Opening Doors to Light: Chemically Gated Diarylethene Photochromism for Sensing and Detection Applications

by

Rameez Raza

M.Sc. (Chemistry), Jamia Millia Islamia, 2014

B.Sc. (Chemistry, Hons.), University of Delhi, 2012

Thesis Submitted in Partial Fulfillment of the
Requirements for the Degree of
Doctor of Philosophy

in the
Department of Chemistry
Faculty of Science

SIMON FRASER UNIVERSITY

Spring 2025

Declaration of Committee

Name:	**Rameez Raza**
Degree:	**Doctor of Philosophy**
Title:	**Opening Doors to Light: Chemically Gated Diarylethene Photochromism for Sensing and Detection Applications**
Committee:	**Chair:** **Paul C. H. Li** Professor, Chemistry
	Neil R. Branda Supervisor Professor, Chemistry
	Vance E. Williams Committee Member Professor, Chemistry
	Peter D. Wilson Committee Member Associate Professor, Chemistry
	Andrew J. Bennet Examiner Professor, Chemistry
	Michael O. Wolf External Examiner Professor, Chemistry University of British Columbia

Abstract

This thesis investigates the gated photochromism of diarylethene photoswitches, focusing on their design, synthesis, characterization, and application as sensors, detectors, and indicators. These sensors aim to detect environmentally and biologically relevant small molecules.

Chapter 2 of this thesis focuses on detecting singlet oxygen, a highly reactive oxygen species. A pro-diarylethene molecule was synthesized, incorporating a furan moiety as the central ring. The molecule lacks a 1,3,5-hexatriene system necessary for the photocyclization until the Diels-Alder reaction with singlet oxygen occurs. This reaction installs the hexatriene system, and the molecule can undergo a visible color change when exposed to UV light.

Chapter 3 presents a diarylethene analog of Hendrickson's reagent to monitor the progress of esterification reactions and detect the alcohols and moisture in solvents. The diarylethene is locked in the parallel conformation through a phosphorus-oxygen-phosphorus bond. Upon adding an O-nucleophile, the phosphorus-oxygen bond breaks, unlocking the molecule's ability to switch to a photoactive form. UV irradiation leads to a color change in the solution.

Chapter 4 introduces a nucleobase-based diarylethene molecule locked in the photoinactive parallel conformation through hydrogen bonds. A photoswitch was designed to bind within a mismatched DNA duplex. A toehold-mediated strand displacement process by the target strand unlocks the molecule, and UV light irradiation leads to a color change. A proof-of-concept model with adenosine and uridine was designed and synthesized to validate the approach.

This work demonstrates the potential of chemically gated diarylethene photoswitches as versatile molecular sensors.

Keywords: Diarylethenes, Gated photochromism, Singlet oxygen, Hendrickson's reagent, Nucleosides

To the challenges that tested me, the setbacks that pushed me,

and the perseverance that kept me going.

To the late nights, the tough moments,

and the small victories that made all the difference.

To those who supported me

and even those who doubted me—both played a part in this journey.

Most of all, to myself—for not giving up. ***This one's for you.***

Acknowledgements

The completion of this degree would not have been possible without the support and guidance of many individuals.

First and foremost, I am deeply grateful to **Neil** for his unwavering support, insightful guidance, and constant patience throughout this journey. His expertise and mentorship have been invaluable in shaping my scientific approach and fostering my critical thinking.

I would also like to extend my sincere gratitude to my supervisory committee, **Vance and Pete**, for their feedback and continuous encouragement. Their guidance has played a crucial role in broadening my scientific perspective and strengthening my research.

A special thanks to **Nabyl** for his mentorship and support throughout my time here. I have learned so much from him, especially about teaching chemistry, and his advice has been invaluable.

I am especially grateful to **Brahmjot and Daina** for their unwavering support, patience, and encouragement. Through every challenge, failed experiment, and moment of frustration, they were always there—offering advice, keeping me motivated, and making even the most tedious tasks more enjoyable. They weren't just lab mates; they became true friends. Whether it was celebrating small victories, commiserating over setbacks, or just finding ways to make the workday more fun, I couldn't have asked for better people to share this experience with. The memories, the laughter, and the countless shenanigans we pulled in the lab will always be some of the best parts of this journey.

I am incredibly thankful for all the fantastic people I had the privilege of meeting and working within this lab—**Khaled, David, Carson, Amir, Tony, Nazanin, Simran, Scott**, and everyone else who was part of this journey. Science can be frustrating at times, but having such a fantastic group of colleagues made even the toughest days more manageable. Whether it was lending a hand with experiments, offering words of encouragement, or simply sharing a laugh after a long day, their support and camaraderie made all the difference. The friendships and memories we built together will always be one of the highlights of my graduate experience.

I would also like to express my appreciation to **PingPing, Paul, Eric, Hongwen, Nathanael**, and others for their assistance with experimental setups and logistical support. A special thanks to **Stacey** for her patience, efficiency, and willingness to assist, which made a world of difference throughout this journey.

Finally, I am forever indebted to my family and the person who has been my constant source of love, patience, and encouragement. Their unwavering belief in me, through every step, every challenge, and every success, has made this journey possible, and I could not have done it without them and their support.

Table of Contents

List of Tables

List of Figures

List of Schemes

List of Acronyms

UV	Ultraviolet
HOMO	Highest Occupied Molecular Orbital
LUMO	Lowest Unoccupied Molecular Orbital
NMR	Nuclear Magnetic Resonance
PSS	Photostationary State
BAPTA	1,2-*bis* (2-aminophenoxy) ethane-*N, N, N′, N′*-tetra acetic acid
EDTA	Ethylenediaminetetraacetic acid
DMSO	Dimethyl Sulfoxide
PMMA	Poly (methyl methacrylate)
DNA	Deoxyribonucleic Acid
ROS	Reactive Oxygen Species
PDT	Photodynamic Therapy
NIR	Near Infrared
EPR	Electron Paramagnetic Response
TEMP	2,3,6,6-Tetramethylpiperidine
TEMPO	(2,2,6,6-Tetramethylpiperidin-1-yl)oxyl
FFA	Furfuryl Alcohol
HPLC	High Performance Liquid Chromatography
PMT	Photomultiplier Tube
THF	Tetrahydrofuran
TLC	Thin Layer Chromatography
EDG	Electron Donating Groups
HRMS	High Resolution Mass Spectrometry
LCMS	Liquid Chromatography Mass Spectrometry
ESI	Electrospray Ionization
TPPO	Triphenyl Phosphine Oxide
GC	Gas Chromatography
IR	Infrared
DFT	Density Functional Theory

TMSD	Toehold Mediated
RNA	Ribonucleic Acid
PCR	Polymerase Chain Reaction
LAMP	Loop-Mediated Isothermal Amplification
SG	SYBR Green I
LSPR	Localized Surface Plasmon Resonance
CTAB	Cetyltrimethylammonium bromide
DMF	Dimethylformamide
DCM	Dichloromethane

Chapter 1.

Introduction

This thesis explores the design and synthesis of chemically gated photochromic systems, where specific molecular interactions modulate the photoisomerization of diarylethene photoswitches. This chemical gating mechanism was leveraged to develop potential sensing and detection applications for reactive oxygen species, oxygen nucleophiles, and nucleic acids.

1.1. Light and Matter

The interaction of light with matter is fundamental and has powerfully impacted numerous scientific disciplines, from physics and chemistry to biology and materials science. The interaction between photons and matter leads to five distinct situations: absorption, transmission, reflection, refraction, and emission.[1,2] When the molecule absorbs light of specific wavelengths, it is excited from a low-energy ground state to a high-energy excited state. Depending on the energy of the light absorbed, this change can be in the vibrational, rotational, or electronic states.[1,2]

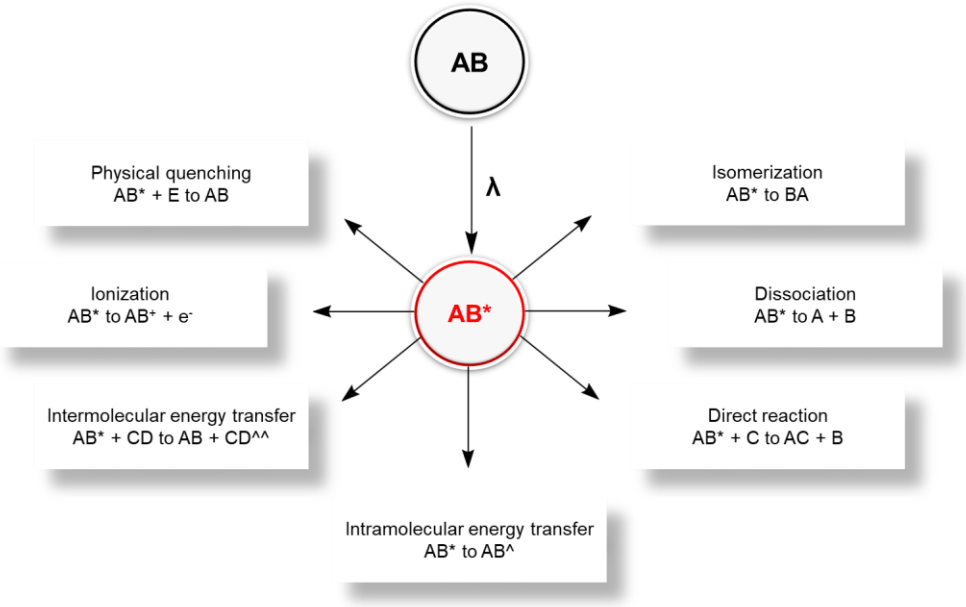

Figure 1-1 The excited state AB* can lose excess energy through different pathways.

In the case of electronic excitation, the excited state AB* is highly energetic and, therefore, short-lived, as the molecule prefers to lose the excess energy.[3] Figure 1 highlights some of the pathways available to the molecule to dissipate the excess energy. One key path for the excited molecule to lose the excess energy is a chemical transformation. These light-induced chemical changes, termed photochemical reactions, form the basis of photochemistry.[1–3]

Light-induced chemical reactions offer several advantages over other reaction modalities. The precise control over light's wavelength, intensity, and duration allows for fine-tuning chemical reactions.[4] Light also enables the specific targeting of regions, thereby providing spatiotemporal control of the chemical reactions.[5] Compared to thermal reactions, photochemical reactions can be conducted under milder reaction conditions (temperature, pressure, and reagents).[6] Another advantage of light over thermal energy is its ability to populate excited states not accessible through thermal energy, which opens new synthetic possibilities.[7]

1.2. Photochromism

Photoexcitation of a molecule followed by structural changes through bond-breaking or bond-forming encompasses a special type of photochemical reaction called photoisomerization.[1,3,8,9] Upon exposure to light, molecules can undergo structural (constitutional) isomerization, such as ring-closing/opening, or spatial (stereo) isomerization, such as cis-trans isomerization. These changes can be reversible or irreversible.

Photoswitches are molecules that undergo a reversible photoisomerization process, meaning they can be toggled between two distinct states upon exposure to light. The two isomers differ in geometrical structure and exhibit different physical and chemical properties, such as absorption spectra, dielectric constants, refractive indices, and oxidation/reduction potentials. Since the two isomers have different absorption spectra (colors), organic photoswitches are often called photochromic molecules.[10–13]

Figure 2 shows some common photoswitch classes: azobenzene[14], spiropyran[15], spirooxazine[16], furylfulgide[17], and diarylethene[18]. Irradiation of isomer A with appropriate light energy, λ^1, induces a photoisomerization reaction leading to isomer B. Azobenzene

molecules undergo a photoinduced *trans-cis* isomerization along the N=N double bond.[14] In the case of spiropyrans and spirooxazines, a C-O bond rearrangement forms a ring-opened isomer from the ring-closed isomer.[15,16] Furylfulgide and diarylethene undergo a pericyclic reaction of the ring-open isomer to yield a colored ring-closed isomer.[17,18] For most systems, this change is accompanied by a change in the molecule's properties, most notably, the color. A sub-classification of the photochromic molecules is based on the ability of isomer B to spontaneously revert to isomer A in the dark (thermally driven). If isomer B is not dark stable, it will revert to isomer A by absorbing heat from the surroundings, and this type of photochromic behavior is called T-type photochromism.

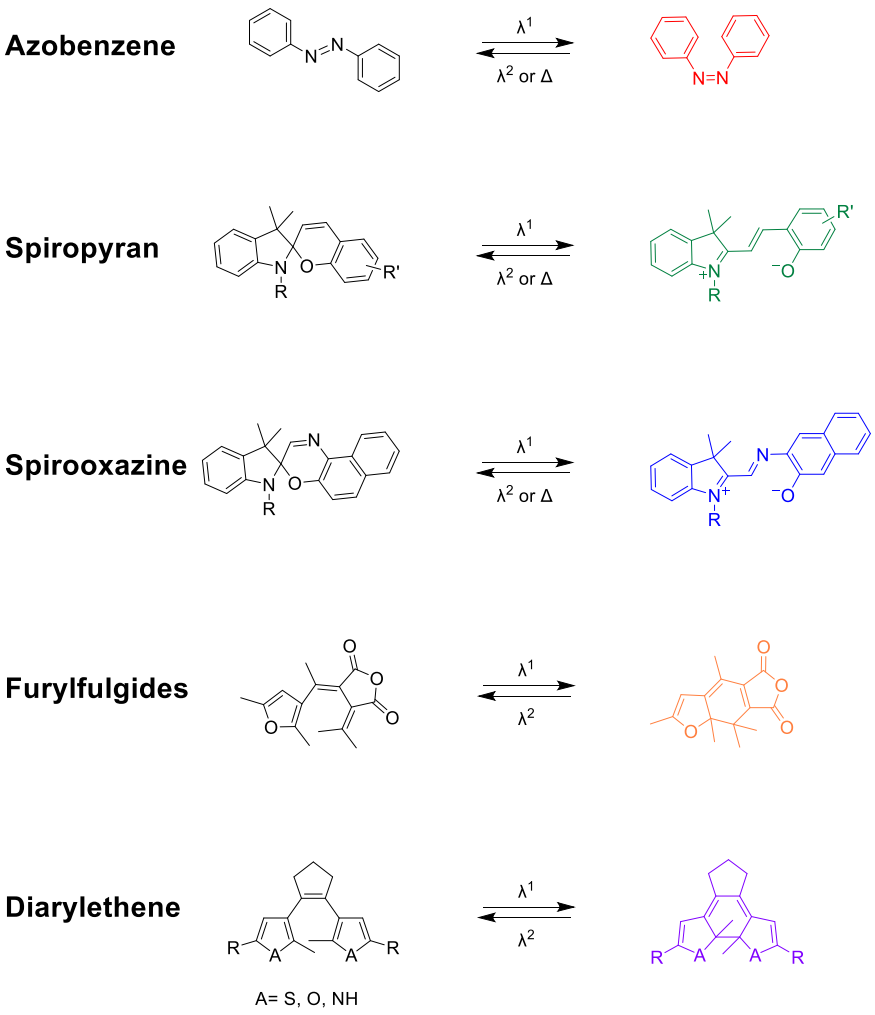

Figure 1-2 Some examples of organic photochromic molecule classes.

The second type is the P-type photochromism, where isomer B is dark stable and reverts to isomer A only when exposed to light of wavelength λ^2 ($> \lambda^1$). Azobenzenes,

spiropyrans, and spirooxazines are typical T-type photochromic molecules[14–16], whereas P-type photochromism is more common in furylfulgides and diarylethenes[17,18].

The successful application of a photochromic molecule in photoresponsive materials and photonic devices hinges on carefully evaluating its inherent properties. The ideal candidate should have a sizeable thermal barrier for reversion in the case of T-type photochromic molecules or, if possible, should display P-type photochromism. Another factor is the photochemical stability of the molecule under prolonged exposure to high-energy light. The photochromic molecules should respond rapidly to light, enabling fast switching between the two states. The ability to tune the photoswitching wavelength through structural modification is also crucial. Lastly, facile modification/functionalization of the molecule is essential for tailoring to specific applications.

Diarylethenes have emerged as a promising photochromic molecule class in recent decades, addressing the critical requirements for applications in molecular switches, sensors, optical data storage, and advanced materials. These molecules offer excellent in-dark stability, high fatigue resistance, ease of modification, and fast response to light of tunable wavelengths.

1.3. Diarylethene Photoswitches

1.3.1. General Description of Diarylethene Photoswitches

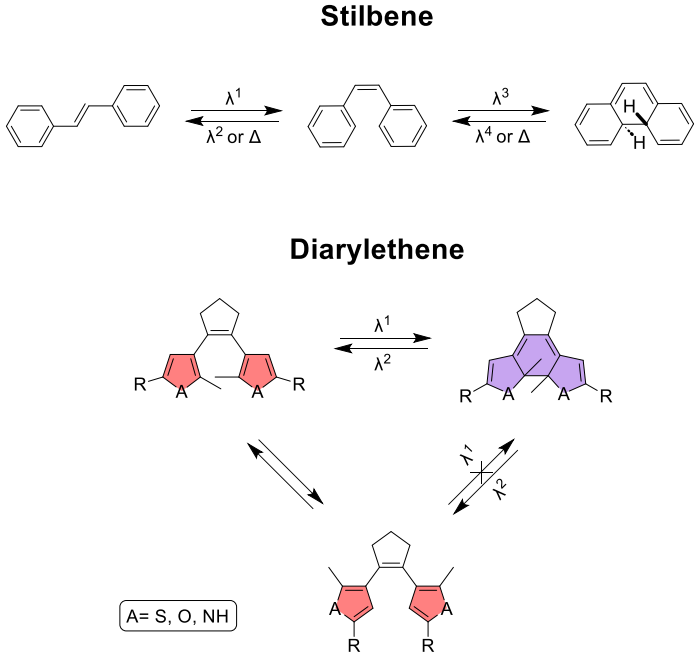

Figure 1-3 Stilbene, a class of photochromic molecules, served as a template for developing diarylethene photoswitches. Replacing the phenyl group with heterocycles improved the photoswitching performance, and the addition of methyl groups in the inner position interrupted the oxidation process of the ring-closed isomer.

The development of diarylethene molecules was inspired by a class of photochromic molecules known as stilbenes, whose general structure consists of an ethylene moiety at the center flanked by phenyl groups.[19] When the ring-open isomer of stilbenes is exposed to UV light, it undergoes a *trans*-*cis* isomerization like azobenzene photoswitches. Further irradiation of the *cis*- isomer leads to the formation of dihydrophenanthrene via 6π electrocyclization. One challenge with the stilbene molecules is the reversion of the ring-closed form, dihydrophenanthrene, to the ring-opened *cis*-isomer in the dark. Another challenge with stilbenes is that dihydrophenanthrene undergoes hydrogen elimination in the presence of oxygen to generate photoinactive phenanthrene. These drawbacks hindered the development of photoresponsive polymers with stilbene groups. Replacement of the phenyl group in the stilbene structure with heterocyclic rings to address the problems led to the development of diarylethene photoswitches. Swapping the hydrogens on the internal position of the

heterocycle with methyl or other functional groups prevented hydrogen elimination and improved stability in oxygenated conditions. Exchanging the bridging ethylene moiety with a ring system like maleic anhydride, maleimide, or cyclopentene locked the molecule in *cis*- or (Z) form. Blocking this *cis-trans* isomerization process enhanced the photoswitching ability compared to stilbenes.[20,21]

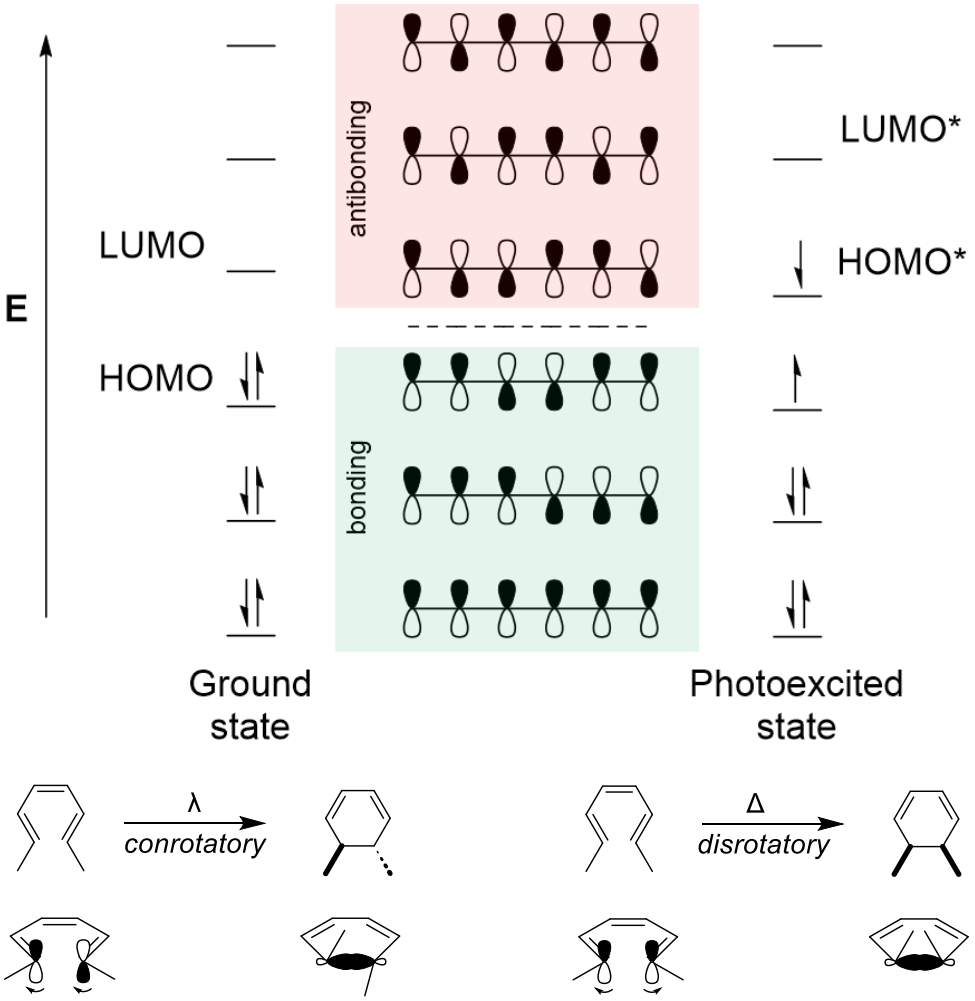

Figure 1-4 The molecular orbital diagram of the 1,3,5-hexatriene system displays the HOMO and LUMO in the ground state and the photoexcited state. Photochemically, the electrocyclization reaction of the 1,3,5-hexatriene system occurs in a conrotatory manner, whereas the thermal electrocyclization occurs in a disrotatory manner.

In diarylethene molecules, a 6π electron system is at the core, formed by the central double bond and the two aromatic rings. Absorption of an appropriate wavelength of light causes electronic rearrangements in a concerted manner, leading to ring closure. Due to the free rotation about the C-C bond between the heterocycle and

the central alkene ring, an equilibrium mixture of *parallel* and *antiparallel* conformations exists in the ring-open isomer. However, only the *antiparallel* conformation can undergo the electrocyclization process, not the *parallel* conformation.[19,21,22] According to Woodward-Hoffman rules for electrocyclization reactions, the 1,3,5-hexatriene system can undergo either a disrotatory thermal cyclization or a conrotatory photocyclization reaction. The inside groups on the aromatic ring do not allow a thermal disrotatory motion in both *parallel* and *antiparallel* conformations because of steric hindrance. For the same reason, the photochemical conrotatory motion in the *parallel* conformation is also not allowed. Thus, only the *antiparallel* conformation with its internal groups in opposite directions can undergo photocyclization.[19–23]

1.3.2. Differences Between the Photoisomers of Diarylethene Photoswitches

The photoisomerization of the diarylethene photoswitches between the ring-open and ring-closed isomers results in distinct physical and chemical properties for each form. These differences have been extensively used for numerous applications in materials science.

Geometric Differences

As mentioned previously, the ring-open isomer exists in two key conformations, *parallel* and *antiparallel*. Based on the symmetry across the double bond in the central ring, the *parallel* conformation possesses a mirror plane symmetry, and the *antiparallel* conformation has a C2 symmetry. This free rotation makes the ring-open structure flexible and allows the functional groups at the internal or external positions of the two heterocycles to converge on each other.

As mentioned before, the ring-open isomer exists in two key conformations, *parallel* and *antiparallel*. Based on the symmetry across the double bond in the central ring, the *parallel* conformation possesses a mirror plane symmetry, and the *antiparallel* conformation has a C2 symmetry. This free rotation makes the ring-open structure flexible and allows the functional groups at the internal or external positions of the two heterocycles to converge on each other.

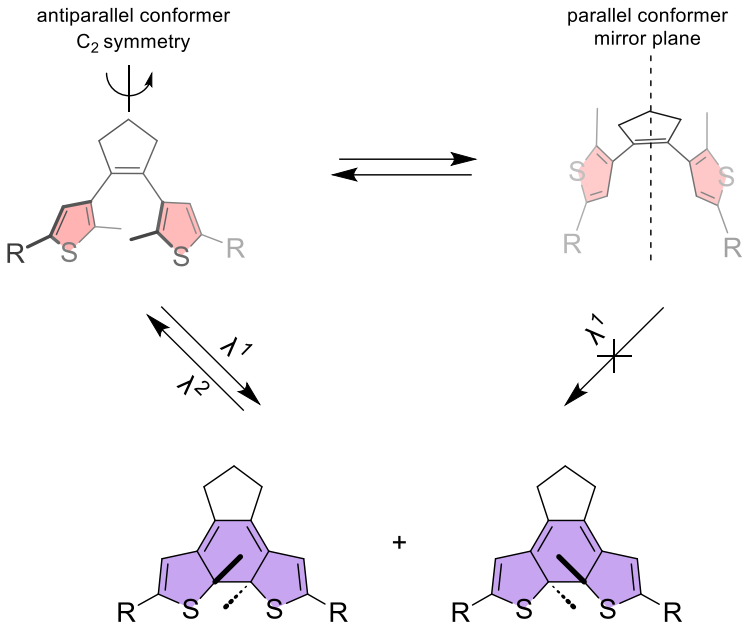

Figure 1-5 The ring-open isomer is flexible and exists in *parallel* and *antiparallel* conformations. The *antiparallel* conformation possesses a C2 symmetry, and the *parallel* conformation possesses a mirror plane. The fused rings in the *ring-closed* isomers impart rigidity.

The ring-closed isomer obtained from photocyclization contains a 1,3-cyclohexadiene ring at its core. This tetracyclic fused ring structure makes the ring-closed isomer structurally rigid. As the two heterocycle rings are now part of this fused ring structure, the functional groups on the internal and external positions diverge from each other.[20,21,23]

Electronic Differences

There are stark differences in the electronic properties of the two isomers of the diarylethene molecules. In the ring-open isomer, the two heterocycle rings across the ethene bridge are electronically insulated from each other, i.e., their π-electron systems are localized. Therefore, the internal (**B**/**C**) and external positions (**A**/**D**) of the heterocycle in the ring-open isomer are electronically connected.

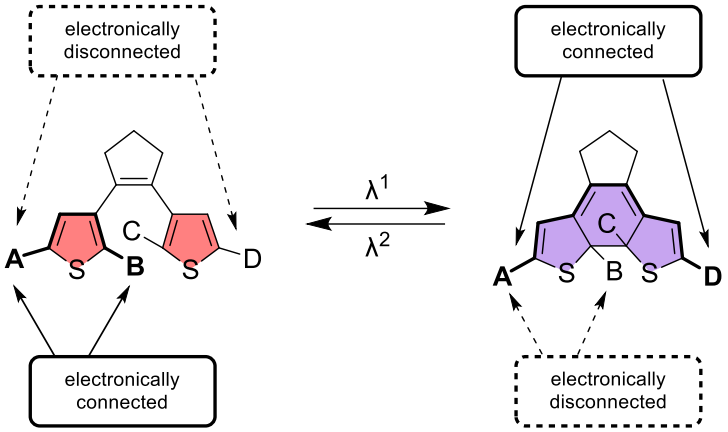

Figure 1-6 In the ring-open isomer, the substituents A and B are electronically connected but disconnected to C and D on the other thiophene. The external positions A and D are electronically connected in the *ring-closed* isomer.

The photocyclization reaction forms a fused ring structure incorporating the two thiophenes, containing a π-conjugated system spread across the diarylethene core. The functional groups in the external positions (**A** and **D**) of the two heterocycles can now communicate with each other through this extended π-conjugation; however, the groups in the internal positions (**B** and **C**) become isolated from them because of the generation of new sp^3 carbons.[21,21,22,24]

Spectroscopic Differences

The ring-open isomer of the diarylethene molecules absorbs in the high-energy UV region as the two thiophene rings are electronically insulated from each other. The ring-open isomer is, therefore, generally colorless and shows absorption bands between wavelengths of approximately 220 nm and 350 nm.

A color change typically accompanies the photocyclization reaction of the ring-open isomer. The extended π-conjugation in the ring-closed isomer absorbs in the visible region and shows absorption bands between 400 and 800 nm.[19,21,25] The color change and UV-visible spectroscopy can be used to easily monitor the photoconversion of the two isomers of diarylethene molecules.

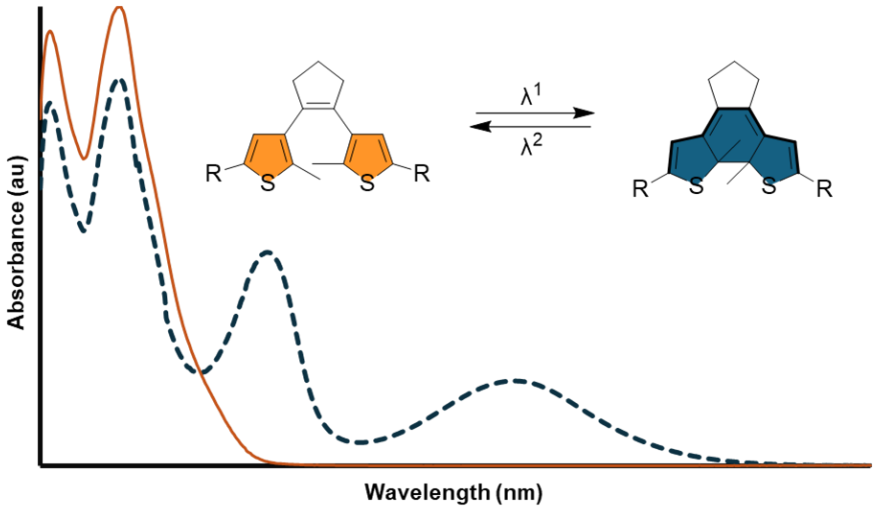

Figure 1-7 Typical UV-visible spectra of the ring-open form (orange line) and the ring-closed form (blue broken line) of the diarylethene photoswitches.

Similar to changes in the UV-visible spectra of the diarylethene molecule on photoisomerization, differences in the ^{1}H NMR of the isomers are occasionally distinct.[26] As mentioned before, the internal position of the thiophene is usually a methyl group to avoid oxidation. The chemical shift of the methyl group protons in the ring-open isomer is dictated by the relative position of the two heterocycles. In the case of the *antiparallel* conformation, the methyl group protons lie in front of the heterocycle rings. The ring current on the aromatic system induces a high magnetic field on the methyl protons, which appear at around 1.7 ppm in the ^{1}H NMR spectrum. This magnetic field effect is absent in the *parallel* conformation, and the methyl protons' signal shifts downfield. For most diarylethene photoswitches, the difference in the ^{1}H NMR spectra of the *parallel* and *antiparallel* conformations is not seen.[27] The time scale for the interchange between the two conformations is extremely small, and a time-averaged signal for the methyl protons is seen in the ^{1}H NMR spectra of the ring-open isomer. In the case of the ring-closed isomer, changes in the chemical shift of the protons on the 4-position (if present) of the heterocycle ring and the methyl protons on the 2-position are apparent. The heterocycle group loses its aromaticity upon photocyclization, and the signal for the 4-position is shifted upfield. In contrast, a downfield shift is observed in the case of the internal methyl protons.[28]

1.4. Salient Features of Diarylethenes

1.4.1. In-dark Stability of Diarylethene Photoswitches

Diarylethene molecules are part of the P-type photoswitch class, i.e., the cycloreversion of the ring-closed form is only possible with light. While this statement is not valid for all heterocycles, it is true for those with thiophenes or benzothiophenes, two of the most commonly used in designing diarylethenes. Another caveat is that a bulky inner group on thiophene or benzothiophene decreases the in-dark stability of diarylethene photoswitches.

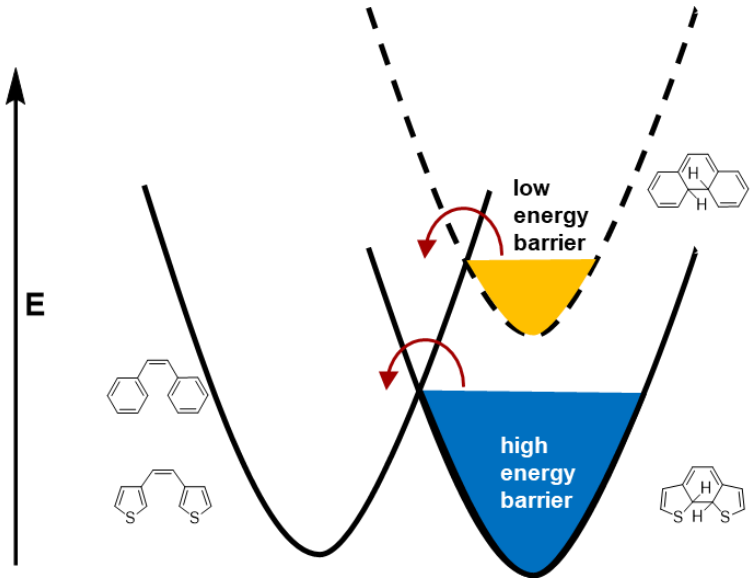

Figure 1-8 Energy diagrams for the ring-open and ring-closed forms of stilbene and diarylethene.

The in-dark stability of the ring-closed isomer is attributed to the low aromatic stabilization energy of the thiophene compared to that of other heterocycles.[23,26] During the photocyclization process, the aromatic character of the heterocycle is lost. Irie and coworkers theoretically calculated the aromatic stabilization energy of various heterocycles and found it to be the highest for the phenyl group and lowest for the thiophene. The ground state energy of the ring-open and the ring-closed isomers is directly connected to the aromatic stabilization energy. Calculations for the ground state energy of the ring-open and the ring-closed isomer showed that the energy difference between the two forms was highest in the case of phenyl and lowest in the case of thiophene. When the ground state energy difference between the two forms is high, the

activation energy barrier is small, as with stilbene, and cycloreversion occurs in the dark. Conversely, the energy barrier for cycloreversion is significant when the ground state energy difference is slight, as in the case of thiophenes and benzothiophenes, and cycloreversion in the dark is extremely difficult.[19,23,26]

1.4.2. Fatigue Resistance of Diarylethene Photoswitches

To alleviate the hydrogen elimination problem analogous to stilbenes, in diarylethenes, the hydrogen on the internal 2-position of thiophene is replaced by another group, in most cases, a methyl group. This modification increases the fatigue resistance of the diarylethene photoswitch, and thus, some diarylethene molecules can undergo thousands of photoswitching cycles without any noticeable change in performance.

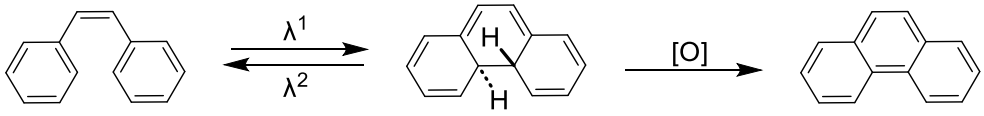

Figure 1-9 The *ring-closed* isomer of stilbene, the first known diarylethene molecule, undergoes oxidation at the bridging carbon-carbon bond to irreversibly form phenanthrene.

Although the fatigue resistance is considerably higher than the stilbene derivatives, diarylethene photoswitches undergo side reactions upon prolonged exposure to UV light.[29] In deaerated conditions, the cyclohexadiene core in the ring-closed isomer rearranges into a condensed-ring byproduct. This stable byproduct possesses the identical absorption spectra as the ring-closed isomer but cannot undergo cycloreversion to the ring-open isomer. Replacing thiophenes with benzothiophenes eliminates this side reaction and increases the fatigue resistance. When oxygen is in the system, the cyclohexadiene core can react with it to form an endoperoxide product, destroying the 1,3-cyclohexadiene core necessary for cycloreversion.[30]

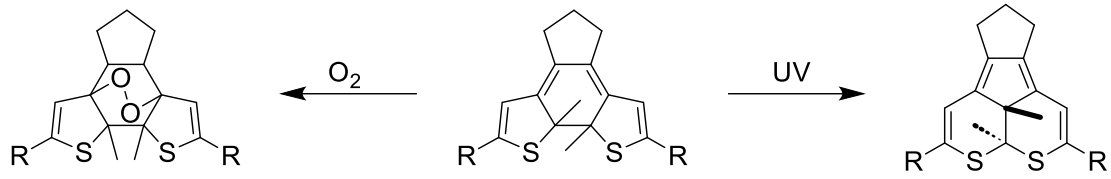

Figure 1-10 Side products from the photocyclization reactions of the diarylethene molecule. Prolonged exposure to high-energy UV light forms a condensed-ring structure that cannot undergo the reverse ring-opening reaction. In the presence of oxygen, the cyclohexadiene core can form endoperoxides.

1.4.3. Photoswitching Performance of Diarylethene Photoswitches

Two crucial parameters, quantum yield and photo-stationary state (PSS), measure the photoswitching performance of photochromic molecules. The quantum yield (Φ) describes the product yield of a photochemical reaction at a particular wavelength, light intensity, and reactant concentration.[13] In terms of photochromic reactions, quantum yield is mathematically described as follows:

$$\Phi(\lambda) = \frac{number\ of\ isomerized\ molecules}{total\ numbers\ of\ photons\ absorbed}$$

Equation 1-1 The mathematical equation for calculating the quantum yield (Φ) of the photochromic process at a given wavelength (λ).

The ideal quantum yield value for the photocyclization and cycloreversion process is 1. The quantum yield for diarylethene molecules is typically below this number. The photocyclization quantum yield of diarylethene molecules is hampered by the free rotation of the heterocyclic rings, which normally leads to a population ratio of 1:1 for *antiparallel* and *parallel* conformations. As only the *antiparallel* conformation undergoes the photocyclization reaction, the quantum yield for the photocyclization reaction is closer to 0.5 for most diarylethene molecules.[19,21,24] Quantum yield for diarylethene molecules can be improved by increasing the population of the *antiparallel* conformation, which can be achieved in several ways. Including the diarylethene molecule in a cyclodextrin cavity favors the *antiparallel* conformation over the *parallel* conformation. Replacing the central cyclopentene ring with heterocyclic aryl groups or replacing the methyl group on the internal 2-position of thiophene with a bulkier group helps in increasing the ratio of *antiparallel* conformation. A photochromic molecule's

photo-stationary state (PSS) is the percentage of isomers A that photocyclizes under specific conditions. Mathematically, PSS is expressed as follows:

$$PSS = \frac{number\ of\ isomerized\ molecules}{total\ numbers\ of\ molecules} * 100$$

Equation 1-2 The mathematical expression for calculating the photo-stationary state of a photochromic molecule.

When the rate of photocyclization reaction of the ring-open isomer becomes equal to the rate of the cycloreversion reaction of the ring-closed isomer, the PSS is said to be reached. The initial irradiation of the diarylethene molecule leads to an increase in the concentration of the ring-closed isomer and a decrease in the concentration of the ring-open isomer. As the ring-closed isomer also absorbs in the UV region, the rate of cycloreversion reaction increases with time. Eventually, the rate of photocyclization and cycloreversion reactions becomes equal, and a steady-state concentration of the ring-open and ring-closed isomers is reached.[21,31]

1.4.4. Versatility of Diarylethene Photoswitches

The most important feature that allows a photochromic molecule to be employed for various applications is its ability to tolerate diverse chemistries and the ease of functionalization. As mentioned earlier, the diarylethene molecule possesses a core of two heterocyclic rings across an ethylene bridge moiety. The 2- or the internal position on the heterocyclic ring commands the reactive carbon undergoing photocyclization. Modifications on this carbon atom modify properties like thermal stability, fatigue resistance, quantum yield, and PSS. The 5- or the external position allows for a wide range of modifications specific to the end use of the molecule. Most of the work on diarylethene molecules is done by attaching various functional moieties, vide infra.

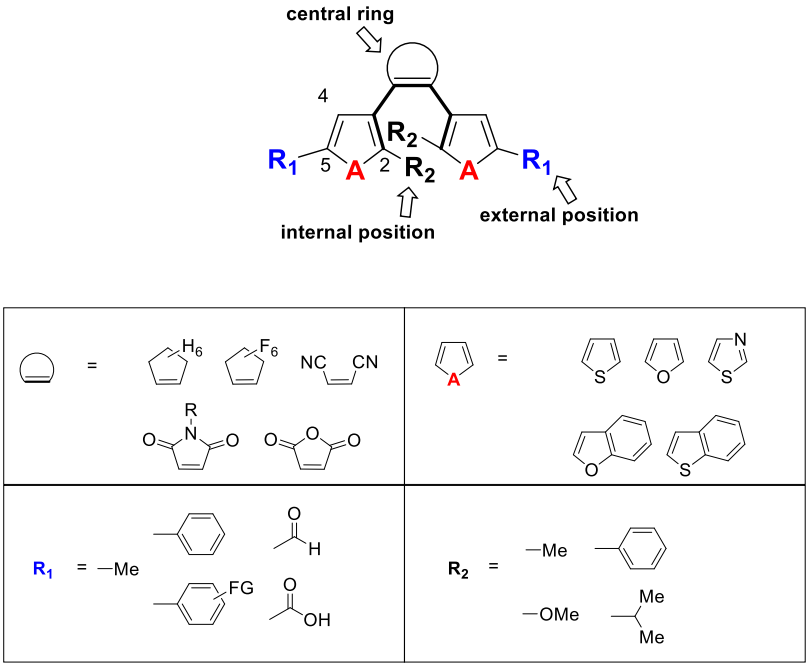

Figure 1-11 Selected examples of the most common modifications done to the central alkene ring, the heterocyclic rings, the internal position, and the external position of the diarylethene are shown here, displaying their versatility.

Though limited, a few examples of modifications at the 4-position are also known. Alterations of the top alkene-bearing ring system can also be done to modify the properties of the diarylethene molecule and to introduce a desired functionality. The versatile nature of diarylethene molecules and the ease of modifications have allowed them to be used for many applications.

1.5. Relationship Between Chemistry and Photochemistry

The previous sections focused on the relationship between light and chemical reactions, the photochromic molecules, diarylethene photoswitches, their photochromic behavior, and their associated properties. The following sections will explore the connection between light, chemical reactions, and the photochromism of diarylethene molecules.

The triad of light, chemical reactivity, and photochromism can be employed in two fundamental approaches to create new technologies and improve upon the existing ones in materials science, chemistry, and biosciences. The first method controls a

chemical reaction by controlling diarylethene molecules' light and photochromic behavior. In this method, the changes in physical and chemical properties associated with the photoisomerization of the diarylethene are employed to influence a chemical reaction. The second method is to use a chemical reaction to control the photochromism of the diarylethene molecule. Here, the diarylethene molecule is non-photoresponsive, but a chemical reaction unlocks the photochromic behavior of the diarylethene molecule. Both methods have been utilized extensively to develop photoresponsive catalysts, reagents, and colorimetric sensors.

1.6. Photochemistry Gates Chemistry

Synthetic chemists have long toiled with the idea of controlling chemical transformations, asserting that spatiotemporal control over a chemical reaction allows for developing complex materials. One path is to use light and the photochromic behavior of a photoswitch to gate or control the chemical reaction. The differences in the structure or electronics of the photochromic molecule upon irradiation with light can be employed to modulate a chemical reaction. The photochromic molecule will be chemically inert in one isomeric form and facilitate a chemical reaction in the other form. In this way, the chemistry can be said to be ‘gated’ using photochemistry.

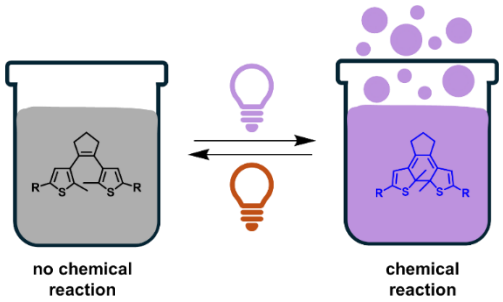

Figure 1-12 The gated chemistry approach is where only one isomer is chemically active.

1.6.1. Modulation Using Steric Differences

The flexibility of the ring-open isomer of diarylethene photoswitches allows it to exist in two conformations: the *parallel* and the *antiparallel* form. Because of the free rotation of the thiophenes, groups attached to the external and internal positions can converge on each other. In the case of the *parallel* conformation, the convergence of the

functional groups leads to the formation of a binding pocket. On the other hand, the ring-closed isomer is structurally rigid, and the functional groups on the thiophenes diverge from each other. These structural differences between the two photocyclized forms of the diarylethene photoswitches have been used to create molecular tweezers. Diarylethene photoswitches are used as spacers and offer dynamic control over substrate binding. The binding groups are attached as the substituents on the thiophene moieties in either external or internal positions. In the ring-open isomer, the binding groups converge on each other and create a cavity for substrate binding, while the ring-closed isomer shows a low affinity for substrate binding.

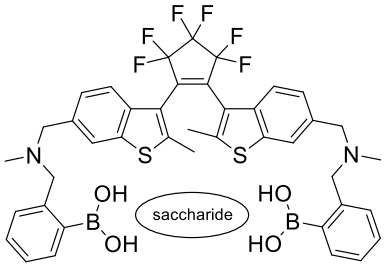

Figure 1-13 Photoswitchable host for saccharides synthesized by Irie and coworkers.

Irie and coworkers used the concept of photoswitchable tweezers to create a saccharide receptor. The benzothiophene-based diarylethene photoswitch contains boronic acid groups in the external positions. These groups can converge on each other in the *parallel* conformation of the ring-open isomer and create a cavity for binding saccharides via boronate linkages. In the case of the ring-closed isomer, the rigid fused ring structure separates the two boronic acid groups, and saccharide binding to form a complex is inhibited.[32]

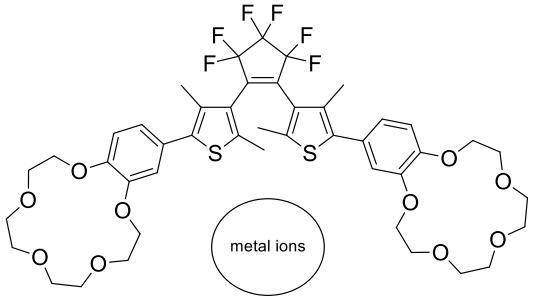

Figure 1-14 Crown ether-based diarylethene photoswitch for binding metal ions.

Building upon the same concept, Irie[33] and Kawai[34] attached crown ethers across the diarylethene photoswitch spacer. The crown ether groups converge on each other in the *parallel* conformer of the ring-open isomer and create a binding site for large alkali metal cations like K^+, Rb^+, and Cs^+. Aqueous solutions of metal picrates were extracted with the organic solvent solution of the diarylethene photoswitch. The amount of metal picrates extracted by the ring-open isomer solution was considerably higher than that by the PSS mixture solution. The photocyclization quantum yield for the crown ether-substituted diarylethene photoswitches was studied in the presence of large alkali metal cations. A significant decrease in the quantum yield of the diarylethene photoswitch was attributed to the complex formation between the photoinactive *parallel* conformation and the metal cations.

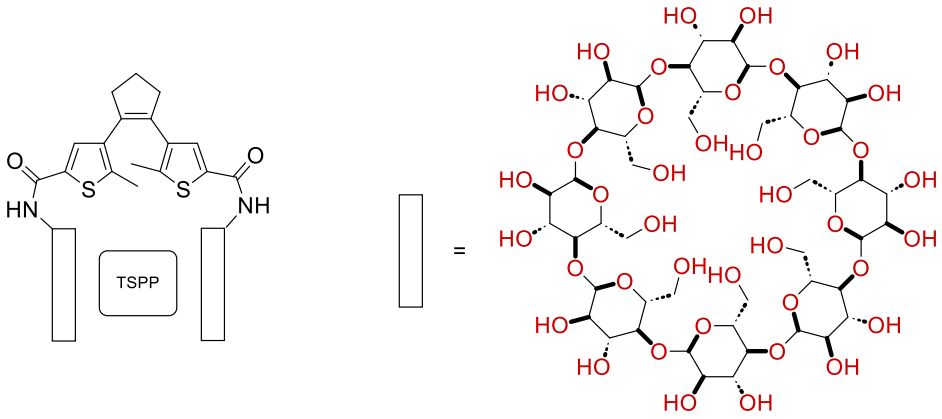

Figure 1-15 β-cyclodextrin substituted diarylethene photoswitch for binding tetrakis(4-sulfonate phenyl) porphyrin.

Reinhoudt and coworkers synthesized a β-cyclodextrin-substituted diarylethene photoswitch to demonstrate the photo-release of encapsulated guest molecules.[35] Tetrakis (4-sulfonatophenyl) porphyrin, which forms a 1:1 complex with beta-cyclodextrin dimers, was used to study the binding affinity. The binding of porphyrin with the ring-open isomer was 35 times higher than that with the ring-closed isomer. Irradiation of the complex with 313 nm UV light resulted in the release of the porphyrin molecule in the solution as the photocyclization reaction proceeded.

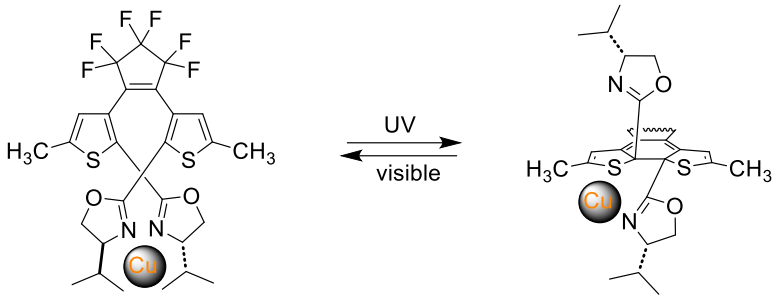

Figure 1-16 *Bis*(oxazoline)-diarylethene for control over metal-catalyzed reaction. The flexible ring-open isomer binds Cu and displays stereoselectivity and enantioselectivity for a reaction between styrene and ethyl diazoacetate. In contrast, no such observation was made with the rigid *ring-closed* isomer.

Branda and coworkers prepared a *bis*(oxazoline) substituted diarylethene photoswitch to control a metal-catalyzed reaction.[36] The oxazoline group was attached to the internal 2-position of the thiophene and, in the flexible ring-open isomer, provided a C2-symmetric chiral environment for metal ions such as Cu to reside. In the ring-closed isomer, rigidity does not allow a suitable coordination environment for Cu binding. A model reaction of styrene with ethyl diazoacetate, catalyzed by the copper-*bis*(oxazoline) diarylethene, was performed to study the difference between the catalytic activity of the two photoisomers. The ring-open isomer-catalyzed reaction showed stereoselectivity and enantioselectivity, whereas no such observation was seen with the ring-closed isomer.

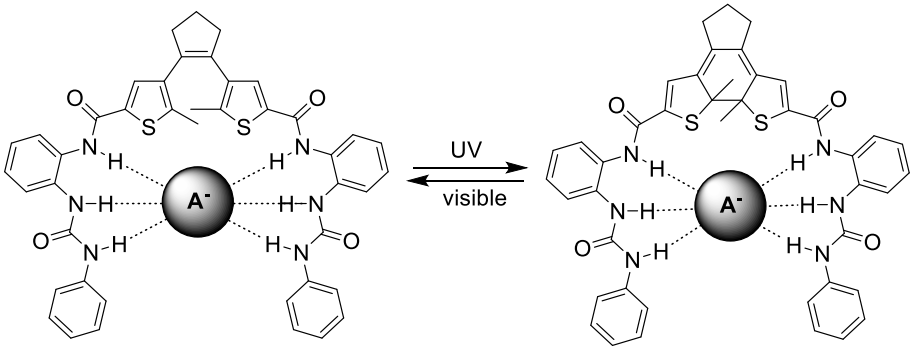

Figure 1-17 The amide functional groups in the diarylethene synthesized by Liu and coworkers can bind Cl^- and Br^- ions. The *ring-closed* isomer has a lower binding affinity to anions than the ring-open isomer.

Liu and coworkers designed a diarylethene photoswitch with amide and urea functionalization and studied the molecule as a receptor for halide anions.[37] The ring-

closed isomer showed a lower affinity for the chloride ion than the ring-open isomer. Theoretical calculations demonstrated that the rigid structure of the ring-closed isomer leads to a larger cavity than the ring-open isomer.

1.6.2. Modulation Using Electronic Differences

As previously discussed, the photocyclization reaction changes the electronic structure of the diarylethene molecules. In the case of the ring-open isomer, the thiophene groups across the ethene bridge are isolated. Thus, the substituents on individual thiophene groups' internal and external positions (of the same ring) can sense each other. On the other hand, the ring-closed isomer possesses an extended π-conjugated system, connecting the external positions of the two thiophene moieties.

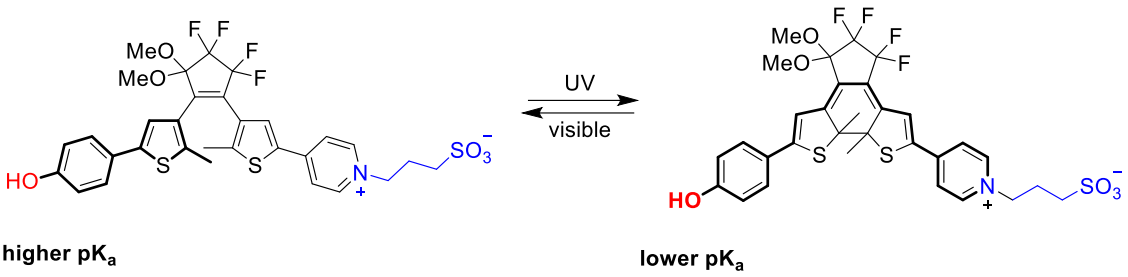

Figure 1-18 Diarylethene with pyridinium group on one side and phenol on the other. The acidity of the phenol is higher in the ring-closed isomer than in the ring-open isomer. The phenol group experiences the electron-withdrawing effect of the pyridinium group through the extended conjugation in the ring-closed isomer.

Lehn and coworkers utilized the change in the electronics of the diarylethene molecule upon photocyclization to control the *pKa* of the phenol group by an electron-withdrawing pyridinium group.[38] In the ring-open isomer, the pyridinium group on one of the thiophenes is isolated from the phenol on the other thiophene. Photocyclization to the ring-closed isomer allows the pyridinium group to sense the phenol group on the other side via the extended π-conjugation, and the *pKa* decreases.

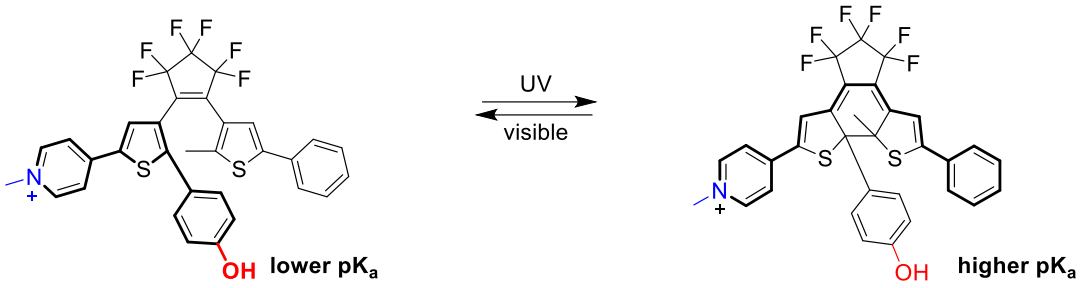

Figure 1-19 The phenol group in the ring-open isomer experiences the electron-withdrawing effect of the pyridinium group. The acidity of the phenol group increases upon photocyclization as it is now isolated on a sp^3-hybridized carbon.

Irie and coworkers modified this system by functionalizing the two groups on the same thiophene.[39] Communication is possible between the external and internal positions of the thiophene in the ring-open isomer. Photocyclization disrupts this conjugation, as the phenol is now attached to a sp^3-hybridized carbon atom, and the *pKa* increases.

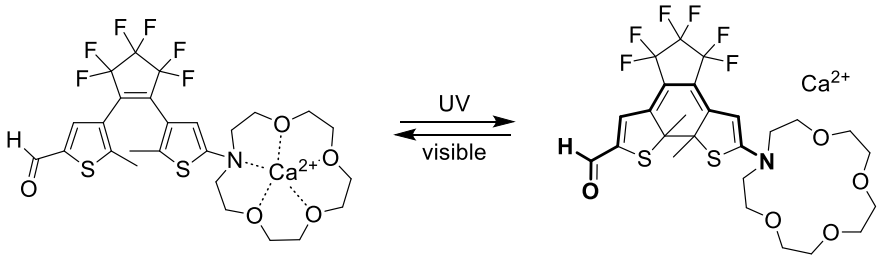

Figure 1-20 Azacrown-based diarylethene photoswitches can bind metal ions in the ring-open isomer. Photocyclization leads to extended conjugation, and the electron-withdrawing group reduces the electron density in the azacrown, thereby releasing the metal ion.

Lapouyade and coworkers synthesized an azacrown-based diarylethene photoswitch capable of binding and releasing cations.[40] The diarylethene photoswitch was designed with an azacrown ether on one thiophene and an electron-withdrawing aldehyde group on the other. In the ring-open isomer of the diarylethene photoswitch, the azacrown moiety acts as an ionophore and binds with metal cations like $Ca^{2+,}$ as demonstrated by the authors. The binding affinity of the azacrown decreases, and the metal cation is released during the photocyclization reaction. In the ring-closed isomer, the communication between the azacrown moiety and the electron-withdrawing carbonyl

group is established through extended π-conjugation, which decreases the binding affinity.

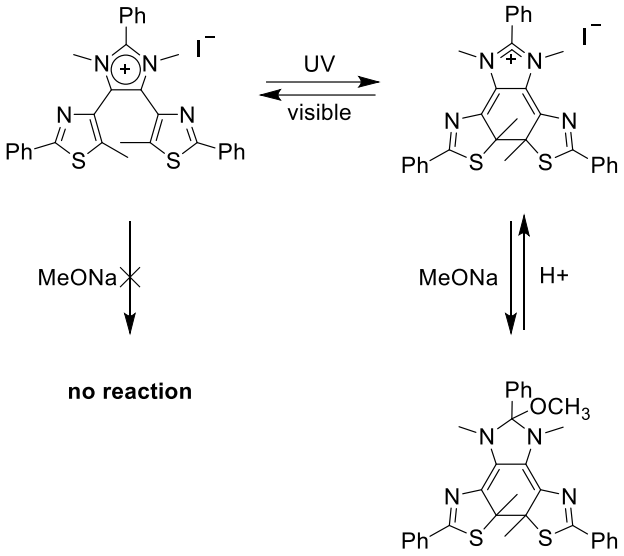

Figure 1-21 The ring-open form of the imidazolium-based diarylethene cannot undergo a nucleophilic reaction with methoxide due to its aromaticity. On the other hand, the *ring-closed* isomer can undergo the reaction as the imidazolinium ring is no longer aromatic.

Kawai and coworkers reported a diarylethene photoswitch with the cyclopentene ring replaced by an aromatic imidazolium ring.[41] The aromaticity of the imidazolium ring inhibits the nucleophilic addition of methoxide on it. Irradiation with 313 nm light produces the ring-closed system with an imidazolinium ion devoid of aromatic stabilization, which can now reversibly react with the methoxide group.

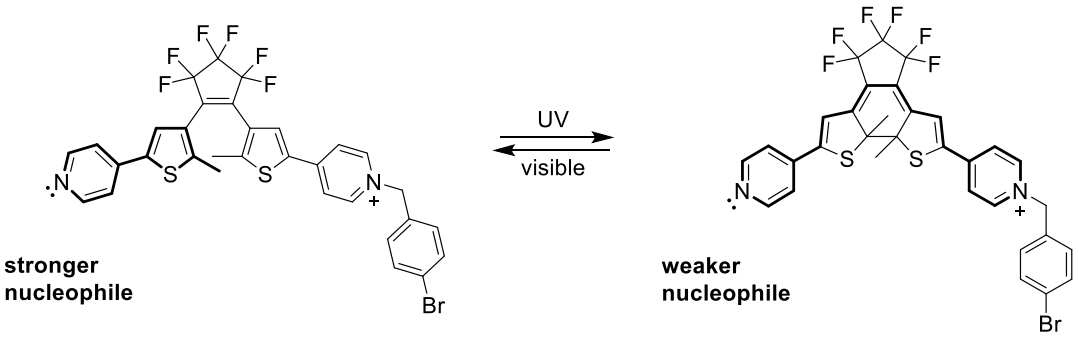

Figure 1-22 The nucleophilicity of the pyridine group is higher in the ring-open form compared to the *ring-closed* form. The extended conjugation leads to the electron-withdrawing effect of the pyridinium group to be sensed by the pyridine ring on the other side.

Branda and coworkers modulated the nucleophilicity of a free pyridine group by controlling the electronic structure of a diarylethene photoswitch.[42] One thiophene group contains the pyridine, and the other has an electron-withdrawing pyridinium group. The two groups are electronically insulated in the ring-open isomer, and the alkylation reaction is fast. Photocyclization creates a connection between the two groups, and the pyridinium group's electron-withdrawing effect reduces the pyridine's nucleophile strength. The reduced nucleophilic character resulted in a decrease in the rate of alkylation reaction.

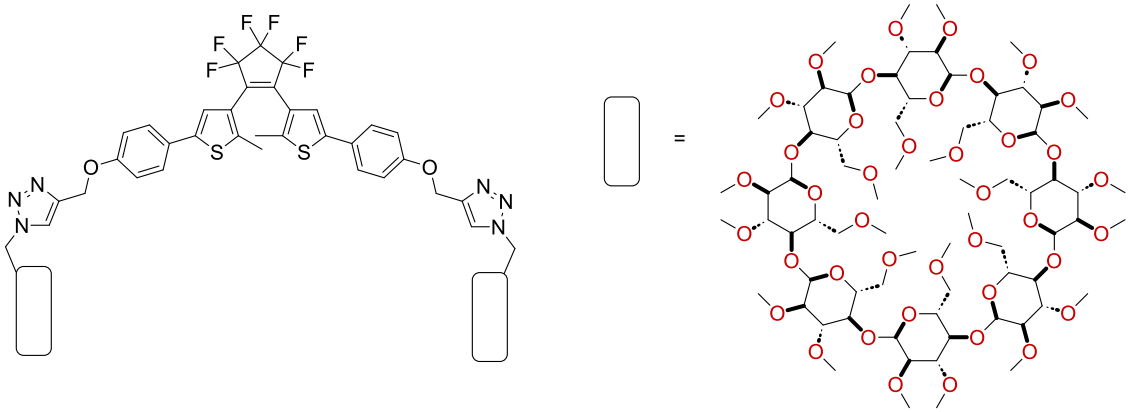

Figure 1-23 Methyl-β-cyclodextrin-based diarylethene synthesized by Liu and coworkers for singlet oxygen generation in 1% ethanol solutions.

Liu and coworkers developed a supramolecular host-guest assembly that produced singlet oxygen in 1% ethanol aqueous solution.[43] Methyl β-cyclodextrin was appended to a diarylethene core, and tetra sulfonatophenyl porphyrin was added as a guest. The porphyrin resides in the cavity of the β-cyclodextrin units of two diarylethene photoswitches to form a supramolecular structure. In the ring-closed isomer of diarylethene, the photosensitizer can transfer energy to the diarylethene molecule over triplet oxygen, and singlet oxygen production is inhibited. The same energy transfer to diarylethene is not possible in the ring-open isomer; thus, the photosensitizer can transfer the energy to triplet oxygen and produce singlet oxygen.

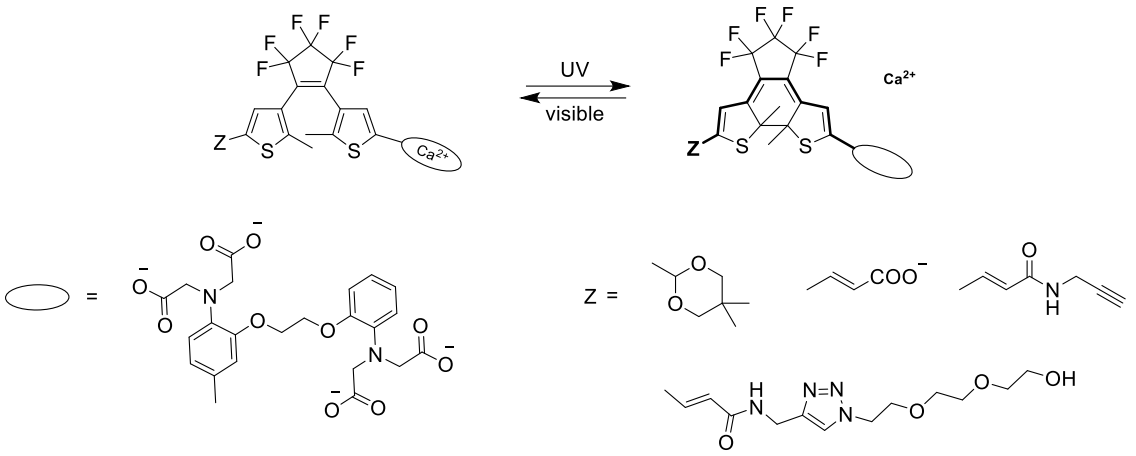

Figure 1-24 The 1,2-*bis* (2-aminophenoxy) ethane-*N,N,N′,N′*-tetra acetic acid (BAPTA) group attached to the diarylethene molecule chelates calcium ions in the ring-open isomer. Photocyclization lowers the electron density of BAPTA and reduces the chelation strength.

Plaza and coworkers synthesized a diarylethene photoswitch with a calcium-chelating 1,2-*bis* (2-*a*minophenoxy) ethane-*N,N,N′,N′*-tetra acetic acid (BAPTA) group on one thiophene and an electron-withdrawing group on the other.[44] The two groups are insulated in the ring-open isomer, and the BAPTA group can freely chelate calcium ions. Photocyclization allows intramolecular charge transfer between the electron-withdrawing group and the nitrogen atom of the BAPTA group, which reduces calcium ion binding by 3-4 times.

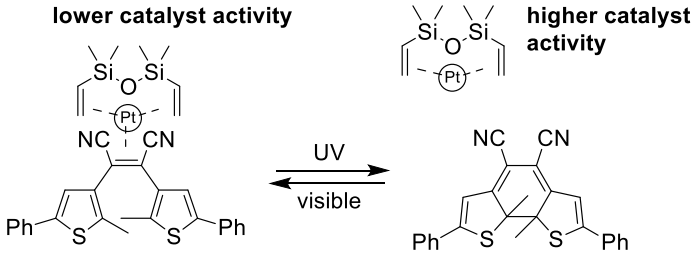

Figure 1-25 The ethylene bridge in the ring-open isomer can bind with the platinum, reducing the catalytic activity. On the other hand, the *ring-closed* isomer cannot bind similarly, and the catalytic activity is unaffected.

Branda and coworkers displayed control of Karstedt's catalyst, which is used for the hydrosilylation reactions, with the dicyano-diarylethene photoswitch.[45] The ring-open isomer includes an electron-deficient double bond because of the electron-withdrawing effect of the cyano groups. Thus, the ring-open isomer can bind with the platinum center

of Karstedt's catalyst through the double bond, reducing the catalytic activity. The double bond is absent in the ring-closed isomer, and the diarylethene photoswitch cannot bind to the catalyst. Thus, the catalytic activity of the hydrosilylation reaction using Karstedt's catalyst can be controlled by visible light.

1.7. Chemistry Gated Photochemistry

Just as light and photochromism can regulate chemical reactivity, chemists have used chemical reactions to control or gate the photochromism of photochromic molecules. A photoinactive molecule undergoes a physical or chemical interaction with a stimulus that activates its photochromic behavior.

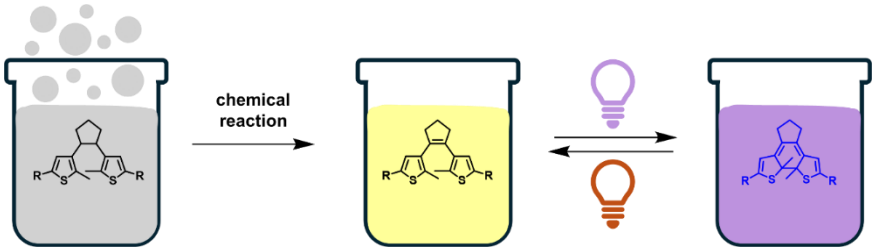

Figure 1-26 Gated photochemistry approach where a chemical event unlocks the photochromism of the molecule.

1.7.1. Modulation Using Geometric Effects

As previously mentioned, the ring-open isomer of diarylethene photoswitches exists in two conformations, i.e., the photoinactive *parallel* conformation and the photoactive *antiparallel* conformation. The molecule can be locked in the parallel conformation via covalent or non-covalent interactions to design a chemical reactivity-gated diarylethene photoswitch. A chemical reaction to break those interactions will allow the diarylethene photoswitch to acquire the photoactive *antiparallel* conformation and unlock the photochemistry of the molecule. This, the photochemistry of the molecule, can be used to indicate whether and to what extent a chemical reaction has occurred.

Irie and coworkers developed diarylethene photoswitches with carboxyl alkyl groups on the benzothiophene rings across the perfluorocyclopentene ring.[46–48] In non-polar solvents, the diarylethene photoswitch displayed no photochromic behavior as the two rings were locked in the photoinactive *parallel* conformation through hydrogen

bonding between the carboxylic acid groups. Adding a polar solvent like ethanol or propylamine or heating the solution to 100° C breaks the hydrogen bonds and unlocks the diarylethene photoswitch towards photocyclization.

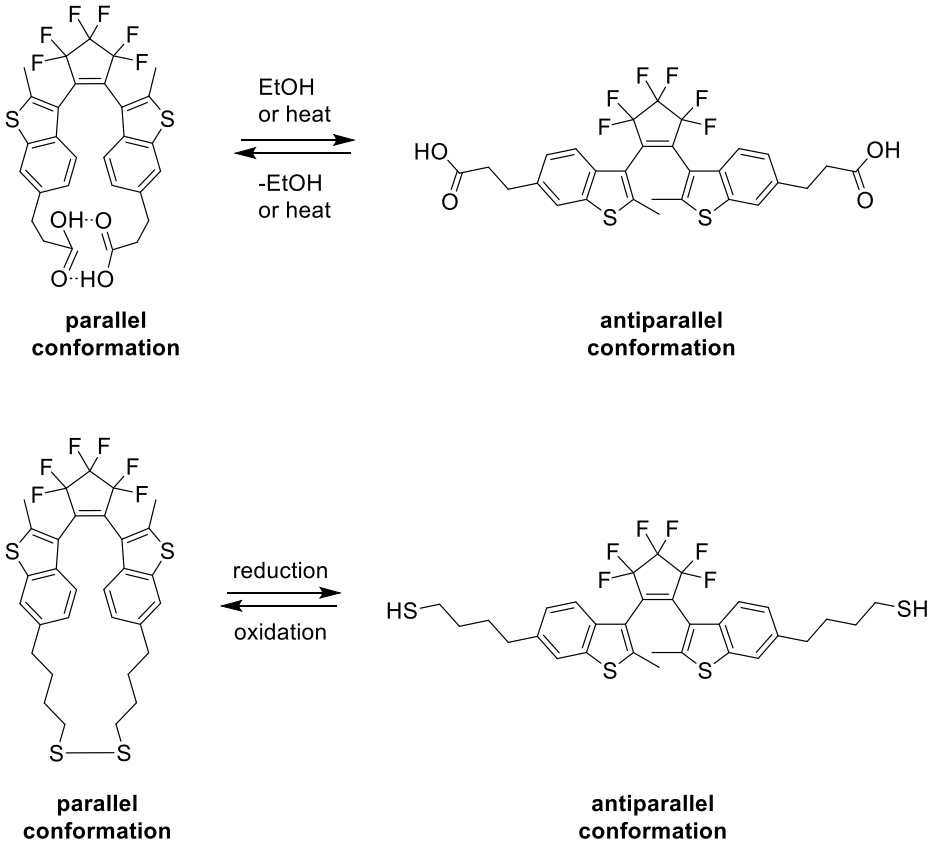

Figure 1-27 The ring-open isomer of the diarylethene molecule locked in the *parallel* conformation by hydrogen bonds in the carboxylic acid derivative and by sulfide bonds in the thiol derivative. Adding a polar solvent or heat to the carboxylic acid derivative breaks the hydrogen bonds. It allows the ring-open isomer to acquire the photocyclizable *antiparallel* conformation, unlocking the photochromism. The oxidation-reduction cycle does the same with the thiol derivative.

In a similar work, a disulfide bond locked a diarylethene photoswitch in a *parallel* conformation.[47] Adding a reducing agent breaks the disulfide bond into thiols, unlocking the molecule's photochromism. Oxidation of the thiols reproduces the disulfide bridges, making the diarylethene molecule photoinactive.

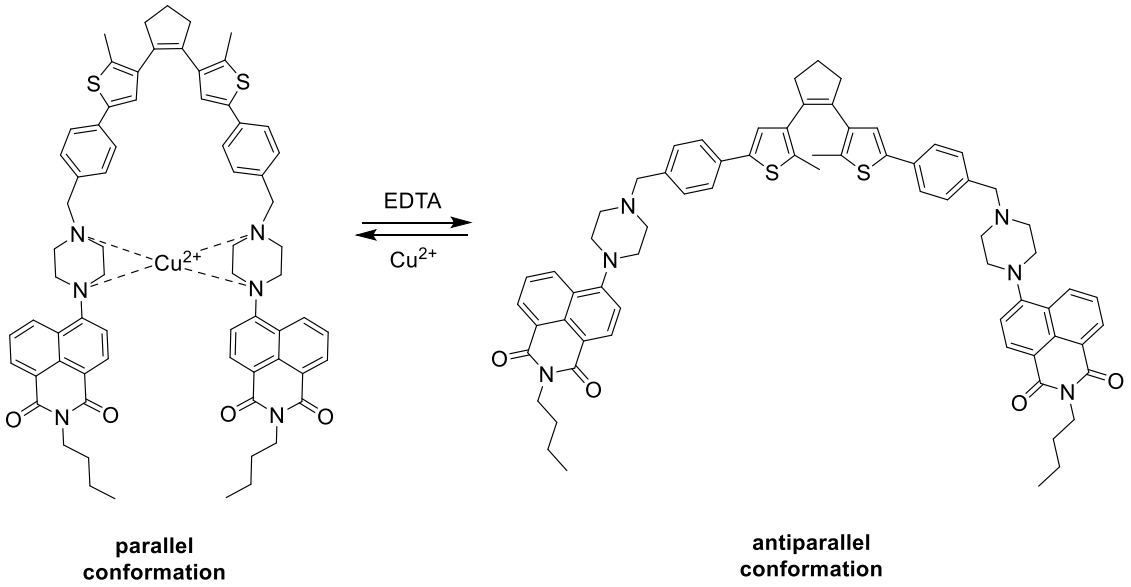

Figure 1-28 The *parallel* conformation of the ring-open isomer can bind to the copper ions through the piperazine groups on the two arms. EDTA chelates the copper ions and unlocks the photochromic behavior of the diarylethene photoswitch.

Tian and coworkers synthesized a diarylethene photoswitch with piperazene-1,8-naphthalimide substitutions as a multi-stimulus device.[49] In the presence of copper ions, the photocyclization process of the ring-open isomer is turned off. The diarylethene photoswitch acquires the *parallel* conformation by coordinating copper ions with the two piperazine units. Adding EDTA, a chelating agent, removes the copper ions from the complex and unlocks the photochromism of the diarylethene molecule. Furthermore, the protonation/deprotonation of the piperazine groups controlled the fluorescent behavior of the diarylethene molecule.

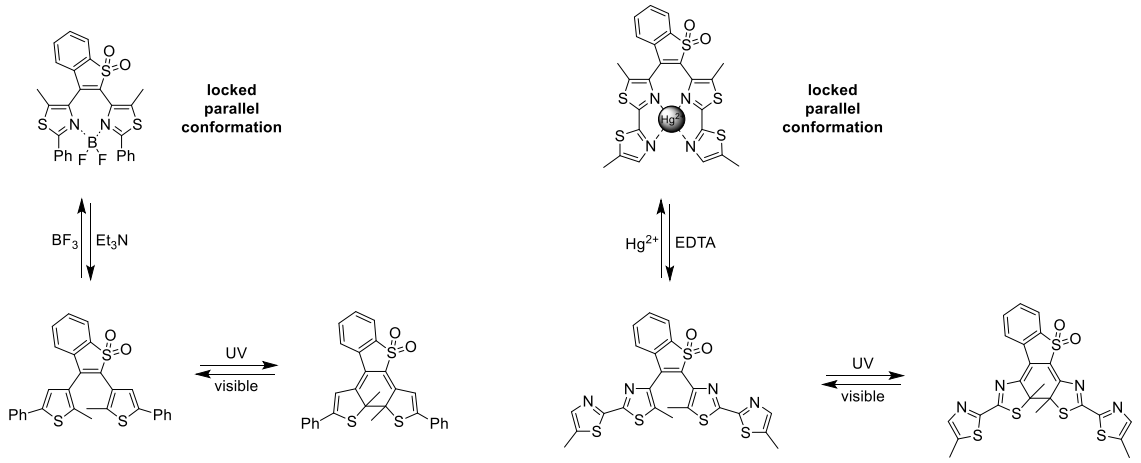

Figure 1-29 Left- Boron trifluoride binds to the nitrogen atoms of the thiazole rings in the *parallel* conformation, locking the photochromic behavior of the diarylethene molecule. Right- Mercury ion is bound to the nitrogen atoms of the thiazole rings in the non-photochromic *parallel* conformation.

Zhu and coworkers created a diarylethene photoswitch that displayed gated photochromism controlled by complexation/dissociation with BF_3.[50] The design of the molecule consisted of thiazole rings attached to the 2- and 3-positions of the benzo[b]thiophene-1,1-dioxide central ring. Addition of $BF_3.Et_2O$ results in locking the photochromic behavior of the diarylethene molecule as BF_3 coordinates to the nitrogen of the thiazole rings. This coordination is only possible in the photo-inactive *parallel* conformation. The photochromic behavior of the molecule is unlocked by adding Et_3N. When Li and coworkers replaced the phenyl group with another thiazole unit, the system displayed reversible binding to mercury ions.[51] The mercury ion coordinates with the nitrogen atoms of the four thiazole groups in the photo-inactive *parallel* conformation. Chelation of the Hg^{2+} with EDTA allows the diarylethene photoswitch to acquire the photoactive *antiparallel* conformation.

1.7.2. Modulation Using Bond Rearrangement

At the core of the ring-open isomer of diarylethene photoswitch is a 1,3,5-hexatriene system that undergoes a conrotatory photocyclization process to yield a ring-closed isomer with a 1,3-cyclohexadiene core. Alterations can be made to the hexatriene or cyclohexadiene systems to control the photocyclization and cycloreversion processes. A chemical reaction is necessary to install the hexatriene or cyclohexadiene core and unlock the photochromic behavior typical of diarylethene photoswitches.

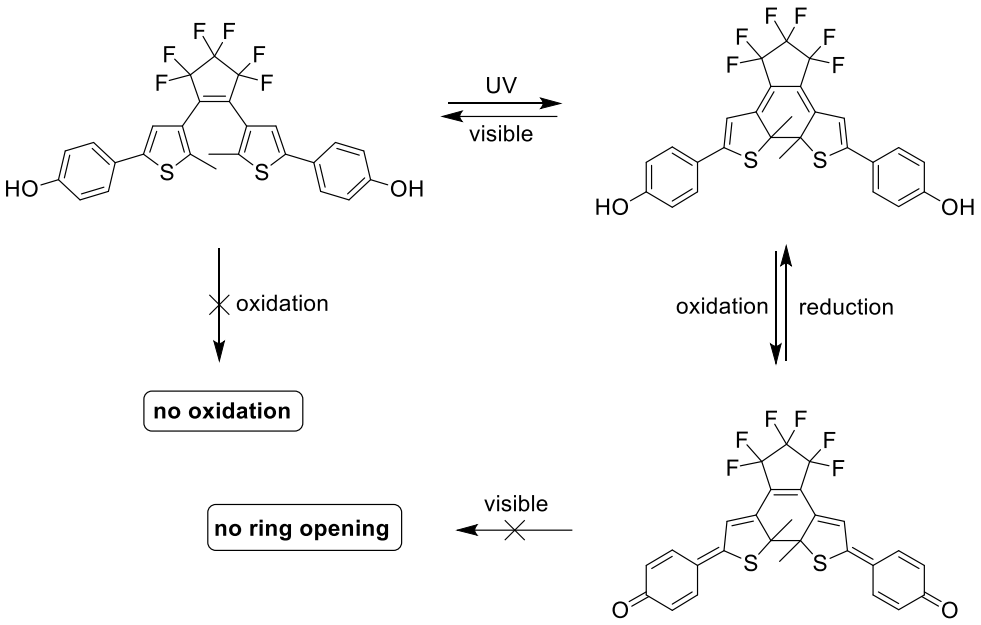

Figure 1-30 The phenol groups in the *ring-closed* isomer oxidize to the non-photochromic quinoid form.

Lehn and coworkers demonstrated a *bis*phenol diarylethene photoswitch, which generally undergoes photocyclization and cycloreversion reactions.[52,53] In the ring-open isomer, the two phenol groups are electronically insulated and, therefore, not reactive towards a redox reaction. The phenol groups are linked through the extended conjugation in the ring-closed isomer. Oxidation of the ring-closed isomer leads to the formation of a quinoid form, which disrupts the cyclohexadiene core. This quinoid form does not undergo a cycloreversion reaction with visible light until a reduction reaction regenerates the cyclohexadiene core.

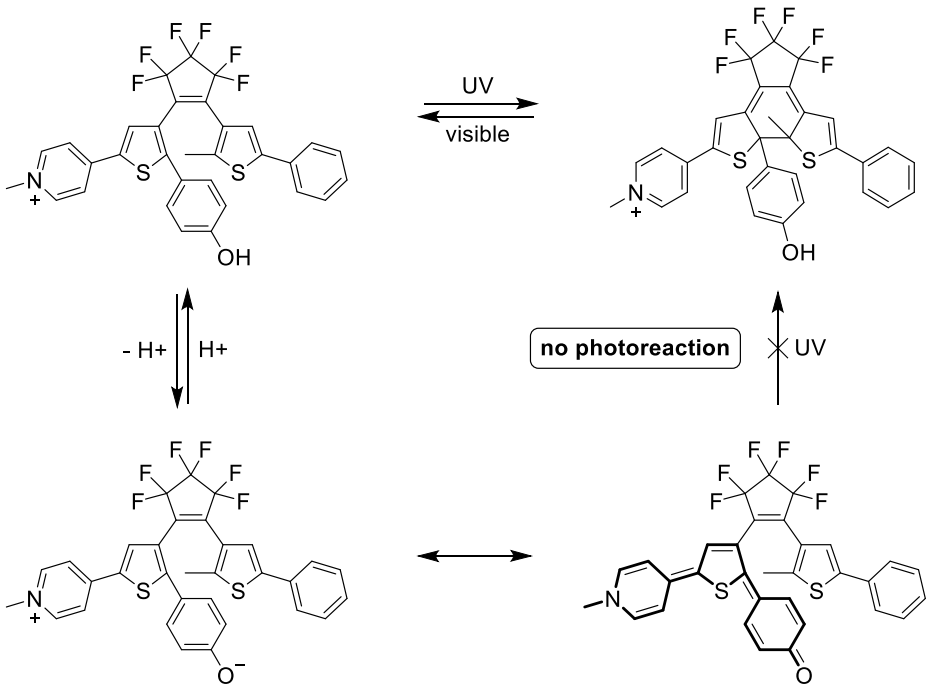

Figure 1-31 Deprotonation of the phenol proton forms a quinoid-type structure in the ring-open isomer. The absence of the 1,3,5-hexatriene system makes the molecule non-photochromic.

Irie and coworkers observed a similar behavior with the diarylethene photoswitch discussed previously.[39] At high pH, the deprotonated form of the ring-open isomer changes to a quinoid-type structure, disrupting the thiophene unit's aromaticity. The ring-open isomer no longer possesses a 1,3,5—hexatriene system, and the molecule cannot photocyclize.

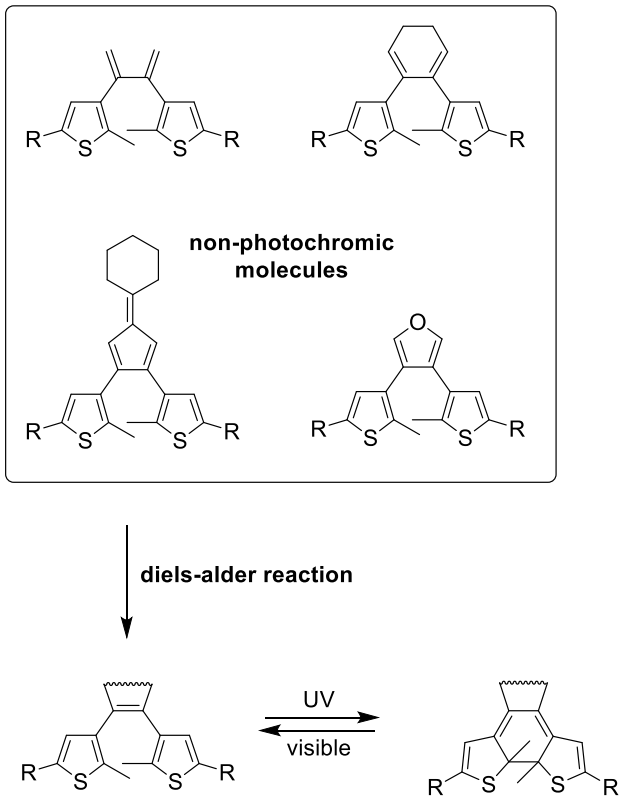

Figure 1-32 Non-photochromic pro-diarylethene derivatives with the central ethene group replaced with 1,3-butadiene, cyclohexadiene, fulvene, or furan. The Diels-Alder reaction on the top ring establishes the 1,3,5-hexatriene system and unlocks the photochromic behavior.

Branda and coworkers synthesized four different pro-diarylethene molecules gated by [4 + 2] cycloaddition reactions. The first molecule was a butadiene derivative that did not contain the necessary hexatriene system for photocyclization.[54] A Diels-Alder reaction with maleic anhydride installed the hexatriene core and unlocked the photocyclization process. A cyclohexadiene derivative was prepared to remove the rotational freedom of the butadiene group.[54] The cyclohexadiene derivative reacted with maleic anhydride similarly to the previous molecule, but at a lower temperature. Based on the same concept, fulvene-based[55] and furan-based[56] pro-diarylethene molecules were synthesized, displaying similar [4 + 2] cycloaddition reactions with dienes to unlock the photochromic behavior.

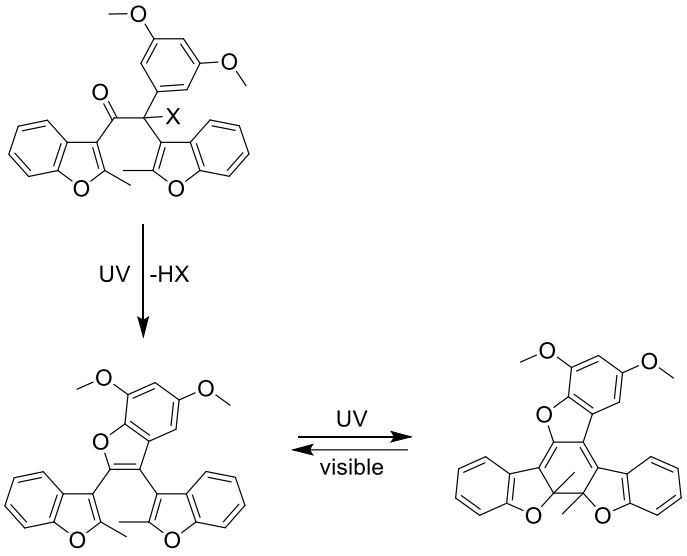

Figure 1-33 A pro-diarylethene molecule with a photocleavable group is located at the bridge between the two benzofuran groups.

Branda and coworkers designed a benzofuran-based pro-diarylethene molecule possessing a dimethoxy benzoin photocage at the bridging unit.[57] The molecule does not have the hexatriene system typical of diarylethene molecules. However, irradiation with UV light leads to photo release of acetic acid, followed by the formation of dimethoxybenzofuran at the central ring. The photocleavage reaction forms the necessary hexatriene system, and the diarylethene molecule undergoes a photocyclization reaction.

Robb and coworkers developed a cyclopentadiene-based diarylethene photoswitch that polymerized with maleimide and changed into a photo-inert pro-diarylethene.[58] Due to the absence of a hexatriene core, no photocyclization reaction was observed with UV light irradiation of the diarylethene-maleimide adduct-based polymer. Mechanical force on the polymer leads to the retro Diels-Alder reaction, creating the hexatriene core for the photocyclization reaction.

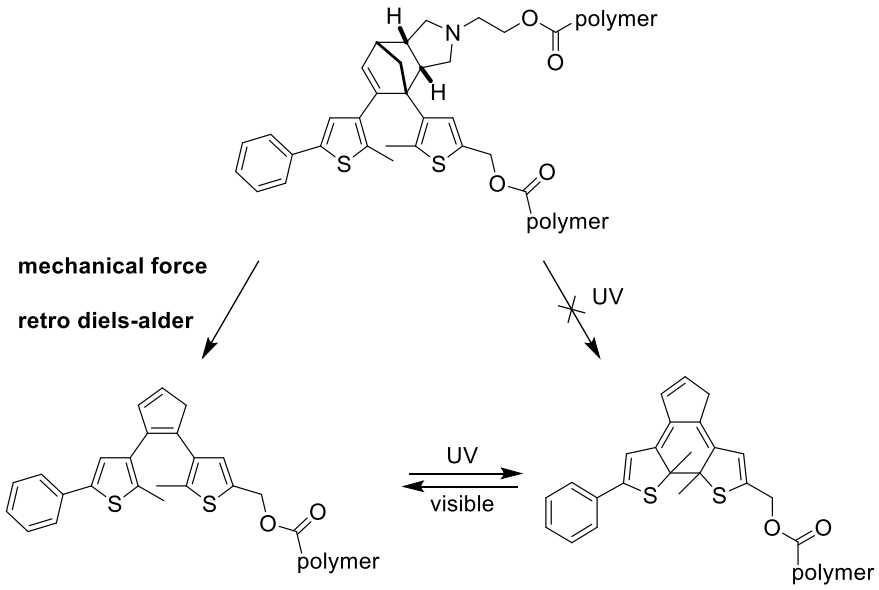

Figure 1-34 The Diels-Alder adduct of the diarylethene molecule is non-photochromic due to the lack of a 1,3,5-hexatriene system. Applying mechanical force leads to a retro Diels-Alder reaction, establishing the hexatriene system and unlocking the photochromic behavior.

1.7.3. Modulation using other effects

As mentioned in Section 1, the excited species can release the absorbed energy via multiple pathways to return to the ground state. These pathways compete with each other depending on the structure of the molecule. Several studies have been conducted on the diarylethene molecules where a competing relaxation process quenches the photochromism process.

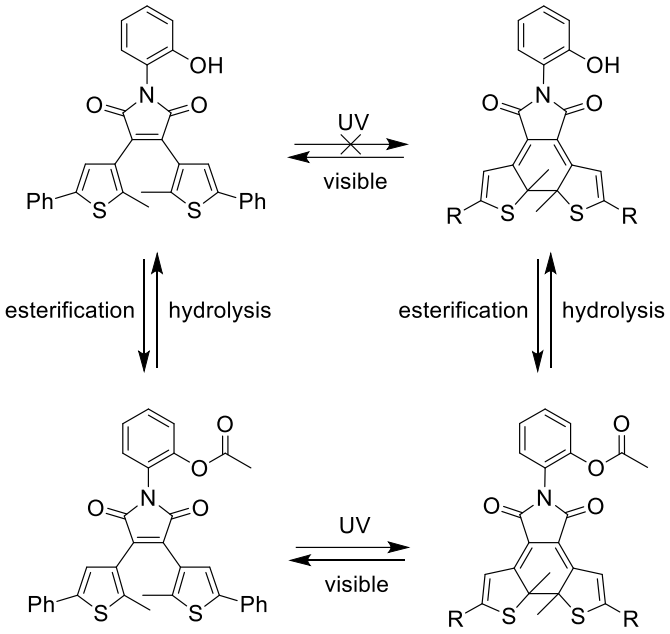

Figure 1-35 Intramolecular proton transfer between the phenol and the maleimide ring inhibits the photochromism of the molecule. Esterification of the phenol ring unlocks the photochromic behavior of the diarylethene photoswitch.

Irie and coworkers synthesized a modified N-(o-hydroxyphenyl) maleimide central ring-based diarylethene molecule.[59] The ring-open isomer of this molecule does not undergo the photocyclization reaction because of the intramolecular proton transfer from the phenol to the oxygen atom of the maleimide carbonyl group. Esterification of the phenol hydroxyl group by a carboxylic acid (acetic anhydride in this case) eliminates the proton transfer process. The formation of the ester derivative unlocks the photochromic behavior of the diarylethene photoswitch.

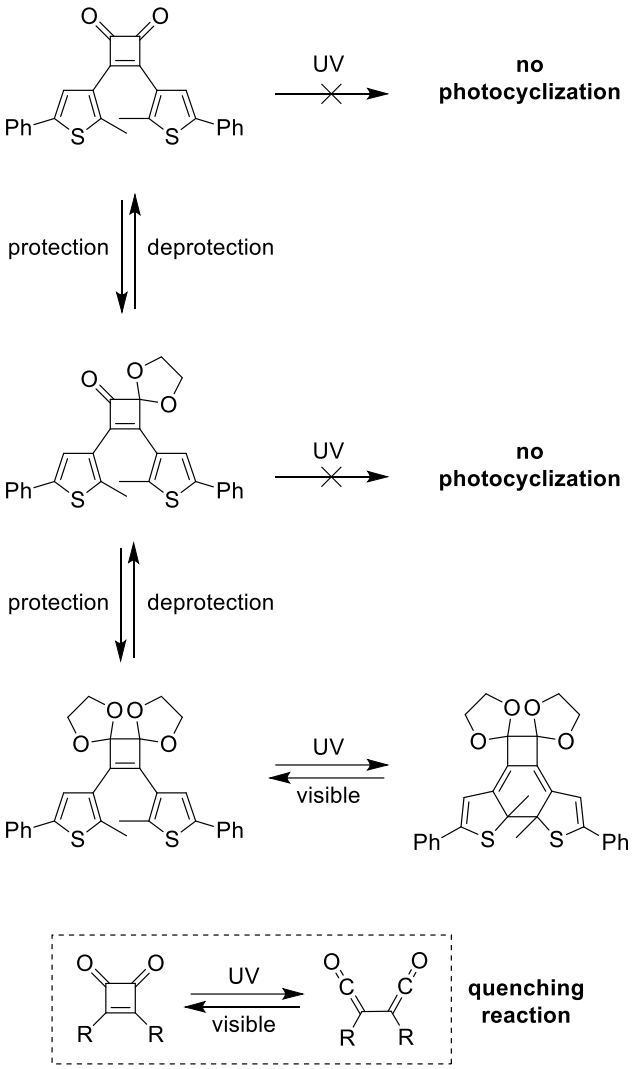

Figure 1-36 Irradiation with UV light leads to the ring-opening of the cyclobutene-1,2-dione ring, thereby quenching the photocyclization process. The reaction of both ketones with diols stops the ring-opening process of the cyclobutene-1,2-dione and unlocks the diarylethene's photochromic behavior.

Belser and coworkers designed a diarylethene molecule with a cyclobutene-1,2-dione ring at the center.[60] No photocyclization was observed upon irradiation of the ring-open isomer with UV light. Instead, a photochemical ring opens up in the cyclobutene ring to 1,2-*bis*ketene, which thermally reverts to the cyclobutene quickly. The reaction of one ketone group with diol did not result in unlocking the photochromic behavior of the molecule. However, the reaction of both ketones with diols suppressed the photochemical ring opening of cyclobutene and unlocked the photochromism of the diarylethene photoswitch.

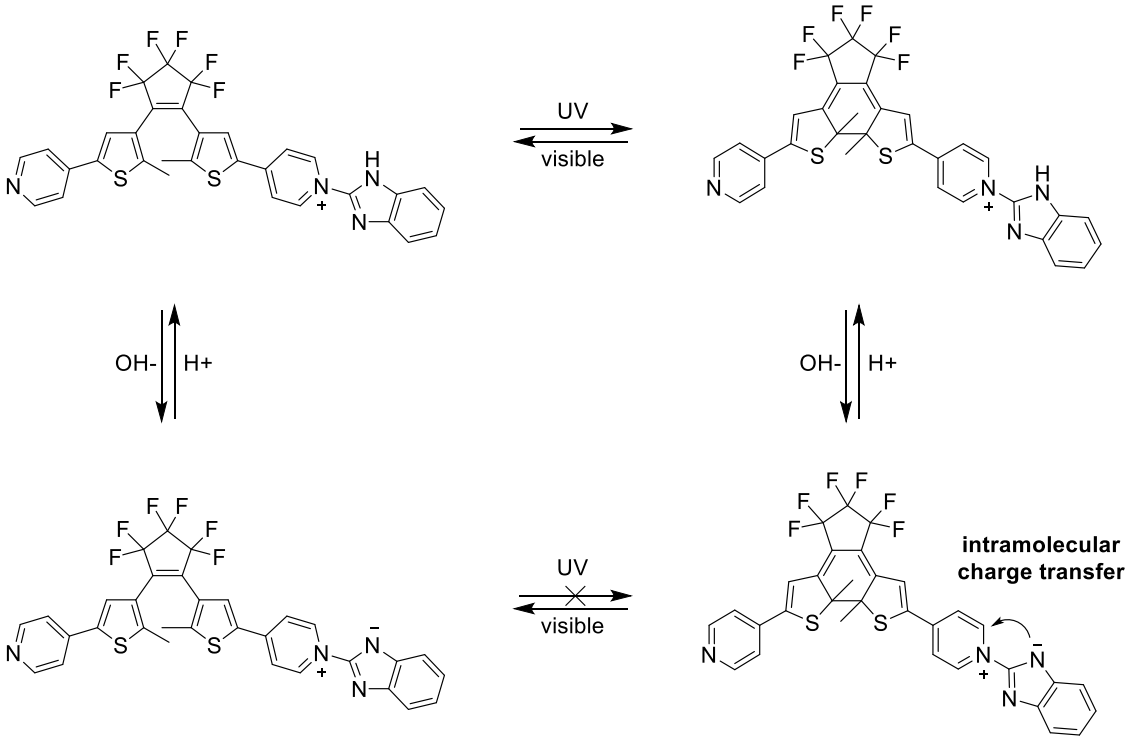

Figure 1-37 Addition of a base deprotonates the nitrogen atom on the benzoimidazole ring, thereby creating a zwitterionic structure. Intramolecular charge transfer locks the photocyclization process of the diarylethene photoswitch.

Zhang and coworkers synthesized two diarylethene photoswitches with pyridinium betaines, one unsymmetrical and the other symmetrical.[61] Both molecules displayed photochromic behavior typical of diarylethene molecules at low pH values. Under basic conditions, deprotonation occurs, thereby creating a zwitterionic moiety. The molecule's photochromic behavior is switched off due to intramolecular charge transfer between the benzimidazole ring and the pyridine ring of the betaine.

1.8. Colorimetric Probes Based on Diarylethene Photoswitches

Devices that detect and analyze the presence of a given chemical species through a physical interaction or a chemical reaction are called chemical sensors. When these interactions or reactions between the sensor and the analyte leads to a change in color as a readout signal, the type of chemical sensor is called a colorimetric sensor. As previously mentioned, photochromic molecules like DTEs exhibit color change between

the two forms on light exposure; thus, this property has been utilized for detecting and sensing chemical species.

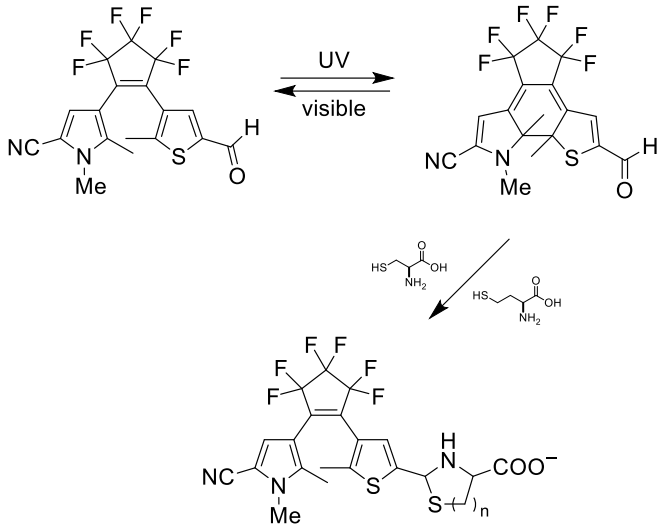

Figure 1-38 Spontaneous cycloreversion of the *ring-closed* isomer of the diarylethene photoswitch occurs in the presence of cysteine and homocysteine. The turquoise to pale yellow color change indicates the presence of cysteine and homocysteine.

Using a formyl group-containing diarylethene photoswitch, Zheng and coworkers synthesized a colorimetric sensor for thiols, cysteine, and homocysteine.[62] The diarylethene molecule demonstrated reversible photocyclization behavior in DMSO solution and PMMA films. Adding cysteine and homocysteine to the colored ring-closed isomer resulted in a rapid color change from turquoise to pale yellow. Cysteine and homocysteine react with the formyl group of the diarylethene photoswitch to form thiazolidines. The authors stated that this reaction increases the diarylethene molecule's thermochromic behavior, and the ring-closed isomer's thermal cycloreversion spontaneously leads to a color change.

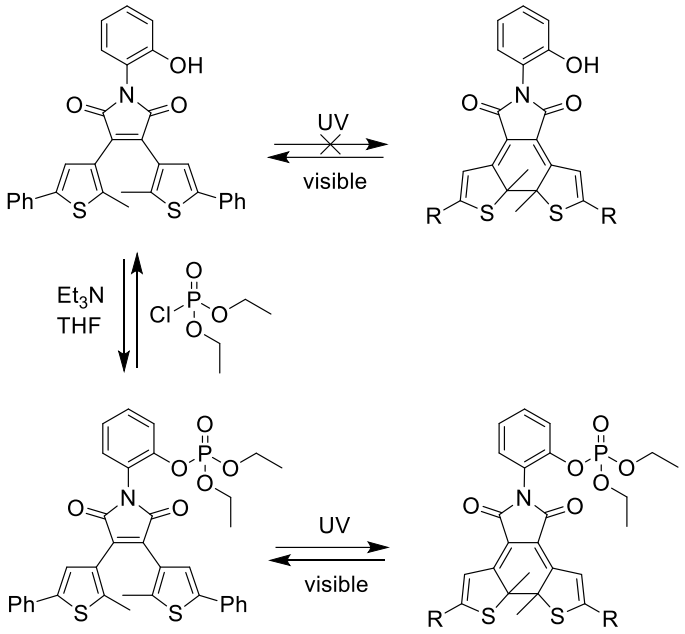

Figure 1-39 The formation of phosphate esters unlocks the diarylethene photoswitch's photochromic behavior. The color change upon UV light irradiation indicates the presence of an organophosphate group like sarin.

Branda and coworkers developed a naked-eye detection system for organophosphorus nerve agents using the *N*-(o-hydroxyphenyl) maleimide diarylethene molecule previously reported by Irie and coworkers.[63] The diarylethene molecule is non-photochromic due to the competing intramolecular proton transfer of the phenolic hydrogen to the maleimide ring. Exposure to organophosphates leads to the formation of phosphate esters with the phenol, unlocking the diarylethene molecule's photochromic behavior.

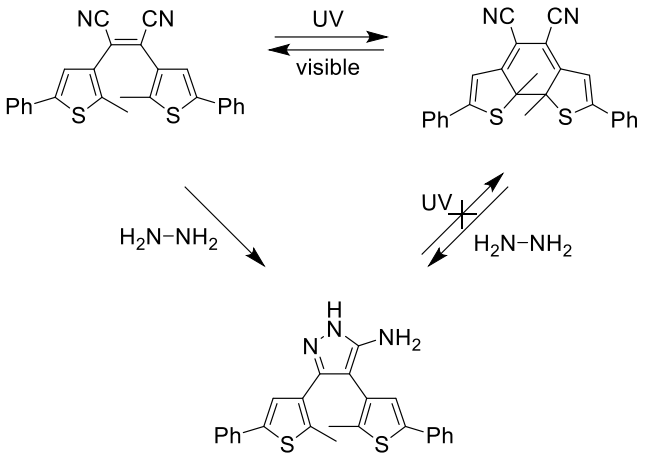

Figure 1-40 Photochromic behavior of the *bis*cyano diarylethene photoswitch is stopped in the presence of hydrazine.

Branda and coworkers reported a diarylethene photoswitch-based probe that combined the colorimetric and fluorescence-based approaches to detecting hydrazine in solution and the vapor phase.[64] The working principle behind this study is the reaction of cyanoethylene with hydrazine to yield aminopyrazoles. When the ring-open and ring-closed isomers of the cyano-diarylethene were treated with hydrazine, a non-photochromic aminopyrazole diarylethene molecule was obtained. The blue color of the ring-closed isomer disappeared, and at the same time, an increase in the fluorescence emission was observed.

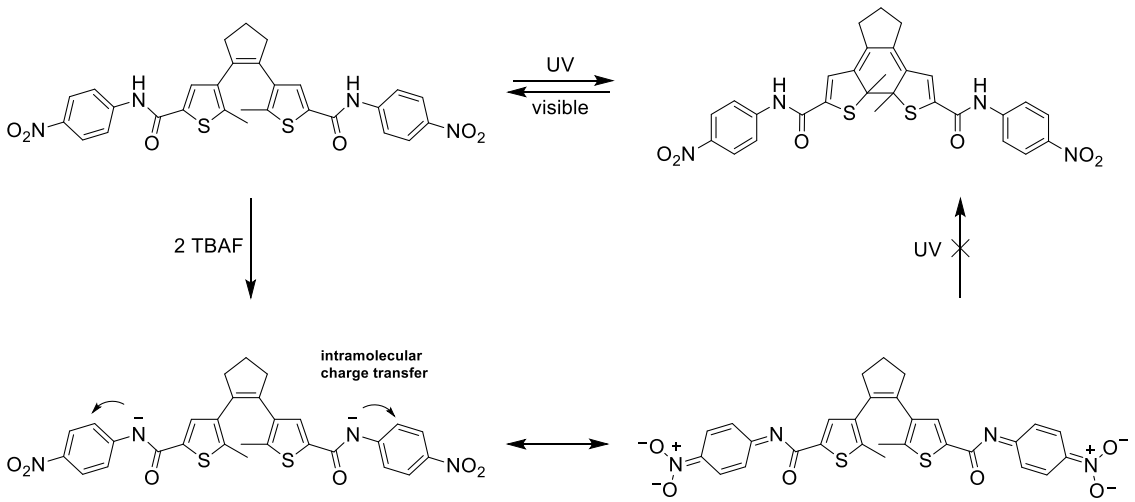

Figure 1-41 Fluoride ions deprotonate the amide nitrogen, leading to intramolecular charge transfer, which stops the photochromic behavior of the diarylethene photoswitch. The ring-open and the *ring-closed* isomers changed color to deep yellow upon adding fluoride ions.

Li and coworkers demonstrated the selective detection of fluoride ions based on an amide diarylethene photoswitch.[65] The addition of excess tetrabutylammonium fluoride salt to the DMSO solution of the ring-open isomer of the amide diarylethene resulted in a color change of the solution from colorless to deep yellow. Similar observations were made with the ring-closed isomer, where the addition of fluoride led to a color change from purple to deep yellow. The authors attributed the color change upon adding fluoride to the charge-transfer interactions between the electron-poor p-nitrophenyl and electron-rich diarylethene groups.

1.9. Thesis Overview

The research detailed in this thesis explores the idea of chemically gated photochromism of diarylethene photoswitches. It focuses on the design, synthesis, characterization, and testing of these gated systems. The end goal of developing such systems is their applicability as sensors and detectors for small molecules of biological and environmental significance.

Chapter 2 of the thesis focuses on detecting reactive oxygen species or, more specifically, singlet oxygen with a pro-diarylethene molecule. Singlet oxygen is a reactive oxygen species and plays both a constructive and destructive role in numerous natural and synthetic processes. A furan-based derivative of the pro-diarylethene molecule was designed and synthesized, but it cannot undergo the photocyclization process due to the absence of the 1,3,5-hexatriene system. The Diels-Alder reaction between furan and singlet oxygen generates the necessary structure for the photocyclization of the diarylethene photoswitch to proceed with UV light. The color change of the solution indicates the presence of singlet oxygen.

In Chapter 3, diarylethene analogues of Hendrickson’s reagent were designed and synthesized to detect 1) alcohols, 2) moisture in organic solvents, and 3) the extent of the esterification reaction. The Hendrickson’s reagent is an alternative to the Mitsunobu reaction and is used mainly for the esterification reaction of carboxylic acids and alcohols. Two phosphine oxide molecules react in the presence of triflic anhydride to form phosphorus-oxygen-phosphorus bonds that are highly reactive to oxygen nucleophiles. In the diarylethene molecule, Hendrickson’s reagent is formed by the intramolecular reaction of two phosphine oxides in the non-photoactive *parallel*

conformation. The covalent phosphorus-oxygen-phosphorus bonds gate the photocyclization reaction until an oxygen nucleophile, such as alcohol or water, breaks one of the phosphorus-oxygen bonds. This bond breakage allows the diarylethene photoswitch to acquire the photochromic *antiparallel* conformation, and a color change is observed when UV light is irradiated.

Chapter 4 of the thesis discusses the gated photochromic systems based on the hydrogen bonds between complementary nucleobases. The project's central idea was to detect nucleic acids by a toehold-mediated strand displacement in a diarylethene photoswitch. A diarylethene photoswitch was designed to bind across a mismatched DNA duplex in the non-photoactive *parallel* conformation. A more complementary strand will break the duplex via toehold-mediated strand displacement, allowing the diarylethene photoswitch to acquire the photoactive *antiparallel* conformation. Irradiation with UV light will lead to a color change, indicating the presence of the target strand. A proof-of-concept model was designed and synthesized based on adenine and uridine nucleobases, and the system was studied as an auxiliary to the DNA duplex-based scheme.

1.10. References

(1) Coyle, J. D. Introduction to Organic Photochemistry; John Wiley & Sons, 1991.

(2) Rohatgi-Mukherjee, K. K. Fundamentals of Photochemistry; New Age International, 1978.

(3) Barltrop, J. A.; Coyle, J. D. Excited States in Organic Chemistry; Wiley, 1975.

(4) Wang, F.; Liu, X. Upconversion Multicolor Fine-Tuning: Visible to Near-Infrared Emission from Lanthanide-Doped NaYF4 Nanoparticles. J. Am. Chem. Soc. 2008, 130 (17), 5642–5643. https://doi.org/10.1021/ja800868a.

(5) Göstl, R.; Senf, A.; Hecht, S. Remote-Controlling Chemical Reactions by Light: Towards Chemistry with High Spatio-Temporal Resolution. Chem. Soc. Rev. 2014, 43 (6), 1982–1996. https://doi.org/10.1039/C3CS60383K.

(6) Marzo, L.; Pagire, S. K.; Reiser, O.; König, B. Visible-Light Photocatalysis: Does It Make a Difference in Organic Synthesis? Angew. Chem. Int. Ed. 2018, 57 (32), 10034–10072. https://doi.org/10.1002/anie.201709766.

(7) Strieth-Kalthoff, F.; Glorius, F. Triplet Energy Transfer Photocatalysis: Unlocking the Next Level. Chem 2020, 6 (8), 1888–1903. https://doi.org/10.1016/j.chempr.2020.07.010.

(8) Turro, N. J. *Modern Molecular Photochemistry*; University Science Books, 1991.

(9) Balzani, V.; Ceroni, P.; Juris, A. Photochemistry and Photophysics: Concepts, Research, Applications; John Wiley & Sons, 2024.

(10) Brown, G. H. Photochromism; Wiley-Interscience, 1971.

(11) Crano, J. C.; Guglielmetti, R. J. Organic Photochromic and Thermochromic Compounds: Volume 1: Photochromic Families; Springer Science & Business Media, 1999.

(12) New Frontiers in Photochromism; Irie, M., Yokoyama, Y., Seki, T., Eds.; Springer Japan: Tokyo, 2013. https://doi.org/10.1007/978-4-431-54291-9.

(13) Bouas-Laurent, H.; Durr, H. Photochromism: Molecules and Systems; Elsevier Amsterdam, 2003.

(14) Hartley, G. S. The Cis-Form of Azobenzene. Nature 1937, 140 (3537), 281–281. https://doi.org/10.1038/140281a0.

(15) Fischer, E.; Hirshberg, Y. Formation of Coloured Forms of Spirans by Low-Temperature Irradiation. Journal of the Chemical Society, 1952, 4522–4524.

(16) Chu, N. Y. C. Photochromism of spiroindolinonaphthoxazine. I. Photophysical properties. Can. J. Chem. 1983, 61 (2), 300–305. https://doi.org/10.1139/v83-054.

(17) Heller, H. G.; Oliver, S. Photochromic Heterocyclic Fulgides. Part 1. Rearrangement Reactions of (E)-α-3-Furylethylidene(Isopropylidene)Succinic Anhydride. J Chem Soc Perkin Trans 1 1981, No. 0, 197–201. https://doi.org/10.1039/P19810000197.

(18) Irie, M.; Mohri, M. Thermally Irreversible Photochromic Systems. Reversible Photocyclization of Diarylethene Derivatives. J. Org. Chem. 1988, 53 (4), 803–808. https://doi.org/10.1021/jo00239a022.

(19) Irie, M. Diarylethene Molecular Photoswitches: Concepts and Functionalities; Wiley-VCH: Weinheim, 2021.

(20) Hanazawa, M.; Sumiya, R.; Horikawa, Y.; Irie, M. Thermally Irreversible Photochromic Systems. Reversible Photocyclization of 1,2-*Bis* (2-Methylbenzo[b]Thiophen-3-Yl)Perfluorocyclocoalkene Derivatives. J. Chem. Soc. Chem. Commun. 1992, No. 3, 206–207. https://doi.org/10.1039/C39920000206.

(21) Irie, M. Diarylethenes for Memories and Switches. Chem. Rev. 2000, 100 (5), 1685–1716. https://doi.org/10.1021/cr980069d.

(22) Feringa, B. L. Molecular Switches, 2nd ed.; John Wiley & Sons, Incorporated: Hoboken, 2011.

(23) Nakamura, S.; Irie, M. Thermally Irreversible Photochromic Systems. A Theoretical Study. J. Org. Chem. 1988, 53 (26), 6136–6138. https://doi.org/10.1021/jo00261a035.

(24) Tian, H.; Yang, S. Recent Progresses on Diarylethene Based Photochromic Switches. Chem. Soc. Rev. 2004, 33 (2), 85–97. https://doi.org/10.1039/B302356G.

(25) Matsuda, K.; Irie, M. Diarylethene as a Photoswitching Unit. J. Photochem. Photobiol. C Photochem. Rev. 2004, 5 (2), 169–182. https://doi.org/10.1016/j.jphotochemrev.2004.07.003.

(26) Nakamura, S.; Yokojima, S.; Uchida, K.; Tsujioka, T.; Goldberg, A.; Murakami, A.; Shinoda, K.; Mikami, M.; Kobayashi, T.; Kobatake, S.; Matsuda, K.; Irie, M. Theoretical Investigation on Photochromic Diarylethene: A Short Review. J. Photochem. Photobiol. Chem. 2008, 200 (1), 10–18. https://doi.org/10.1016/j.jphotochem.2008.05.005.

(27) Yam, V. W.-W.; Ko, C.-C.; Zhu, N. Photochromic and Luminescence Switching Properties of a Versatile Diarylethene-Containing 1,10-Phenanthroline Ligand and Its Rhenium(I) Complex. J. Am. Chem. Soc. 2004, 126 (40), 12734–12735. https://doi.org/10.1021/ja047446q.

(28) Jong, J. J. D. de; Lucas, L. N.; Hania, R.; Pugzlys, A.; Kellogg, R. M.; Feringa, B. L.; Duppen, K.; Esch, J. H. van. Photochromic Properties of Perhydro- and Perfluorodithienylcyclopentene Molecular Switches. Eur. J. Org. Chem. 2003, 2003 (10), 1887–1893. https://doi.org/10.1002/ejoc.200200719.

(29) Higashiguchi, K.; Matsuda, K.; Kobatake, S.; Yamada, T.; Kawai, T.; Irie, M. Fatigue Mechanism of Photochromic 1,2-*Bis*(2,5-Dimethyl-3-Thienyl)Perfluorocyclopentene. Bull. Chem. Soc. Jpn. 2000, 73 (10), 2389–2394. https://doi.org/10.1246/bcsj.73.2389.

(30) Taniguchi, H.; Shinpo, A.; Okazaki, T.; Matsui, F.; Irie, M. Photodegradation Mechanism of Photochromic Diarylethene Derivatives. Nippon Kagaku Kaishi 1992, No. 10, 1138–1140. https://doi.org/10.1246/nikkashi.1992.1138.

(31) Kodani, T.; Matsuda, K.; Yamada, T.; Kobatake, S.; Irie, M. Reversible Diastereoselective Photocyclization of a Diarylethene in a Single-Crystalline Phase. J. Am. Chem. Soc. 2000, 122 (40), 9631–9637. https://doi.org/10.1021/ja001350o.

(32) Takeshita, M.; Uchida, K.; Irie, M. Novel Saccharide Tweezers with a Diarylethene Photoswitch. Chem. Commun. 1996, No. 15, 1807. https://doi.org/10.1039/cc9960001807.

(33) Takeshita, M.; Irie, M. Photoresponsive Tweezers for Alkali Metal Ions. Photochromic Diarylethenes Having Two Crown Ether Moieties. J. Org. Chem. 1998, 63 (19), 6643–6649. https://doi.org/10.1021/jo980290q.

(34) Kawai, S. H. Photochromic *Bis*(Monoaza-Crown Ether)s. Alkali-Metal Cation Complexing Properties of Novel Diarylethenes. Tetrahedron Lett. 1998, 39 (25), 4445–4448. https://doi.org/10.1016/S0040-4039(98)00843-0.

(35) Mulder, A.; Jukovic, A.; N. Lucas, L.; Esch, J. van; L. Feringa, B.; Huskens, J.; N. Reinhoudt, D. A Dithienylethene-Tethered β-Cyclodextrin Dimer as a Photoswitchable Host. Chem. Commun. 2002, 0 (22), 2734–2735. https://doi.org/10.1039/B208692A.

(36) Sud, D.; Norsten, T. B.; Branda, N. R. Photoswitching of Stereoselectivity in Catalysis Using a Copper Dithienylethene Complex. Angew. Chem. Int. Ed. 2005, 44 (13), 2019–2021. https://doi.org/10.1002/anie.200462538.

(37) Li, Z.; Zhang, C.; Ren, Y.; Yin, J.; Liu, S. H. Amide- and Urea-Functionalized Dithienylethene: Synthesis, Photochromism, and Binding with Halide Anions. Org. Lett. 2011, 13 (22), 6022–6025. https://doi.org/10.1021/ol202491e.

(38) Kawai, S. H.; Gilat, S. L.; Lehn, J.-M. Photochemical *pKa*-Modulation and Gated Photochromic Properties of a Novel Diarylethene Switch. Eur. J. Org. Chem. 1999, 1999 (9), 2359–2366. https://doi.org/10.1002/(SICI)1099-0690(199909)1999:9<2359::AID-EJOC2359>3.0.CO;2-#.

(39) Odo, Y.; Matsuda, K.; Irie, M. *pKa* Switching Induced by the Change in the π-Conjugated System Based on Photochromism. Chem. – Eur. J. 2006, 12 (16), 4283–4288. https://doi.org/10.1002/chem.200501292.

(40) Malval, J.-P.; Gosse, I.; Morand, J.-P.; Lapouyade, R. Photoswitching of Cation Complexation with A Monoaza-Crown Dithienylethene Photochrome. J. Am. Chem. Soc. 2002, 124 (6), 904–905. https://doi.org/10.1021/ja0167203.

(41) Nakashima, T.; Goto, M.; Kawai, S.; Kawai, T. Photomodulation of Ionic Interaction and Reactivity: Reversible Photoconversion between Imidazolium and Imidazolinium. J. Am. Chem. Soc. 2008, 130 (44), 14570–14575. https://doi.org/10.1021/ja802986y.

(42) Samachetty, H. D.; Branda, N. R. Photomodulation of Lewis Basicity in a Pyridine-Functionalized 1,2-Dithienylcyclopentene. Chem. Commun. 2005, No. 22, 2840–2842. https://doi.org/10.1039/B501779C.

(43) Liu, G.; Xu, X.; Chen, Y.; Wu, X.; Wu, H.; Liu, Y. A Highly Efficient Supramolecular Photoswitch for Singlet Oxygen Generation in Water. Chem. Commun. 2016, 52 (51), 7966–7969. https://doi.org/10.1039/C6CC02996E.

(44) Dozova, N.; Pousse, G.; Barnych, B.; Mallet, J.-M.; Cossy, J.; Valeur, B.; Plaza, P. A Novel Diarylethene-Based Photoswitchable Chelator for Reversible Release and Capture of Ca2+ in Aqueous Media. J. Photochem. Photobiol. Chem. 2018, 360, 181–187. https://doi.org/10.1016/j.jphotochem.2018.04.029.

(45) Kaur, B.; Raza, R.; Stashick, M. J.; Branda, N. R. Using Light to Control the Inhibition of Karstedt's Catalyst. Org. Chem. Front. 2019, 6 (8), 1253–1256. https://doi.org/10.1039/C9QO00221A.

(46) Irie, M.; Miyatake, O.; Uchida, K. Blocked Photochromism of Diarylethenes. J. Am. Chem. Soc. 1992, 114 (22), 8715–8716. https://doi.org/10.1021/ja00048a063.

(47) Irie, M.; Miyatake, O.; Sumiya, R.; Hanazawa, M.; Horikawa, Y.; Uchida, K. Photochromism of Diarylethenes With Intralocking Arms. Mol. Cryst. Liq. Cryst. Sci. Technol. Sect. Mol. Cryst. Liq. Cryst. 1994, 246 (1), 155–158. https://doi.org/10.1080/10587259408037805.

(48) Irie, M.; Miyatake, O.; Uchida, K.; Eriguchi, T. Photochromic Diarylethenes with Intralocking Arms. J. Am. Chem. Soc. 1994, 116 (22), 9894–9900. https://doi.org/10.1021/ja00101a010.

(49) Zhang, J.; Tan, W.; Meng, X.; Tian, H. Soft Mimic Gear-Shift with a Multi-Stimulus Modified Diarylethene. J. Mater. Chem. 2009, 19 (32), 5726–5729. https://doi.org/10.1039/B908707A.

(50) Wu, Y.; Chen, S.; Yang, Y.; Zhang, Q.; Xie, Y.; Tian, H.; Zhu, W. A Novel Gated Photochromic Reactivity Controlled by Complexation/Dissociation with BF3. Chem. Commun. 2011, 48 (4), 528–530. https://doi.org/10.1039/C1CC15824D.

(51) Wu, Y.; Zhu, W.; Wan, W.; Xie, Y.; Tian, H.; Li, A. D. Q. Reversible Photoswitching Specifically Responds to Mercury(II) Ions: The Gated Photochromism of *Bis*(Dithiazole)Ethene. Chem. Commun. 2014, 50 (91), 14205–14208. https://doi.org/10.1039/C4CC06372D.

(52) Kawai, S. H.; Gilat, S. L.; Ponsinet, R.; Lehn, J.-M. A Dual-Mode Molecular Switching Device: *Bis*phenolic Diarylethenes with Integrated Photochromic and Electrochromic Properties. Chem. – Eur. J. 1995, 1 (5), 285–293. https://doi.org/10.1002/chem.19950010505.

(53) Kawai, S. H.; Gilat, S. L.; Lehn, J.-M. A Dual-Mode Optical–Electrical Molecular Switching Device. J. Chem. Soc. Chem. Commun. 1994, No. 8, 1011–1013. https://doi.org/10.1039/C39940001011.

(54) Lemieux, V.; Branda, N. R. Reactivity-Gated Photochromism of 1,2-Dithienylethenes for Potential Use in Dosimetry Applications. Org. Lett. 2005, 7 (14), 2969–2972. https://doi.org/10.1021/ol050971p.

(55) Lemieux, V.; Gauthier, S.; Branda, N. R. Selective and Sequential Photorelease Using Molecular Switches. Angew. Chem. Int. Ed. 2006, 45 (41), 6820–6824. https://doi.org/10.1002/anie.200601584.

(56) Erno, Z.; Asadirad, A. M.; Lemieux, V.; Branda, N. R. Using Light and a Molecular Switch to ‘Lock’ and ‘Unlock’ the Diels–Alder Reaction. Org. Biomol. Chem. 2012, 10 (14), 2787–2792. https://doi.org/10.1039/C2OB06908C.

(57) Wu, T.; Tang, H.; Bohne, C.; Branda, N. R. Reporting the Release of Caged Species by a Combination of Two Sequential Photoreactions, a Molecular Switch, and One Color of Light. Angew. Chem. Int. Ed. 2012, 51 (11), 2741–2744. https://doi.org/10.1002/anie.201108336.

(58) Hu, X.; McFadden, M. E.; Barber, R. W.; Robb, M. J. Mechanochemical Regulation of a Photochemical Reaction. J. Am. Chem. Soc. 2018, 140 (43), 14073–14077. https://doi.org/10.1021/jacs.8b09628.

(59) Ohsumi, M.; Fukaminato, T.; Irie, M. Chemical Control of the Photochromic Reactivity of Diarylethene Derivatives. Chem. Commun. 2005, No. 31, 3921–3923. https://doi.org/10.1039/B506801K.

(60) Kühni, J.; Belser, P. Gated Photochromism of 1,2-Diarylethenes. Org. Lett. 2007, 9 (10), 1915–1918. https://doi.org/10.1021/ol070487h.

(61) Chen, Z.; Zhao, S.; Li, Z.; Zhang, Z.; Zhang, F. Acid/Alkali Gated Photochromism of Two Diarylperfluorocyclopentenes. Sci. China Ser. B Chem. 2007, 50 (5), 581–586. https://doi.org/10.1007/s11426-007-0114-9.

(62) Zheng, C.; Pu, S.; Liu, G.; Chen, B.; Dai, Y. A Highly Selective Colorimetric Sensor for Cysteine and Homocysteine Based on a New Photochromic Diarylethene. Dyes Pigments 2013, 98 (2), 280–285. https://doi.org/10.1016/j.dyepig.2013.02.022.

(63) Nourmohammadian, F.; Wu, T.; Branda, N. R. A 'Chemically-Gated' Photoresponsive Compound as a Visible Detector for Organophosphorus Nerve Agents. Chem Commun 2011, 47 (39), 10954–10956. https://doi.org/10.1039/C1CC13685B.

(64) Kaur, B.; Raza, R.; R. Branda, N. A Dual-Mode Visual Detector for Toxic Hydrazine. RSC Adv. 2021, 11 (37), 22835–22841. https://doi.org/10.1039/D1RA03677G.

(65) Li, Z.; Zhang, H.; Zhang, H.; Xie, Y.; Chen, H.; He, C.; Wang, Y.; Ya, H.; Guo, H. A Photoswitchable Colorimetric Sensor for Fluoride Based on a Dithienylethene Unit. J. Chem. Res. 2018, 42 (6), 305–308. https://doi.org/10.3184/174751918X15287323806534.

Chapter 2.

Unlocking Photochemistry: A Diels-Alder Reaction-Based Colorimetric Approach for Singlet Oxygen Detection

Abstract

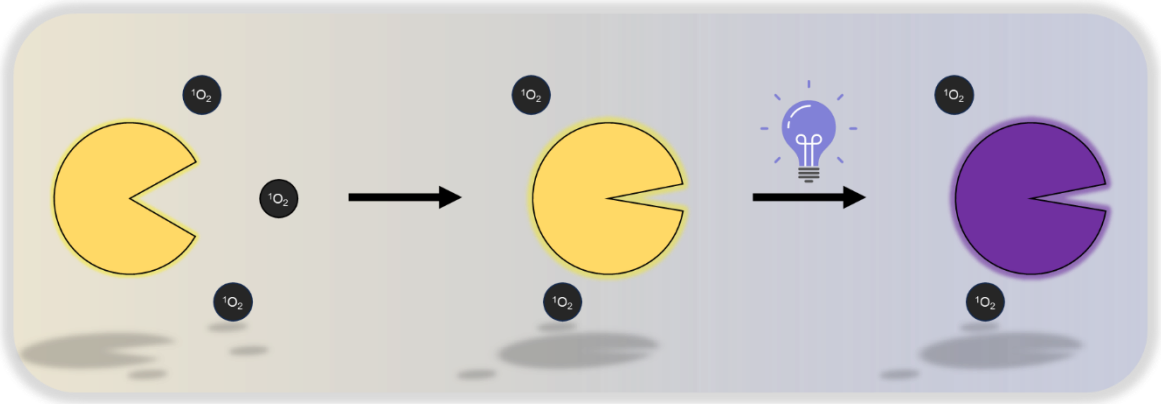

Various biological, environmental, and industrial processes generate singlet oxygen and other reactive oxygen species. Their extreme reactivity with organic molecules works both in positive and negative approaches. Thus, the detection and quantification of these species is of utmost importance and has led to the development of numerous detection methods. A new approach to detecting singlet oxygen is proposed based on a non-photochromic molecule that reacts with singlet oxygen through the Diels-Alder reaction. This chemical reaction installs the necessary structural arrangement in the molecule and unlocks the photochemistry. Exposure to UV light induces a color change in the system, indicating the presence of singlet oxygen.

2.1. Introduction

According to molecular orbital theory, ground-state dioxygen (O_2) molecules have two electrons with parallel spins in their highest occupied molecular orbital, making it a spin triplet. However, most organic molecules exist in the singlet state, and reactions between different electronic states are forbidden due to spin conservation rules. This difference in spin multiplicity limits directivity reactivity between molecular oxygen and organic molecules. However, the biradical-like character allows reaction with organic molecules through radical or enzymatic mechanisms, such as aerobic respiration. This symmetry-controlled reactivity prevented the rapid and unrestricted oxidation of the building blocks of life and enabled life to exist on Earth.[1]

Redox reactions of molecular oxygen generate molecules with extreme reactivity termed reactive oxygen species (ROS). Hydrogen peroxide (H_2O_2), a widely used oxidizing agent in synthetic chemistry, is the most well-known ROS. In biological systems, superoxide anion ($O_2^{\bullet-}$) is the precursor, and the disproportion of $O_2^{\bullet-}$ leads to the formation of H_2O_2, which in turn can produce hydroxyl radicals (HO•), hydroxyl ions (HO^-), and singlet oxygen ($^1O_2$). Among these, HO• and $^1O_2$ are the most destructive, playing a key role in numerous biological and non-biological processes.[1,2]

An imbalance between the production and destruction of reactive oxygen species in biological systems causes oxidative stress. Damage from oxidative stress is linked to several diseases and disorders. Environmentally, ROS contribute to atmospheric pollution. Industrially, they play a crucial role in the degradation of polymers and organic electronics. Reactive oxygen species are also a fundamental cause of food spoilage.[1–3]

Thus, detecting and tracking ROS, especially hydroxyl radicals and singlet oxygen, is essential for monitoring critical biological, environmental, and industrial processes. Methodologies for detecting and tracking these reactive oxygen species are the subject of ongoing research. Herein, a novel absorption-based approach for detecting singlet oxygen is proposed, where a probe goes from a colorless state to a colored state upon exposure.

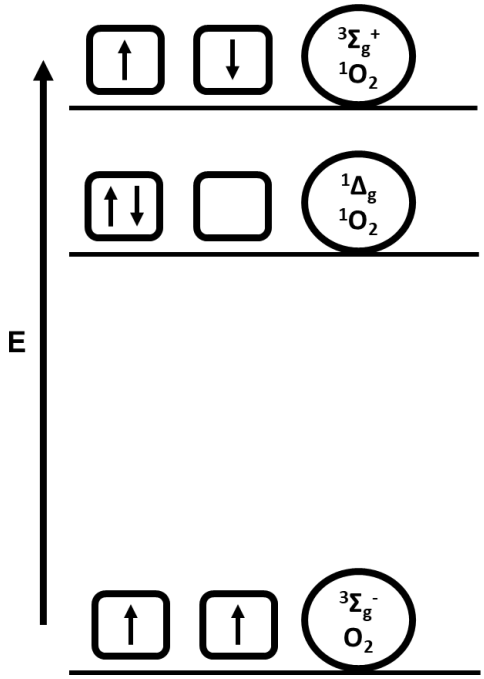

Figure 2-1 Electron spins and pairing in the HOMO of the ground triplet state and the two excited singlet states of molecular oxygen. The two excited singlet states are 94 and 157 kJ/mol, higher than the ground triplet state.

2.1.1. What is Singlet Oxygen?

$^1O_2$ is one of the most studied reactive oxygen species because of its involvement in numerous processes. The triplet-state oxygen, ($^3\Sigma_g^-$) $^3O_2$, can absorb energy and transition to higher energy excited states. The two lowest excited states of molecular oxygen are in the electronic singlet state. One of the two forms of singlet-state oxygen is the closed-shell singlet state, ($^1\Delta_g$) $^1O_2$, in which the two electrons are spin-paired. The second form is the open-shell singlet state, ($^3\Sigma_g^+$) $^1O_2$, which possesses unpaired electrons with antiparallel spins.[1,3,4] The energies of the two forms are 94 and 157 kJ/mol, higher than that of the triplet ground state, respectively.[4] The higher-energy singlet state ($^3\Sigma_g^+$)$^1O_2$ is short-lived and relaxes to ($^1\Delta_g$) $^1O_2$ in solutions, and in the gas phase, it transitions to the ground triplet state. The closed-shell singlet excited state ($^1\Delta_g$) has a higher lifetime of the two forms in the gas and solution phase, and thus, singlet oxygen ($^1O_2$) commonly refers to this species.

2.1.2. Synthetic Reactions of Singlet Oxygen

Reactions of molecules with triplet-state oxygen are spin-forbidden; however, singlet oxygen no longer has this limitation. A wide variety of organic reactions are possible with molecules because of the multiplicity and higher-energy nature of the excited state of oxygen vs. the ground state. This combination results in the spontaneous reaction of singlet-state oxygen with organic and inorganic compounds, generating significant interest in the research community. The extreme reactivity of singlet oxygen shows destructive and constructive effects in various processes.

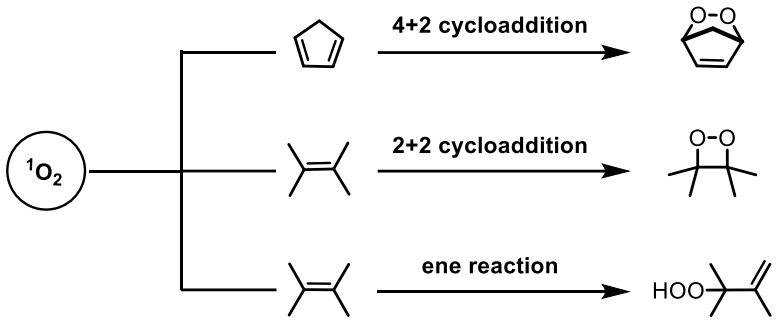

Figure 2-2 Singlet oxygen reactivity with alkenes. With 1,3-dienes, it undergoes 4+2 cycloaddition or Diels-Alder type reaction. With alkenes, it either forms dioxetanes via 2+2 cycloaddition or allylic hydroperoxides via a Schenck ene reaction.

Singlet oxygen reacts readily with electron-rich species such as alkenes, aromatics, sulfides, and amines. It forms hydroperoxides by abstracting hydrogen from organic molecules that contribute to their oxidative degradation. Singlet oxygen can also undergo addition reactions with alkenes, cyclic, acyclic, and aromatic conjugated dienes.[5,6] It acts as a dienophile and undergoes the Diels-Alder reaction to form a 6-membered endoperoxide ring.[5,6] [2 + 2]-Cycloaddition reactions of singlet oxygen with electron-rich alkenes to form 4-membered ring peroxides called 1,2-dioxetanes have been well studied. 'Ene' reactions with alkenes lead to the formation of allylic hydroperoxides.[5,6] These reactions of singlet oxygen have helped chemists synthesize novel molecules used in drug discovery and form the basis for several detection methodologies.

2.1.3. Presence in Biological Systems

Singlet oxygen plays an essential role in biological processes. There are two pathways for singlet oxygen production in biological systems.[7] The first pathway involves 'light reactions' in which the photoexcitation of a triplet-state molecule and a subsequent energy transfer to ground-state oxygen leads to the formation of singlet oxygen. An example is in plants, where singlet oxygen is generated as a byproduct of the photosynthesis reaction via the excitation of chlorophyll molecules that can transfer energy to ground-state oxygen to produce singlet oxygen. The second pathway concerns 'dark reactions,' where singlet oxygen production occurs through a chemical reaction. Enzymatic reactions catalyzed by dioxygenases, lipoxygenases, myeloperoxidases, and cytochromes are a few examples of singlet oxygen generation that is not light-mediated.[7–9]

Due to its extreme reactivity, singlet oxygen has a destructive effect on biological processes. Oxidative damage to biomolecules through the reaction of singlet oxygen with lipids is widespread. Amino acids such as histidine, tyrosine, tryptophan, and methionine react with singlet oxygen, producing short-lived endoperoxides. Singlet oxygen can also react with the nucleobases in DNA, damaging and breaking the strands. Guanine is the most reactive nucleobase to singlet oxygen.[10] Singlet oxygen-mediated oxidative damage is considered one of the leading causes of diseases such as asthma, glaucoma, diabetes, skin cancer, and psoriasis.[11] It is also considered a factor that induces photoaging of the skin. On the other hand, the cytotoxic effects of singlet oxygen are utilized in photodynamic therapy (PDT) for cancer treatment. Singlet oxygen is produced at the cancer site using photosensitizers to destroy cancer cells.[12]

2.1.4. Significance in Industries

Singlet oxygen, because of its higher reactivity, can accelerate the rancidity of oils. It reacts with the alkene groups in unsaturated fatty acids, generating epoxides, free radicals, and other reactive species that promote and accelerate the oxidation process. For the dairy industry, singlet oxygen is one of the leading causes of spoilage. Singlet oxygen can be generated when milk is exposed to light, resulting in lipid peroxidation of milk fats. This process leads to unpleasant odors and a rancid taste known as the sunlight flavor. Milk components such as riboflavin and ascorbic acid can react with

singlet oxygen, accelerating milk degradation.[13] Photosensitized oxidation of food products containing edible dyes is also a significant challenge attributed to singlet oxygen.[14] In the paper and pulp industry, singlet oxygen is used for bleaching purposes, but overexposure leads to an adverse reaction with lignin, resulting in loss of structural integrity.[4]

Singlet oxygen is a significant factor in the modification and degradation of polymeric structures. Impurities or photosensitizers in polymers can generate singlet oxygen, which reacts with the polymers and produces reactive species that increase the oxidation rate. Polybutadiene, polyisoprene, and conjugated polymers are highly susceptible to singlet oxygen-mediated oxidative degradation. Singlet oxygen is shown to negatively impact or degrade organo-electronic materials, such as organic photovoltaics, organic field-effect transistors, organic light-emitting diodes, organic semiconductors, and organic thin films.[15]

An area where singlet oxygen finds constructive use is in the electrochemical treatment of wastewater. Singlet oxygen reacts with organic contaminants in wastewater to neutralize them and efficiently inactivates the pathogens present through its cytotoxic effects.[16]

2.1.5. How Singlet Oxygen is Generated

Naturally, singlet oxygen is present in small amounts in the upper atmosphere, where it is excited by molecular oxygen through solar radiation. Polluted urban centers and other locations with high ozone concentration levels promote the formation of singlet oxygen.[17]

Photosensitization of dyes is commonly used for the controlled, on-demand generation of singlet oxygen. In this process, organic or inorganic molecules known as photosensitizers absorb light energy and are promoted to an electronically excited singlet state. This excited singlet state undergoes intersystem crossing to the excited triplet state, which is usually long-lived. The excited triplet state of the photosensitizer can then transfer the excitation energy to molecular oxygen, converting it to singlet oxygen. Methylene blue, rose bengal, erythrosine B, and acridine derivatives are some examples of photosensitizers used to generate singlet oxygen.[4,18]

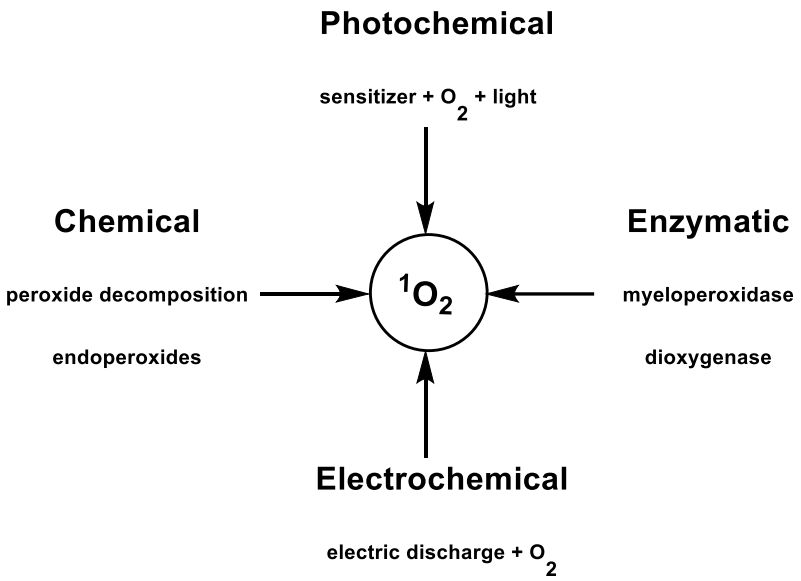

Figure 2-3 Various methods for singlet oxygen generation.

Chemically, singlet oxygen is produced by the decomposition of hydrogen peroxide. Hydrogen peroxide decomposes into water and singlet oxygen, but the decomposition rate is slow at room temperature. Catalysts such as sodium hypochlorite (NaOCl), calcium hydroxide ($Ca(OH)_2$), and molybdate anion (MoO_4^{2-}) improve the rate of decomposition of hydrogen peroxide. The reaction between H_2O_2 and NaOCl is the most common method to demonstrate singlet oxygen production. Other chemical methods of generation include a) the decomposition of ozonides such as triphenylphosphine ozonide, b) the interaction of superoxide with perhydroxyl radicals, and c) cycloreversion of endoperoxides such as diphenyl anthracene endoperoxide.[19]

Other methods of singlet oxygen generation include the electric discharge technique, where an electrical discharge produces singlet oxygen from the pure gaseous oxygen stream.[20] Thermal or light exposure can also induce surface-mediated reactions in metal oxide particles such as silicon dioxide (SiO_2), aluminum oxide (Al_2O_3), titanium dioxide (TiO2), and calcium oxide (CaO).[21]

2.1.6. Current Methods of Detection

The detection and quantification of singlet oxygen is essential because of its involvement in various biological, environmental, and industrial processes. It is necessary to gauge the presence and reactivity of singlet oxygen within these systems.

The highly reactive nature, combined with the versatility of chemistry, has allowed chemists to develop different techniques for detecting singlet oxygen. It can be detected directly through luminescence or indirectly through reactions with molecular probes.

Direct Detection Methods

The easiest direct detection method for singlet oxygen production is to mix H_2O_2 with NaOCl and observe the intense red glow produced. Khan and Kasha, in 1963, observed that the intense red glow was centered around 633 and 703 nm. This photoluminescence of singlet oxygen is attributed to the dimol emission, which occurs when two singlet oxygen molecules combine and form a singlet complex that transitions into two triplet-state oxygen molecules.[22]

Bader and Ogryzalo, in 1964, demonstrated near-infrared luminescence emission of singlet oxygen at 1270 nm.[23] The spin-unrestricted transition of excited singlet oxygen to ground triplet oxygen leads to this weak phosphorescence. Germanium or indium gallium arsenide (InGaAs)-based photodiodes and NIR photomultiplier tubes are extensively used for monitoring this weak emission. Recently, single-photon avalanche detectors (SPAD), superconducting nanowire single-photon detectors (SNSPDS), and singlet oxygen detection systems (SODS) have been used to design devices for detection purposes.

Indirect Detection Methods

Indirect detection methods utilize the chemical reactivity of singlet oxygen with organic molecules. Chemical reactions on the probe alter the molecule's properties and give a readout signal. Molecular probes are usually combined with analytical instruments such as spectrometers and chromatograms.

Electron Paramagnetic Resonance (EPR)

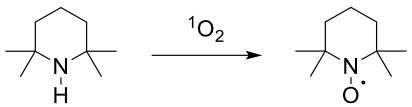

Figure 2-4 Singlet oxygen reacts with TEMP to form nitroxide radical TEMPO, which is detectable by EPR.

Electron paramagnetic resonance (EPR) spectroscopy is one of the most accurate methods for detecting singlet oxygen. Highly reactive chemical traps react

selectively and rapidly with singlet oxygen to produce radical species. The probes most used for EPR have sterically hindered amines such as 2,3,6,6-tetramethylpiperidine (TEMP) and its analogues. These sterically hindered amines react with singlet oxygen to form nitroxide radicals detected via EPR spectroscopy.[24]

Luminescence-based Probes

The luminescence-based molecular probes work on the same principle as the EPR probes. Reaction with singlet oxygen alters the molecule's electronic and molecular structure. These changes in electronic or molecular structure are the guiding principles for photoluminescent, chemiluminescent, or absorption-based sensors.

Photoluminescent Probes

Photoluminescence-based probes are the most common tools for singlet oxygen detection. These probes exhibit four distinct response modes: a) fluorescence turn-on response, b) fluorescence turn-off response, c) phosphorescence turn-on response, and d) ratiometric fluorescence response. The basic design of these molecular probes contains a singlet oxygen-reactive species. 1,3-diphenylisobenzofuran (DPBF), anthracene, and their derivatives are the most widely used reactive groups for these systems. These molecules react via a Diels-Alder reaction with singlet oxygen, generating a corresponding endoperoxide.

DPBF is a standalone molecule that detects singlet oxygen and works in the fluorescence turn-off response mode. Photoexcitation of DPBF in the UV region (λ_{abs} = 414 nm) produces fluorescence emission (λ_{em} = 455 nm). Upon reaction with singlet oxygen, DPBF-endoperoxide is formed, which subsequently rearranges into 1,2-dibenzoylbenzene. This transformation results in quenching of the visible fluorescence emission of the molecule.[25]

Probes with a fluorescence or phosphorescence turn-on response utilize a singlet oxygen-reactive species attached to a fluorophore or a phosphor. Photoinduced electron transfer (PET) in the case of fluorescence turn-on response probes and triplet-triplet energy transfer (TTET) in the case of phosphorescence turn-on response probes quench the photoluminescence of the probes. These two processes (PET and TTET) are either limited or eliminated when singlet oxygen interacts with the reactive species. Anthracene and its derivatives are the most widely used singlet oxygen-reactive species,

whereas fluorescein, rhodamine, BODIPY, and their derivatives are the most common fluorophores.[26]

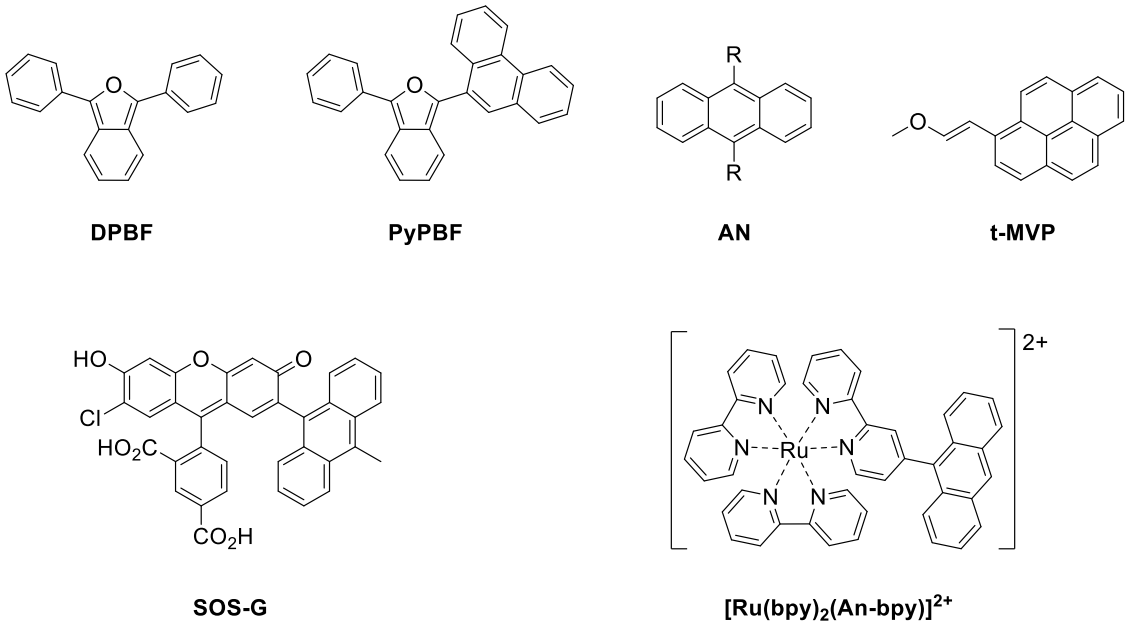

Figure 2-5 Luminescence-based probes for singlet oxygen detection. Most probes have a furan or anthracene moiety that reacts with singlet oxygen.

The commercially available singlet oxygen sensor-green probe (SOS-G) contains fluorescein (fluorophore and electron acceptor) covalently linked to anthracene (reactive species and electron donor). Intramolecular PET quenching deactivates the fluorescence emission of the molecule. When singlet oxygen is present, anthracene readily reacts with it and forms anthracene endoperoxide. This transformation stops the PET process and turns on the fluorescence of the fluorescein molecule.

Phosphorescence turn-on response-based systems use metal complexes (Re, Ru, Eu, or Tb) as the phosphor and anthracene and its derivatives as the singlet oxygen reactive species. One such system is a modified Ruthenium-bipyridine complex, $[Ru(bpy)_3]^{2+}$. The anthracene group was covalently attached to the bipyridine ligands. The anthracene moiety quenches the phosphorescence of the complex via TTEP. The conversion of anthracene to anthracene endoperoxide breaks the TTEP process and activates the phosphorescence behavior of the molecule.[27]

Ratiometric fluorescent probes work by conjugating the fluorophore with the singlet oxygen-reactive species. The π-conjugation is spread over the molecule, but the

reaction with singlet oxygen shortens the conjugation, leading to a blue shift in fluorescence emission. Several probes of this type were created using DPBF as the reactive moiety and replacing one of the aryl groups with phenanthrene, pyrene, and 4-(diphenylamino)stilbene as the fluorophores. The blue shift in the fluorescence emission wavelength and the change in fluorescence intensity were observed in all molecules upon reaction with singlet oxygen.[28]

Chemiluminescent Probes

Whereas most photoluminescent probes use a Diels-Alder reaction between singlet oxygen and the reactive species, chemiluminescent probes work via reactions of alkenes to form 1,2-dioxetane. The 1,2-dioxetane moiety is a high-energy species that undergoes spontaneous thermolysis, forming an excited-state carbonyl group. Radiative deactivation of this excited-state carbonyl group generates chemiluminescence. trans-1-(2-methoxyvinyl) pyrene reacts with singlet oxygen to form a 1,2-dioxetane product which subsequently dissociates to form pyrene-1-carboxaldehyde with chemiluminescence emission.[29]

Absorption-based Probes

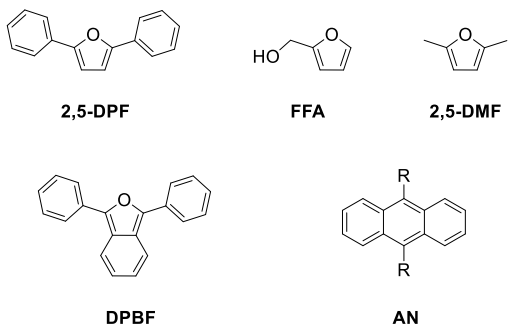

Figure 2-6 Absorption-based probes use furan as the reactive species with singlet oxygen.

Absorption-based probes are the simplest of all detection methods available. Changes in the absorption spectra of a reactive species upon its reaction with singlet oxygen form the basis of this technique. The requirement for an absorption-based probe is simple: the molecule must possess a π-conjugated diene system. The molecules can undergo a Diels-Alder reaction with singlet oxygen to form cyclic endoperoxides. These changes shorten the π-conjugation in the system and result in either a hypochromic or a blue shift. Almost all absorption-based systems have an absorption-bleaching response

to singlet oxygen. The 5-membered heteroarenes and acenes are the two classes of molecules that are used for this purpose. Naphthalene and anthracene are two acene groups widely used in absorption-based singlet oxygen detection. Amongst heteroarenes, furan and its derivatives react highly toward singlet oxygen. Furfuryl alcohol (FFA) is the most well-known absorption-based probe for singlet oxygen. 2,5-dimethylfuran, 2,5-diphenylfuran, and 1,3-diphenylisobenzofuran have all been used for the absorption-based detection of singlet oxygen as a standalone probe or in conjunction with HPLC.[30–32]

2.1.7. Challenges with Detection

As a reactive oxygen species, singlet oxygen presents many challenges when designing a system for its detection. It is a highly reactive species and readily reacts with other molecules in its surroundings. Also, this extreme reactivity gives singlet oxygen a short lifetime, especially in aqueous environments, with a lifetime of a few microseconds. Another major hurdle in singlet oxygen detection is the low concentration of singlet oxygen, especially in biological systems. All singlet oxygen detection systems have their advantages and disadvantages.

The major advantage of the direct systems is the real-time detection and analysis of the singlet oxygen release. The other significant benefit is the ability to provide the lifetime of singlet oxygen in a given process. Since these techniques examine the luminescence generated from the singlet oxygen itself, they are not dependent on the microenvironment of the release process. Therefore, direct methods are the most advantageous and desirable for singlet oxygen detection. However, the luminescence of singlet oxygen at 1270 nm is weak and is the major drawback in utilizing these techniques. The nonradiative processes that compete with the radiative transition are faster, which leads to extremely low emission efficiency. Additionally, processes in which a low concentration of singlet oxygen is released exacerbate the already weak signal and lead to low sensitivity and low signal-to-noise ratio. PMT tubes and photodiodes are usually employed to increase the signal-to-noise ratio, but using specialized equipment makes the whole process cost-ineffective.

Indirect or probe-based methods alleviate the issue of weak signals in direct methods. The emission efficiency is much higher in the case of luminescence-based

probes than the direct emission from singlet oxygen. The probe-based techniques are also more sensitive towards singlet oxygen, except for the absorption or photo-bleaching methods. The disadvantages of these systems, however, are that these systems rely on microenvironment conditions, do not provide real-time detection, and do not give any information about the lifetime of singlet oxygen in the monitoring process. The other major disadvantage of probe-based systems is their invasive nature and the probable cytotoxic effect that can arise from it.

EPR spectroscopy provides reasonable specificity for singlet oxygen but suffers from high costs and complicated procedures associated with the instrument. Luminescence-based probes are highly sensitive, show reasonable selectivity and specificity towards singlet oxygen, and do not require specialized equipment. However, they suffer from the problem of self-photosensitization. Photoluminescent probes are sensitive to the environment's color and have a lower signal-to-noise ratio than chemiluminescent probes. The major drawback of the chemiluminescent probes, on the other hand, is their delayed response to singlet oxygen detection. Absorption-based systems provide easy detection and convenient usage and are incredibly cost-effective but are limited by their color dependence, low sensitivity, and low signal-to-noise ratio.

	Direct		Indirect			
	NIR-luminescence	Dimol emission	EPR	Photo-luminescence	Chemi-luminescence	Absorbance
Color dependence	No	No	No	Yes	No	Yes
Convenience	Low	Low	Low	Low	Low	High
Cost/Specialized equipment	High	High	High	Low	Low	Low
Ease of detection	No	No	No	Yes	Yes	Yes
Emission efficiency	Low	Low	-	High	High	-
Invasive	No	No	Yes	Yes	Yes	Yes
Lifetime information	Yes	Yes	No	No	No	No
Microenvironment dependency	No	No	Yes	Yes	Yes	Yes
Possible cytotoxicity	-	-	Yes	Yes	Yes	Yes
Real time detection	Yes	Yes	No	No	No	No
Selectivity	-	-	Good	Good	Good	Good
Self-photosensitization	-	-	-	Yes	Yes	-
Sensitivity	Low	Low	High	High	High	Low
Signal-to-noise ratio	Low	Low	-	Low	High	Low
Specificity	High	High	High	Low	Low	Low

Table 2-1 Advantages and disadvantages of various singlet oxygen detection systems.

2.2. Proposed Research

Herein, an absorption-based system is proposed for the detection of singlet oxygen. This system employs the Diels-Alder reaction of singlet oxygen with a molecular probe to provide a colorimetric readout signal. The basic design of this system consists of a 1,3-butadiene moiety with thiophene groups attached at the C2 and C3 positions. The modified diarylethene molecule or pre-diarylethene is non-photochromic because of the absence of the 1,3,5-hexatriene system at its core. The Diels-Alder reaction of the 1,3-butadiene moiety with singlet oxygen generates an endoperoxide that installs the necessary 1,3,5-hexatriene core of the open-ring form of diarylethene. Thus, a chemical reaction unlocks the photochemistry of the molecule. Exposure to light of appropriate wavelength will allow the ring-open form to undergo cyclization to give the ring-closed form. A readout signal in the form of color change is expected to be observed.

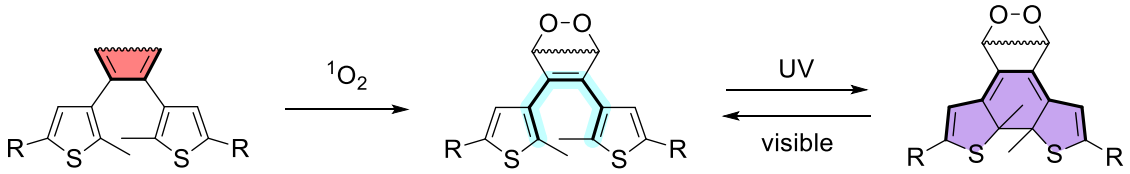

Scheme 2-1 Proposed 1,3-butadiene-based pre-diarylethene system that undergoes Diels-Alder reaction with singlet oxygen. The reaction unlocks the photochemistry of the molecule and allows it to undergo reversible photoisomerization.

Motivation for the System

The design for this system was guided by the non-photoactive pre-diarylethene molecules containing a 1,3-butadiene moiety synthesized by the Branda group.[33–35] These molecules were shown to undergo the Diels-Alder reaction with a dienophile to unlock their photochromic behavior.

Current absorption-based singlet oxygen detection systems lose the extended π-conjugation from their system, leading to a blue shift or a decrease in absorbance intensity. The new approach creates an extended π-conjugated system within the molecule, thereby inducing a red shift.

Advantages and Applications of the System

The main advantage of this system is that it provides a better readout signal for singlet oxygen detection compared to photobleaching-based techniques. Another advantage is that visual color change is a quick and straightforward qualitative detection method that does not require sophisticated instruments. Systems that go from colorless to colored also provide higher sensitivity than those that undergo photobleaching. These systems also have a slightly higher signal-to-noise ratio than the photobleaching methods, as the molecule's color change (signal) can be differentiated in most cases relative to the background color (noise). Overall, this alternate approach retains most of the advantages of the currently known absorption-based systems, like low cost and convenience, and alleviates some disadvantages, like low sensitivity and low signal-to-noise ratio.

This approach can be used in various processes where quick and easy visual detection of singlet oxygen is needed. One such example is the photodegradation of polymers by singlet oxygen. These colorimetric probes can be added to the polymer matrix, where they can function as a quencher for singlet oxygen and give a readout signal for the degradation site.

2.3. Experimental Design

2.3.1. Probe Selection

The first consideration in designing a colorimetric singlet oxygen detection system was finding an appropriate molecule that could work as a probe. Several pre-diarylethene (pre-diarylethene) molecules with the 1,3-butadiene system at the core are known. These molecules do not undergo reversible photocyclization reactions until the Diels-Alder reaction generates the desired 1,3,5-hexatriene system. The first reported example of this molecule type was a bicyclohexene derivative synthesized by Wang and coworkers. The pre-diarylethene molecule was subjected to a Diels-Alder reaction with maleic anhydride or N-ethylmaleimide. Lemieux and coworkers expanded on this concept and synthesized the pre-diarylethene butadiene, cyclohexadiene, and fulvene-based derivatives.[33,34] All three derivatives underwent the Diels-Alder reaction, like the work done by Wang and coworkers. Zach Erno and coworkers replaced the

cyclopentene ring in a diarylethene with a furan ring known to undergo a Diels-Alder reaction with a suitable dienophile.[35] In all systems, the absence of a 1,3,5-hexatriene system at the molecule's core prohibited photocyclization upon exposure to light. Diels-Alder reaction on the molecules installed the 1,3,5-hexatriene system, unlocking their photoswitching ability.

Theoretically, all the above systems can undergo a Diels-Alder reaction with singlet oxygen and yield a photoswitchable endoperoxide molecule. However, several factors dictated the choice of dithienylfuran as the probe molecule for singlet oxygen detection. The butadiene derivative of diarylethene photoswitch was shown to undergo a Diels-Alder reaction only in the absence of solvents, as it acquires the unreactive *s-trans* 1,3-butadiene configuration in solvents. The ease of synthesis and the availability of extensive literature on the endoperoxide product dictated using the furan derivative over the bicyclohexene, cyclohexadiene, and fulvene-based pre-diarylethene photoswitches. The reaction of furan with singlet oxygen is well-known among synthetic chemists. Furans undergo the [4 + 2] cyclization reaction with singlet oxygen, producing a bicyclic endoperoxide.[36–38] This bicyclic endoperoxide will install the 1,3,5-hexatriene system in the molecule's core, unlocking its photochemistry.

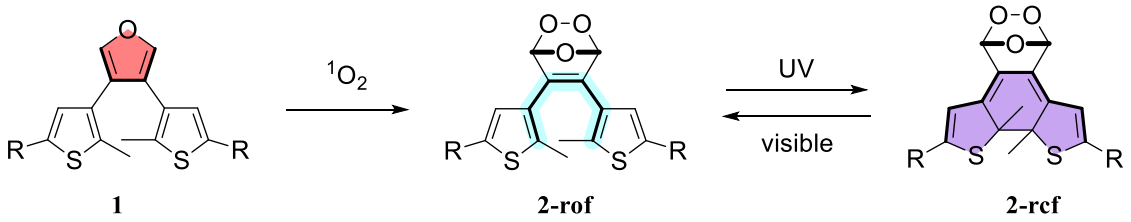

1 **2-rof** **2-rcf**

R = COOEt

Scheme 2-2 The reaction of singlet oxygen with *bis*-ester *dithienylfuran*, 1, unlocks the molecule's photochemistry and gives a color change as a readout signal on exposure to UV light.

Of the four furan derivatives synthesized by Erno and coworkers, the *bis*-ester derivative of dithienylfuran was selected as the model probe to perform the Diels-Alder reaction with singlet oxygen. The *bis*-chloro derivative of the dithienylfuran molecule degrades under ambient conditions, rendering it unsuitable for reaction with already highly reactive singlet oxygen. Although stable, the *bis*-acid derivative had problems with solubility in organic solvents required for the tests. The phenyl derivative did not undergo the Diels-Alder reaction with singlet oxygen. The *bis*-ester derivative was stable when

stored at ambient conditions, soluble in organic solvents, and reactive towards singlet oxygen.[35]

The synthesis procedure for the *bis*-ester derivative of dithienylfuran was modified from that proposed previously by Zach Erno and coworkers. This new synthesis protocol a) eliminated the need to synthesize the unstable *bis*-chloro derivative as a precursor, b) reduced the number of reaction steps, and c) increased the overall yield of the final product.

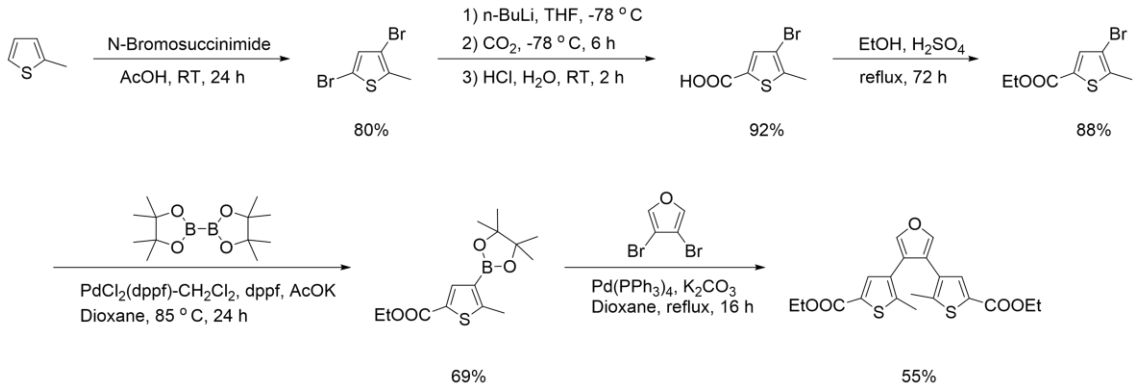

Scheme 2-3 Synthesis procedure for *bis*-ester dithienylfuran, 1.

Bis-ester dithienylfuran was synthesized by a two-fold Suzuki cross-coupling of a boronic ester of thiophene with 2,3-dibromofuran. The boronic ester of thiophene was prepared by the bromination of 2-methyl thiophene to 3,5-dibromo-2-methyl thiophene. Lithiation with n-BuLi, followed by quenching with CO_2, converted 3,5-dibromo-2-methyl thiophene into 4-bromo-5-methylthiophene-2-carboxylic acid, which gave the thiophene ester after Fischer esterification reaction with ethanol. The Miyaura borylation of the thiophene ester with *bis*(pinacolato)diboron yielded the pinacol boronic ester of thiophene. 2,3-dibromofuran was prepared from trans-2,3-dibromo-butene-1,4-diol using conc. sulfuric acid and potassium dichromate via a known literature procedure.[43]

2.3.2. Source Selection

Singlet oxygen can be generated by various methods in laboratory settings. Both chemical and photosensitized sources of singlet oxygen were used to test the hypothesis. Endoperoxides such as those of diphenyl anthracene were not used, as the released singlet oxygen can react with the anthracene molecule.

Calcium peroxide diperoxohydrate appeared to be the most viable chemical source of singlet oxygen for the experiment. It is an environmentally benign singlet oxygen source because of its insolubility in organic solvents. Thermolysis of the molecule leads to the formation of singlet oxygen via the disproportionation of hydrogen peroxide. The product of the reaction is a cream-colored, insoluble, anhydrous calcium peroxide residue. This insoluble residue can be easily removed from the reaction mixture via centrifugation or filtration after the completion of the reaction.[39]

Calcium peroxide octahydrate is the storable precursor to calcium peroxide diperoxohydrate and is prepared by the reaction of calcium chloride with hydrogen peroxide at -4 °C for seven days. Calcium peroxide diperoxohydrate is prepared by stirring calcium peroxide octahydrate with hydrogen peroxide at -15 °C for 2 hours. The molecule is only stable at -80 °C and spontaneously releases singlet oxygen above this temperature, so it is freshly prepared before each use.

For the photooxidation of *bis*-ester dithienylfuran, photosensitizers such as rose bengal and methylene blue that absorb in the visible region were ruled out because they absorb in the same region as the ring-closed form of diarylethenes. The solutions of these photosensitizers are colored similarly to the expected ring-closed products, which will interfere with the expected color change observation. This restriction limited the choice of photosensitizers to those that absorb in the UV-A region, as they would mostly form colorless solutions. Amongst the most commonly available UV-A photosensitizers are acetophenone, benzophenone, and duroquinone.[40,41] Benzophenone is an additive added to polymers to prevent photodegradation. It is also used as a photo-initiator, while acetophenone is widely used as a precursor to resins for coatings and inks.

2.3.3. Test Conditions and Absorption Measurements

Chemical Method

Aubry and coworkers observed that methanol and tetrahydrofuran were the most suitable solvents for singlet oxygen generation with calcium peroxide diperoxohydrate. The singlet oxygen yield was 25% and 21% in methanol and tetrahydrofuran, respectively.[39] The singlet oxygen yield was in single digits in solvents such as acetonitrile and chloroform. High boiling point solvents like dimethylformamide and dimethylsulfoxide were unsuitable for the experiment if the solvent had to be removed.

To test the viability of the singlet oxygen reaction with *bis*-ester dithienylfuran, the reaction was tested in both tetrahydrofuran and methanol. Since many singlet oxygen detections are done in aqueous environments, the viability of the calcium peroxide diperoxohydrate was tested in water-methanol or water-tetrahydrofuran mixtures. The solubility of *bis*-ester dithienylfuran was tested in different water-organic solvent ratios, and ultimately, a 3:1 THF/methanol-deionized water mixture worked best. Aubry and coworkers reported that it takes about 3 hours at 50 °C for calcium peroxide diperoxohydrate to release all the available singlet oxygen. Since singlet oxygen detection needs to be conducted at ambient conditions, the reaction temperature was set at 25 °C for this study, and the mixture was stirred for a longer duration.

Freshly prepared calcium peroxide diperoxohydrate (8 equivalents) was added to *bis*-ester dithienylfuran (1 equivalent) solutions in suitable solvents and stirred in a water bath set at 25 °C. The reaction progress was monitored by thin-layer chromatography (TLC). When the TLC showed the complete consumption of *bis*-ester dithienylfuran in the reaction mixture, the suspension was filtered under vacuum and washed with a small amount of solvent. The filtrate was evaporated to dryness under a vacuum, weighed, and redissolved in an appropriate solvent to prepare 25 millimolar stock solutions. Appropriate dilutions were carried out, and UV-visible spectra were obtained by irradiating the sample with 254 nm light at an interval of 5 seconds to monitor the changes in the absorption spectra.

Photooxidation Method

Benzophenone or duroquinone (3 equivalents) was added to a *bis*-ester dithienylfuran (1 equivalent) solution prepared in different aerated solvents for photosensitized singlet oxygen generation. The reaction mixture was stirred and irradiated with 254 nm UV light at a distance of 1 cm. Aliquots were drawn from the solution after 300 seconds of exposure, diluted, and the UV-visible spectra were recorded.

Water-organic solvent mixtures were excluded from the photosensitization method because of the solubility constraints with duroquinone. Chlorinated solvents were also excluded because they form reactive radical species on exposure to high-energy UV light.

Reaction with Other Reactive Oxygen Species

To evaluate the selectivity of this system, *bis*-ester dithienylfuran was reacted with other reactive oxygen species. Fenton's reagent, a strong oxidizer utilized by chemists in synthesis, produces hydroxyl radicals and hydroxyl ions. Hydroxyl radicals are highly reactive, like singlet oxygen, but they are not very selective in the type of reaction. Fenton's reagent was used to assess the stability and selectivity of *bis*-ester dithienylfuran with hydroxyl radicals and hydroxyl ions. A stock solution of Fenton's reagent was prepared by mixing $FeSO_4.7H_2O$ and H_2O_2 and adding to a stirred *bis*-ester dithienylfuran solution in methanol. The reaction was stirred at room temperature and monitored with TLC.

2.4. Results and Discussions

Reaction with Calcium Peroxide Diperoxohydrate as the Source

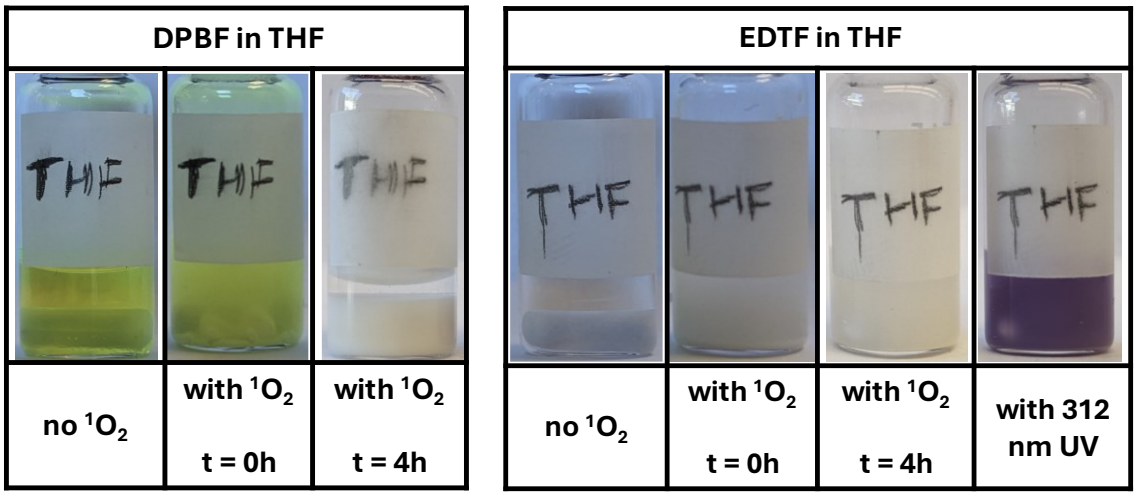

Figure 2-7 The reaction of 1,3-diphenylisobenzofuran (left) and *bis*-ester dithienylfuran (right) with singlet oxygen generated by thermolysis of calcium peroxide diperoxohydrate.

1,3-Diphenylisobenzofuran, a typical absorption-based singlet oxygen probe, was used to assess the reactivity of the singlet oxygen source, calcium peroxide diperoxohydrate, in tetrahydrofuran as a solvent. Four equivalents of the singlet oxygen source were added to a 1 mM probe solution and stirred for 4 hours in a water bath set at 25 °C. The yellow color of the solution bleached slowly, eventually becoming

colorless. The same reaction in methanol takes longer to bleach due to the partial solubility of the probe in the solvent.

Similarly, five equivalents of calcium peroxide diperoxohydrate were added to a 1 mM solution of *bis*-ester dithienylfuran in tetrahydrofuran, and the reaction was stirred for 4 hours in a water bath set at 25 °C. The turbid cream-colored solution was then irradiated with 312 nm UV light for 60 seconds, and the color changed to purple. Irradiation with visible light (<450 nm) bleached the purple color of the solution. TLC of this reaction mixture indicated unreacted dithienylfuran. To find the equivalence of the singlet oxygen source needed for the complete conversion of dithienylfuran, 1mM solutions of dithienylfuran in tetrahydrofuran and methanol were stirred with five to ten equivalents of calcium peroxide diperoxohydrate overnight at 25 °C. TLC of the reaction mixture for eight equivalents of singlet oxygen source showed complete conversion of the probe in both solvents.

TLC for the reaction of *bis*-ester dithienylfuran with singlet oxygen in tetrahydrofuran as the solvent showed the formation of multiple reaction products. Five product spots were visible on the TLC plate with 25% ethyl acetate in hexane as eluent. Three spots at Rf = 0.69, 0.50, and 0.31 were non-photochromic, whereas spots with Rf = 0.11 and the one at baseline changed color on exposure to 254 nm UV light.

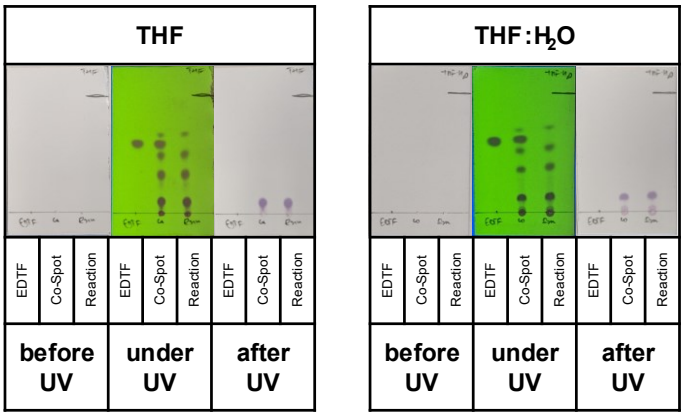

Figure 2-8 Thin-layer chromatography plates showing photochromic spots for a singlet oxygen reaction with *bis*-ester dithienylfuran in tetrahydrofuran and tetrahydrofuran-water mixture.

Similarly, the reaction in 25% water in a tetrahydrofuran solvent mix showed five products on the TLC plate: three non-photochromic and two photochromic spots. The Rf values of photochromic spots were 0.68, 0.52, and 0.36, whereas the photochromic spots were at Rf =0.12 and the baseline.

UV-visible absorption spectroscopy monitored the photoinduced ring-closing of the products in a tetrahydrofuran and tetrahydrofuran-water solvent mixture. Aliquots were taken from the reaction mix and diluted to make 7.5 × 10-5 M solutions of reaction products in the respective solvents. The cuvette was kept at a 1 cm distance from the UV lamp and irradiated with 254 nm light. The absorption spectra were acquired after regular 5-second irradiation intervals.

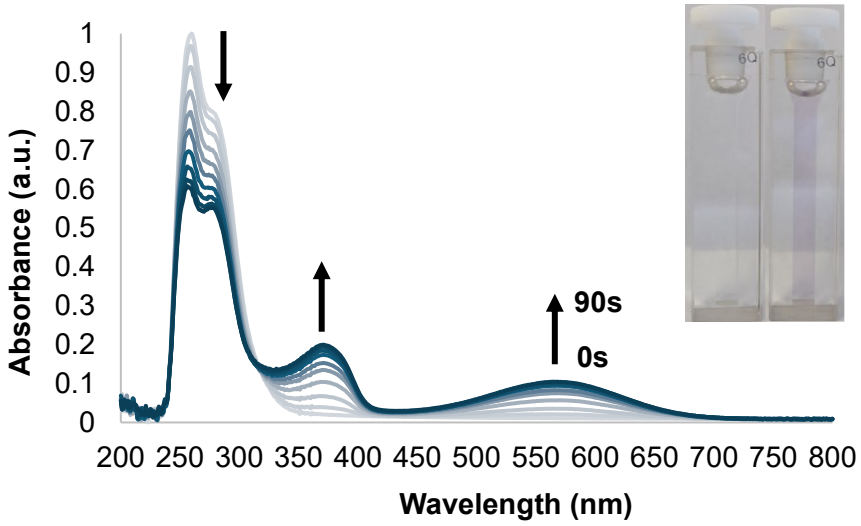

Figure 2-9 UV-visible absorption spectrum of the mixture of products from the reaction of *bis*-ester dithienylfuran (7.5 × 10^{-5} M) with singlet oxygen in tetrahydrofuran before and after irradiation with 254 nm UV light.

The absorption spectra of the reaction products in tetrahydrofuran at 0 seconds of UV exposure showed peaks centered at 256 nm. Irradiation of the solution with UV light decreased the intensity of the absorption peaks in the UV region. Two new absorption peaks centered around 369 nm and 563 nm appeared, and the colorless solution changed to purple. After 90 seconds of irradiation, no change in absorption was observed in both solvent systems, meaning the PSS was reached. Irradiation with visible light (>450 nm) bleached the purple solution back to colorless.

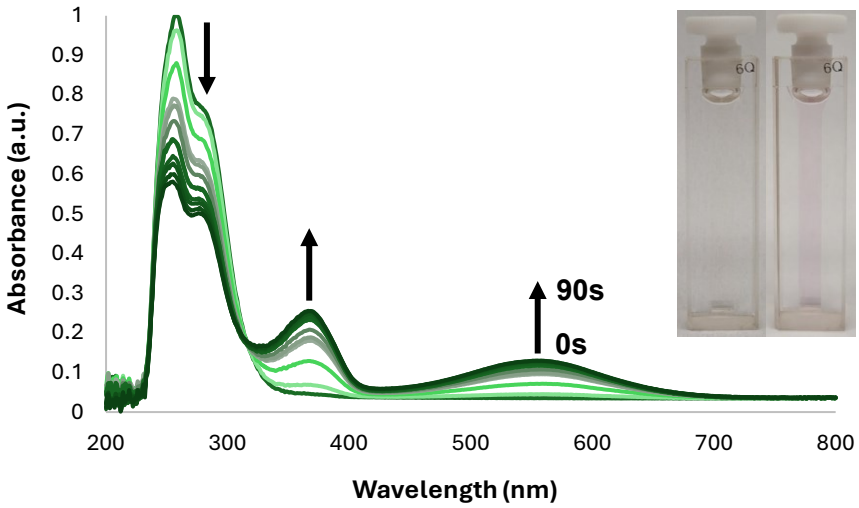

Figure 2-10 UV-visible absorption spectrum of the mixture of products from the reaction of *bis*-ester dithienylfuran (7.5×10^{-5} M) with singlet oxygen in the tetrahydrofuran-water solvent mix before and after irradiation with 254 nm UV light.

As observed on the TLC, the reaction of *bis*-ester dithienylfuran with singlet oxygen in methanol yielded two products: one at the baseline and the other at Rf = 0.10 with 25 % ethyl acetate in hexane as eluent. Both spots change color when exposed to 254 nm UV light.

Similarly, the photochromic molecules are the major products in the water-methanol solvent system. The TLC showed two photochromic product spots at Rf = 0.11 and at the baseline on exposure to 254 nm UV light.

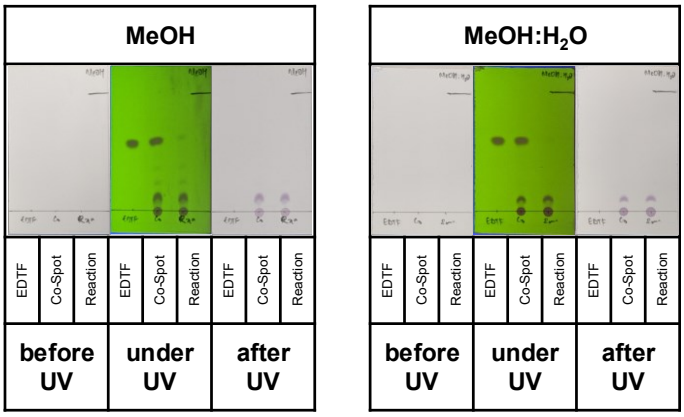

Figure 2-11 The TLC plate for singlet oxygen reaction with bis-ester dithienylfuran in methanol (left) and methanol-water mix (right) shows photochromic spots.

UV-visible absorption spectroscopy monitored the photoinduced ring-closing of the products in a methanol and methanol-water solvent mixture. Aliquots were taken from the reaction mix and diluted to make 7.5×10^{-5} M solutions of reaction products in the respective solvents. The cuvette was kept at a 1 cm distance from the UV lamp and irradiated with 254 nm light. The absorption spectra were acquired after regular 5-second irradiation intervals.

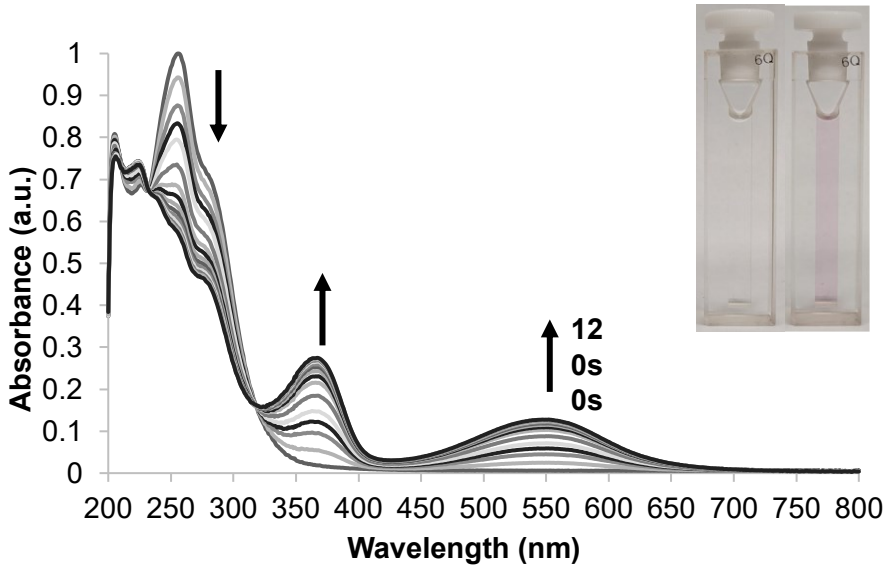

Figure 2-12 The UV-visible absorption spectrum of the mixture of products from the reaction of *bis*-ester dithienylfuran with singlet oxygen before and after irradiation with 254 nm UV light in methanol.

The absorption spectra of the reaction products in methanol at 0 seconds of UV exposure showed peaks centered at 254 nm. Irradiation of the solution with UV light decreased the intensity of the absorption peaks in the UV region. Two new absorption peaks centered around 364 nm and 554 nm appeared, and the colorless solution changed to purple. After 90 seconds of irradiation, no change in absorption was observed, meaning the PSS had reached. Irradiation with visible light (>450 nm) bleached the purple solution back to colorless.

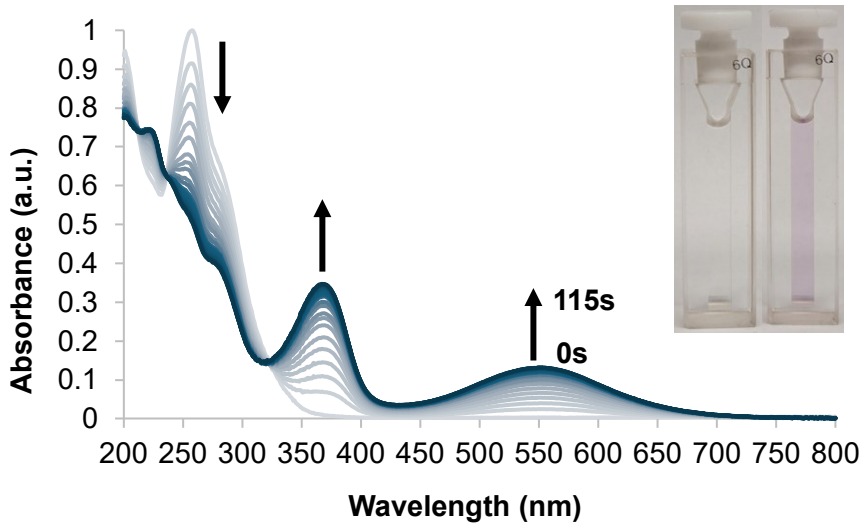

Figure 2-13 The UV-visible absorption spectrum of the mixture of products from the reaction of *bis*-ester dithienylfuran with singlet oxygen before and after irradiation with 254 nm UV light in the methanol-water solvent mix.

Endoperoxide Rearrangement

As evidenced by thin-layer chromatography, multiple photochromic and non-photochromic spots were detected as the reaction of singlet oxygen with dithienylfuran proceeded. This observation can be attributed to the instability or reactivity of the furan endoperoxide product.

Due to the combination of the weak O–O peroxide bond and the ring strain, the furan endoperoxide has limited thermal stability at ambient conditions and is known to be stable only at very low temperatures. At ambient temperatures, they can rearrange or react spontaneously with another molecule, forming a mixture of products. The rearrangement or reaction pathways are initiated via the cleavage of the O–O bond or the C–O bond. The reaction environment and the substitution pattern of furan dictate the mechanistic pathway taken. The main products of 2,5-substituted furans are 1,4-dicarbonyl compounds, and in the case of 3,4-substituted furans, 2-furanone derivatives are usually the major products.[36,37,42]

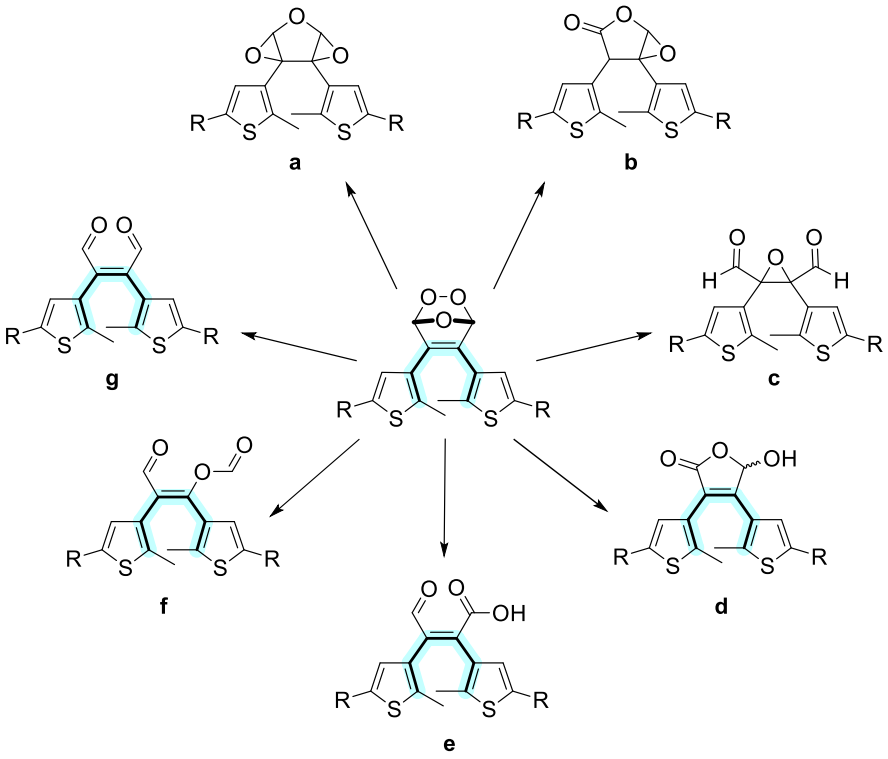

Figure 2-14 Expected products from the furan endoperoxide rearrangement in aprotic solvents. Except for products a, b, and c, the other species possess the necessary 1,3,5-hexatriene system typical of diarylethene photoswitches.

The influence of solvents on the mechanistic pathway has been extensively studied in the literature. In aprotic solvents, the expected endoperoxide rearrangement pathways lead to the formation of epoxides (diepoxide and epoxy lactone), 1,4-dicarbonyl, 4-oxo-2-ene carboxylic acid, and 3-oxo-1-ene-1-formate derivatives. Epoxide derivatives are formed via the homolytic cleavage of the O–O bond. Cleavage of the C–O bond leads to the formation of a 2-hydroxy-5-hydroperoxide intermediate derivative, which can rearrange further to give 4-oxo-2-ene carboxylic acid and 3-oxo-1-ene-1-formate derivatives.[36,37,42]

In alcoholic solvents, the *cis*- and *trans*-2-alkoxy-5-hydroperoxide derivatives are formed as the major intermediate product. The alkoxy hydroperoxide can undergo dehydration to form a 5-alkoxy furan-2-one derivative. For the reaction in methanol, if the hydroperoxide reacts with a water molecule, the 5-methoxy-2-hydroxy derivative is obtained; however, if the hydroperoxide reacts with a methanol molecule, a 2,5-dimethoxy derivative of 2,5-dihydrofuran forms. Since the homolytic cleavage of the O–O

bond, and the C–O bond cleavage and rearrangement are also possible in alcohols, epoxides, and other products observed in aprotic solvents can also be obtained.[36,37,42]

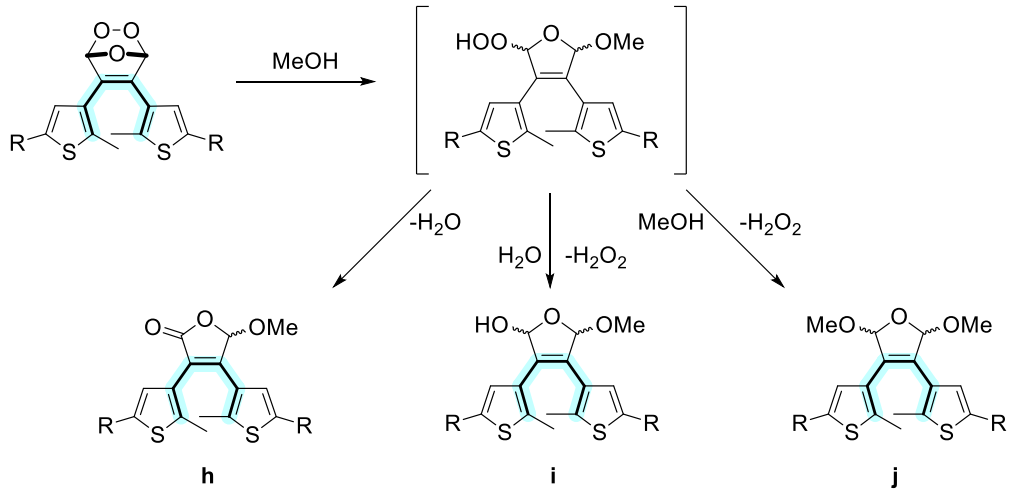

Figure 2-15 Some expected furan endoperoxide products in methanol as solvent.

Due to the unstable nature of some of the molecules, isolation and characterization of all the reaction products were not practical. Since the project aimed to create a hexatriene system in the dithienylfuran molecule, and tetrahydrofuran reactions generated non-photochromic products, further analysis of the reaction mixture was not undertaken. However, mass spectrometry provided preliminary evidence supporting the predicted reaction pathways. The exact mass of all the expected products except the dialdehyde product (g), as shown in Scheme 4, is 436.1 g/mol. This corresponded to the molecular ion peak observed in the mass spectrum of the tetrahydrofuran reaction mixtures.

The number of probable reaction products is far greater in the case of methanol reactions than in the tetrahydrofuran reaction. Expected products **a** to **f** and **h** have an exact mass of 436.1 g/mol; product **g** is 420.1 g/mol, product **i** is 452.1 g/mol, and product **j** is 464.1 g/mol. The molecular ion peaks in the mass spectrum of the methanol reaction mixture corresponded to product **i**. Microscale column chromatography was performed to isolate and analyze the reaction products using silica gel as the stationary phase. Elution was done with a gradient of 0% to 100% ethyl acetate in hexane solvent system, and 1 mL fractions were collected. The spot with Rf = 0.10 was successfully

isolated. However, the baseline product did not elute even with 100% ethyl acetate or 100% methanol. This suggests that the components at the baseline are highly polar or strongly adsorbed to the silica gel.

The ^{1}H NMR of all the stereoisomers of the expected product i was predicted individually and as mixtures using the ACD Labs NMR prediction software. The predicted data for the crucial signals of the products were then compared with the ^{1}H NMR of the isolated product. Most of the signals in the expected spectrum matched the product's 1H NMR. However, four signals in the aromatic region were observed instead of the expected two for each of the thiophenes. Additional singlets were also observed in the 1H NMR spectrum around 3.80 ppm. Since the decomposition product of the calcium peroxide diperoxohydrate is calcium hydroxide, it was hypothesized that the transesterification of the ethyl ester groups with the solvent methanol was taking place in the reaction mixture. The ^{1}H NMR of the four esterification products was predicted again, and four signals in the aromatic region and the singlets around 3.80 ppm were observed in the expected spectrum, which matched with that of the isolated product. Since the transesterification reaction did not affect the formation of the hexatriene core on the diarylethene system, further analysis was not taken up.

Photooxidation

Initial tests of photosensitized reactions of *bis*-ester dithienylfuran with singlet oxygen were conducted in three different solvents: acetonitrile, benzene, and methanol. Equimolar benzophenone and duroquinone solutions with *bis*-ester dithienylfuran were prepared in aerated solvents. The solutions were then stirred, placed 1 cm away from the UV light source, and irradiated for 60-second intervals alongside the controls. Irradiation with high-energy UV light for over 300 seconds led to a discernible color change in the control solutions. Therefore, the samples were only irradiated for a total of 300 seconds.

For benzophenone (B) photosensitized reactions, the benzene solution turned pale blue, and the acetonitrile solution changed to light grey upon UV light exposure. A very faint change in the methanol solution was observed.

Figure 2-16 Benzophenone (B) and duroquinone (DQ) photosensitized solutions of *bis*-ester dithienylfuran solutions in benzene, acetonitrile, and methanol, before (top) and after (bottom) irradiation with 254 nm UV light.

The duroquinone (DQ) solutions showed a more profound color change in all three solvents. After UV irradiation, the benzene solution turned blue, the acetonitrile solution changed to bluish-grey, and the methanol solution turned deep purple.

Aliquots were taken from the mixtures before and after irradiation with UV light and diluted to make 2.25×10^{-4} M solutions of *bis*-ester dithienylfuran reaction products. UV-visible absorption spectra were collected for the samples, which showed a typical diarylethene behavior. Since the mixture also contained benzophenone or duroquinone, which was absorbed in a region similar to the ring-open form of the diarylethene photoswitches, no change in absorption bands was visible upon irradiation. However, new bands in the area where the ring-closed form absorbs started to appear, as seen with the calcium peroxide diperoxohydrate as the singlet oxygen source.

Aliquots were taken from the mixtures before and after irradiation with UV light and diluted to make 2.25×10^{-4} M solutions of *bis*-ester dithienylfuran reaction products. UV-visible absorption spectra were collected for the samples, which showed a typical diarylethene behavior. Since the mixture also contained benzophenone or duroquinone, which was absorbed in a region similar to the ring-open form of the diarylethene photoswitches, no change in absorption bands was visible upon irradiation. However, new bands in the area where the ring-closed form absorbs started to appear, as seen with the calcium peroxide diperoxohydrate as the singlet oxygen source.

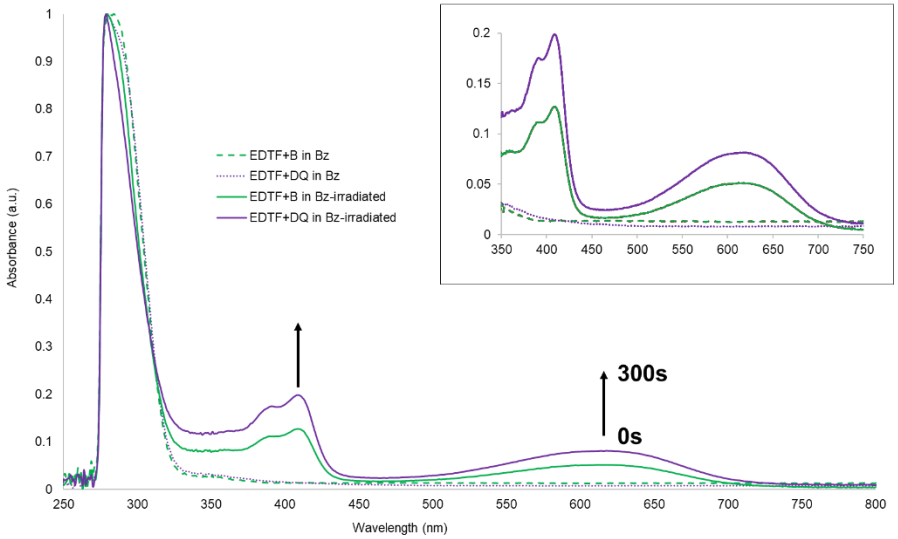

Figure 2-17 UV-visible absorption spectrum of the mixture of benzophenone (B) and duroquinone (DQ) of *bis*-ester dithienylfuran with singlet oxygen before and after irradiation with 254 nm UV light in methanol.

It is worth mentioning here that photosensitized oxidation reactions with benzophenone and duroquinone can proceed through both Type I and Type II processes. The Type II process involves singlet oxygen as the oxidizing agent, while the Type I process proceeds through photoinduced electron transfer. The reactive oxygen species generated in the Type I process are the superoxide anion radical and the hydroperoxyl radical. Since the experiment's motivation was to photooxidize the dithienylfuran molecule, no distinction was made on whether the Type I or Type II process was followed in these reactions.

Reaction with Other Reactive Oxygen Species

Adding 50 % hydrogen peroxide to a solution of *bis*-ester dithienylfuran in methanol did not result in any observable changes, even after stirring for 24 hours at room temperature. However, the reaction with Fenton's reagent yielded a mix of photochromic molecules, similar to the reaction with singlet oxygen.

The active reactive oxygen species groups in Fenton's reagent are hydroxyl anion, hydroxyl radicals, and hydroperoxyl radicals. Upon adding Fenton's reagent, the colorless solution changed to deep orange. The TLC of the mixture showed new photochromic spots, two of which were the most prominent at Rf values of 0.14 and 0.40. The reaction mixture was irradiated with 254 nm UV light; however, no color

change was observed in the orange solution. The reaction mixture was extracted with ethyl acetate, evaporated to dryness, and redissolved in methanol. Irradiation of this solution with 254 nm UV light resulted in a color change from colorless to purple.

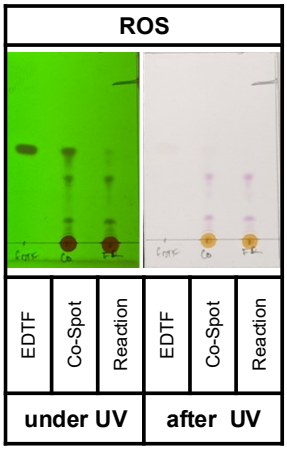

Figure 2-18 TLC plate for the reaction of *bis*-ester dithienylfuran with Fenton's reagent showing photochromic spots.

Similar to the endoperoxide reaction, multiple products were expected and observed in the reaction of *bis*-ester dithienylfuran with Fenton's reagent. The hydroxyl radical attacks the 2- and 5-positions of furan and forms 2,5-dihydroxy-2,5-dihydrofuran intermediate species. If this intermediate species reacts with methanol, it forms a 5-methoxy-2-hydroxy derivative of 2,5-dihydrofuran, which can further react with the second methanol molecule to form a 2,5-dimethoxy derivative. If the intermediate species reacts with the hydrogen peroxide, one of the hydroxy groups is oxidized to give the 5-hydroxy-furan-2-one derivative, which can react with alcohol to provide a 5-methoxy-furan-2-one derivative.

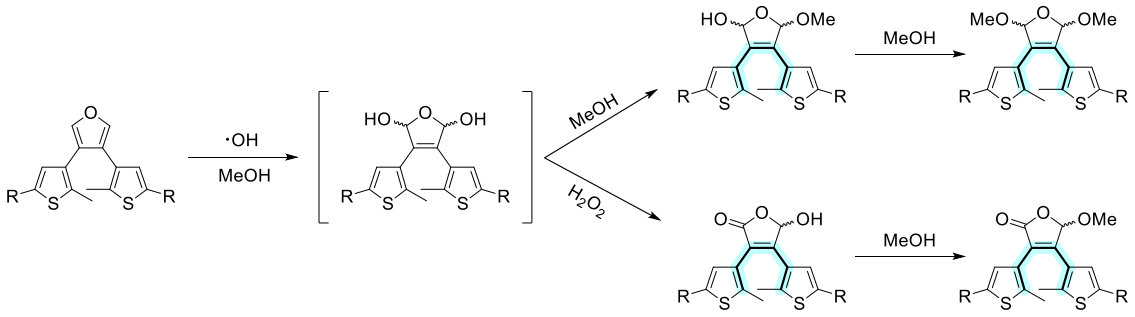

Figure 2-19 Expected products from the reaction of dithienylfuran with hydroxyl radicals in methanol.

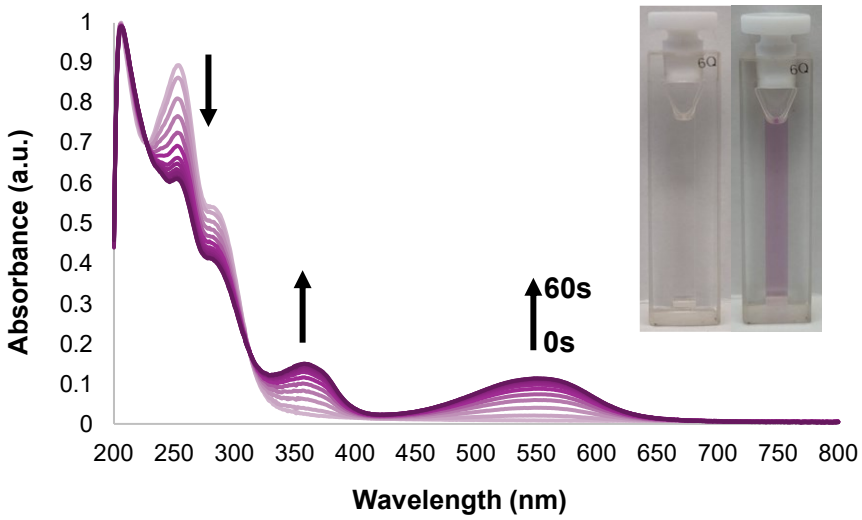

Figure 2-20 The UV-visible absorption spectrum of the products (1.25×10^{-5} M) was obtained from the reaction between *bis*-ester dithienylfuran and Fenton's reagent before and after irradiation with 254 nm UV light.

UV-visible absorption spectroscopy monitored the photoinduced ring-closing of the products in methanol. Aliquots were taken from the methanol solution of reaction products and diluted to make a 1.25×10^{-5} M solution. The cuvette was kept at a 1 cm distance from the UV lamp and irradiated with 254 nm light. The absorption spectra were acquired after regular 5-second irradiation intervals. The absorption spectra of the reaction products in methanol at 0 seconds of UV exposure showed peaks centered at 254 nm. Irradiation of the solution with UV light decreased the intensity of the absorption peaks in the UV region. Two new absorption peaks centered around 358 nm and 554 nm appeared, and the colorless solution changed to purple. After 60 seconds of irradiation, no change in absorption was observed, meaning the PSS was reached. Irradiation with visible light (>450 nm) bleached the purple solution back to colorless.

2.5. Limitations

This new absorption-based system for singlet oxygen detection shares some limitations with other indirect detection methods. First, the detection process consumes singlet oxygen to give a readout signal, making it unsuitable for monitoring processes where singlet oxygen interacts with another target. Second, the microenvironment affects indirect detection systems, especially in biological processes. An external factor,

such as the presence of other reactive species, may influence the color change, producing a false positive or negative result.

Furthermore, colorimetric sensors are limited by their suitability in colored environments. Observing color changes in a deep-colored solution or solid matrix is challenging. This limitation makes the system unsuitable for detecting singlet oxygen released from photosensitizers that absorb in the visible region, such as methylene blue and rose Bengal, especially at high concentrations.

2.6. Future Work

The following vital steps in optimizing the colorimetric detection method are a) designing a probe that forms a more stable endoperoxide and b) modifying the system for testing in purely aqueous environments.

The biggest challenge with heteroarene-based endoperoxides is their stability at ambient temperatures. Furan endoperoxide is unstable at temperatures above -15 ˚C, but several furan derivatives are known to form stable endoperoxides.[37]

Figure 2-21 Proposed dithienylfuran derivatives that may form room-temperature stable endoperoxides.

EDG in positions 2- and 5- of the furan increases the corresponding endoperoxide's stability. Endoperoxide of 2,5-dimethylfuran is known to be stable up to 20 ˚C. Similarly, the 2,5-diphenylfuran endoperoxides are stable at room temperature.

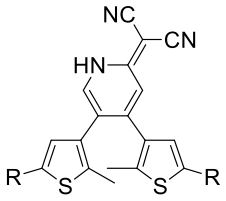

Figure 2-22 Proposed 1,2-dihydropyridine-based pre-diarylethene that may form stable catch and release photoswitches for singlet oxygen.

Other butadiene-containing groups can also be tested in place of furan. 1,2-dihydropyridine and its analogues also undergo a Diels-Alder reaction with singlet oxygen and have emerged as stable traps for singlet oxygen. Some analogues of 1,2-dihydropyridine were demonstrated to store singlet oxygen as endoperoxides and thermally release it at 50 ˚C.

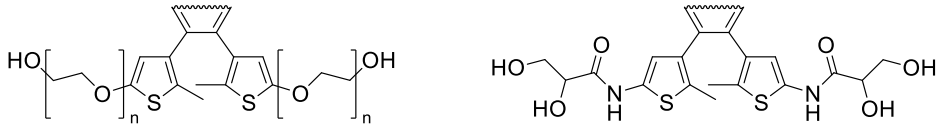

Figure 2-23 Proposed polyethylene glycol and 2,3-dihydroxypropylamide side groups based pre-diarylethene photoswitches for increased water solubility.

The versatile nature of diarylethene molecules is due to the ability to modify the R groups on the thiophene. Depending on the sensing requirement, the R group can easily be modified. For sensing applications in aqueous conditions, groups such as 2,3-dihydroxypropylamide or polyethylene glycol groups can be added to increase water solubility. The “R” group modification ability also allows combining this approach with other detection techniques like fluorescence.

2.7. Materials and Instrumentation

Solvents, reagents, catalysts, and precursors used for synthesis, chromatography, UV-visible spectroscopy, and photochemical studies were purchased from Aldrich, Alfa Aesar, Anachemia, Caledon Labs, and Fisher Scientific and used as received. Solvents used for moisture-sensitive reactions were dried by passing through silica gel and leaving on 3 Å / 4 Å molecular sieves for at least 48 hours or passing through steel columns containing activated alumina under nitrogen using an MBraun solvent purification system. Solvents used for the singlet oxygen trapping reaction were degassed via the freeze-thaw cycle. Deuterated solvents for NMR spectroscopy were purchased from Cambridge Isotope Laboratories and Aldrich and used as received or dried with 4 Å molecular sieves for at least 48 hours. Column chromatography was done using silica gel 60 (0.015-0.040 mm or 0.063 to 0.200 mm) purchased from Silicycle Inc.

The ^{1}H and ^{13}C NMR characterizations were performed on a Bruker Avance-400 instrument with a 5 mm inverse probe operating at 400.13 MHz for the ^{1}H NMR and

100.61 MHz for the ^{13}C NMR. Chemical shifts (δ) are reported in parts per million (ppm) relative to tetramethylsilane using the residual solvent peak as a reference. The coupling constants (J) are reported in Hertz. UV-visible absorption spectra were recorded on Varian Cary 300 Bio UV-visible spectrophotometer. High-resolution mass spectroscopy (HRMS) measurements were performed using an Agilent 6210 TOF LC / MS instrument in ESI-(+) mode. Ring-closing reactions were carried out using a lamp to visualize TLC plates at 254 nm (Spectroline E series, 470 μW/cm^2). The ring-opening reactions were carried out using the light of a 150 W halogen photo-optic source passed through a 435 nm cut-off filter to eliminate higher-energy light.

Synthesis

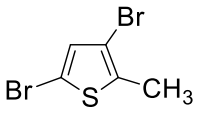

3,5-dibromo-2-methylthiophene- N-bromosuccinimide (89 g, 0.5 mol, 2 eq) was slowly added over 10 minutes to a stirring solution of 2-methylthiophene (24.3 mL, 0.25 mol, 1 eq) in glacial acetic acid (250 mL) at room temperature. The reaction mixture was stirred for an additional 2 hours at room temperature before neutralizing with the addition of aqueous NaOH solution (8% w/v). The reaction mixture was extracted with dichloromethane (3 × 100 mL), and organic phases were combined and washed with saturated aqueous sodium thiosulfate, water, and brine solution. The organic phase was dried over anhydrous $MgSO_4$, filtered, and concentrated under a vacuum to give a dark, oily crude product. The crude product was purified by vacuum distillation to provide 51 g (80%) of 3,5-dibromo-2-methylthiophene as a clear, colorless oil.

^1H NMR- (400 MHz, $CDCl_3$)- δ- 6.86 (s, 1H), 2.34 (s, 3H)

^{13}C NMR- (101 MHz, $CDCl_3$)- δ- 136.0, 131.1, 108.9, 108.6, 14.9

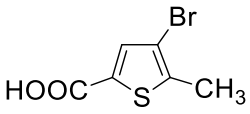

4-bromo-5-methylthiophene-2-carboxylic acid- To a stirred solution of 3,5-dibromo-2-methylthiophene (25.96 g, 0.1 mol, 1 eq) in dry tetrahydrofuran (250 mL) at -78 ^oC, n-

BuLi (2M in hexanes, 50 mL, 0.1 mol, 1 eq) was added for 30 minutes. The reaction mixture was stirred at -78 °C for 30 minutes, and then CO_2 gas was bubbled in the solution for 3 hours. The reaction mixture was allowed to slowly warm to room temperature, and the reaction was stirred for an additional 3 hours. Hydrochloric acid 6N (100 mL) was carefully added dropwise, and the reaction mixture was extracted with diethyl ether (4 × 50 mL). The combined organic layers were washed with brine, dried in anhydrous $MgSO_4$, filtered, and concentrated under vacuum to give 20.34 g (92%) of 4-bromo-5-methylthiophene-2-carboxylic acid as a white solid.

^{1}H NMR- (400 MHz, $CDCl_3$) δ- 13.02 (br s, 1H), 7.60 (s, 1H), 2.42 (s, 3H)

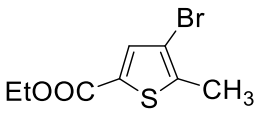

Ethyl 4-bromo-5-methylthiophene-2-carboxylate- To a stirred solution of 4-bromo-5-methylthiophene-2-carboxylic acid (11.05 g, 0.05 mol, 1 eq) in ethanol (150 mL), 12N Hydrochloric acid (6.5 mL) was added, and the reaction was refluxed for 72 hours. Most of the ethanol was evaporated under vacuum, and the remaining mixture was redissolved in dichloromethane. The mixture was washed with saturated aqueous sodium bicarbonate, water, and brine solution. The organic phase was dried over anhydrous $MgSO_4$, filtered, and concentrated under a vacuum to give 10.96 g (88%) of ethyl 4-bromo-5-methylthiophene-2-carboxylate as a brown oil.

^{1}H NMR- (400 MHz, $CDCl_3$) δ- 7.55 (s, 1H), 4.30 (q, 2H), 2.40 (s, 3H), 1.33 (t, 3H)

^{13}C NMR- (101. MHz, $CDCl_3$) δ- 161.1, 142.05, 135.4, 130.5, 110.1, 61.2, 15.3, 14.2

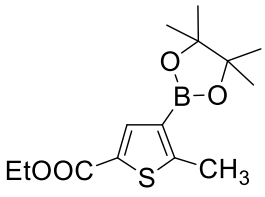

Ethyl 5-methyl-4-(4,4,5,5-tetramethyl-1,3,2-dioxaborolan-2-yl)thiophene-2-carboxylate- Ethyl 4-bromo-5-methylthiophene-2-carboxylate (6.23 g, 0.025 mol, 1 eq), *bis*(pinacolato)diboron (6.98 g, 0.0275 mol, 1.1 eq), $PdCl_2$(dppf)-CH_2Cl_2 adduct (0.612 g, 0.75 mmol, 0.03 eq), dppf (0.416 g, 0.75 mmol, 0.03 eq) and potassium acetate (4.9 g,

0.05 mol, 2 eq) were added in 1,4-dioxane (200 mL) and the mixture was bubbled with Argon gas for 30 minutes. The reaction mixture was heated at 85 °C for 48 hours in an oil bath. After cooling, water (50 mL) was added and extracted with ethyl acetate (3 × 100 mL). Organic layers were combined, washed with brine, dried in anhydrous $MgSO_4$, and concentrated under a vacuum. The crude product was purified by column chromatography on silica gel (0-40% EtOAc/Hexane) to yield 5.11 g (69%) of ethyl 5-methyl-4-(4,4,5,5-tetramethyl-1,3,2-dioxaborolan-2-yl) thiophene-2-carboxylate as an off white solid.

^{1}H NMR- (400 MHz, $CDCl_3$) δ- 7.88 (s, 1H), 4.28 (q, 2H), 2.68 (s, 3H), 1.33 (t, 3H), 1.31 (s, 12H)

HRMS (ESI): m/z (M+H) calculated for $C_{14}H_{21}BO_4S$: 197.133712, found: 197.133746

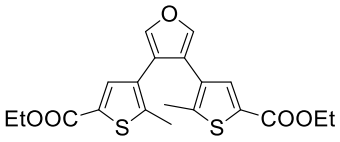

Diethyl 4,4'-(furan-3,4-diyl)*bis*(5-methylthiophene-2-carboxylate) (1)- 3,4-Dibromo furan (1.13 g, 0.005 mol, 1 eq), ethyl 5-methyl-4-(4,4,5,5-tetramethyl-1,3,2-dioxaborolan-2-yl)thiophene-2-carboxylate (3.7 g, 0.0125 mol, 2.5 eq), $Pd(PPh_3)_4$ (1.1 g, 0.001 mol, 0.2 eq) and K_2CO_3 (2.76 g, 0.02 mol, 4 eq) were added to 1,4-dioxane (100 mL) and the mixture was bubbled with Argon gas for 1 hour. The reaction mixture was then refluxed overnight. After being cooled to room temperature, water was added, and the reaction mixture was extracted with ethyl acetate (3 × 75 mL). The combined organic phases were washed with brine, dried in anhydrous $MgSO_4$, filtered, and concentrated under a vacuum. Purifying the crude with silica gel (0-20% EtOAc/Hexane) yielded a gel-like solid. Recrystallization of the gel with methanol yielded 1.11 g (55%) of Diethyl 4,4'-(furan-3,4-diyl) *bis*(5-methylthiophene-2-carboxylate) as white crystals.

^{1}H NMR- (400 MHz, $CDCl_3$) δ 7.51 (s, 2H), 7.39 (s, 2H), 4.31 (q, 4H), 2.2 (s, 6H), 1.34 (t, 3H)

^{13}C NMR- (101 MHz, $CDCl_3$) δ- 162.0, 143.7, 141.0, 135.1, 129.9, 120.3, 61.0, 14.5

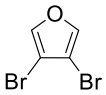

3,4-Dibromofuran- Trans-2,3-dibromo-butene-1,4-diol (24.59 g, 0.1 mol, 1 eq) was added to 7.5% sulfuric acid (80 mL) and heated to 85 °C. Potassium dichromate (29.42 g, 0.1 mol, 1 eq), and conc. Sulfuric acid (25 mL) was added to water (125 mL) to prepare a solution, and this solution was added to the previous reaction mixture dropwise for 5 hours, with the simultaneous steam distillation of the product. After the addition was complete, the distillation was continued for another 1 hour. The distillate was extracted with dichloromethane (4 × 100 mL), and the combined organic layers were dried over anhydrous $MgSO_4$, filtered, and concentrated under vacuum to yield 6.77 g (30%) of 3,4-dibromofuran as a clear colorless liquid. 3,4-Dibromofuran degrades rapidly, even at -18 °C; storing it as a hexane solution slows down the degradation.

^{1}H NMR- (400 MHz, $CDCl_3$) δ- 7.45 (s, 2H)

^{13}C NMR- (101 MHz, $CDCl_3$) δ- 141.1, 104.2

Calcium peroxide octahydrate - A solution of calcium chloride (6.71 g, 0.061 mol) and 50% H_2O_2 (17.6 mL, 0.3 mol) in water (232 mL) was prepared in a volumetric flask. Half of this solution was added to a 250 mL Erlenmeyer flask and covered with perforated parafilm. The Erlenmeyer flask was placed inside a closed vessel containing 14% aqueous ammonia (200 mL). The whole system was kept at 4 °C for one week, after which the crystalline precipitate was collected by filtration, washed with cold water and acetone, and produced 9.1 g (69%) of $CaO_2.8H_2O$ as white crystals.

Calcium peroxide diperoxohydrate – Calcium peroxide octahydrate (1 g, 4.6 mmol) crystals were ground to a fine powder with a mortar and pestle. 6 mL of 50% hydrogen peroxide was added to this, and the turbidity of the suspension decreased rapidly initially and then increased as a new precipitate formed. The precipitate is quickly filtered after stirring the suspension at -15 °C for 1 hour. The precipitate is stirred in 6 mL of 50% hydrogen peroxide for an additional 1 hour at -15 °C, filtered rapidly, and stored at -78 °C. The yield of the residue was 0.58 g (90%).

General oxidation reactions of *bis*-ester dithienylfuran

With calcium peroxide diperoxohydrate as the source: A solution of *bis*-ester dithienylfuran **1** (10.0 mg, 0.025 mmol, 1 eq) in 500 µl of solvent was treated with freshly prepared $CaO_2.2H_2O_2$ (17.5 mg, 0.125 mmol, 5 eq). The reaction mixture was stirred in a 25 °C water bath and monitored by TLC. After the dithienylfuran was consumed, the cream-colored suspension was filtered to remove the insoluble residue, and the solvent was evaporated to obtain the reaction product mixture as an off-white solid.

With benzophenone as the source: To a solution of *bis*-ester dithienylfuran **1** (1.0 mg, 0.0025 mmol, 1 eq) in 500 µl of aerated solvent, benzophenone (1.37 mg, 0.0075 mmol, 3 eq) was added. The solution was stirred and irradiated with 254 nm UV light from a distance of 1 cm, and the reaction progress was monitored with TLC.

With duroquinone as the source: To a solution of *bis*-ester dithienylfuran **1** (1.0 mg, 0.0025 mmol, 1 eq) in 500 µl of aerated solvent, duroquinone (1.23 mg, 0.0075 mmol, 3 eq) was added. The solution was stirred and irradiated with 254 nm UV light from a distance of 1 cm, and the reaction progress was monitored with TLC.

With Fenton’s reagent- Ferrous sulfate heptahydrate (6.95 mg, 0.025 mmol, 1 eq) was dissolved in 474 µl of distilled water, and 3% w/w hydrogen peroxide (26.0 µl, 0.025 mmol, 1 eq) was added to it while stirring to prepare a 0.025 mmol solution of Fenton's reagent. *Bis*-ester dithienylfuran (10.0 mg, 0.025 mmol, 1 eq) was dissolved in 1 mL of methanol, and freshly prepared Fenton's reagent was added to it dropwise over 5 minutes. The clear solution was stirred at room temperature and monitored with TLC. When the reaction reached equilibrium, 2 mL of ethyl acetate was added, and the organic layer was separated. After drying with anhydrous $MgSO_4$, the solvent was evaporated under a vacuum to yield a white solid.

2.8. References

(1) Ciesielka, A. Singlet Oxygen Discovery. Eur. J. Clin. Exp. Med. 2021, 19 (4), 318–321. https://doi.org/10.15584/ejcem.2021.4.5.

(2) Bayr, H. Reactive Oxygen Species: Crit. Care Med. 2005, 33 (Suppl), S498–S501. https://doi.org/10.1097/01.CCM.0000186787.64500.12.

(3) Kearns, D. R. Physical and Chemical Properties of Singlet Molecular Oxygen. Chem. Rev. 1971, 71 (4), 395–427. https://doi.org/10.1021/cr60272a004.

(4) DeRosa, M. Photosensitized Singlet Oxygen and Its Applications. Coord. Chem. Rev. 2002, 233–234, 351–371. https://doi.org/10.1016/S0010-8545(02)00034-6.

(5) Ohloff, G. Singlet Oxygen: A Reagent in Organic Synthesis. In Organic Synthesis; Elsevier, 1975; pp 481–502. https://doi.org/10.1016/B978-0-408-70725-1.50014-8.

(6) Wasserman, H. H.; Ives, J. L. Singlet Oxygen in Organic Synthesis. Tetrahedron 1981, 37 (10), 1825–1852. https://doi.org/10.1016/S0040-4020(01)97932-3.

(7) Devasagayam, T. P. A.; Kamat, J. P. Biological Significance of Singlet Oxygen. Indian J Exp Biol. 2002, 40 (6), 680-92.

(8) Politzer, I. R.; Griffin, G. W.; Laseter, J. L. Singlet Oxygen and Biological Systems. Chem. Biol. Interact. 1971, 3 (2), 73–93. https://doi.org/10.1016/0009-2797(71)90088-3.

(9) Koh, E.; Fluhr, R. Singlet Oxygen Detection in Biological Systems: Uses and Limitations. Plant Signal. Behav. 2016, 11 (7), e1192742. https://doi.org/10.1080/15592324.2016.1192742.

(10) Di Mascio, P.; Martinez, G. R.; Miyamoto, S.; Ronsein, G. E.; Medeiros, M. H. G.; Cadet, J. Singlet Molecular Oxygen Reactions with Nucleic Acids, Lipids, and Proteins. Chem. Rev. 2019, 119 (3), 2043–2086. https://doi.org/10.1021/acs.chemrev.8b00554.

(11) Davies, M. J. Singlet Oxygen-Mediated Damage to Proteins and Its Consequences. Biochem. Biophys. Res. Commun. 2003, 305 (3), 761–770. https://doi.org/10.1016/S0006-291X(03)00817-9.

(12) Cui, S.; Guo, X.; Wang, S.; Wei, Z.; Huang, D.; Zhang, X.; Zhu, T. C.; Huang, Z. Singlet Oxygen in Photodynamic Therapy. Pharmaceuticals 2024, 17 (10), 1274. https://doi.org/10.3390/ph17101274.

(13) Bradley, D. G.; Lee, H. O.; Min, D. B. Singlet Oxygen Detection in Skim Milk by Electron Spin Resonance Spectroscopy. J. Food Sci. 2003, 68 (2), 491–494. https://doi.org/10.1111/j.1365-2621.2003.tb05700.x.

(14) Min, D. B.; Boff, J. M. Chemistry and Reaction of Singlet Oxygen in Foods. Compr. Rev. Food Sci. Food Saf. 2002, 1 (2), 58–72. https://doi.org/10.1111/j.1541-4337.2002.tb00007.x.

(15) Enko, B.; Borisov, S. M.; Regensburger, J.; BäumLer, W.; Gescheidt, G.; Klimant, I. Singlet Oxygen-Induced Photodegradation of the Polymers and Dyes in Optical Sensing Materials and the Effect of Stabilizers on These Processes. J. Phys. Chem. A 2013, 117 (36), 8873–8882. https://doi.org/10.1021/jp4046462.

(16) Nidheesh, P. V.; Boczkaj, G.; Ganiyu, S. O.; Oladipo, A. A.; Fedorov, K.; Xiao, R.; Dionysiou, D. D. Generation, Properties, and Applications of Singlet Oxygen for Wastewater Treatment: A Review. Environ. Chem. Lett. 2025, 23 (1), 195–240. https://doi.org/10.1007/s10311-024-01798-0.

(17) Eisenberg, W. C.; DeSilva, M. Atmospheric Gas Phase Generation of Singlet Oxygen by Homogeneous Photosensitization. Tetrahedron Lett. 1990, 31 (41), 5857–5860. https://doi.org/10.1016/S0040-4039(00)97978-4.

(18) Schmidt, R. Photosensitized Generation of Singlet Oxygen. Photochem. Photobiol. 2007, 82 (5), 1161–1177. https://doi.org/10.1562/2006-03-03-IR-833.

(19) You, Y. Chemical Tools for the Generation and Detection of Singlet Oxygen. Org. Biomol. Chem. 2018, 16 (22), 4044–4060. https://doi.org/10.1039/C8OB00504D.

(20) Hicks, A.; Norberg, S.; Shawcross, P.; Lempert, W. R.; Rich, J. W.; Adamovich, I. V. Singlet Oxygen Generation in a High Pressure Non-Self-Sustained Electric Discharge. J. Phys. Appl. Phys. 2005, 38 (20), 3812–3824. https://doi.org/10.1088/0022-3727/38/20/007.

(21) Kiselev, V. M.; Kislyakov, I. M.; Burchinov, A. N. Generation of Singlet Oxygen on the Surface of Metal Oxides. Opt. Spectrosc. 2016, 120 (4), 520–528. https://doi.org/10.1134/S0030400X16040123.

(22) Khan, A. U.; Kasha, M. Red Chemiluminescence of Molecular Oxygen in Aqueous Solution. J. Chem. Phys. 1963, 39 (8), 2105–2106. https://doi.org/10.1063/1.1734588.

(23) Bader, L. W.; Ogryzlo, E. A. Reactions of O2(1ΔG) and O2(1Σ+g). Discuss. Faraday Soc. 1964, 37, 46. https://doi.org/10.1039/df9643700046.

(24) Nardi, G.; Manet, I.; Monti, S.; Miranda, M. A.; Lhiaubet-Vallet, V. Scope and Limitations of the TEMPO/EPR Method for Singlet Oxygen Detection: The Misleading Role of Electron Transfer. Free Radic. Biol. Med. 2014, 77, 64–70. https://doi.org/10.1016/j.freeradbiomed.2014.08.020.

(25) Krieg, M. Determination of Singlet Oxygen Quantum Yields with 1,3-Diphenylisobenzofuran in Model Membrane Systems. J. Biochem. Biophys. Methods 1993, 27 (2), 143–149. https://doi.org/10.1016/0165-022X(93)90058-V.

(26) Umezawa, N.; Tanaka, K.; Urano, Y.; Kikuchi, K.; Higuchi, T.; Nagano, T. Novel Fluorescent Probes for Singlet Oxygen. Angew. Chem. Int. Ed. 1999, 38 (19), 2899–2901. https://doi.org/10.1002/(SICI)1521-3773(19991004)38:19<2899::AID-ANIE2899>3.0.CO;2-M.

(27) Ye, Z.; Song, B.; Yin, Y.; Zhang, R.; Yuan, J. Development of Singlet Oxygen-Responsive Phosphorescent Ruthenium(Ii) Complexes. Dalton Trans. 2013, 42 (40), 14380. https://doi.org/10.1039/c3dt52020j.

(28) Song, D.; Cho, S.; Han, Y.; You, Y.; Nam, W. Ratiometric Fluorescent Probes for Detection of Intracellular Singlet Oxygen. Org. Lett. 2013, 15 (14), 3582–3585. https://doi.org/10.1021/ol401421r.

(29) Sugioka, K.; Nakano, M.; Kurashige, S.; Akuzawa, Y.; Goto, T. A Chemiluminescent Probe with a Cypridina Luciferin Analog, 2-methyl-6-phenyl-3,7-dihydroimidazo[1,2-a]Pyrazin-3-one, Specific and Sensitive for O2− Production in Phagocytizing Macrophages. FEBS Lett. 1986, 197 (1–2), 27–30. https://doi.org/10.1016/0014-5793(86)80291-5.

(30) Shellum, C. L.; Birks, J. W. Photochemical Amplifier for Liquid Chromatography Based on Singlet Oxygen Sensitization. Anal. Chem. 1987, 59 (14), 1834–1841. https://doi.org/10.1021/ac00141a021.

(31) Denham, K.; Milofsky, R. E. Photooxidation of 3-Substituted Pyrroles: A Postcolumn Reaction Detection System for Singlet Molecular Oxygen in HPLC. Anal. Chem. 1998, 70 (19), 4081–4085. https://doi.org/10.1021/ac980416j.

(32) Oliveira, M. S.; Severino, D.; Prado, F. M.; Angeli, J. P. F.; Motta, F. D.; Baptista, M. S.; Medeiros, M. H. G.; Di Mascio, P. Singlet Molecular Oxygen Trapping by the Fluorescent Probe Diethyl-3,3′-(9,10-Anthracenediyl)*Bis*acrylate Synthesized by the Heck Reaction. Photochem. Photobiol. Sci. 2011, 10 (10), 1546–1555. https://doi.org/10.1039/c1pp05120b.

(33) Lemieux, V.; Branda, N. R. Reactivity-Gated Photochromism of 1,2-Dithienylethenes for Potential Use in Dosimetry Applications. Org. Lett. 2005, 7 (14), 2969–2972. https://doi.org/10.1021/ol050971p.

(34) Lemieux, V.; Gauthier, S.; Branda, N. R. Selective and Sequential Photorelease Using Molecular Switches. Angew. Chem. Int. Ed. 2006, 45 (41), 6820–6824. https://doi.org/10.1002/anie.200601584.

(35) Erno, Z.; Asadirad, A. M.; Lemieux, V.; Branda, N. R. Using Light and a Molecular Switch to ‘Lock’ and ‘Unlock’ the Diels–Alder Reaction. Org. Biomol. Chem. 2012, 10 (14), 2787–2792. https://doi.org/10.1039/C2OB06908C.

(36) Gollnick, K.; Griesbeck, A. Singlet Oxygen Photooxygenation of Furans. Tetrahedron 1985, 41 (11), 2057–2068. https://doi.org/10.1016/S0040-4020(01)96576-7.

(37) Feringa, B. L. Photo-Oxidation of Furans. Recl. Trav. Chim. Pays-Bas 2010, 106 (9), 469–488. https://doi.org/10.1002/recl.19871060902.

(38) Altınok, E.; Friedle, S.; Thomas, S. W. Furan-Containing Singlet Oxygen-Responsive Conjugated Polymers. Macromolecules 2013, 46 (3), 756–762. https://doi.org/10.1021/ma3025656.

(39) Pierlot, C.; Nardello, V.; Schrive, J.; Mabille, C.; Barbillat, J.; Sombret, B.; Aubry, J.-M. Calcium Peroxide Diperoxohydrate as a Storable Chemical Generator of Singlet Oxygen for Organic Synthesis. J. Org. Chem. 2002, 67 (8), 2418–2423. https://doi.org/10.1021/jo010766x.

(40) Cuquerella, M. C.; Lhiaubet-Vallet, V.; Cadet, J.; Miranda, M. A. Benzophenone Photosensitized DNA Damage. Acc. Chem. Res. 2012, 45 (9), 1558–1570. https://doi.org/10.1021/ar300054e.

(41) Darmanyan, A. P.; Foote, C. S. Solvent Effects on Singlet Oxygen Yield from n,. Pi.* and. Pi.,. Pi.* Triplet Carbonyl Compounds. J. Phys. Chem. 1993, 97 (19), 5032–5035.

(42) Badovskaya, L. A.; Povarova, L. V. Oxidation of Furans (Review). Chem. Heterocycl. Compd. 2009, 45 (9), 1023–1034. https://doi.org/10.1007/s10593-009-0390-8.

(43) Mee, S. P. H.; Lee, V.; Baldwin, J. E.; Cowley, A. Total Synthesis of 5,5′,6,6′-Tetrahydroxy-3,3′-Biindolyl, the Proposed Structure of a Potent Antioxidant Found in Beetroot (Beta Vulgaris). Tetrahedron 2004, 60 (16), 3695–3712. https://doi.org/10.1016/j.tet.2004.02.043.

Chapter 3.

Chemically Gated Diarylethene-Based Hendrickson's Reagent as a Tool for Reaction Monitoring and O-Nucleophile Detection

Abstract

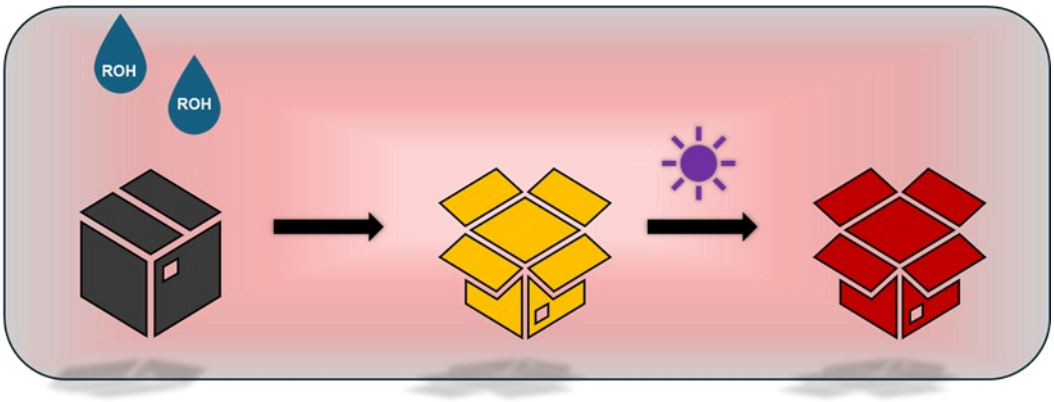

This chapter explores the chemistry-gated photochemistry of a diarylethene molecule to monitor the progress of a reaction and to detect oxygen nucleophiles like alcohol or water. The diarylethene molecule is an analog of Hendrickson's reagent and is locked in the parallel conformation by a P-O-P bond. Hendrickson's reagent is used stoichiometrically for an esterification reaction where the alcohol reacts with one of the electron-deficient phosphorus atoms in the P-O-P bond, breaking one of the phosphorus-oxygen bonds. In the case of the diarylethene analog, the alcohol in the esterification reaction will break one of the phosphorus-oxygen bonds and allow it to acquire the antiparallel conformation necessary for photocyclization. The subsequent color change produced on exposure to light can indicate the reaction's extent. This process can also be utilized for the detection of alcohols, water, and other oxygen nucleophiles.

3.1. Introduction

Tertiary phosphines and their derivatives- ylides, oxides, sulfides, imines, and phosphonium salts- have been extensively employed in synthetic organic chemistry as stoichiometric reagents, nucleophilic organocatalysts, and ligands in coordination complexes. The Appel, Staudinger, Wittig, and Mitsunobu reactions are conventional name reactions that employ tertiary phosphines as stoichiometric reagents.

3.1.1. Mitsunobu Reaction- Mechanism and Drawbacks

The Mitsunobu reaction, discovered by Mitsunobu and Yamada in 1967, is a widely employed method for reactions involving alcohols.[1] Initially reported for the esterification of carboxylic acids, it has since been extended to other functional group transformations, such as ethers, epoxides, azides, and disulfides.

The mechanism involves the formation of a protonated betaine intermediate from the reaction between triphenylphosphine and dialkyl azodicarboxylate. This protonated betaine then reacts with an alcohol to form an oxyphosphonium salt and converts it into a good leaving group. Nucleophilic attack via an SN2-type reaction produces the desired product and phosphine oxide byproduct. The significant drawbacks of the Mitsunobu reaction are: 1) the use of toxic and explosive dialkyl dicarboxylate, 2) the difficult separation of hydrazine and phosphine oxide byproducts from the reaction products, and 3) a competing side reaction involving N-alkylation of the hydrazine dicarboxylate.

3.1.2. Hendrickson's Reagent

In 1975, Hendrickson and Schwartzman proposed a reagent capable of dehydrating alcohols prepared from triphenylphosphine oxide (TPPO) and trifluoromethane sulfonic anhydride (Tf_2O).[2] They initially proposed the reactive species as a monophosphonium ditriflate salt, which was named Hendrickson's reagent. However, in 1979, Husebye and coworkers determined the actual structure of Hendrickson's reagent to be a triphenylphosphonium anhydride trifluoromethane sulfonate complex.[3]

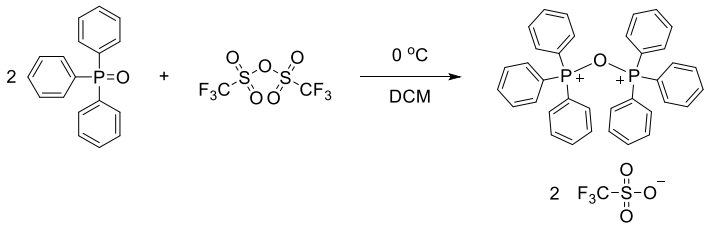

Scheme 3-1 Hendrickson's reagent is prepared by mixing two equivalents of triphenylphosphine oxide (TPPO) and one equivalent of trifluoro sulfonic anhydride (Tf_2O) at 0 °C in anhydrous dichloromethane (DCM).

Hendrickson's reagent is prepared by mixing two equivalents of TPPO and one equivalent of Tf_2O at 0 °C in anhydrous dichloromethane or 1,2-dichloroethane under an inert atmosphere. Initially, a molecule of TPPO reacts with Tf_2O to make a monophosphonium salt, which gets attacked by the second triphenylphosphine oxide molecule, yielding the P-O-P Hendrickson's reagent. The white solid obtained when exposed to air or moisture decomposes rapidly and thus is used without isolation. Structural determination via X-ray crystallography by Kelly and coworkers revealed that the P-O-P bond angle is almost linear at 164.5° and the P-O bond length is approximately 1.60 Å.[4]

3.1.3. Use in Synthetic Organic Chemistry.

Hendrickson's reagent is used as an alternative protocol to the Mitsunobu reaction for various substitution and elimination reactions. Similar to the Mitsunobu reaction, Hendrickson's reagent reacts to form an oxyphosphonium salt, an excellent leaving group. The advantages of using Hendrickson's reagent are 1) toxic and explosive azodicarboxylates are not used, 2) no competing side reaction of hydrazine dicarboxylate, and 3) recovered triphenylphosphine oxide can be reused. However, a notable drawback remains: the removal of triphenylphosphine oxide from the reaction mixture.

Substitution Reactions

Similar to the Mitsunobu reaction, Hendrickson's reagent is mainly used for the esterification reaction between carboxylic acids and alcohols. Adding alcohols to the Hendrickson's reagent results in the formation of an alkoxyphosphonium complex intermediate. A nucleophilic attack of the carboxylic acid on the complex results in the

formation of an ester. If carboxylic acid is added first, acyloxyphosphonium complex forms, which reacts with an alcohol to form esters.[5]

Amides are formed analogously when primary or secondary amines are reacted with carboxylic acids in the presence of Hendrickson's reagent. Amidines are formed when amides react with primary or secondary amines in the presence of Hendrickson's reagent.[5]

Carboxylic acids react with *bis*-nucleophilic species in the presence of Hendrickson's reagent and undergo double dehydration to yield heterocyclic aromatic molecules. The reaction of carboxylic acids with o-phenylenediamine, o-aminophenol, and o-amino thiophenol yields 2-aryl benzimidazoles, 2-aryl benzoxazole, and 2-aryl benzothiazole, respectively.[5]

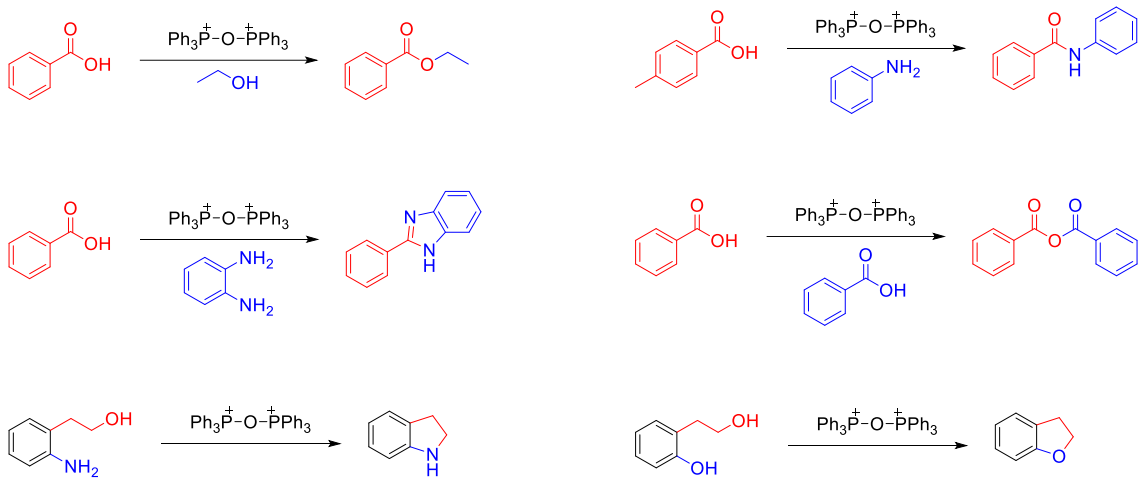

Figure 3-1 Some examples of substitution reactions done with Hendrickson's reagent.

Acid anhydrides are formed when two equivalents of carboxylic acid react with Hendrickson's reagent. The acyloxyphosphonium complex intermediate reacts with the second molecule of carboxylic acid to form an acid anhydride. A base is typically added to the reaction to neutralize the triflic acid formed as the side product.[5]

The reaction of diols and amino alcohols in the presence of a Hendrickson's reagent yields 3-, 5-, and 6-membered cyclic ethers and cyclic amines through intramolecular reactions. In the case of amino alcohols, two nucleophilic groups are present for the phosphonium ion formation; however, the hydroxyl group is preferred due

to a stronger P-O bond compared to the P-N bond. The amine acts as an intramolecular nucleophile, facilitating the ring closure.[6]

Elimination Reactions

Secondary alcohols have been presented to undergo an elimination reaction with Hendrickson's reagent to yield alkenes. Adding Hendrickson's reagent to the secondary alcohol transforms a poor-leaving group (hydroxyl) into a good-leaving group (alkoxyphosphonium salt). Upon heating, the intermediate undergoes an elimination reaction to yield alkenes. When (-)-menthol was treated with Hendrickson's reagent, followed by heating, a mixture of 2-menthene and 3-menthene was observed.[7]

Elimination reactions of secondary alcohols are a template for converting ketones to alkynes. If the alpha-hydrogen is sufficiently acidic, adding Hendrickson's reagent to a ketone results in the formation of an enol-phosphonium intermediate species that undergoes elimination to yield an alkyne.[8]

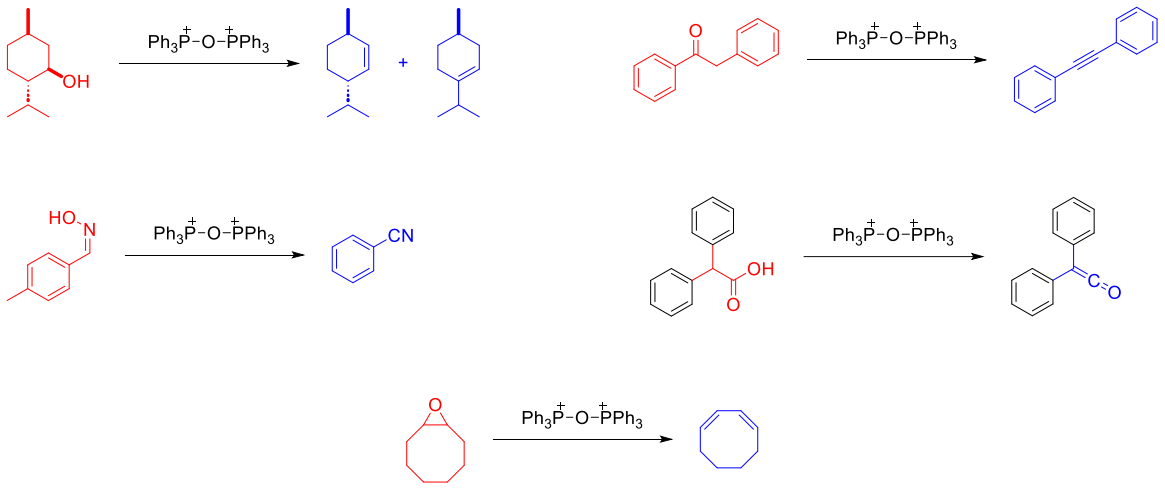

Figure 3-2 Some examples of elimination reactions done with Hendrickson's reagent.

Aldoximes were shown to convert to nitriles when reacted with Hendrickson's reagent. However, unlike the secondary alcohols, the elimination reactions for the aldoximes proceeded at room temperature in most cases.[9]

Carboxylic acids with highly acidic alpha-hydrogen react with Hendrickson's reagent to yield ketenes. In the presence of Hendrickson's reagent, diphenyl acetic acid is dehydrated to yield diphenyl ketene as the product.

Epoxides have been demonstrated to undergo a double-elimination reaction in the presence of a base and heat to yield 1,3-dienes as the product.[10]

3.1.4. Modifications

Since its discovery by Hendrickson, several modifications have been made to Hendrickson's reagent. Crich and Dyker prepared a modification of Hendrickson's reagent with tetrafluoroborate as the counter ion instead of the trifluoromethanesulfonate ion. They demonstrated that the counter ion does not affect the reagent's reactive nature toward dehydration reactions.

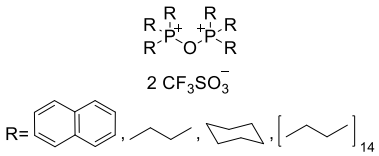

Figure 3-3 Hendrickson's reagent analogues prepared by Mukaiyama and Suda from trinaphthyl-, tributyl-, tricyclohexyl-, and trihexadecyl phosphine oxide.

Mukaiyama and Suda studied the glycosylation reaction of 2,3,5-tri-O-benzyl-D-ribofuranose with cyclohexanol using Hendrickson's reagent prepared from triphenyl-, tributyl-, trinaphthyl-, tricyclohexyl-, and trihexadecylphosphine oxide. Tributylphosphine oxide yielded the best result for the particular reaction, likely due to the optimum balance between steric hindrance and reactivity. The yields from bulkier tricyclohexyl- and trinaphthylphosphine oxides were poor.[11]

While the alternative protocol proposed by Hendricksen solved some of the problems associated with the Mitsunobu reaction, the generation of two equivalents of phosphine oxide still posed a challenge for purification. Due to triphenylphosphine oxide's solubility in most organic solvents, extraction, selective precipitation, or recrystallization is difficult. Large-scale column chromatography is not feasible; hence, reactions that yield triphenylphosphine oxide side products are rarely employed commercially. Therefore, several researchers have done work to alleviate this issue associated with triphenylphosphine oxide.

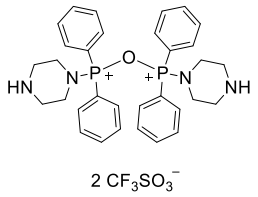

Figure 3-4 Piperazine-based Hendrickson's reagent. The phosphine oxide is soluble in water, facilitating aqueous workup.

Hendrickson and Hussoin reported the preparation of Hendrickson's reagent from 1-(diphenylphosphinyl)piperazine. The reported piperazine-based Hendrickson's reagent can be removed from the reaction mixture by aqueous phase extraction, and the reactivity is demonstrated to be similar to that of the triphenylphosphine oxide-based Hendrickson's reagent.

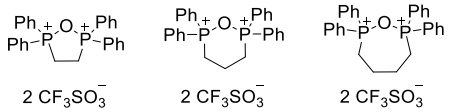

Figure 3-5 Five-, six-, and seven-membered cyclic analogues of Hendrickson's reagent prepared by Jenkins and coworkers.

Jenkins and coworkers synthesized 5-, 6-, and 7-membered cyclic analogues of Hendrickson's reagent from the corresponding *bis*phosphine oxides.[12] The cyclic analogues are advantageous because only one equivalent of phosphine oxide byproduct is produced per reaction, compared to the traditional Hendrickson's reagent, which generates two equivalents of phosphine oxide. Also, the cyclic analogues are more polar as compared to phosphine oxide, which facilitates easier separation by column chromatography. The authors reported using the cyclic Hendrickson's reagents to synthesize esters, amides, 2-oxazolines, and 2-thiazolines.

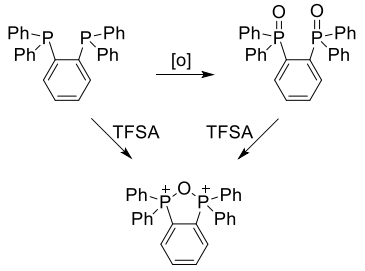

Figure 3-6 The cyclic analog of Hendrickson's reagent prepared by Moussa.

Moussa reported two cyclic analogues prepared from commercially available 1,2-*bis* (diphenylphosphino)benzene. The author oxidized 1,2-*bis* (diphenylphosphino)benzene with hydrogen peroxide to obtain 1,2-*bis* (diphenylphosphoryl)benzene, followed by the addition of triflic anhydride to yield Hendrickson's reagent. The author also reported the formation of Hendrickson's reagent by directly adding one equivalent of triflic anhydride to 1,2-*bis*(diphenylphosphino)benzene, which yielded a mixture of Hendrickson's reagent, 1-(diphenylphosphino)-2 [diphenyl(trifluoromethylsulfonyloxy)phosphonio] benzene and 1,2-*bis*[diphenyl(trifluoromethylsulfonyloxy)phosphonio] benzene with trifluoromethanesufinate as the counter ion in all three.[13]

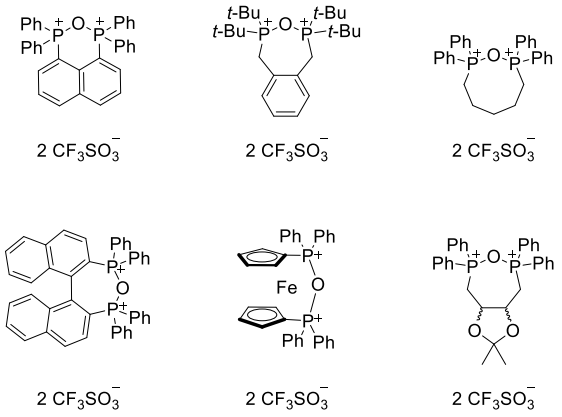

Figure 3-7 Cyclic analogues of Hendrickson's reagent prepared by Walczak and coworkers.

Walczak and coworkers synthesized six new cyclic analogues of Hendrickson's reagent based on the work done by Jenkins and Moussa. The study examined the effects of Hendrickson's reagents' cyclic analogues for preparing *O*-, *N*-, *C*-, and *S*-glycosides. The authors prepared an 8-membered ring derivative similar to the 5-, 6-, and 7-membered rings prepared by Jenkins and coworkers. Like Moussa's Hendrickson's reagent from 1,2-*bis*(diphenyl phosphoryl)benzene, the authors synthesized Hendrickson's reagent from 1,2-*bis*(di-tert-butyl phosphoryl)benzene. Other reported Hendrickson's reagents were prepared from 1,1'-*bis*(diphenylphosphoryl)ferrocene, 1,8-*bis*(diphenylphosphoryl)naphthalene, 2,2'-*bis*(diphenylphosphoryl)(1,1'-binaphthalene), and 2,3-O-isopropylidene-2,3-dihydroxy-1,4-*bis*(diphenylphosphoryl)butane.[14]

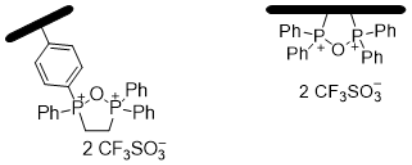

Figure 3-8 Polymer-supported Hendrickson's reagent analogues prepared by Jenkins and coworkers. The polymer can easily be filtered off at the end of the reaction.

Jenkins and coworkers extended the use of the cyclic Hendrickson's reagent analog by incorporating it into polymer support. As Hendrickson's reagent is directly connected to the polymer support, the phosphine oxide byproduct can easily be filtered after the reaction completion.[15] The authors prepared 1,2-*bis*(diphenylphosphinyl)ethane connected to poly(styrene-co-divinylbenzene) and subsequently prepared Hendrickson's reagent by adding Tf_2O. The authors also reported a second polymer-supported Hendrickson's reagent from a commercially available polymer-supported triphenylphosphine. The authors noted that the considerable distance between two phosphoryl groups within the polymer support resulted in a mixture of ditriflate and Hendrickson's reagent.

3.2. Proposed Research

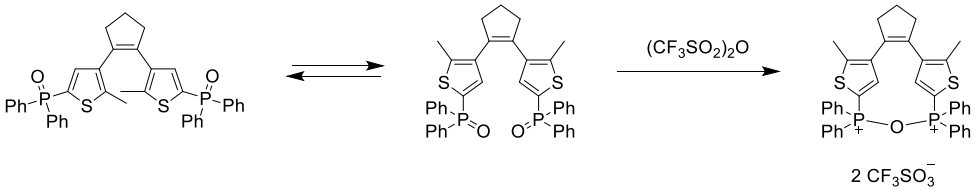

Scheme 3-2 The *parallel* conformation of the *bis*phosphine oxide diarylethene can make Hendrickson's reagent. The molecule will be locked in the photoinactive form.

Based on the cyclic analogues of Hendrickson's reagent prepared by Jenkins, Moussa, and Walczak, a diarylethene-based Hendrickson's reagent is proposed in this research. Several *bis*phosphine oxide-based diarylethene molecules are known in the literature that can be used to form Hendrickson's reagent. The expectation is that adding trifluoromethane sulfonic anhydride to the ring-open form of the *bis*phosphine oxide diarylethene would create the cyclic Hendrickson's reagent in the *anti-parallel* conformer. As per the mechanism of Hendrickson's reagent formation, the Tf_2O activates the first phosphine oxide group to form the triflated phosphine oxide group. Since the thiophene

groups are free to rotate in the ring-open form, the nucleophilic attack of the phosphine oxide group on the phosphine oxide group of the second thiophene will generate the P-O-P bonds. This type of cyclization is only possible when the two thiophene groups in the ring-open form are parallel. Once the intramolecular P-O-P bond is formed, the diarylethene molecule will be locked in the photoinactive *parallel* conformation. A chemical reaction of a nucleophilic species with this photoinactive form will break one of the P-O bonds, allowing the free rotation of the thiophenes. The diarylethene molecule will regain the ability to form the photoactive *anti-parallel* conformation, and irradiation with UV light will induce a color change in the solution because of the photocyclization reaction.

3.2.1. Potential Applications

The electron-deficient phosphonium moiety in Hendrickson's reagent is an electrophilic center. A nucleophilic attack by an electron-rich species will form a new bond between the nucleophile and phosphorus, and the bond between phosphorus and oxygen in P-O-P breaks. In the case of the proposed system, the nucleophilic attack will unlock the thiophene rings and allow the photocyclization process.

The locked Hendrickson's reagent-based diarylethene can be used to monitor the progress of a chemical reaction. The most common reaction where the Hendrickson's reagent is employed is the esterification reaction between a primary alcohol and a carboxylic acid. The first step in the reaction mechanism is the nucleophilic attack of the alcohol's oxygen on the phosphonium group of Hendrickson's reagent, which is also the slowest or rate-determining step. The photocyclization reaction of the diarylethene photoswitch could monitor this slow step. Alternatively, the phosphine oxide photoswitch formation can also be observed after esterification. Irradiation with UV light will generate the colored ring-closed isomer, and as the reaction progresses, an increase in the absorbance value in the visible region will be observed.

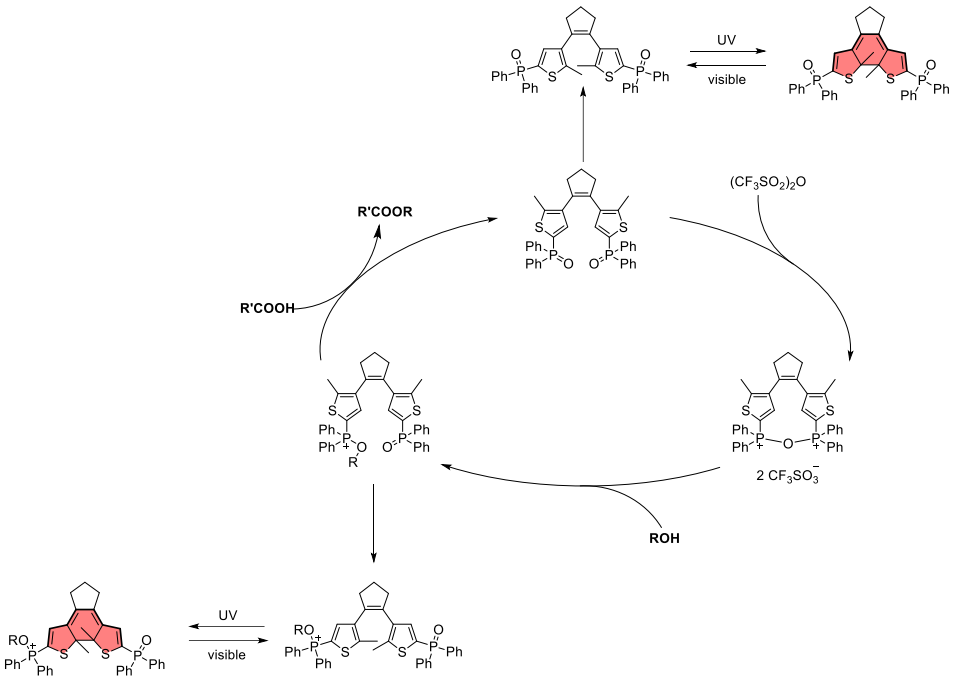

Scheme 3-3 The proposed esterification reaction monitoring system for diarylethene-based Hendrickson's reagent. The color change can be monitored at the slow step or when the *bis*phosphine oxide is reproduced towards the end of the reaction mechanism.

This increase in the absorbance value in the visible region can be correlated to the extent of the chemical reaction as Hendrickson's reagent is used stoichiometrically. In general, the esterification reaction and any other reaction mentioned previously can be monitored by this process.

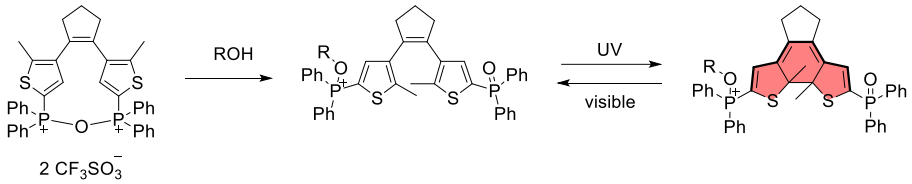

Scheme 3-4 Detection of O-nucleophiles such as alcohols or water by the diarylethene-based Hendrickson's reagent.

. The nucleophilic attack on the locked system can also enable the detection of oxygen-based nucleophilic species. Alcohols are used in many industrial processes and are found in many daily-use items. At elevated concentrations, these alcohols can have profound health implications, such as vision loss or death in case of methanol ingestion. Conventionally, the analysis of alcohols is done with instruments such as HPLC,[16] GC,[17] MS,[18] or IR[19] spectroscopy in combination or separately. These methods provide

sensitive detection of alcohols; however, the on-site detection is complex and expensive. Several optical sensors are available for alcohols based on fluorescence, luminescence, surface plasmon resonance, and colorimetry. Colorimetric methods use-

1. Strong oxidants to oxidize ethanol to acetic acid, followed by photometric analysis.[20]

2. Solvatochromism of dyes like triphenylmethane, Brooker's merocyanine, and Reichardt's betaine.[21]

3. Metal organic frameworks and metalloporphyrins.[22]

Additionally, the sensitivity of Hendrickson's reagent towards water can be used to monitor moisture content in aprotic solvents. Many reactions performed in academic and industrial settings require dry solvents. Water in solvents can lead to side reactions, reagent degradation, or shifting the equilibrium towards reactants. These factors can be highly detrimental in large-scale industrial settings such as pharmaceuticals. Karl Fischer titration is the classical method for determining moisture in organic solvents. Several colorimetric systems have also been developed for quick and easy moisture detection.[23]

3.2.2. Experimental Design

Probe Selection

Branda and coworkers reported the first *bis*phosphine-based diarylethene photoswitch.[24] The perfluorinated *bis*phosphine diarylethene prepared the *bis*phosphine-gold chloride complex and the selenide derivative. Liu and coworkers further developed the concept and synthesized two perhydro-derivatives of the *bis*phosphine diarylethene—one with diphenylphosphine and the other with di-cyclohexylphosphine.[25] The authors also reported the synthesis of phosphine oxide, phosphine selenide, and phosphine sulfuret derivatives of the two *bis*phosphine diarylethene photoswitches.

Out of the three similar *bis*phosphine diarylethene photoswitches reported by Branda and Liu, the perfluoro derivative of the diphenylphosphine oxide diarylethene photoswitch was considered for the initial project assessment. However, preliminary tests with this diarylethene photoswitch did not yield the desired locked photoinactive product. At that point, it was conjectured that the two phosphine oxide groups do not

converge fully for the P-O-P bond to form. Therefore, it was necessary to perform a computational analysis of the structure to ascertain whether the two phosphine oxide arms would converge sufficiently for Hendrickson's reagent formation. Two novel phosphine oxide derivatives were designed with longer flexible arms as controls to ascertain if that would allow the convergence and subsequent bond formation.

Computational Analysis

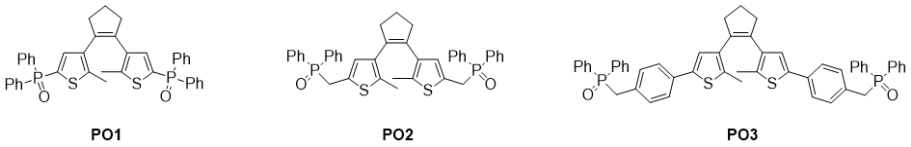

Figure 3-9 Three phosphine oxide derivatives were used for simple computational analysis for Hendrickson's reagent formation.

To screen a suitable diarylethene photoswitch, preliminary computational analysis was done on three *bis*phosphine oxide derivatives, selected based on their ease of synthesis. Molecule PO1, which is the perhydro analog of the perfluoro diarylethene, has the diphenylphosphine oxide group directly attached to the thiophene ring. Molecule PO2 is slightly more flexible, with a methylene group between the thiophene and diphenylphosphine oxide group. Molecule PO3 has a longer extended arm with a benzylic spacer between thiophene and diphenylphosphine oxide. A more flexible arm group was expected to allow the two phosphine oxides to contact each other when the two thiophene groups converge in the *parallel* conformation.

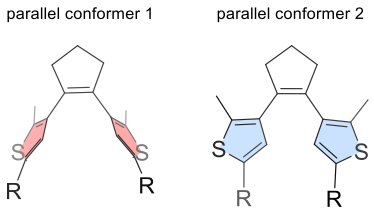

Figure 3-10 The ring-open isomer exists in two *parallel* conformations. The two conformers differ in the relative orientation of the thiophene rings.

The diarylethene molecule can exist in two non-photochromic *parallel* conformations. In the first conformation, the two thiophene rings are perpendicular to the central cyclopentene ring, whereas in the second *parallel* conformation, the two thiophene rings are twisted. Both *parallel* conformations were analyzed for the three phosphine oxide molecules. Simple geometry optimizations were performed using

density functional theory (DFT) with the B3LYP/6-31G(d) level of theory on the structures of PO1, PO2, and PO3 using Gaussian 16 software. However, the electronic properties or the reaction mechanism were not explored. This study was done only to understand how flexibility might influence structural stability.

Synthesis

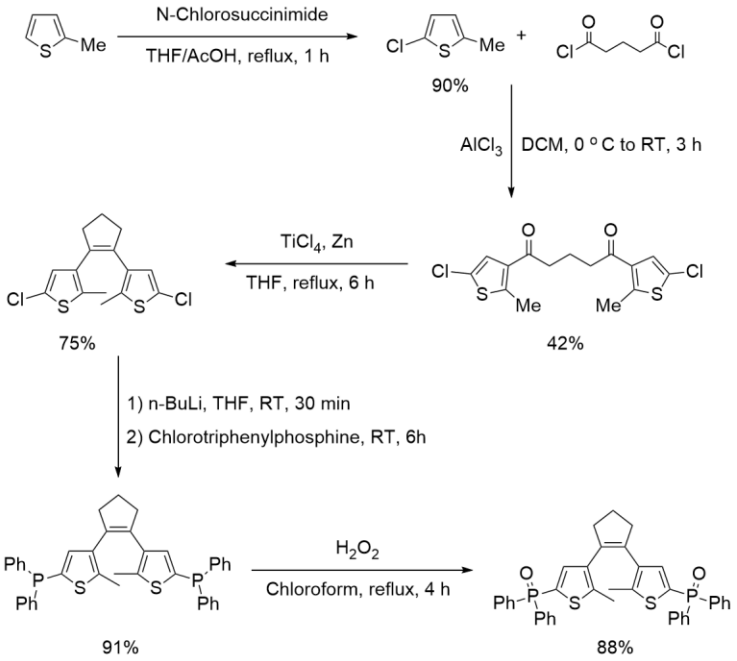

Scheme 3-5 Synthesis scheme for *bis*phosphine oxide diarylethene photoswitch.

The *bisphosphine* oxide diarylethene photoswitch was synthesized by starting with the chlorination of 2-methyl thiophene with *N*-chlorosuccinimide. The subsequently formed 2-chloro-5-methyl thiophene was then reacted with glutaryl chloride using Friedel-Crafts acylation to provide the diketone derivative. Intramolecular McMurry coupling reaction of the diketone with titanium tetrachloride and zinc afforded the dichloro diarylethene photoswitch. The metal halogen exchange reaction of the dichloro diarylethene molecule with n-butyl lithium and subsequent quenching with chlorodiphenylphosphine gives the diphenylphosphine diarylethene molecule. Oxidation of the diphenylphosphine photoswitch with hydrogen peroxide afforded the phosphine oxide photoswitch.

Hendrickson's Reagent Test

To test the formation of Hendrickson's reagent-based diarylethene system, ^{31}P and ^{19}F NMR spectra were collected. When the Hendrickson's reagent forms, the ^{31}P NMR signals are shifted downfield as the phosphorus atoms become more electron deficient. The strong electrophilic phosphorus species experience more deshielding, so the signal moves downfield to a higher ppm. The other marker is the formation of Hendrickson's reagent, the ^{19}F NMR signal for Tf_2O and trifluoromethane sulfonate ion. The ^{19}F NMR signal for Tf_2O appears at -71.7 ppm, whereas the signal for the sulfonate ion appears at -78.1 ppm. One can confirm the formation of Hendrickson's agent by monitoring the changes in the 31P and 19F NMR signals.

The other test is the change in the absorbance spectra of Hendrickson's reagent-based diarylethene. The phosphine oxide diarylethene is photoactive and should display a change in the absorbance spectrum when exposed to the appropriate wavelength of UV light. However, the locked diarylethene should not show any changes upon UV light exposure. Adding alcohol should unlock the photoswitch, and the molecule should show the typical diarylethene behavior again.

Esterification Reaction Test

Esterification is the most commonly used reaction to which Hendrickson's reagent is applied. A model esterification reaction between benzyl alcohol and benzoic acid to form benzyl benzoate was designed to test the applicability of the diarylethene-based system toward reaction monitoring. The changes in the ^{1}H and ^{13}C NMR signals of the α-protons and the α-carbons on the benzyl alcohol and benzyl benzoate can be tracked to monitor the progress of the reaction. The α-protons on benzyl alcohol appear around 4.51 ppm in the ^{1}H NMR, and the α-carbon appears around 64.70 ppm in the ^{13}C NMR. In the case of benzyl benzoate, the α-protons appear at 5.37 ppm in the ^{1}H NMR, and the α-carbon appears around 66.69 ppm in the ^{13}C NMR. A comparative study with Hendrickson's reagent prepared from triphenylphosphine oxide was done as a control.

3.3. Results and Discussion

3.3.1. Computational Analysis

The test for Hendrickson's reagent-based diarylethene from the perfluoro *bis*phosphine oxide photoswitch didn't turn out as expected. One equivalent Tf_2O was added to the anhydrous CD_2Cl_2 solution of the *bis*phosphine oxide at 0 °C and mixed for 1 hour. There was no precipitation. However, the solution turned yellow. When this solution was exposed to UV light, a color change to red was observed. This color change suggested that either the locked Hendrickson's reagent was not formed or the structure was a dimer. Simple computational analysis was done to test the hypothesis that the molecule can converge and form the locked P-O-P structure. Two novel phosphine oxide diarylethene photoswitches were designed with flexible arms to test if convergence was an issue. Geometry optimization of all three molecules was done in both parallel conformations. The perhydro analogue was optimized instead of the perfluoro because of the ease of synthesis.

Geometry optimization results for all three photoswitches displayed that they can form the locked structures in both *parallel* conformations. In all cases, the calculated phosphorus-oxygen bond length was 1.65 Å, almost the same as in the regular Hendrickson's reagent (1.60 Å).

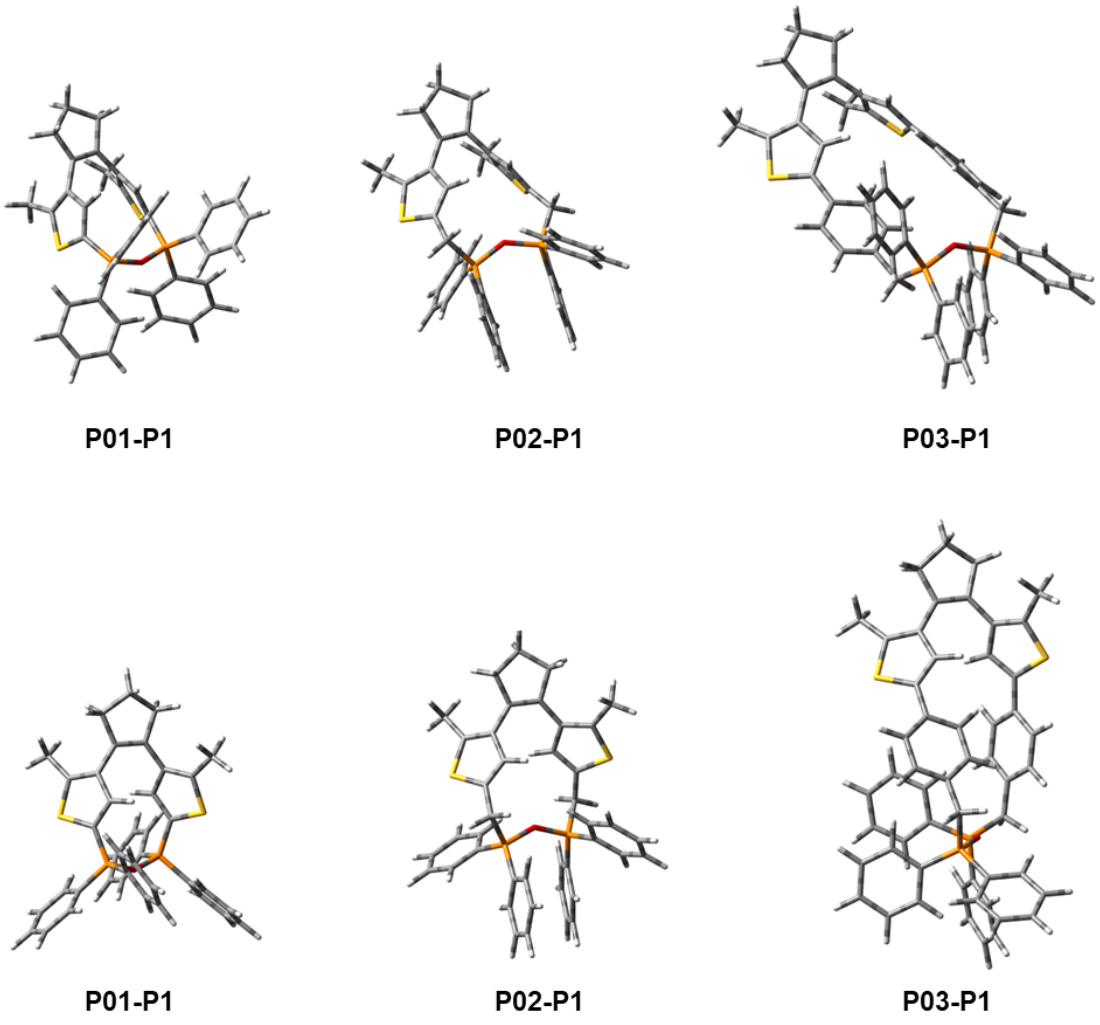

Figure 3-11 Geometry optimized structures of the three *bis*phosphine oxide diarylethenes.

Name	P-O-P bond angle	P-O bond length (Avg)
P01-P1	152.14°	1.65 Å
P01-P2	147.96°	1.66 Å
P02-P1	138.90°	1.65 Å
P02-P2	141.89°	1.65 Å
P03-P1	137.87°	1.65 Å
P03-P2	137.31°	1.65 Å

Table 3-1 The calculated P-O-P bond angle and P-O bond length for the two parallel conformers of the three *bis*phosphine oxide diarylethene molecules.

The P-O-P bond angle for the *parallel* conformation 1 of the *bis*phosphine oxide diarylethene was calculated as 152.14 Å. It was closest to the bond angle of Hendrickson's reagent from triphenylphosphine oxide. The *bis*phosphine oxide molecule with a benzylic spacer had the smallest calculated P-O-P bond angle amongst the structure. The preliminary results suggested that the perhydro diphenylphosphine oxide molecule should be able to form the inactive locked structure. A further literature review was done to find similar cyclic analogues. The procedure used by Jenkins and coworkers was tried, where they kept the molecule at -18 °C for 12 hours to favor intramolecular P-O-P bond formation over the intermolecular P-O-P formation.

3.3.2. Hendrickson's Reagent Formation

Jenkins and co-workers reported 5-, 6-, and 7-membered cyclic Hendrickson's reagent analogs. Their observation was that the *bis*phosphine oxide molecules initially formed intermolecular P-O-. After leaving the solution overnight at -18 °C, the molecule changed to intramolecular P-O-P formation, which they confirmed through ^{31}P NMR. The ^{31}P and ^{19}F NMR of Hendrickson's reagent-based diarylethene was compared to that of the triphenylphosphine oxide-based Hendrickson's reagent.

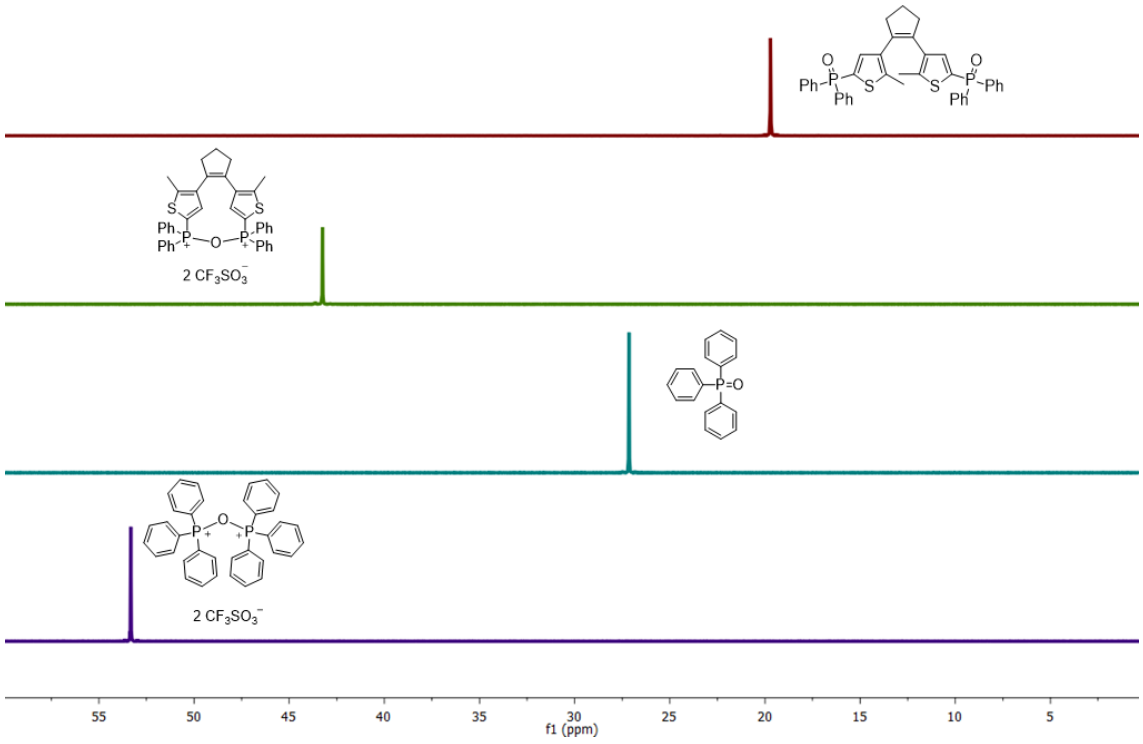

Figure 3-12 ^{31}P NMR spectra of Hendrickson's reagent-based diarylethene and TPPO-based Hendrickson's reagent. A downfield shift is observed in both cases.

The ^{31}P NMR spectra of Hendrickson's reagent-based diarylethene and standard TPPO-based Hendrickson's reagent were collected before and after the addition of Tf_2O. In both cases, a downfield shift in the phosphorus signal was observed due to the electrophilic nature of the positively charged phosphorus in Hendrickson's reagent. The absence of other signals in the diarylethene case suggests that only one species is present in the reaction mixture. A similar observation was seen in the ^{19}F NMR spectra of the two Hendrickson's reagent molecules. The signal at -78.1 ppm corresponds to the trifluoromethane sulfonate ion. This further confirmed the identity of the diarylethene as a Hendrickson's reagent analog.

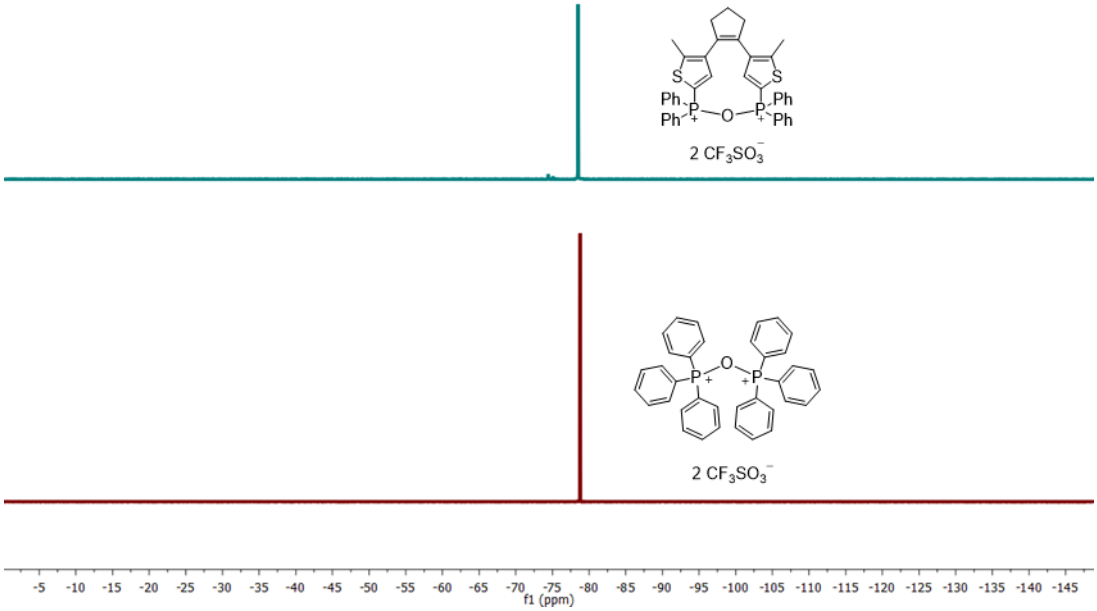

Figure 3-13 The ^{19}F NMR of the two Hendrickson reagents shows the presence of the same counter ions, the trifluoromethane sulfonate ion.

3.3.3. Test with Alcohol

To test whether the species formed is an actual Hendrickson's reagent analog, absorbance spectroscopy was performed on the *bis*phosphine oxide diarylethene photoswitch, the Hendrickson's reagent analog, and after methanol addition. The *bis*phosphine oxide diarylethene displayed typical photochromic behavior. Irradiation with 254 nm UV light led to a change in color of the 2.5×10^{-5} M solution in dichloromethane. A new absorbance centered around 510 nm was observed, and the PSS reached after 60 seconds of irradiation. Irradiation with a visible lamp bleached the solution in 300 seconds, and the solution became the initial yellow color.

A second 2.5×10^{-5} M solution of Hendrickson's reagent-based diarylethene was prepared, and absorbance spectra were collected after irradiation with 254 nm UV light at regular intervals. An increase in a band centered around 380 nm was observed, and a decrease in the visible region was observed. The sample was irradiated with 254 nm UV light for a total of 180 seconds. After this, the sample was placed in front of the visible lamp; however, no change in the absorbance spectra was observed.

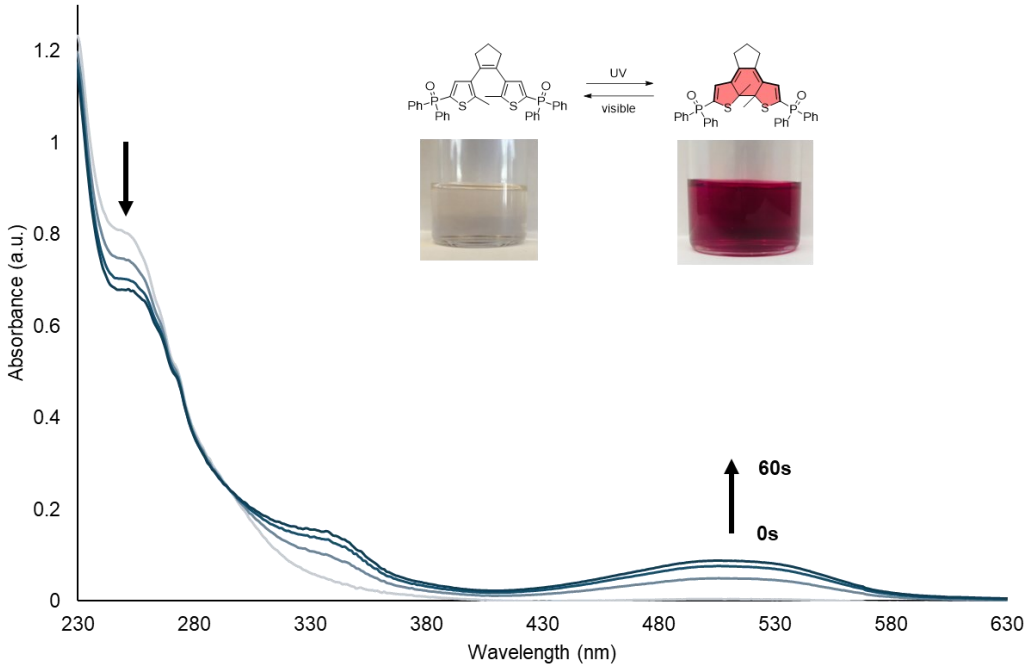

Figure 3-14 The absorbance spectra of *bis*phosphine oxide diarylethene photoswitch. A new band centered around 510 nm appears in the visible region.

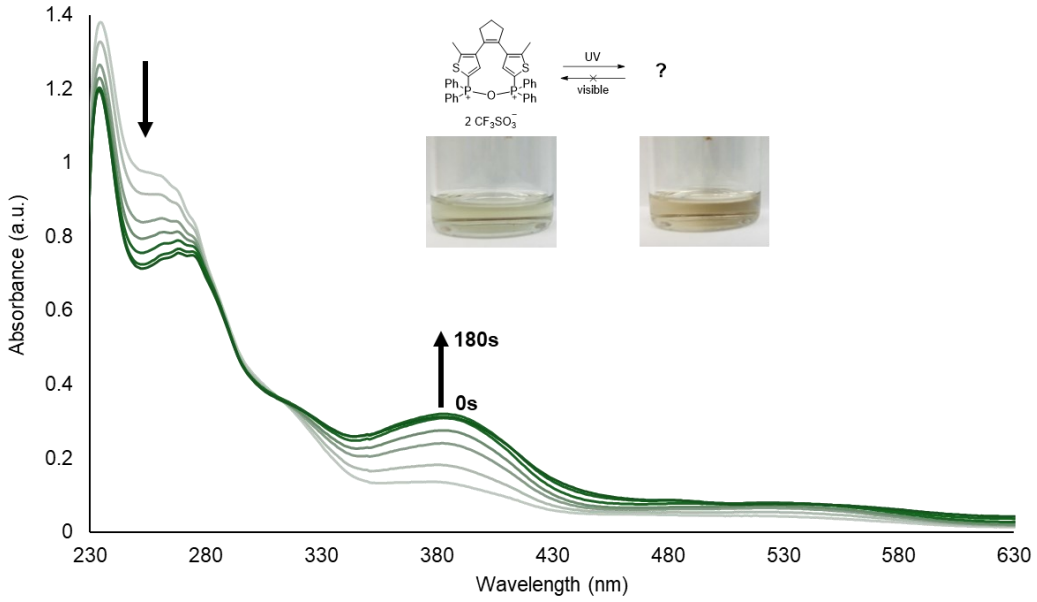

Figure 3-15 The absorbance spectra of Hendrickson's reagent-based diarylethene molecule, which undergoes an irreversible change after irradiation with 254 nm UV light.

When an equivalent amount of methanol was added to Hendrickson's reagent mixture and irradiated with 254 nm UV light, the photochromic behavior of the molecule returned. After 60 seconds of irradiation with UV light, the color of the solution changed to wine red, and a new band in the visible region centered around 520 nm appeared. Irradiation with visible light returned the original pale-yellow color in 240 seconds.

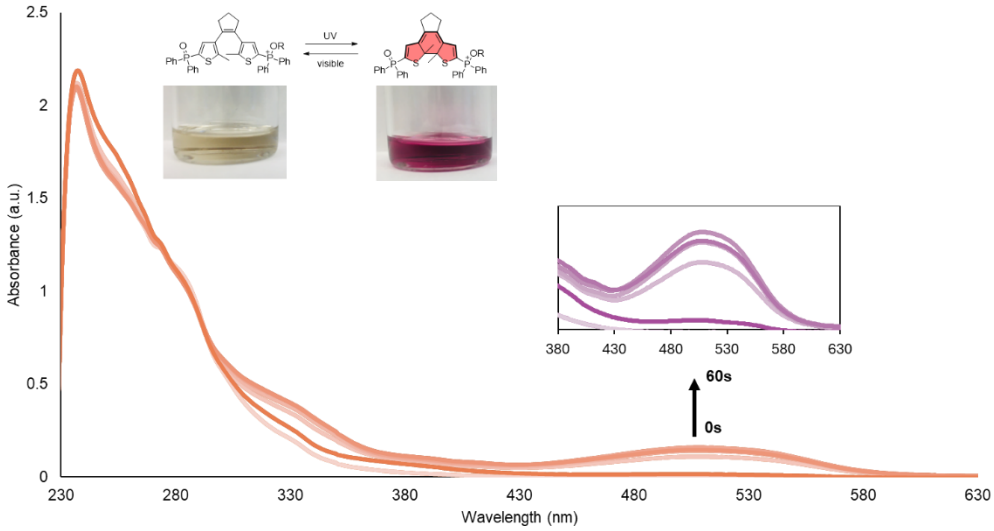

Figure 3-16 The absorbance spectra of Hendrickson's reagent-based diarylethene after adding methanol, which unlocks the photochromic behavior of the diarylethene switch.

3.3.4. Esterification Reaction Test

Hendrickson's reagent is used for many reactions; however, esterification is the most common reaction where this reagent is applied. To prove that Hendrickson's reagent analog of the diarylethene can perform as a reagent, a model reaction between benzyl alcohol and benzoic acid was performed. A control reaction was done with standard Hendrickson's reagent and monitored by ^{1}H and ^{13}C NMR spectroscopy.

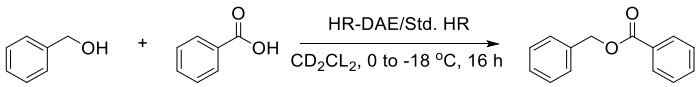

Scheme 3-6 A model reaction between benzyl alcohol and benzoic acid was performed with Hendrickson's reagent analog, diarylethene, and a control reaction with TPPO.

The α-proton and carbon of the benzyl alcohol were monitored to assess the conversion to benzyl benzoate.

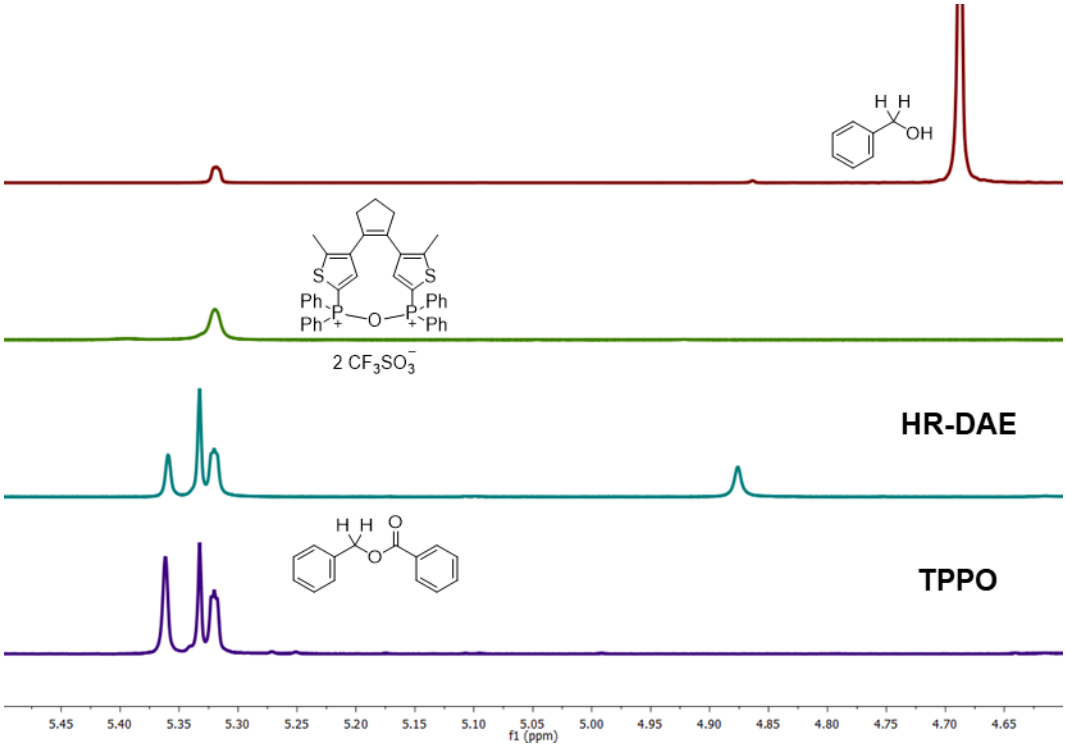

Figure 3-17 The benzyl signal at 4.67 ppm in the ^{1}H NMR is not present in both reactions. A new signal at 5.37 appears, corresponding to benzoyl benzoate.

The 1H NMR of the reactions showed that the benzyl alcohol was completely consumed in the reaction. The α-proton signals of benzyl alcohol were not present in both reactions after 1 hour of mixing. However, in the case of the diarylethene reaction, an additional singlet was observed at 4.87 ppm, the identity of which could not be confirmed.

The 13C spectra of the reaction mixture confirmed the complete consumption of benzyl alcohol in the reaction. Signals for the α-carbon on benzyl alcohol and benzyl benzoate were visible on both spectra of the esterification reaction.

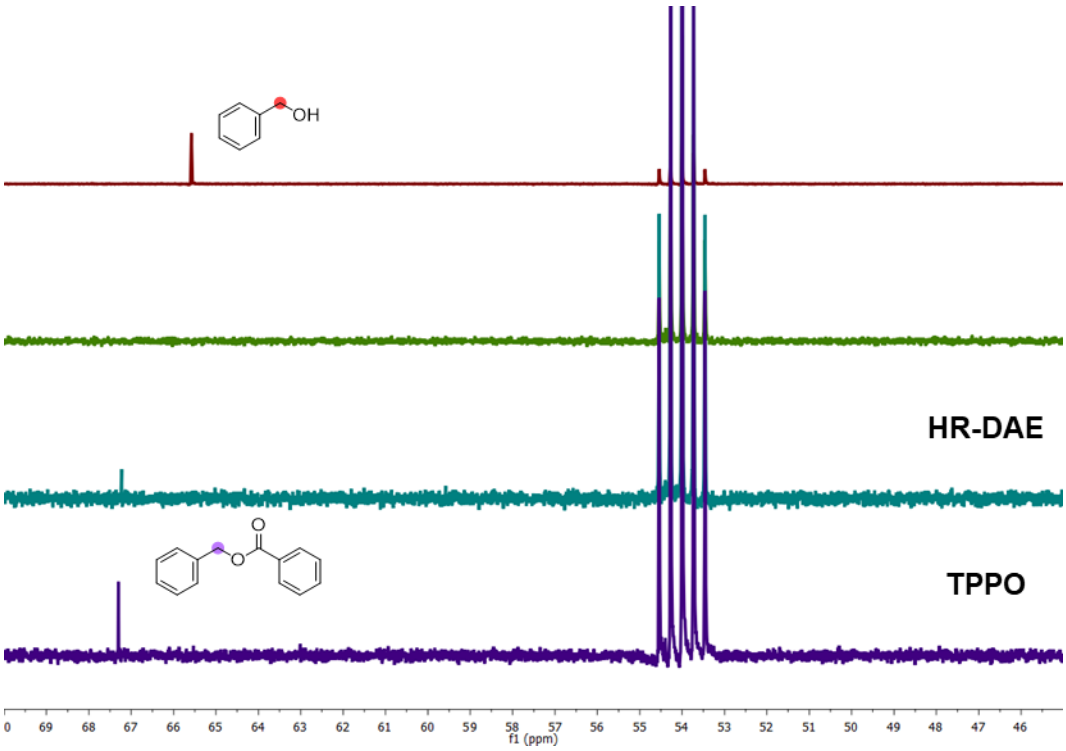

Figure 3-18 ^{13}C spectra of the benzyl alcohol and benzoic acid esterification reaction with the diarylethene analog of Hendrickson's reagent and TPPO.

3.4. Limitations

The proposed Hendrickson's reagent-based detection system has some notable limitations. The most challenging problem is the reagent's instability in the open atmosphere. The significant advantage of colorimetric detections is that they are easy to use. This aspect of colorimetric detection is limited by the fact that the proposed system will work only under an inert atmosphere. The reagent could be placed in a sealed tube inside a secondary housing as a workaround. The solvent or nucleophile could be injected into the secondary housing, and breaking the sealed tube will release Hendrickson's reagent for the reaction.

The second major limitation of this proposed system as a detector is the lack of selectivity and specificity. The electrophilic centers in the molecule are susceptible to nucleophilic attack. Since the electronic properties of the diarylethene photoswitch are not influenced by the type of nucleophile attached to the phosphonium group, the color

change will remain the same in all cases. The lack of specificity and selectivity may cause false positive results and limit the applicability of this method.

As the reaction-extent indicator, the diarylethene-based Hendrickson's reagent is limited to colorless reaction mixtures. If the reaction itself is colored or produces colored products, the color changes observed will be a mixture of the reagent and the reaction. Isolation of the color change due to the reagent will be difficult as it will be masked or hidden by the color of the reaction. Also, the system will be less sensitive as the initial changes will be challenging to observe. The color of the solution will be dictated by the reaction mixture rather than the ring-closed form of the diarylethene photoswitch.

Similarly, the viability of such a system falters in a large-scale reaction setup, even if the reaction mixture or products are colorless. The precise tracking of the reaction progress will be hindered as a slight change in concentration of the ring-closed form of the diarylethene photoswitch may not produce a noticeable color change in the reaction solution.

3.5. Future Work

Polymer Support

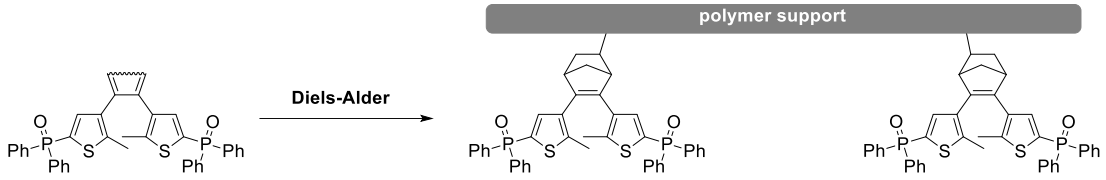

Figure 3-19 Proposed polymer supported diarylethene analog of Hendrickson's reagent.

Similar to the work done by Jenkins and coworkers, the diarylethene photoswitch could be appended to polymer support. One possible method could be to create a phosphine oxide pre-diarylethene with a diene central ring. The Diels-Alder reaction of the diene central ring with a dienophile in the polymer chain will make a photochromic phosphine oxide diarylethene. In some of the current polymer-supported Hendrickson's reagent systems proposed in the literature, an equilibrium mixture of ditriflate and anhydride species is observed. This difference from the regular Hendrickson's reagent is because some phosphine oxide may not be near a second phosphine oxide group.

Since, in the diarylethene-based system, the two phosphine oxide groups will be on the same species, the probability of the formation of ditriflate is low. Similarly, the polymer support could be designed so that two diarylethene groups are far apart to favor the intramolecular phosphine oxide attack over the intermolecular one.

Analogs

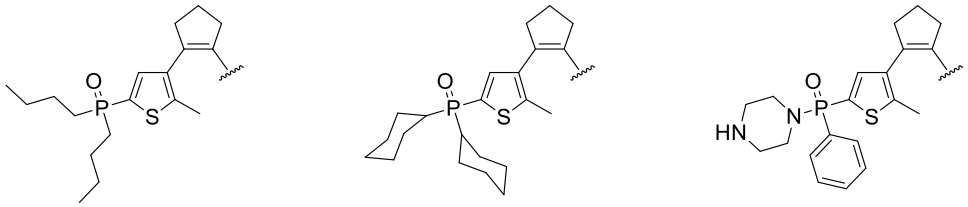

Figure 3-20 Replacement of phenyl rings with other groups may help with the stability, reactivity, and solubility of the phosphine oxide derivatives.

Hendrickson's reagent is generally prepared from triphenylphosphine oxide; however, other groups have been tried instead of the phenyl rings. A similar approach could be taken with the diarylethene-based Hendrickson's reagent. A piperazine-based phosphine oxide diarylethene group could be synthesized to facilitate the removal of the reagent with aqueous workup. Similarly, other groups like butyl or cyclohexyl could be tried to see the effect on the reactivity and stability of the system.

Moisture Detection

Since the Hendrickson's reagent is sensitive to water, studies on moisture content detection need to be done. Different ratios of solvent-water mixtures need to be prepared and then titrated with the Hendrickson's reagent to form a calibration curve. Then the unknown ratios need to be titrated with the reagent followed by UV exposure and finally absorbance measurements.

3.6. Materials and Instrumentations

All solvents and reagents used for synthesis, chromatography, UV-visible spectroscopy, and photochemical studies were purchased from Aldrich, Anachemia, Alfa Aesar, Caledon Labs, and Fisher Scientific and used as received. Tetrahydrofuran used for Suzuki coupling reactions was dried and degassed by passing through steel columns containing activated alumina under nitrogen using an MBraun solvent purification system. Dichloromethane for Hendrickson's reagent synthesis was dried on 4Å molecular sieves over 48 hours. Deuterated solvents for NMR analysis were purchased from Cambridge Isotope Laboratories and used as received or dried with 4Å molecular sieves over at least 48 hours. Column chromatography was performed using silica gel 60 (230–400 mesh) from Silicycle Inc.

^{1}H, ^{13}C, ^{19}F, and ^{31}P NMR characterizations were performed on a Bruker Avance-400 instrument with a 5 mm inverse probe operating at 400.13 MHz for ^{1}H NMR and 100.61 MHz for ^{13}C NMR. Chemical shifts (δ) are reported in parts per million (ppm) relative to tetramethylsilane using the residual solvent peak as a reference. Coupling constants (J) are reported in Hertz. UV-visible absorption spectra were recorded on a Shimadzu UV-3600Plus spectrophotometer. High-resolution mass spectroscopy (HRMS) measurements were performed using an Agilent 6210 TOF LC/MS in ESI-(+) mode. Ring-closing reactions were carried out using a lamp for visualizing TLC plates at 312 nm (Spectroline E series, 470 W/cm2). The ring-opening reactions were carried out using the light of a 150 W halogen photo-optic source passed through a 435 nm cut-off filter to eliminate higher energy light.

Synthesis

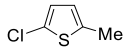

2-chloro-5-methylthiophene- 2-methylthiophene (100 g, 1.02 mol, 1 eq) and *N*-chlorosuccinimide (152 g, 1.14 mol, 1.1 eq) were added to a 1:1 mixture of tetrahydrofuran and acetic acid (800 mL), and the reaction was stirred at room temperature for 30 minutes followed by reflux for 1.5 hours. The reaction mixture was cooled, and 3 M aqueous NaOH solution (300 mL) was added slowly. The mixture was transferred to a separatory funnel and washed with 3 M aqueous NaOH solution (3 × 300 mL), followed by brine. The combined organic phase was dried with anhydrous

$MgSO_4$, filtered, and the solvent removed under vacuum to yield a brown liquid. Purification by vacuum distillation yielded 121.7 g (90%) of 5-chloro-2-methylthiophene as a clear, colorless liquid.

^{1}H NMR- (400 MHz, $CDCl_3$) δ- 6.71 (d, 1H), 6.53 (d, 1H), 2,4 (d, 3H)

^{13}C NMR- (101 MHz, $CDCl_3$) δ- 138.55, 128.55, 125.8, 124.56, 15.55

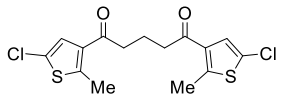

1,5-*bis*(5-chloro-2-methylthiophen-3-yl)pentane-1,5-dione- Aluminum trichloride (60 g, 0.45 mol, 1,2 eq) was added carefully in portions to carbon disulfide (250 mL) at 0 °C and stirred vigorously. Glutaryl chloride (63.4 g, 0.375 mol, 1 eq) was added dropwise to the suspension, and the mixture was stirred for 15 minutes at 0 °C. To this suspension, 2-chloro-5-methylthiophene (49.75 g, 0.375 mol, 1 eq) was added dropwise. The reaction mixture was allowed to warm to room temperature and stirred for 3 hours, after which 100 g of ice was added over 30 minutes. The organic layer was separated, and the aqueous layer was washed with diethyl ether (3 × 100 mL). The combined organic layers were washed with brine, dried with anhydrous $MgSO_4$, filtered, and the solvent evaporated under vacuum to yield a black tar. The black tar was redissolved in dichloromethane, dry-loaded on Celite, and passed through a pad of silica gel with 20 % ethyl acetate in hexane as the eluent. Recrystallization with hot ethanol yielded 56.9 g (42%) of 1,5-*bis*(5-chloro-2-methylthiophen-3-yl)pentane-1,5-dione as solid white crystals.

^{1}H NMR- (400 MHz, $CDCl_3$) δ- 7.16 (s, 2H), 2.86 (t, 4H), 2.68 (s, 6H), 2.08 (m, 2H)

^{13}C NMR- (101 MHz, $CDCl_3$) δ- 194.1, 147.4, 134.2, 126.6, 125.0, 40.7, 18.4, 16.1

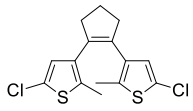

1,2-*bis*(5-chloro-2-methylthiophen-3-yl)cyclopent-1-ene- Titanium tetrachloride (8.52 mL, 0.08 mol, 8 eq) was added dropwise to a suspension of zinc powder (7.5 g, 0.115 mol, 11.5 eq) in dry tetrahydrofuran (100 mL) at 0 °C and the reaction mixture was heated to reflux for 1 hour. After that, the reaction was cooled to 0 °C, and 1,5-*bis*(5-

chloro-2-methylthiophen-3-yl)pentane-1,5-dione (3.61 g, 0.01 mol, 1 eq) was added in portions. The reaction mixture was refluxed again and monitored with TLC. After 3 hours, all the starting material was consumed, and the reaction mixture was cooled to room temperature and quenched with 10% aqueous K_2CO_3 (5 mL) solution. The reaction mixture was then filtered over a pad of Celite and washed with ethyl acetate (3 × 100 mL). The combined organic layers were dried with anhydrous $MgSO_4$, filtered, and the solvent evaporated under vacuum. Purification by column chromatography on silica gel using *n*-hexane as eluent yielded 2.47 g (75%) of 1,2-*bis*(5-chloro-2-methylthiophen-3-yl)cyclopent-1-ene as a white crystalline solid.

^{1}H NMR- (400 MHz, $CDCl_3$) δ- 6.56 (s, 2H), 2.69 (t, 4H), 2.02 (q, 2H), 1.88 (s, 6H)

^{13}C NMR- (100 MHz, $CDCl_3$) δ- 134.6, 134.2, 133.1, 126.5, 125.2, 38.27, 22.67, 14.12

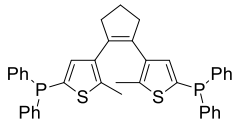

1,2-*bis*(5-(diphenylphosphine)-2-methylthiophen-3-yl) cyclopent-1-ene- n-BuLi (3 mL, 0.0075 mol, 2.5 eq, 2.5 M in hexane) was added dropwise to a solution of 1,2-*bis*(5-chloro-2-methylthiophen-3-yl)cyclopent-1-ene (1.00 g, 0.003 mol, 1 eq) in dry tetrahydrofuran (60 mL) at room temperature over 30 minutes. The reaction mixture was monitored with TLC and stirred for 30 minutes. Diphenylphosphine chloride (1.25 mL, 0.00675 mol, 2.25 eq) was added at once using a syringe to quench the reaction, and the mixture was stirred overnight. Ethyl acetate (30 mL) and water (30 mL) were added to the reaction flask, and the organic layer was separated. The aqueous layer was extracted with ethyl acetate (3 × 30 mL), dried with anhydrous $MgSO_4$, filtered, and the solvent evaporated under vacuum. Purification with column chromatography on silica gel using 33 % dichloromethane in petroleum ether yielded 1.72 g (91%) of 1,2-*bis*(5-(diphenylphosphine)-2-methylthiophen-3-yl) cyclopent-1-ene as a white fluffy solid.

^{1}H NMR-- (400 MHz, $CDCl_3$) δ- 7.34-7.21 (m, 20H), 7.01 (d, 2H), 2.72 (t, 4H), 2.01-2.05 (m, 2H), 1.94 (s, 6H)

^{31}P NMR-- (125 MHz, $CDCl_3$) δ- -20.08 (s, P)

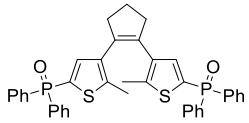

(Cyclopentane-1-ene-1,2-diyl*bis*(5-methylthiophene-4,2-diyl)) *bis* (diphenylphosphine oxide)- Hydrogen peroxide (50% aqueous solution, 7 mL) was added to a solution of 1,2-*bis*(5-(diphenylphosphine)-2-methylthiophen-3-yl) cyclopent-1-ene (0.63 g, 0.001 mol, 1 eq) in chloroform (100 mL) and the mixture was heated to reflux for 4 hours. The mixture was cooled to room temperature, added water (30 mL), and extracted with chloroform (3 × 75 mL). The combined organic layers were dried with anhydrous $MgSO_4$, and the solvent evaporated under vacuum. Purification by column chromatography on silica gel using 20 % acetone in dichloromethane yielded 0.75 g (88%) of (cyclopent-1-ene-1,2-diyl*bis*(5-methylthiophene-4,2-diyl))*bis*(diphenylphosphine oxide) as a white, fluffy solid.

^{1}H NMR-- (400 MHz, $CDCl_3$) δ- 7.39-7.70 (m, 20H), 7.07 (d, 2H), 2.71 (t, 4H), 1.91-2.01 (m, 2H), 1.92 (s, 6H)

^{13}C NMR-- (101 MHz, $CDCl_3$) δ- 143.78, 137.5, 137.19, 134.88, 133.29, 132.09, 131.50, 129.99, 128.45, 38.16, 22.76, 14.45

^{31}P NMR-- (121.5 MHz, $CDCl_3$) δ- 19.81

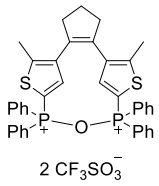

Hendrickson's reagent-based diarylethene synthesis- In a flame-dried round-bottom flask equipped with a stir bar, *bis*phosphine oxide diarylethene (66.1 mg, 0.1 mmol, 1 eq) was dissolved in anhydrous dichloromethane (2 mL) under argon atmosphere and placed in an ice bath at 0 °C. Trifluoromethane sulfonic anhydride (0.17 mL, 0.1 mmol, 1 eq) was added dropwise to the chilled solution via a syringe. The reaction mixture was stirred at 0 °C for 4 hours and then kept in a freezer at -18 °C for 12 hours to yield POP-diarylethene.

^{31}P NMR-- (121.5 MHz, $CDCl_3$) δ- 43.33

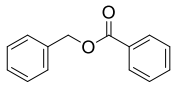

General procedure for ester synthesis- To the freshly prepared Hendrickson's reagent-based diarylethene solution in an NMR tube, benzyl alcohol (0.054 mL, 0.5 mmol, 1 eq), benzoic acid (0.061 g, 0.5 mmol, 1 eq), and diisopropylethylamine (0.19 mL, 1.1 mmol, 2.2 eq) were added successively. The reaction mixture was allowed to warm to room temperature with occasional stirring. ^{1}H, ^{13}C, ^{19}F, and ^{31}P NMR were collected at appropriate times.

3.7. Reference

(1) Mitsunobu, O.; Yamada, M.; Mukaiyama, T. Preparation of Esters of Phosphoric Acid by the Reaction of Trivalent Phosphorus Compounds with Diethyl Azodicarboxylate in the Presence of Alcohols. Bull. Chem. Soc. Jpn. 1967, 40 (4), 935–939. https://doi.org/10.1246/bcsj.40.935.

(2) Hendrickson, J. B.; Schwartzman, S. M. Triphenyl Phosphine Ditriflate: A General Oxygen Activator. Tetrahedron Lett. 1975, 16 (4), 277–280. https://doi.org/10.1016/S0040-4039(00)71842-9.

(3) Aaberg, A.; Gramstad, T.; Husebye, S. The Preparation and Molecular Structure of a Diphosphonium Salt with a Linear P—O—P System. Acta Chem Scand A 1980, 34 (10).

(4) You, S.; Razavi, H.; Kelly, J. W. A Biomimetic Synthesis of Thiazolines Using Hexaphenyloxodiphosphonium Trifluoromethanesulfonate. Angew. Chem. 2003, 115 (1), 87–89. https://doi.org/10.1002/ange.200390029.

(5) Hendrickson, J. B.; Hussoin, M. S. Reactions of Carboxylic Acids with Phosphonium Anhydrides. J. Org. Chem. 1989, 54 (5), 1144–1149.

(6) Hendrickson, J. B.; Hussoin, M. S. Facile Cyclodehydrations of Diols and Amino Alcohols with Phosphonium Anhydrides. Synlett 1990, 1990 (07), 423–424.

(7) Elson, K. E.; Jenkins, I. D.; Loughlin, W. A. The Hendrickson's Reagent and the Mitsunobu Reaction: A Mechanistic Study. Org Biomol Chem 2003, 1 (16), 2958–2965. https://doi.org/10.1039/B305375J.

(8) Hendrickson, J. B.; Hussoin, M. S. Facile Dehydration of Activated Ketones to Alkynes. Synthesis 1989, 1989 (03), 217–218.

(9) Hendrickson, J. B.; Hussoin, M. S. Seeking the Ideal Dehydrating Reagent. J. Org. Chem. 1987, 52 (18), 4137–4139.

(10) Hendrickson, J. B.; Walker, M. A.; Varvak, A.; Hussoin, M. S. Direct Elimination of Epoxides to Dienes with Phosphonium Anhydrides. Synlett 1996, 1996 (07), 661–662.

(11) Mukaiyama, T.; Suda, S. Diphosphonium Salts as Effective Reagents for Stereoselective Synthesis of 1, 2-Cis-Ribofuranosides. Chem. Lett. 1990, No. 7, 1143–1146.

(12) Elson, K. E.; Jenkins, I. D.; Loughlin, W. A. Cyclic Analogues of the Hendrickson 'POP' Reagent. Aust. J. Chem. 2004, 57 (4), 371. https://doi.org/10.1071/CH03223.

(13) Moussa, Z. Cyclic Aromatic Analogues of the Hendrickson Reagent; NMR Studies and Electrophilic Properties. Synthesis 2012, 44 (03), 460–468. https://doi.org/10.1055/s-0031-1289998.

(14) Dyapa, R.; Dockery, L. T.; Walczak, M. A. Dehydrative Glycosylation with Cyclic Phosphonium Anhydrides. Org. Biomol. Chem. 2017, 15 (1), 51–55. https://doi.org/10.1039/C6OB01812B.

(15) Fairfull-Smith (née Elson), K. E.; Jenkins, I. D.; Loughlin, W. A. Novel Polymer-Supported Coupling/Dehydrating Reagents for Use in Organic Synthesis. Org Biomol Chem 2004, 2 (14), 1979–1986. https://doi.org/10.1039/B406770C.

(16) Tagliaro, F.; Dorizzi, R.; Ghielmi, S.; Marigo, M. Direct Injection High-Performance Liquid Chromatographic Method with Electrochemical Detection for the Determination of Ethanol and Methanol in Plasma Using an Alcohol Oxidase Reactor. J. Chromatogr. B. Biomed. Sci. App. 1991, 566 (2), 333–339. https://doi.org/10.1016/0378-4347(91)80249-C.

(17) Wang, M.-L.; Choong, Y.-M.; Su, N.-W.; Lee, M.-S. A Rapid Method for Determination of Ethanol in Alcoholic Beverages Using Capillary Gas Chromatography. J. Food Drug Anal. 2003, 11 (2), 3.

(18) Creaser, C. S.; Lamarca, D. G.; Brum, J.; Werner, C.; New, A. P.; Freitas dos Santos, L. M. Reversed-Phase Membrane Inlet Mass Spectrometry Applied to the Real-Time Monitoring of Low Molecular Weight Alcohols in Chloroform. Anal. Chem. 2002, 74 (1), 300–304.

(19) Lachenmeier, D. W.; Godelmann, R.; Steiner, M.; Ansay, B.; Weigel, J.; Krieg, G. Rapid and Mobile Determination of Alcoholic Strength in Wine, Beer and Spirits Using a Flow-through Infrared Sensor. Chem. Cent. J. 2010, 4 (1), 5. https://doi.org/10.1186/1752-153X-4-5.

(20) Lau, O.-W.; Luk, S.-F. Spectrophotometric Method for the Determination of Ethanol in Beverages and Beer Samples Using Cerium (IV) as Reagent. Int. J. Food Sci. Technol. 1994, 29 (4), 469–472.

(21) Dickert, F. L.; Geiger, U.; Lieberzeit, P.; Reutner, U. Solvatochromic Betaine Dyes as Optochemical Sensor Materials: Detection of Polar and Non-Polar Vapors. Sens. Actuators B Chem. 2000, 70 (1–3), 263–269. https://doi.org/10.1016/S0925-4005(00)00578-5.

(22) Sasaki, S.; Kotegawa, Y.; Tamiaki, H. Trifluoroacetyl-Chlorin as a New Chemosensor for Alcohol/Amine Detection. Tetrahedron Lett. 2006, 47 (28), 4849–4852. https://doi.org/10.1016/j.tetlet.2006.05.026.

(23) Kumar, P.; Ghosh, A.; Jose, D. A. Chemical Sensors for Water Detection in Organic Solvents and Their Applications. ChemistrySelect 2021, 6 (4), 820–842. https://doi.org/10.1002/slct.202003920.

(24) Sud, D.; McDonald, R.; Branda, N. R. Synthesis and Coordination Chemistry of a Photoswitchable *Bis*(Phosphine) Ligand. Inorg. Chem. 2005, 44 (17), 5960–5962. https://doi.org/10.1021/ic050429x.

(25) Yin, J.; Lin, Y.; Cao, X.; Yu, G.-A.; Tu, H.; Liu, S. H. The Synthesis and Photochromic Properties of Two *Bis*(Phosphine) Ligands Based on Dithienylethene Backbone and Their Oxides, Sulfurets and Selenides. Dyes Pigments 2009, 81 (2), 152–155. https://doi.org/10.1016/j.dyepig.2008.10.006.

Chapter 4.

Locked Tight: The Struggle to Break a Single Base Pair in a Model for Toehold-Mediated Displacement

Abstract

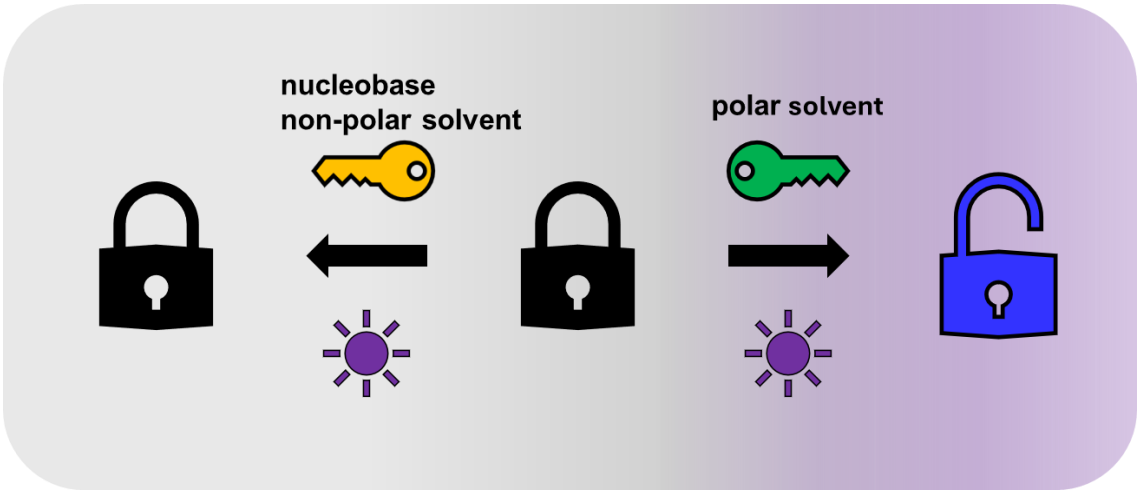

Nucleic acid detection has revolutionized medicine, forensics, food safety, and environmental monitoring. There are several detection methods available. However, most of them are fluorophore-based. This chapter discusses the attempt to prepare a toehold-mediated strand displacement (TMSD) process to create a colorimetric sensor based on the diarylethene molecule. The diarylethene molecule will be locked in the photoinactive parallel conformation. The TMSD process will unlock the molecule and allow it to acquire the photoactive anti-parallel conformation. A single nucleobase pair was attached to the diarylethene molecule as proof of concept. However, the strong hydrogen bonding between the complementary nucleobases hindered the intended conformational switching of the diarylethene molecule.

4.1. Introduction

The presence of nucleic acids in every living cell on Earth is a testament to their role as the fundamental building block of life. The discovery and subsequent research on the structure of nucleic acids accelerated the progression of fields such as biotechnology, medicine, genetic engineering, and evolutionary sciences.

Two primary classes of nucleic acids are ribonucleic acid (RNA) and deoxyribonucleic acid (DNA), each with a distinct structure and role. These large linear biopolymers are made up of monomeric units called nucleotides, which comprise three subunits: a phosphate group, a pentose sugar (deoxyribose in DNA and ribose in RNA), and a nucleobase (purines or pyrimidines).[1–3] The purines are adenine [A] and guanine [G], while the pyrimidines are cytosine [C] and thymine [T] in DNA / uracil [U] in RNA. The phosphates connect the sugars, forming the backbone, while the nucleobases participate in base-pairing interactions. In DNA, two strands coil into a double-helix structure, held together by hydrogen bonds between complementary base pairs – A with T or U and C with G. RNA is a single strand with exposed bases; however, internal base pairing allows some regions to fold into secondary structures. The stability and functions of nucleic acids depend on the base-pairing rules.[1–3]

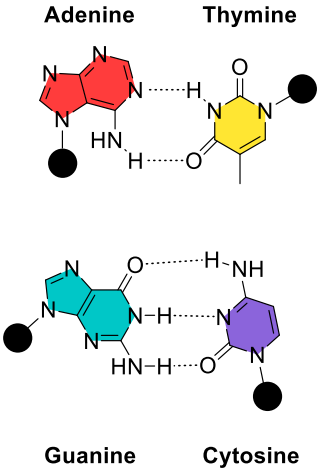

Figure 4-1 Purines [T and C] and pyrimidines [G and T] and hydrogen bonding between the complementary pairs.

Nucleic acids determine many biological functions in living organisms. Genes, which are specific DNA nucleotide sequences, form the basis for all individual organism's traits and characteristics. These specific sequences control all cellular

activities, such as cell development, maintenance, and regulation. The stored data in DNA carries the instructions for making proteins through gene expression, ensuring proper cell function. DNA replication allows genetic information to be passed on before cell division. Some RNA molecules help regulate gene expression by preventing unwanted protein production. On the other hand, viruses use host cells to replicate their nucleic acids, leading to infections and diseases.[1–4]

4.2. Where and Why is the Detection of Nucleic Acids Needed?

The demand and need for fast and consistent nucleic acid detection has grown significantly over the past few decades, particularly in diagnostics, forensics, and environmental monitoring. The replacement of slower traditional methods, such as pathogen culture, with faster and more efficient alternatives has improved scientific and industrial applications.

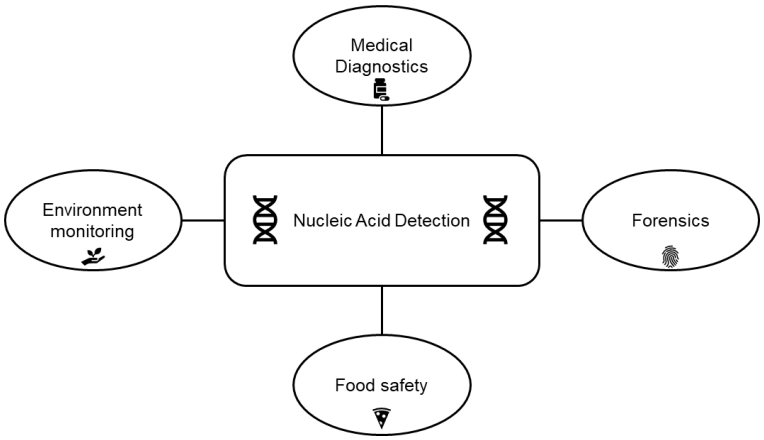

Figure 4-2 Nucleic acid detection is crucial in many fields.

Medical diagnostics and therapeutics – Quick and accurate identification of pathogens based on their genetic material has become possible due to the advances in nucleic acid detection, making this approach invaluable in medical diagnostics. Fast detection of infections caused by pathogens has facilitated quick vaccine development. This became especially clear during the COVID-19 pandemic and helped track and control the spread of the virus. Detecting genetic disorders is another field that new nucleic acid detection technologies have transformed. Identification of mutations in DNA allows early diagnosis of inherited conditions. Fast detection of circulating tumor DNA

(ctDNA), a biomarker for cancer, has proved to be a less invasive alternative to traditional biopsy. This has allowed continuous tracking of disease progression and the effectiveness of the treatment.[1,2,5]

Forensics—The discovery of DNA's uniqueness made it possible to establish identification databases. Minute traces of biological material—such as blood, saliva, or hair—can be analyzed to determine the source. DNA evidence is crucial in identifying victims and suspects and exonerating individuals who have been wrongfully convicted.[6]

Environmental monitoring – Nucleic acid detection is valuable for assessing ecological health. Pathogens posing significant risks to humans, animals, and plants are present in water, soil, and air. Investigation of antibiotic-resistant bacteria such as Mycobacterium tuberculosis can help develop new drugs. Analysis of environmental nucleic acids (eDNA and eRNA) makes tracking and monitoring invasive or endangered species easier. DNA barcoding allows for identifying and profiling endangered species, supporting efforts to combat poaching and the illegal wildlife trade. Certain microorganisms play a role in bioremediation, i.e., they help break down contaminants such as oil spills and heavy metals. Identification of these helpful microorganisms helps enhance environmental cleanup efforts.[7]

Food Safety – Nucleic acid detection is used to identify contaminants and detect food fraud. The 2013 horsemeat scandal in Europe, where undeclared horse DNA was found in beef products, is a recent example of the usefulness of DNA detection techniques. Labeling fish and other food items ensures that consumers receive the correct products. In food production, nucleic acid detection helps monitor microbial populations to ensure food safety for consumption. It can also be used to identify toxins produced by certain microorganisms. Additionally, this technology detects genetically modified organisms (GMOs) in food products to comply with regulatory requirements.[8]

4.3. What Techniques are Used for Nucleic Acid Detection?

Nucleic acids are complex structures inside cells, organized into tightly coiled and condensed assemblies wrapped around proteins. Nucleic acid analysis is done either *in situ* (within the cell) or in a test tube after isolation from the cell (*in vitro*). *In vitro* procedures require the extraction, purification, and amplification of the nucleic acids

before analysis, whereas *in situ* methods do not require any work. This chapter will focus on the *in vitro* nucleic acid analysis as the method of detection discussed later in this chapter deals with that.

4.3.1. Isolation

The first step in nucleic acid analysis is the cell lysis process, which breaks open the cell wall.[9] This can be achieved through:

- Chemical methods (detergents, chaotropic salts, or organic salts)
- Mechanical methods (bead beating, sonication)
- Enzymatic methods (proteases, lysozymes, lytic enzymes)

4.3.2. Purification

Following the lysis process, purification separates proteins, lipids, and other contaminants that may interfere with the downstream analysis.[9–11] Standard purification techniques include:

- Phenol-chloroform extraction – Separates nucleic acids from proteins using organic solvents.

- Silica-based purification – A simple process where the nucleic acids bind to the silica in the presence of chaotropic salts, and weakly bound proteins and polysaccharides are removed by washing.

- Magnetic bead-based purification – Coated magnetic beads can selectively bind to nucleic acids under specific buffer conditions, followed by isolation using a magnetic rod.

4.3.3. Amplification

In many cases, the number of nucleic acids received after purification is insufficient for direct analysis. Amplification techniques are deployed to increase the quantity of nucleic acids to detectable levels.[12–14]

Polymerase Chain Reaction (PCR) is a widely used DNA amplification technique. Amplification takes place in three steps: denaturation (heating the sample to break the duplex), annealing (cooling to bind the short single-stranded DNA sequences called primers), and extension (formation of complementary strands).[15]

Isothermal amplification is a notable alternate procedure that does not require thermal cycling. Instead, these methods use specialized enzymes that facilitate DNA replication at a constant temperature. Some examples of the isothermal amplification processes are Loop-Mediated Isothermal Amplification (LAMP),[16] which uses strand-displacing polymerase and multiple primers to generate large amounts of DNA; Recombinase Polymerase Amplification (RPA), which employs recombinase enzymes to facilitate primer binding and strand exchange at lower temperatures; and Nicking Enzyme Amplification Reaction (NEAR), which utilizes nicking enzymes to generate continuous DNA replication in real time.[15,17]

4.3.4. Detection

Post amplification, two distinct approaches for nucleic acid detection are indirect and direct.

The indirect methods monitor the byproducts of the amplification process rather than the nucleic acids themselves. The approach relies on detecting physical changes (e.g., solution turbidity) or chemical variations (e.g., pH variations, phosphate release). While the indirect methods are simple, they can suffer from reduced specificity, increasing the risk of false-negative or false-positive results.[18]

The direct detection methods rely on identifying nucleic acids based on their sequence, minimizing errors in nucleic acid identification.[18–20] Subsequent sections outline some of the direct detection methods for nucleic acids.

Visual Detection Methods for Nucleic Acids

Visual detection probes are the widely used tools for the direct detection of nucleic acids. The different strategies for visual detection can broadly be classified into two classes:

- Binding-based strategies

- Hybridization-based strategies

Both strategies allow for fast and reliable detection of nucleic acids, although some methods lack specificity.

Binding-based Strategies

Small molecules can interact with nucleic acids in various ways, and these interactions have been utilized to develop detection strategies.[21] The primary binding modes are:

a. **Intercalation**: Small planar, positively charged molecules called intercalators insert between two stacked DNA or RNA duplex base pairs. The duplex unwinds to open space between the stacked nucleobase pairs, leading to lengthening of the strand, which distorts the stacking pattern. This structural distortion increases the fluorescence intensity of the intercalator, allowing for sensitive detection.

b. **Groove binding**: The base pair arrangement and the sugar-phosphate backbone in the DNA double helix are asymmetrical, leading to grooves in the structure. The broader and deeper groove is called the major groove, while the shallower and narrower groove is called the minor groove. Molecules can bind to the grooves through hydrogen bonds, van der Waals forces, or electrostatic interactions with the base pairs. Structurally, the molecule must be flexible enough to twist around the double helix sufficiently.

c. **Electrostatic interactions**: Due to the phosphate groups, nucleic acid's negatively charged backbone facilitates electrostatic interactions with cationic species. These interactions are non-specific due to the intense negative charge density inherent to nucleic acids.

Absorbance-based Probes

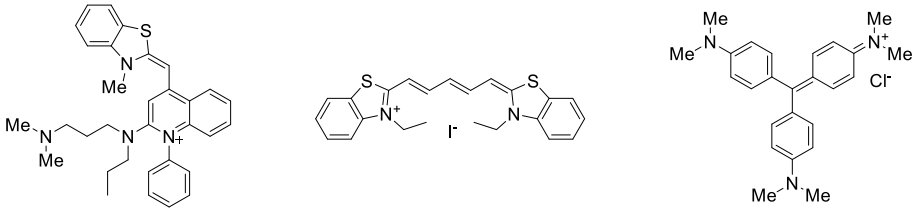

SYBER GREEN I DISC$_2$(5) CRYSTAL VIOLET

Figure 4-3 Absorbance-based probes are used for the binding-based detection of nucleic acids.

SYBR Green I (SG), an intercalating fluorescent dye, also changes color upon interaction with DNA. The unbound SG color is orange and changes to green upon intercalation.[22] DISC$_2$(5) is a cyanine dye that binds in the minor groove of the DNA double helix, and the binding process results in a blue shift in the absorption (λ_{max} = 647 nm to λ_{max} = 590 nm).[23] Crystal violet is a major groove-binding dye for DNA detection. The addition of excess sodium sulfite converts the purple-colored crystal violet into a colorless leuco crystal violet form. An equilibrium exists between the two forms, favoring the leuco form due to the excess sodium sulfite.[24]

Hybridization Process

Complementary base-pairing is leveraged in hybridization-based detection methods, often offering enhanced sensitivity and specificity over binding-based detection strategies. Hybridization can occur in two distinct ways: a) two complementary single strands coming together to form a double strand, and b) a complementary single strand displacing a strand from a duplex. Several strategies have been developed to incorporate the hybridization process in nucleic acid detection and quantification methods.

Nanoparticles provide a versatile platform for nucleic acid detection because of the ability to control their size, shape, surface chemistry, and optical properties. Both direct and post-amplification techniques have been used for nucleic acid detection. Gold nanoparticles (AuNP) are the most widely used nucleic acid detection systems. Color change due to the shift in localized surface plasmon resonance, observed upon aggregation of AuNPs, forms the basic principle for colorimetric detection of nucleic

acids. Basic design strategies for nucleic acids detection based on AuNPs are listed below:

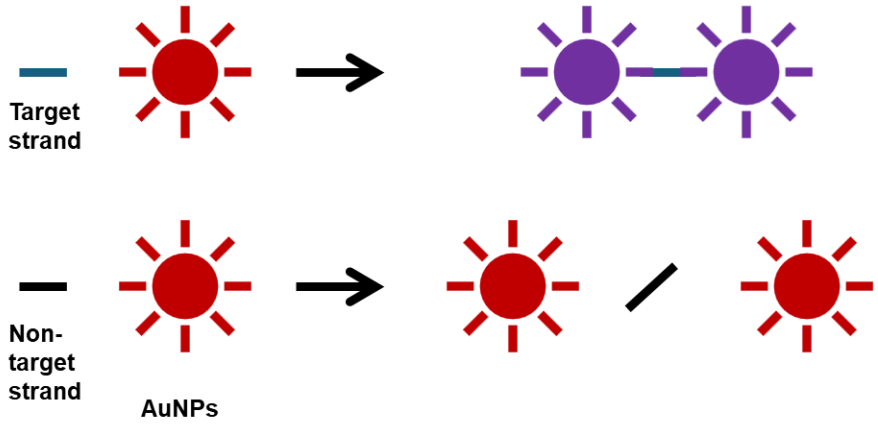

Figure 4-4 Crosslinking process for nucleic acid detection by AuNPs.

Crosslinking approach: Labeling AuNPs with thiolated oligonucleotides allowed for developing a cross-linking-based approach for nucleic acid detection. This approach labels AuNPs with oligonucleotides complementary to one-half of the target nucleic acid sequence. Adding the complementary target strand results in the hybridization process. Aggregation of the AuNPs occurs as a result, leading to a color change from red to purple.[25,26]

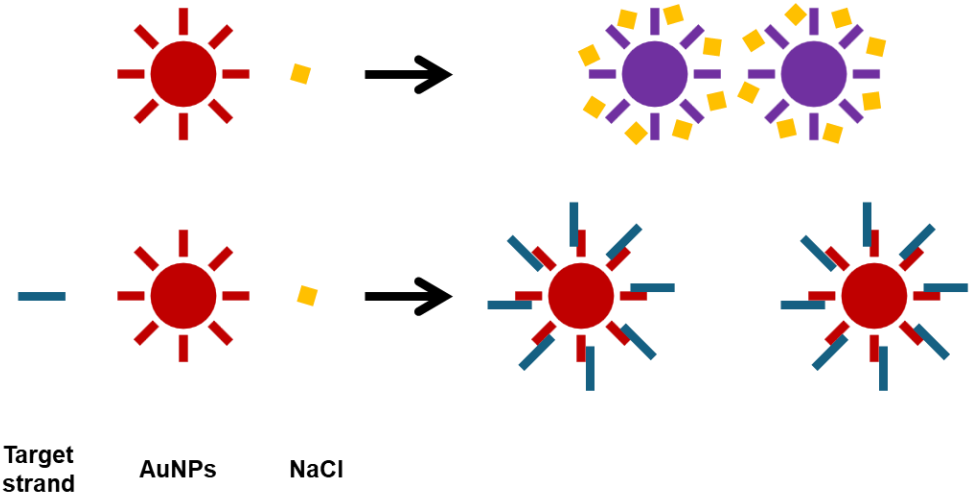

Figure 4-5 Non-crosslinking process for nucleic acid detection by AuNPs.

Non-crosslinking approach: In this approach, ssDNA strands complementary to the target strand are attached to the AuNP surface. In the absence of the non-

complementary target strand, high NaCl concentrations lead to aggregation of the AuNPs, causing a color change from red to purple. However, in the presence of the target strand, hybridization occurs between the AuNP surface-bound probe ssDNA and the target strand. This hybridization increases the stability of the AuNP, preventing NaCl-induced aggregation, and the solution remains red.[25,27]

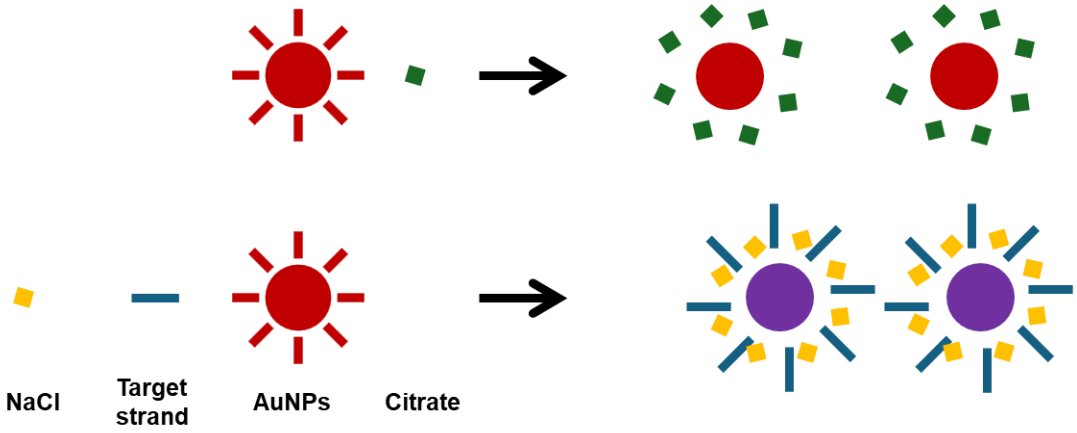

Figure 4-6 Sandwich-mode probes for nucleic acid detection by AuNPs.

Sandwich mode: Non-functionalized AuNP: AuNPs are capped with citrate to create a negatively charged surface that inhibits aggregation. SsDNA or RNA, with their exposed nucleobases, can adsorb on the surface of the AuNP through non-covalent interactions. This adsorption process increases the overall charge density on the AuNP surface and stabilizes the colloid against NaCl-induced aggregation. In contrast, dsDNA cannot adsorb on the AuNP surface similarly; thus, NaCl addition leads to a decrease in electrostatic repulsion, and subsequently, aggregation occurs, causing the color change from red to purple.[28]

Similar to AuNPs, silver nanoparticles (AgNP) have been used for colorimetric detection of nucleic acids. Colloidal solutions of AgNPs exhibit a yellow color due to localized surface plasmon resonance (LSPR). Aggregation leads to a visible color change to red.[29]

Other colorimetric techniques for nucleic acid detection use the peroxidase-like enzyme activity of nanomaterials like G-quadruplex-based nanostructures[30], magnetic NPS[31], and graphene oxide. These nanomaterials can catalyze the oxidation of chromogenic substrates like 2,2'-azino*bis*(3-ethylbenzothiozoline)-6-sulfonic acid

(ABTS), 3,3',5,5'-tetramethylbenzidine (TMB), o-phenylenediamine (OPD) in presence of oxidizing agents like hydrogen peroxide (H_2O_2) and singlet oxygen ($^1O_2$). In the presence of the target nucleic acid, the peroxidase-like activity of these nanomaterials turns on, leading to a color change.

Toehold-mediated Strand Displacement (TMSD)

TMSD is a powerful technique used in nucleic acid detection, utilizing the unique properties of DNA and RNA to create highly specific and controllable interactions.[32,33] The mechanism of TMSD involves the following steps:

- Initial complex – A double-stranded DNA complex consisting of a shorter protector strand and a longer target strand. This creates an overhanging "toehold" region in the target strand.
- Invading strand—The initial complex introduces an RNA or a single-stranded DNA complementary to the target strand.
- Toehold binding – The invading strand binds to the toehold region, thereby initiating a displacement process.
- Branch migration – The invading strand progressively replaces the protector strand through a process known as branch migration.
- Displacement – At the end of the process, the protector strand is wholly displaced, leaving the target strand bound to the invading strand.

4.4. Proposed Research

The applicability of diarylethene photoswitches in biological systems has been widely demonstrated in the literature. Several research groups have worked on the sensing and imaging applications of the diarylethene photoswitches, while others have tried to incorporate the nucleobases in the photoswitch itself.

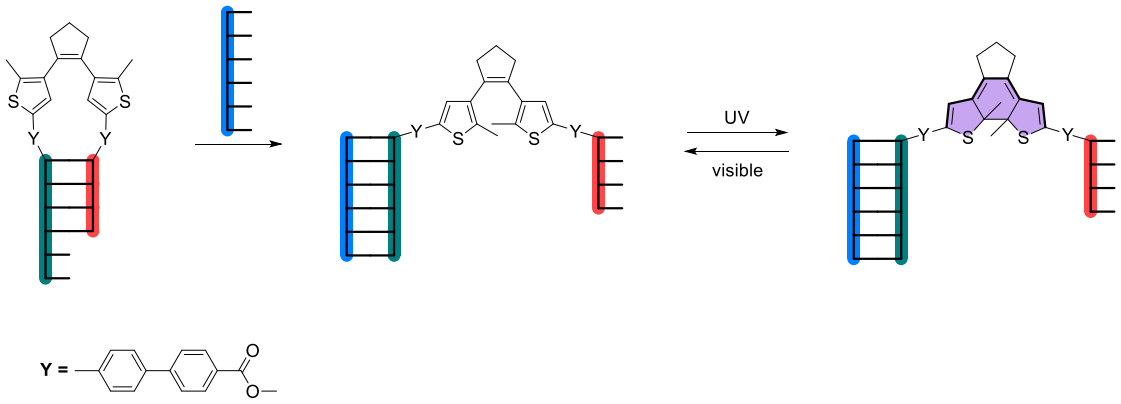

Scheme 4-1 A toehold-mediated detection strategy is based on locking the diarylethene in parallel conformation.

This research proposes a nucleic acid detection system based on the toehold-mediated strand displacement process. The proposed system features a pair of nucleic acid strands of different lengths positioned across the diarylethene molecule. The two thiophenes will converge in the parallel conformation to form a duplex with a toehold. This arrangement will lock the diarylethene photoswitch in the non-photochromic parallel conformation. When a target strand with higher complementarity to the longer strand is introduced in the system, strand displacement will occur. The duplex will break, allowing the diarylethene photoswitch to acquire the photoactive anti-parallel conformation. Irradiating with light of appropriate wavelength induces the photocyclization reaction in the diarylethene, resulting in a color change. This color change will be used as the optical readout signal for the presence of the analyte strand.

The proposed system can potentially be used in medical diagnostics and monitoring processes. The longer strand could be designed to complement a unique segment of the nucleic acid genome of a virus or bacterium. Similarly, the DNA sequences or mutations associated with certain tumors, cancers, and genetic disorders could be used as targets for diagnostic purposes. Monitoring the extent of the color change can assess the progression of a disease or the amount of harmful pathogens present.

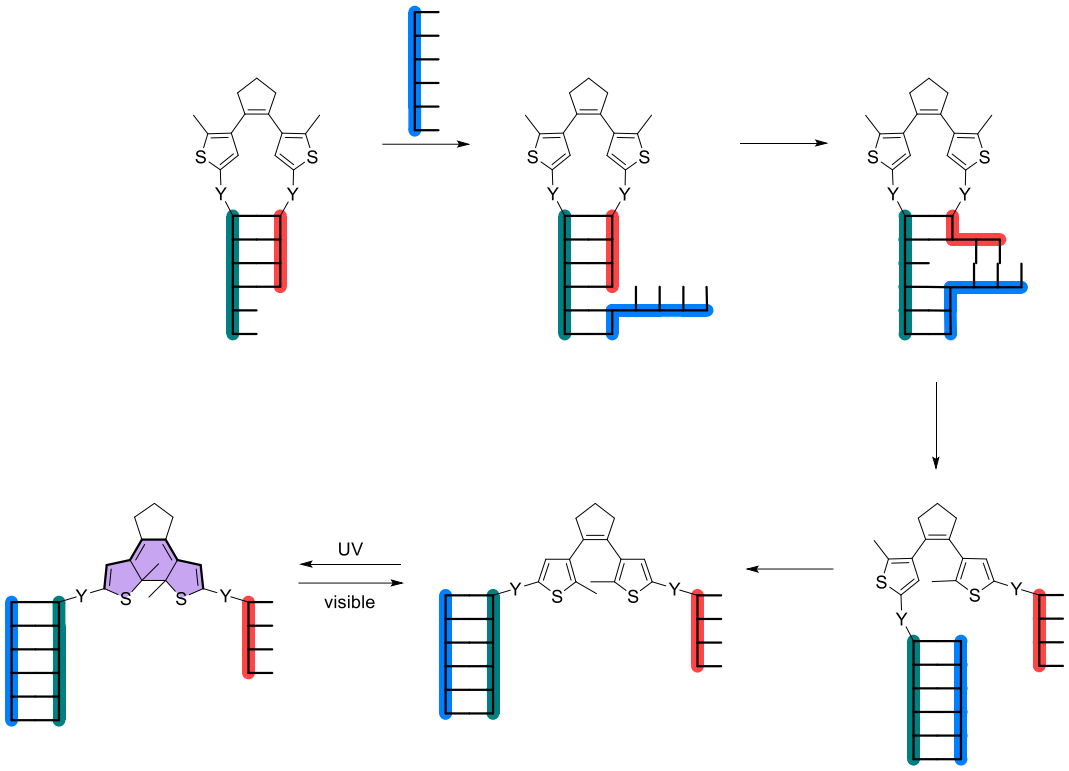

Figure 4-7 Each step of the Toehold-mediated strand displacement process mentioned previously.

The proposed nucleic acid detection system offers several advantages. The toehold-mediated strand displacement process is highly specific, making the color change only possible when the perfectly complementary target strand is present. Ideally, the system will go from colorless to colored, making it sensitive even at low concentrations of target strands. The proposed system is also versatile, allowing the detection of a wide range of nucleic acid sequences by simply changing the target strand. The system's relative ease and simple design make it suitable for point-of-care diagnostics and on-the-field applications.

4.4.1. Proof of Concept

As proof of concept for the diarylethene-based nucleic acid detection system, the initial idea was to design and synthesize a diarylethene molecule with one pair of complementary nucleobases on each thiophene arm. The design of the diarylethene molecule also had to incorporate the dimensions of the DNA duplex. The diameter of a DNA duplex is approximately 18-20 Å; thus, the end-to-end length of the diarylethene

photoswitch in the anti-parallel conformation should be greater than this. If the photoswitch is shorter than the DNA diameter, the diarylethene molecule can acquire photochromic anti-parallel conformation. The other important consideration is the choice of a functional group on the diarylethene molecule for the covalent binding of the nucleic acid strand. The convention for the directionality or orientation of the single strand of a nucleic acid is based on the ribose sugar. The nucleic acid strand contains a 5’ end where the phosphate group is attached to the hydroxyl group on the carbon 5 of the ribose ring and a 3’ end where the hydroxyl group is on carbon 3. Amine or thiol functional groups are commonly used as the end groups in commercially available single strands of nucleic acids.

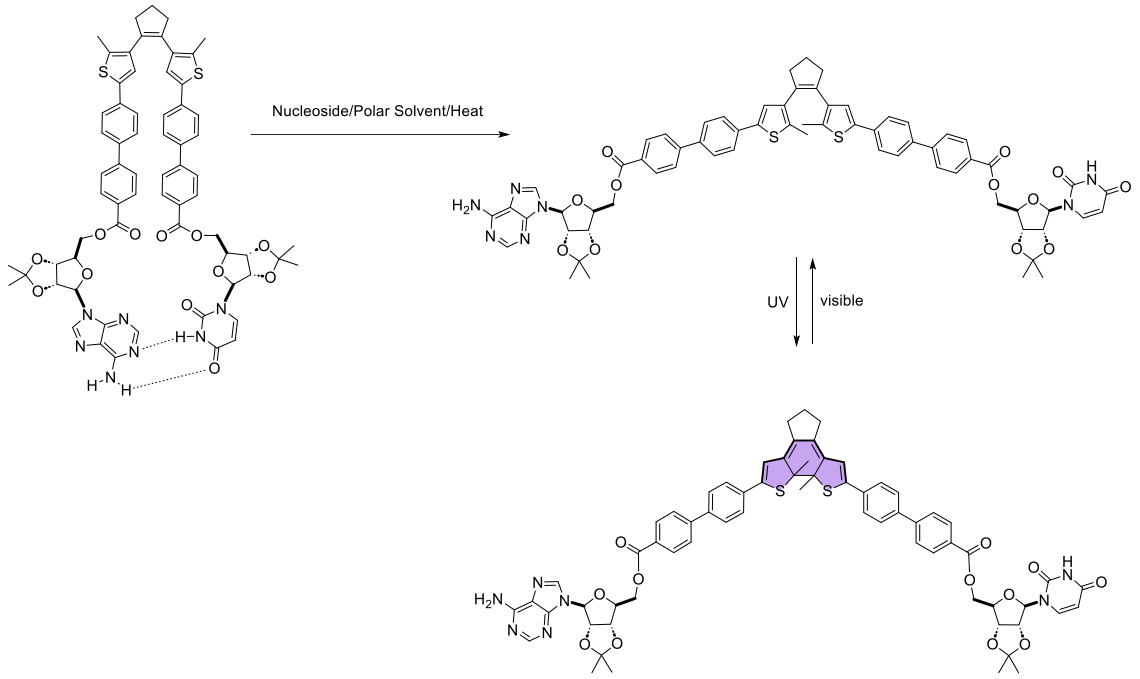

Scheme 4-2 Proof of concept based on a single nucleobase pair across the thiophene arms.

Several diarylethene photoswitch structures were considered with different functional groups that can undergo chemistry with the commercially available single strands. A biphenyl group connected to the thiophene group was envisaged to achieve the optimum length. For the proof of concept, 2′,3′-O-Isopropylidene derivatives of adenosine and uridine were selected to attach to the diarylethene photoswitch. Since there is a free primary hydroxyl group on the ribose ring, carboxylic acid was chosen as

the functional group on the diarylethene molecule, as esterification is one of the most straightforward chemical reactions.

After designing the molecule, computational structure analysis was done using the Gaussian 09 software. The geometry of the anti-parallel conformation was optimized using the Hartree-Fock method with a 6-31G,d basis set. The end-to-end length between the carboxyl groups in the anti-parallel conformation in the optimized structure was 27 Å. The biphenyl groups on thiophene impart rigidity to the structure, allowing the length in anti-parallel conformation to be longer than the diameter of the DNA duplex.

4.4.2. Synthesis

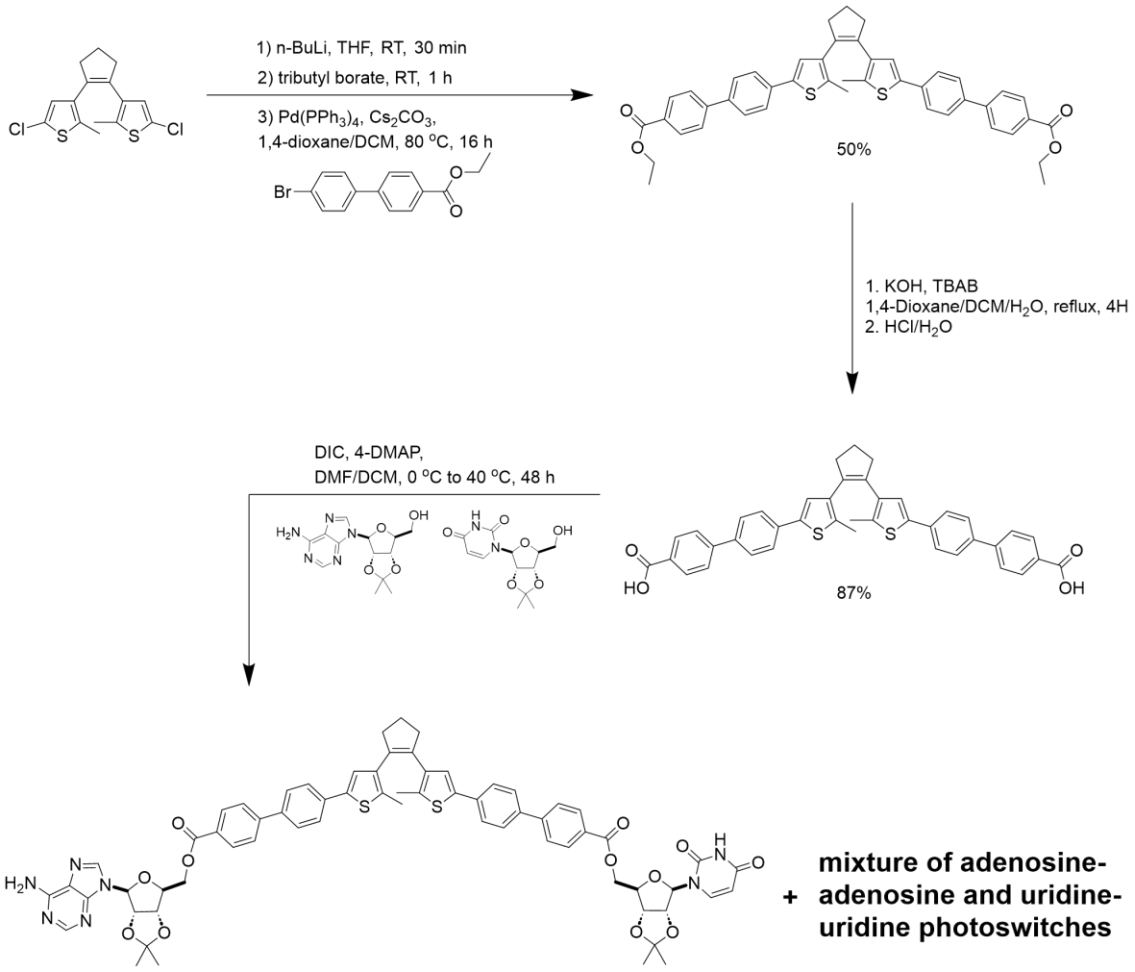

Scheme 4-3 Synthesis scheme for the nucleobase diarylethene photoswitch.

The *bis*-chloro diarylethene precursor was synthesized by the process described in Chapter 3. The biphenyl arm was synthesized by the Suzuki coupling reaction of 4-

bromobenzene boronic acid and methyl-4-iodobenzoate. Metal-halogen exchange of the *bis*-chloro diarylethene molecule with n-BuLi, followed by the Suzuki coupling with biphenyl ester, gave the *bis*-ester diarylethene. This *bis*-ester diarylethene photoswitch was hydrolyzed with a base to yield the *bis*-acid diarylethene molecules. Steglich esterification of the protected nucleosides with the *bis*-acid diarylethene molecules using carbodiimides gave a mixture of adenosine-adenosine, adenosine-uridine, and uridine-uridine diarylethene photoswitches.

4.5. Results and Discussions

4.5.1. Computational Analysis

To test whether the two nucleobases can form a hydrogen-bonded pair in the parallel conformation of the diarylethene, a simple computational analysis was performed using the DFT method with a 6-31G, d basis set. The structure was designed in the *parallel* conformation, and the two nucleobases were kept close. Geometry optimization was done to observe the final optimized structure and determine if hydrogen bonding will occur naturally.

The optimized structure showed a planar arrangement of adenosine and uridine units in the *parallel* conformation. The hydrogen bond lengths were measured at 1.78 Å and 1.90 Å, confirming the formation of N-H---O and N-H---N hydrogen bonds. This reinforced that the diarylethene molecule should be able to achieve the locked state upon base pairing, thus restricting its photochromic activity. Since this simple experiment aimed to assess whether such a configuration was possible, no further higher-level analysis was carried out.

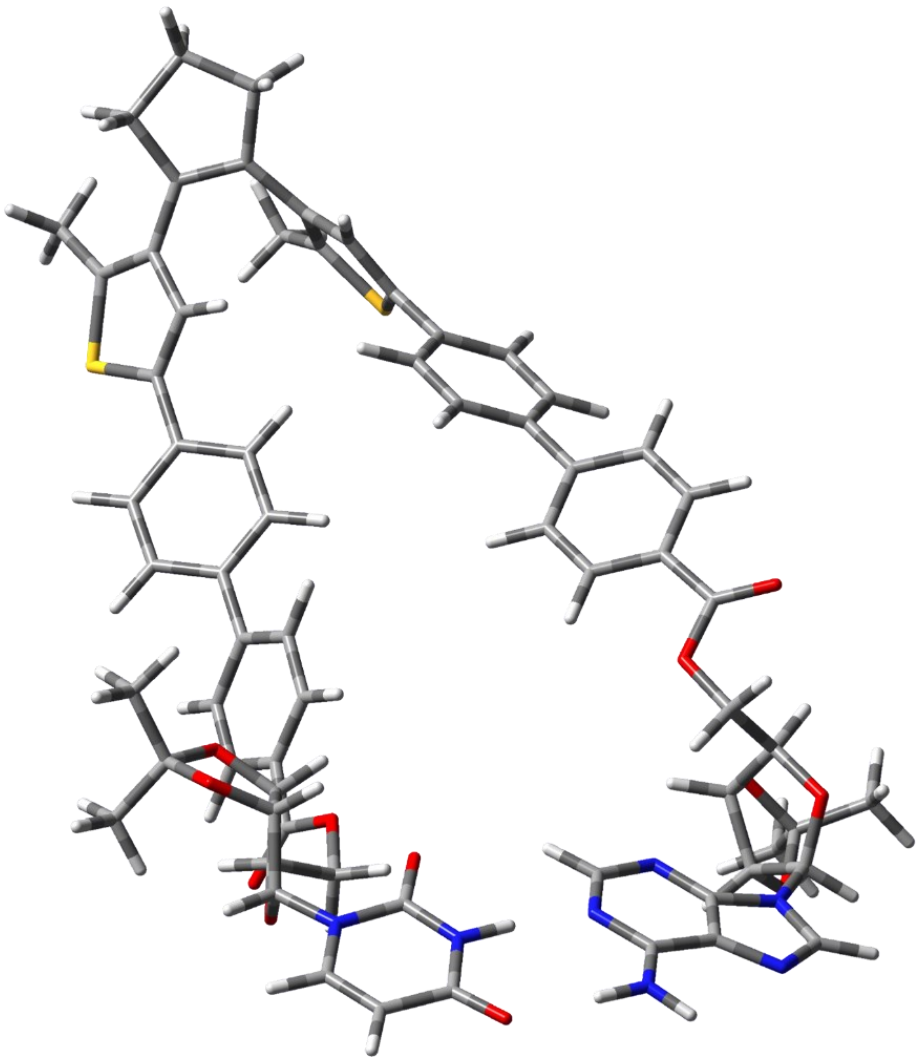

Figure 4-8 Figure 4-8 Optimized structure of diarylethene in parallel conformation with planar arrangement of nucleobases.

4.5.2. Synthesis Challenges

Initially, attempts were made to synthesize the biphenyl carboxylic acid instead of the ester to minimize the number of synthesis steps. However, this proved challenging as the molecule was highly polar, with several overlapping spots on the TLC, which made the purification difficult. This prompted the switch to ethyl esters to facilitate the purification of the diarylethene photoswitch. The Suzuki coupling reaction was initially tried in a toluene/ethanol/water mixture; however, only a tiny amount of disubstituted

product was recovered from the reaction mixture, with mostly monosubstituted product. Attempts to perform the metal-halogen exchange reaction on the monosubstituted product were unsuccessful, followed by the Suzuki coupling reaction to make the disubstituted product. The reaction yielded multiple overlapping products, as evidenced by TLC. A water-free Suzuki coupling reaction was performed in 1,4-dioxane with cesium carbonate as the base at reflux and 80 °C temperature. The yield increased slightly compared to the previous solvent mixture at both temperatures; however, the monosubstituted diarylethene was still the major product. It was observed that as the reaction proceeded, an insoluble precipitate formed. Filtration and analysis of the precipitate revealed that the precipitate was the monosubstituted product. The solubility of this product was checked in different solvents, and it was found that the molecule was only soluble in dichloromethane or chloroform. The reaction was repeated in 1,4-dioxane mixtures with dichloromethane or chloroform at 80 °C. In the case of the dichloromethane reaction, fresh solvent was added as soon as the precipitate appeared, most likely due to solvent evaporation. The yield for the disubstituted production improved significantly for the dichloromethane reaction. The same issue occurred with the hydrolysis reaction of the ester. Adding dichloromethane did not favor hydrolysis; the same precipitation issue was observed. The addition of cetyltrimethylammonium bromide (CTAB), a phase transfer agent, helped with the hydrolysis reaction of the ester. The esterification reaction with nucleobases was then performed in a mixture of *N, N*-dimethylformamide and dichloromethane.

4.5.3. Locking and Unlocking Tests

Absorbance spectroscopy was performed to test the hypothesis that changing the environment in the solution locks and unlocks the nucleobase diarylethene. DMSO was selected as a highly polar solvent that can break the hydrogen bonding between nucleobases to observe the photochromic performance of the nucleobase diarylethene. A 0.025 mM solution of the diarylethene was prepared, and the absorbance spectrum was collected without irradiation with 365 nm UV light. The spectrum at t=0s showed a band in the visible region. The sample was kept in front of a visible lamp with a >450 nm cutoff filter for 10 minutes; however, no change in the spectrum was observed. Further irradiation with 365 nm UV light increased the band in the visible region centered around 563 nm, and PSS was reached after 50 seconds of irradiation.

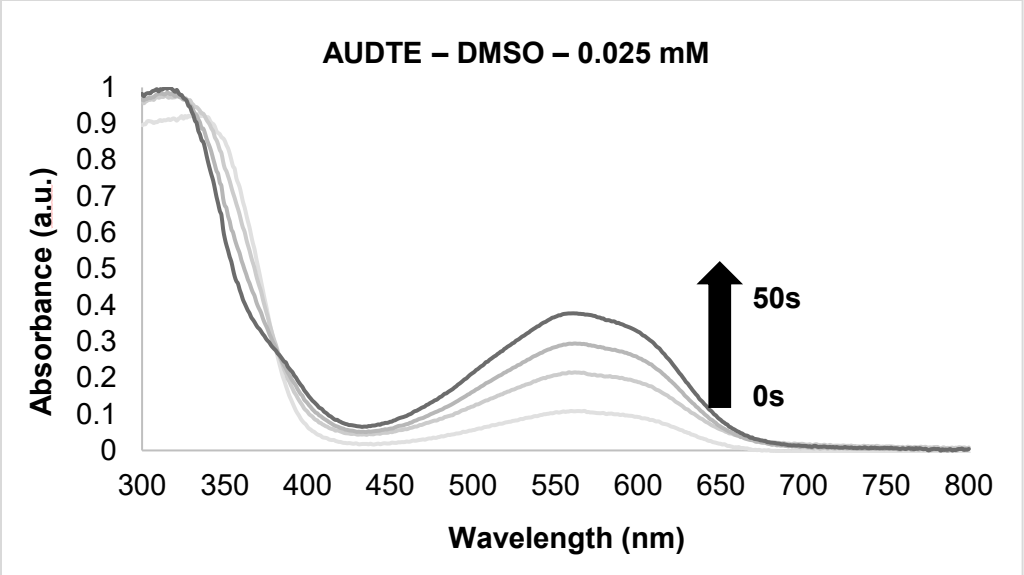

Figure 4-9 The absorbance spectra of nucleobase diarylethene in DMSO (0.025 mM).

Since chloroform is one of the solvents that completely dissolves the nucleobase diarylethene and is relatively less polar than DMSO, the same experiment was performed to see whether the solvent would allow the locking of the photoswitch in the *parallel* conformation.

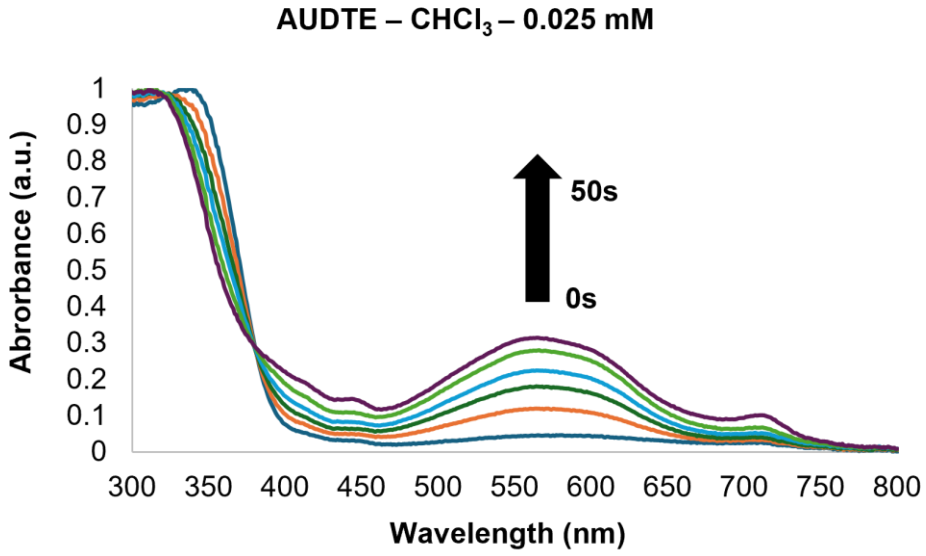

Figure 4-10 The absorbance spectra of nucleobase diarylethene in chloroform (0.025 mM).

However, an increase in the bands in the visible region centered at 566 nm was observed with UV light irradiation (365 nm), and the PSS was reached after 50 seconds of irradiation. It was hypothesized that this was probably due to the water present in the solvent. However, only a slight decrease in the band intensity was observed when dry solvent was used.

During an NMR run, the tube was accidentally exposed to light. However, the sample remained colorless. This prompted an inquiry into trying the locking process in deuterated solvents. Since the solubility of diarylethene is best in dichloromethane, the next attempt was to lock the molecule in dry CD_2Cl_2.

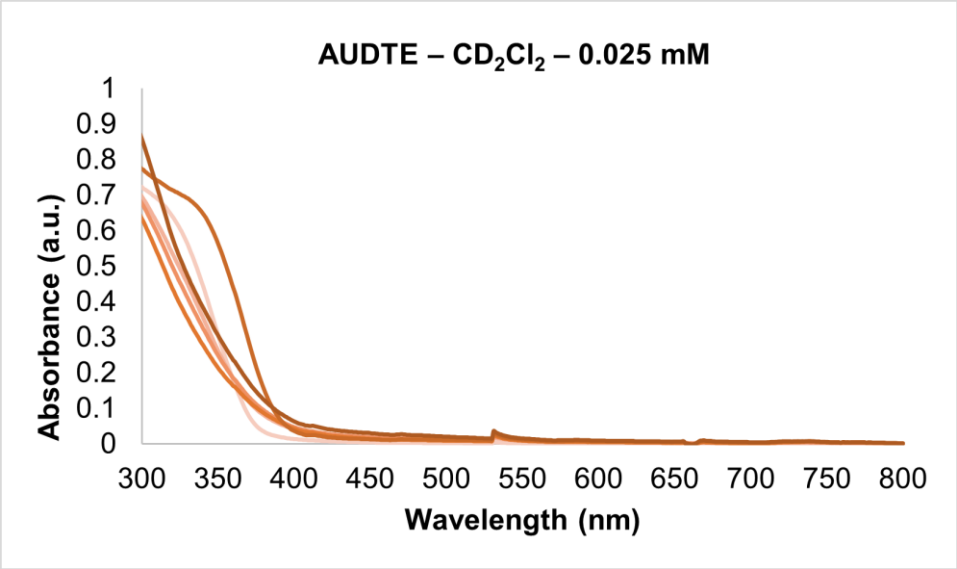

Figure 4-11 The absorbance spectra of nucleobase diarylethene in deuterated dichloromethane (0.025 mM).

A 0.025 mM solution of the diarylethene photoswitch was prepared in dry deuterated dichloromethane, and the absorbance spectra were collected. The sample was irradiated with 365 nm UV light for 180 seconds, but no change in absorbance spectra was observed. The addition of adenine in 100 µL of methanol and DMSO also did not result in any change in the spectra. Similar observations were seen with deuterated chloroform as the solvent.

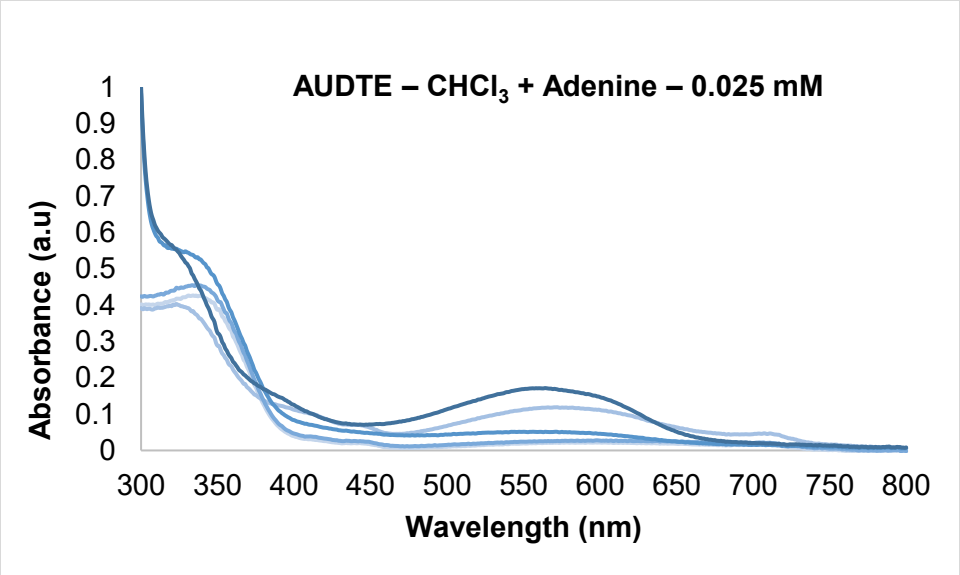

Figure 4-12 The absorbance spectra of nucleobase diarylethene in chloroform with adenine (0.025 mM).

Since there was no change in the absorbance spectra of the deuterated solvents, dry chloroform was again tested. The solvent was dried thoroughly on 4 Å molecular sieves and deoxygenated with freeze-pump-thaw. A 0.025 mM solution was prepared, and absorbance spectra were collected. The addition of adenine in DMSO to the mix resulted in an increase in bands in the visible region. However, the same was also observed when only DMSO was added. Irradiation with UV light resulted in an increase in bands in the visible region. This observation made the whole experiment inconclusive about whether the unlocking was due to adenine or the solvent.

At this point, it was hypothesized that the protons in chloroform and dichloromethane disrupt the hydrogen bonding. That disruption is minimized in deuterated solvents such as $CDCl_3$ and CD_2Cl_2, and the diarylethene can lock through the hydrogen bonding between the nucleobases. To check for this hypothesis, the absorbance spectra were recorded in CCl_4, which possesses no protons, and the solubility of the photoswitch is similar to that in the case of chloroform and dichloromethane. The results for the tests in CCl_4 were identical to those in the case of deuterated chloroform and dichloromethane. The addition of DMSO, methanol, and adenine did not unlock the diarylethene photoswitch.

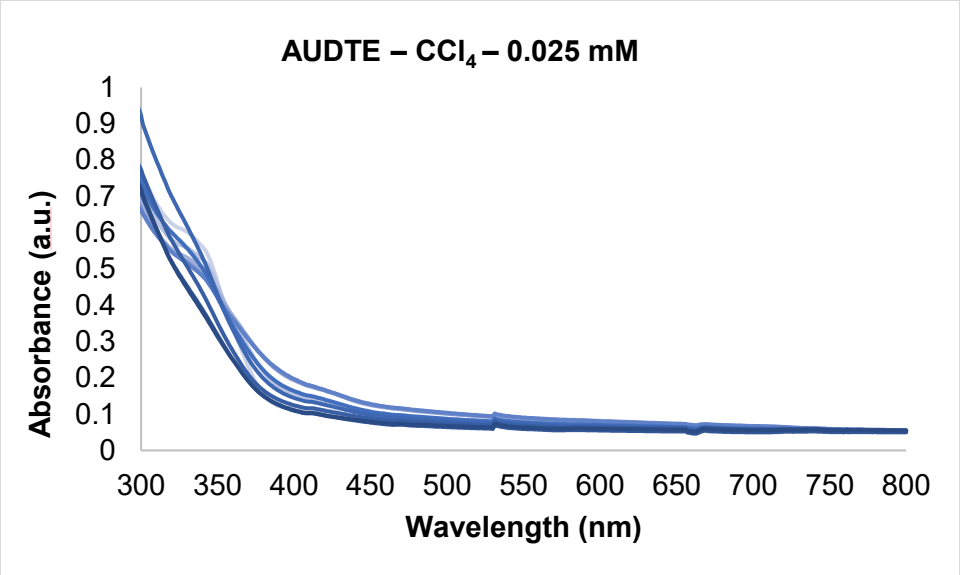

Figure 4-13 The absorbance spectra of nucleobase diarylethene in CCl_4 (0.025 mM).

Several other solvents were also tried; however, the result was more or less the same in each case. Polar solvents kept the molecule unlocked, while hydrogen bonding tightly held the molecule in a parallel conformation in non-polar solvents. In the case of highly non-polar solvents (hexanes, cyclohexane, and heptane), the molecule crashed out.

4.6. Limitations

There are several challenges and limitations in toehold-mediated strand displacement systems for nucleic acid detection. The target nucleic acid and the toehold need to be very specific. If the target nucleic acid has a similar or partial sequence somewhere other than the end, binding from a site different from the one intended might occur, which may only result in a partial displacement. This situation may also arise in complex systems where multiple analytes are present. Unintended interactions between a non-target analyte and the toehold might occur, stopping the intended analyte from attaching.

Similarly, a non-target species like blood or saliva may interact with the nucleic acid duplex of the diarylethene system. The changes in pH and temperature also affect the binding of the nucleic acid strands. Spontaneous displacement of the strands, referred to as leakage, might also occur, increasing the background noise. These

limitations reduce the specificity of this system towards the analyte and increase the chances of false-positive or false-negative results.

The length of the toehold is also critical, as a shorter or suboptimal toehold might result in slower reaction kinetics. This would result in incomplete strand displacement reactions, leading to a false negative result. Lastly, the sensitivity of such a system will not be very high unless an amplification method is used. The detection system and the analyte react in 1:1 stoichiometry. The color intensity will be weak and difficult to assess for samples with low analyte concentrations.

4.7. Future Work

The next step in the project will be to weaken the nucleobase interaction to afford the breakage of the hydrogen bonds. The adenine group can be replaced with inosine, a purine found in transfer RNA (tRNA), which can bind to adenine, cytosine, and uracil. Since uracil can also hydrogen bond with guanine, its addition should ideally break the duplex. Alternatively, a less hydrogen bonding derivative of uracil can also be used alongside adenine. A thorough computational analysis of the binding process must be performed to analyze the hydrogen bonding strengths before synthesizing and analyzing the modified structures. Regarding the design of the diarylethene, one of the phenyl groups from the biphenyl arm could be replaced with a linker long enough to maintain the size considerations. This will help solve the solubility challenges during the synthesis. Other functional groups that can react with the OH of the sugar could also be tried. Once these problems are solved, actual nucleic acid strands need to be attached to the diarylethene photoswitch, and the hypothesis with the toehold-mediated strand displacement process needs to be tested. The lengths of the two strands will be critical, as well as the length of the toehold. The other important aspect will be the number of mismatches in the duplex. If the number of mismatches is large, spontaneous displacement of strands may occur.

4.8. Materials and Instrumentations

Solvents, reagents, catalysts, and precursors used for synthesis, chromatography, UV-visible spectroscopy, and photochemical studies were purchased from Aldrich, Alfa Aesar, Anachemia, Caledon Labs, and Fisher Scientific and used as received. Solvents used for moisture-sensitive reactions were dried by passing through silica gel and leaving on 3 Å / 4 Å molecular sieves for at least 48 hours or passing through steel columns containing activated alumina under nitrogen using an MBraun solvent purification system. Deuterated solvents for NMR spectroscopy were purchased from Cambridge Isotope Laboratories and Aldrich and used as received or dried with 4 Å molecular sieves for at least 48 hours. Column chromatography was done using silica gel 60 (0.015-0.040 mm or 0.063 to 0.200 mm) purchased from Silicycle Inc.

^{1}H, and ^{13}C NMR characterizations were performed on a Bruker Avance-400 instrument with a 5 mm inverse probe operating at 400.13 MHz for ^{1}H NMR and 100.61 MHz for ^{13}C NMR. Chemical shifts (δ) are reported in parts per million (ppm) relative to tetramethylsilane using the residual solvent peak as a reference. Coupling constants (J) are reported in Hertz. UV-visible absorption spectra were recorded on a Shimadzu UV-3600Plus spectrophotometer. High-resolution mass spectroscopy (HRMS) measurements were performed using an Agilent 6210 TOF LC/MS in ESI-(+) mode. Ring-closing reactions were carried out using a lamp for visualizing TLC plates at 312 nm (Spectroline E series, 470 W/cm2). The ring-opening reactions were carried out using the light of a 150 W halogen photo-optic source passed through a 435 nm cut-off filter to eliminate higher energy light.

Synthesis

Bis-chloro diarylethene photoswitch was prepared using the synthesis procedure described in Chapter 3.

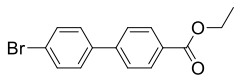

Ethyl 4'-bromo-[1,1'-biphenyl]-4-carboxylate- 4-Bromobenzeneboronic acid (4.02 g, 20 mmol, 1 eq), ethyl-4-iodobenzoate (5.24 g, 20 mmol, 1 eq), and $Pd(PPh_3)_4$ (2.31 g, 2 mmol, 0.1 eq) were dissolved in a mixture of toluene (100 mL) and ethanol (60 mL). 2M

aqueous Na_2CO_3 solution (20 mL) was added, and the reaction mixture was refluxed and monitored with TLC for 16 hours. After the reactants were consumed, the reaction was cooled to room temperature, and water (50 mL) was added. The mixture was extracted with ethyl acetate (3 × 100 mL), the combined organic phases were washed with brine, dried over $MgSO_4$, and the solvent was evaporated to dryness. Purification with silica gel column chromatography using 10 % ethyl acetate in hexanes yielded 4.66 g (80%) of ethyl 4'-bromo-[1,1'-biphenyl]-4-carboxylate as a white solid.

^{1}H NMR-- (400 MHz, $CDCl_3$) δ- 8.1 (dt 2H), 7.60 (tt, 4H), 7.48 (dt, 2H), 4.39 (q, 2H), 1.42(t, 3H)

^{13}C NMR- (101 MHz, $CDCl_3$) δ- 166.4, 144.6, 138.9, 133.0, 130.2, 128.8, 126.8, 122.5, 61.2, 14.5

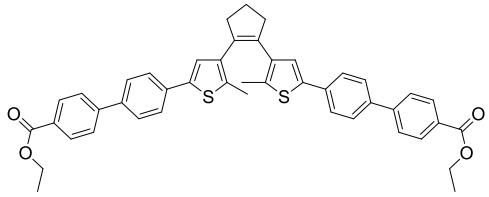

Diethyl 4',4'''-(cyclopent-1-ene-1,2-diyl*bis*(5-methylthiophene-4,2-diyl))*bis*([1,1'-biphenyl]-4-carboxylate)- n-BuLi (3 mL, 7.5 mmol, 2.5 eq, 2.5 M in hexane) was added dropwise to a solution of 1,2-*bis*(5-chloro-2-methylthiophen-3-yl)cyclopent-1-ene (1.00 g, 3 mmol, 1 eq) in dry tetrahydrofuran (60 mL) at room temperature over 30 minutes. The reaction mixture was monitored with TLC and stirred for an additional 30 minutes. Tributyl borate (3.22 mL, 12 mmol, 4 eq) was added, and the reaction was stirred at room temperature for a further 1 h. In a separate round-bottom flask, ethyl 4'-bromo-4-biphenylcarboxylate (3.49 g, 12 mmol, 4 eq) and $Pd(PPh_3)_4$ (700 mg, 0.6 mmol, 0.2 eq) were dissolved in toluene (50 mL) and ethanol (30 mL) followed by the addition of 2M aqueous Cs_2CO_3 solution (30 mL). The mixture was heated to around 60 °C to obtain a clear solution, and the previously prepared boronic ester was added dropwise. The reaction was refluxed for 16 h and monitored with TLC. After completion, the reaction was cooled to room temperature and added water (50 mL). The mixture was extracted with dichloromethane (3 × 75 mL), the combined organic phases were washed with brine, dried over $MgSO_4$, and the solvent evaporated to dryness. Purification with silica gel column chromatography using 50% dichloromethane in hexanes yielded 0.92 g

(50%) of diethyl 4',4'''-(cyclopent-1-ene-1,2-diyl*bis*(5-methylthiophene-4,2-diyl))*bis*([1,1'-biphenyl]-4-carboxylate) as a grey solid.

^{1}H NMR-(400 MHz, $CDCl_3$) δ- 8.10 (d, 4H), 7.66, (d, 4H), 7.60 (s, 8H), 7.11 (s, 2H), 4.40 (q, 4H), 2.86 (t, 4H), 2.11 (m, 2H), 2.03 (s, 6H), 1.41 (t, 6H)

^{13}C NMR- (101 MHz, $CDCl_3$) δ- 166.8, 145.1, 139.2, 138.6, 137.0, 135.2, 134.9, 134.5, 130.1, 127.7, 126.8, 125.9, 124.6, 60.9, 38.1, 23.2, 14.6, 14.5

HRMS (ESI): m/z (M+H) calculated for $C_{45}H_{41}O_4S_2$: 709.245609, found: 709.245680

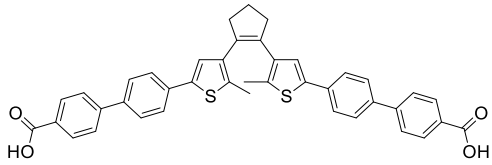

4',4'''-(Cyclopent-1-ene-1,2-diyl*bis*(5-methylthiophene-4,2-diyl))*bis*([1,1'-biphenyl]-4-carboxylic acid))- In a round bottom flask, 80 mL of 1:1 (v:v) 1,4-dioxane/water mixture was added, followed by the dimethyl 4',4'''-(cyclopent-1-ene-1,2-diyl*bis*(5-methylthiophene-4,2-diyl))*bis*([1,1'-biphenyl]-4-carboxylate) (680 mg, 1 mmol, 1 eq) and 1.5 g KOH (crushed pellets). The mixture was refluxed for 16 h under stirring. After completion, the reaction was cooled to room temperature, and the pH value was adjusted to around pH=2 with 2 M HCl. A grey precipitate formed which was centrifuged to collect, washed with water, and dried under vacuum to yield 0.57 g (87%) of 4',4'''-(Cyclopent-1-ene-1,2-diyl*bis*(5-methylthiophene-4,2-diyl))*bis*(([1,1'-biphenyl]-4-carboxylic acid)) as a grey solid.

^{1}H NMR-(400 MHz, DMSO-d) δ- 12.95 (bs, 2H), 8.02 (d, 4H), 7.82 (d, 4H), 7.69 (d, 4H), 7.65 (d, 4H), 7.44 (s, 2H), 2.86 (t, 4H), 2.04 (m, 2H), 1.94 (s, 6H)

HRMS (ESI): m/z (M+H) calculated for $C_{41}H_{33}O_4S_2$: 653.181478, found: 653.182218

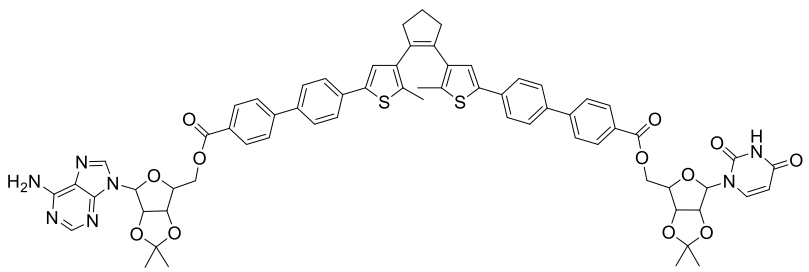

Procedure for adenine-uridine diarylethene- In a flame-dried round bottom flask, 2',3'-O-isopropylideneadenosine (84 mg, 0.275 mmol, 1.1 eq) and 2',3'-O-isopropylideneuridine (78 mg, 0.275 mmol, 1.1 eq) were dissolved in 10 mL (1:1, v: v) anhydrous DMF/dichloromethane mixture. 4-dimethylamonipyridine (0.008g, 0.0625 mmol, 0.25 eq) and *N,N'*-diisopropylcarbodiimide (0.098 mL, 0.625 mmol, 2.5 eq) were subsequently added and stirred for 15 min. *bis*-carboxylic acid diarylethene (0.25 mmol, 1 eq) was dissolved in 5 mL anhydrous DMF and added dropwise to the previously stirring solution of nucleosides. The reaction was stirred at room temperature for 48 hours. After completion of the reaction, water (10 mL) was added and extracted with DCM (3 × 30 mL). The combined organic phase was washed with brine, dried over $MgSO_4$, and the solvent evaporated to dryness. Purification on silica gel column chromatography (chloroform/methanol, 0 to 10% gradient) yielded the compound as a purple oil.

^{1}H NMR--(400 MHz, DMSO-d6) δ- 11.45 (s, 1H), 8.31 (s, 1H), 8.15 (s, 1H), 8.05 – 7.75 (aromatic H, 16H), 7.31 (s, 1H), 7.27 (s, 2H), 6.24 (s, 1 H), 5.81 (s, 1H), 5.57 (d, 1H), 5.21 (s, 1H), 5.18 (s, 1H), 4.98 (s, 1H), 4.61 (s, 1H), 4.55 – 4.31 (m, 6 H), 2.67 (t, 4H), 2.07 (m, 2H), 2.01 (s, 6H), 1.51 (s, 3H) 1.51 (s, 3H), 1.28 (s, 3H), 1.26 (s, 3H).

4.9. References

(1) Rapley, R. Nucleic Acid Structure and Basic Analysis. In Genomics and Clinical Diagnostics; Whitehouse, D., Rapley, R., Eds.; The Royal Society of Chemistry, 2019; p 0. https://doi.org/10.1039/9781782628217-00001.

(2) Minchin, S.; Lodge, J. Understanding Biochemistry: Structure and Function of Nucleic Acids. Essays Biochem. 2019, 63 (4), 433–456. https://doi.org/10.1042/EBC20180038.

(3) The Biochemistry of the Nucleic Acids; Elsevier, 1972. https://doi.org/10.1016/B978-0-12-205350-4.X5002-1.

(4) Molecular Biology of the Cell, 4th ed.; Alberts, B., Ed.; Garland Science: New York, 2002.

(5) Dutta, A.; Banerjee, N.; Chaudhuri, M.; Chatterjee, S. Nucleic Acid in Diagnostics. In Nucleic Acid Biology and its Application in Human Diseases; Chatterjee, S., Chattopadhyay, S., Eds.; Springer Nature Singapore: Singapore, 2023; pp 213–269. https://doi.org/10.1007/978-981-19-8520-1_7.

(6) Żarczyńska, M.; Żarczyński, P.; Tomsia, M. Nucleic Acids Persistence—Benefits and Limitations in Forensic Genetics. Genes 2023, 14 (8), 1643. https://doi.org/10.3390/genes14081643.

(7) Littlefair, J. E.; Rennie, M. D.; Cristescu, M. E. Environmental Nucleic Acids: A Field-based Comparison for Monitoring Freshwater Habitats Using eDNA and eRNA. Mol. Ecol. Resour. 2022, 22 (8), 2928–2940. https://doi.org/10.1111/1755-0998.13671.

(8) Qiao, J.; Zhao, Z.; Li, Y.; Lu, M.; Man, S.; Ye, S.; Zhang, Q.; Ma, L. Recent Advances of Food Safety Detection by Nucleic Acid Isothermal Amplification Integrated with CRISPR/Cas. Crit. Rev. Food Sci. Nutr. 2024, 64 (32), 12061–12082. https://doi.org/10.1080/10408398.2023.2246558.

(9) Boom, R.; Sol, C. J.; Salimans, M. M.; Jansen, C. L.; Wertheim-van Dillen, P. M.; Van Der Noordaa, J. Rapid and Simple Method for Purification of Nucleic Acids. J. Clin. Microbiol. 1990, 28 (3), 495–503. https://doi.org/10.1128/jcm.28.3.495-503.1990.

(10) Ali, N.; Rampazzo, R. D. C. P.; Costa, A. D. T.; Krieger, M. A. Current Nucleic Acid Extraction Methods and Their Implications to Point-of-Care Diagnostics. BioMed Res. Int. 2017, 2017, 1–13. https://doi.org/10.1155/2017/9306564.

(11) Yin, J.; Hu, J.; Sun, J.; Wang, B.; Mu, Y. A Fast Nucleic Acid Extraction System for Point-of-Care and Integration of Digital PCR. The Analyst 2019, 144 (23), 7032–7040. https://doi.org/10.1039/c9an01067j.

(12) Botella, J. R. Point-of-Care DNA Amplification for Disease Diagnosis and Management. Annu. Rev. Phytopathol. 2022, 60 (1), 1–20. https://doi.org/10.1146/annurev-phyto-021621-115027.

(13) Sun, W. Nucleic Extraction and Amplification. In Molecular Diagnostics; Elsevier, 2010; pp 35–47. https://doi.org/10.1016/B978-0-12-369428-7.00004-5.

(14) Monis, P.; Giglio, S. Nucleic Acid Amplification-Based Techniques for Pathogen Detection and Identification. Infect. Genet. Evol. 2006, 6 (1), 2–12. https://doi.org/10.1016/j.meegid.2005.08.004.

(15) Fakruddin, M.; Mannan, K. B.; Chowdhury, A.; Mazumdar, R.; Hossain, M.; Islam, S.; Chowdhury, M. Nucleic Acid Amplification: Alternative Methods of Polymerase Chain Reaction. J. Pharm. Bioallied Sci. 2013, 5 (4), 245. https://doi.org/10.4103/0975-7406.120066.

(16) Das, D.; Lin, C.-W.; Chuang, H.-S. LAMP-Based Point-of-Care Biosensors for Rapid Pathogen Detection. Biosensors 2022, 12 (12), 1068. https://doi.org/10.3390/bios12121068.

(17) Garrido-Maestu, A.; Prado, M. Naked-Eye Detection Strategies Coupled with Isothermal Nucleic Acid Amplification Techniques for the Detection of Human Pathogens. Compr. Rev. Food Sci. Food Saf. 2022, 21 (2), 1913–1939. https://doi.org/10.1111/1541-4337.12902.

(18) Wolcott, M. J. Advances in Nucleic Acid-Based Detection Methods. Clin. Microbiol. Rev. 1992, 5 (4), 370–386.

(19) Azeem, M. M.; Shafa, M.; Aamir, M.; Zubair, M.; Souayeh, B.; Alam, M. W. Nucleotide Detection Mechanism and Comparison Based on Low-Dimensional Materials: A Review. Front. Bioeng. Biotechnol. 2023, 11. https://doi.org/10.3389/fbioe.2023.1117871.

(20) Kricka, L. J. Nucleic Acid Detection Technologies — Labels, Strategies, and Formats. Clin. Chem. 1999, 45 (4), 453–458. https://doi.org/10.1093/clinchem/45.4.453.

(21) Zhang, H.; Li, F.; Dever, B.; Li, X.-F.; Le, X. C. DNA-Mediated Homogeneous Binding Assays for Nucleic Acids and Proteins. Chem. Rev. 2013, 113 (4), 2812–2841. https://doi.org/10.1021/cr300340p.

(22) Zipper, H. Investigations on DNA Intercalation and Surface Binding by SYBR Green I, Its Structure Determination and Methodological Implications. Nucleic Acids Res. 2004, 32 (12), e103–e103. https://doi.org/10.1093/nar/gnh101.

(23) Wang, M.; Holmes-Davis, R.; Rafinski, Z.; Jedrzejewska, B.; Choi, K. Y.; Zwick, M.; Bupp, C.; Izmailov, A.; Paczkowski, J.; Warner, B.; Koshinsky, H. Accelerated Photobleaching of a Cyanine Dye in the Presence of a Ternary Target DNA, PNA Probe, Dye Catalytic Complex: A Molecular Diagnostic. Anal. Chem. 2009, 81 (6), 2043–2052. https://doi.org/10.1021/ac702519k.

(24) Wakelin, L. P. G.; Adams, A.; Hunter, C.; Waring, M. J. Interaction of Crystal Violet with Nucleic Acids. Biochemistry 1981, 20 (20), 5779–5787. https://doi.org/10.1021/bi00523a021.

(25) Wang, G.; Akiyama, Y.; Shiraishi, S.; Kanayama, N.; Takarada, T.; Maeda, M. Cross-Linking versus Non-Cross-Linking Aggregation of Gold Nanoparticles Induced by DNA Hybridization: A Comparison of the Rapidity of Solution Color Change. Bioconjug. Chem. 2017, 28 (1), 270–277. https://doi.org/10.1021/acs.bioconjchem.6b00410.

(26) Tanaka, Y.; Hirao, G.; Fukuzumi, N.; Asahi, T.; Maeda, M.; Ogawa, A.; Zako, T. Effect of DNA Density on Nucleic Acid Detection Using Cross-Linking Aggregation of DNA-Modified Gold Nanoparticles. Langmuir 2025, acs.langmuir.4c04343. https://doi.org/10.1021/acs.langmuir.4c04343.

(27) Sato, K. Non-Cross-Linking Gold Nanoparticle Aggregation as a Detection Method for Single-Base Substitutions. Nucleic Acids Res. 2005, 33 (1), e4–e4. https://doi.org/10.1093/nar/gni007.

(28) Li, T.; Xu, X.; Zhang, G.; Lin, R.; Chen, Y.; Li, C.; Liu, F.; Li, N. Nonamplification Sandwich Assay Platform for Sensitive Nucleic Acid Detection Based on AuNPs Enumeration with the Dark-Field Microscope. Anal. Chem. 2016, 88 (8), 4188–4191. https://doi.org/10.1021/acs.analchem.6b00535.

(29) Teengam, P.; Siangproh, W.; Tuantranont, A.; Vilaivan, T.; Chailapakul, O.; Henry, C. S. Multiplex Paper-Based Colorimetric DNA Sensor Using Pyrrolidinyl Peptide Nucleic Acid-Induced AgNPs Aggregation for Detecting MERS-CoV, MTB, and HPV Oligonucleotides. Anal. Chem. 2017, 89 (10), 5428–5435. https://doi.org/10.1021/acs.analchem.7b00255.

(30) Detection of Human Leptin in Serum Using Chemiluminescence Immunosensor: Signal Amplification by Hemin/G-Quadruplex DNAzymes and Protein Carriers by Fe3O4/Polydopamine/Au Nanocomposites. Sens. Actuators B Chem. 2015, 221, 792–798. https://doi.org/10.1016/j.snb.2015.07.022.

(31) Xu, S.; Duo, H.; Zheng, C.; Zhao, S.; Song, S.; Simon, G. Novel Approach to Fabrication of DNA Biosensor Based on a Carboxylated Graphene Oxide Decorated with Fe3O4 NPs for the Detection of Typhoidal Salmonella. Int. J. Electrochem. Sci. 2019, 14 (2), 1248–1269. https://doi.org/10.20964/2019.02.44.

(32) Li, S.; Zhu, L.; Lin, S.; Xu, W. Toehold-Mediated Biosensors: Types, Mechanisms, and Biosensing Strategies. Biosens. Bioelectron. 2023, 220, 114922. https://doi.org/10.1016/j.bios.2022.114922.

(33) Tang, L.; Luo, T.; Fan, S.; Liu, Y.; Song, J. Principles of Nucleic Acid Toehold Mediated Strand Displacement (TMSD) Reaction Model and Its Applications in Cell Environment. Biomater. Sci. 2023, 11 (15), 5060–5077. https://doi.org/10.1039/D3BM00476G.

Chapter 5.

Conclusion

The chemistry-gated photochemistry approach paves the way for developing sensors and detectors based on the diarylethene photoswitches. The research on using the photoinactive parallel conformation of diarylethene photoswitches for sensing and detection applications is limited. Most of the research on these photochromic molecules still caters to the photochemistry-gated chemistry approach. Similarly, many modifications on the central ring have been done to improve the photochemistry of these molecules, and very little has been done to create novel systems that can turn on photochromism through chemical bond rearrangements. The main focus of this thesis was to highlight one area related to diarylethenes that has enormous potential.

Chapter 2 of the thesis focused on detecting singlet oxygen, a highly reactive oxygen species, by utilizing the Diels-Alder reaction with the furan central ring on the pro-diarylethene molecule. The synthesis procedure of the molecule was revised to avoid reactive intermediates, which helped increase the yield and decreased the number of steps required. The reaction of the furan ring was tried with calcium peroxide diperoxohydrate, a benign source of singlet oxygen, photooxidation with benzophenone and duroquinone, and Fenton's reagent. The main drawback or challenge was the stability of the endoperoxide product. This volatile reaction product rearranges to form numerous other products at room temperature. This made the analysis and isolation of the reaction products difficult. Additionally, the system was not exclusive to singlet oxygen, as evident from the photochromic product appearance in Fenton's reagent reaction. Additionally, under certain conditions, non-photochromic products also formed. A more stable molecule could be placed at the central ring, creating a stable endoperoxide. This way, singlet oxygen could be trapped and released on command for Photodynamic Therapy.

Chapter 3 of the chapter focussed on the development of a covalently locked diarylethene system, an analog of the Hendrickson's reagent. The covalent bonds hold the molecule in the photoinactive state unless a chemical reaction breaks one of the bonds, allowing the molecule to acquire the photoactive *antiparallel* conformation. In this

case, the P-O-P bond is highly reactive with the oxygen nucleophiles due to the electrophilic nature of the two phosphorus. The Hendrickson's reagent is primarily used for the esterification reaction. The diarylethene-based reagent performed the esterification reaction almost equally well as the standard Hendrickson's reagent. The color change of the solution upon reaction progress can be used as a TLC replacement to detect reaction progress. Alternatively, the susceptibility of the P-O-P group towards O-nucleophiles was exploited to demonstrate the ability to detect alcohols. The biggest problem faced in the process was the stability of the molecule. A slight exposure to moisture led to the decomposition of the reagent. This propensity to moisture could be utilized to make sensors for moisture in organic solvents in the future.

Chapter 4 of the thesis focussed on creating a nucleic acid detector based on the toehold-mediated strand displacement reaction. The project's premise was to bind the parallel form of the diarylethene switch across a DNA double helix with a long target strand and a short protective strand with mismatches. A single strand complementary to the target strand will replace the protective strand, allowing the photochromic molecule to acquire the photoactive form. Before trying the DNA, a single nucleobase pair was attached across the diarylethene arms as a proof of concept. Unlocking the molecule by adding an excess of a nucleobase was tried. However, the hydrogen bonding between the pair was strong enough to resist the unlocking in non-polar solvents. In polar solvents, the molecule showed typical behavior. The biggest challenge in the project was the limited solubility of some of the intermediates in organic solvents. The project can be taken forward by finding a non-polar solvent to hold the two nucleobases through hydrogen bonding but polar enough to break it when another nucleobase is added. The strong binding also suggests that if the molecule is appended on a DNA double helix, only the toehold-mediated strand displacement process will be able to unlock the molecule apart from heat and polar solvents.

Appendix A. NMRs from Chapters 2, 3, and 4

CDCl3
3.2
1.0
Br
S
Br
f1 (ppm)

Br
S
HO
O
CDCl3
3.3
1.0
f1 (ppm)

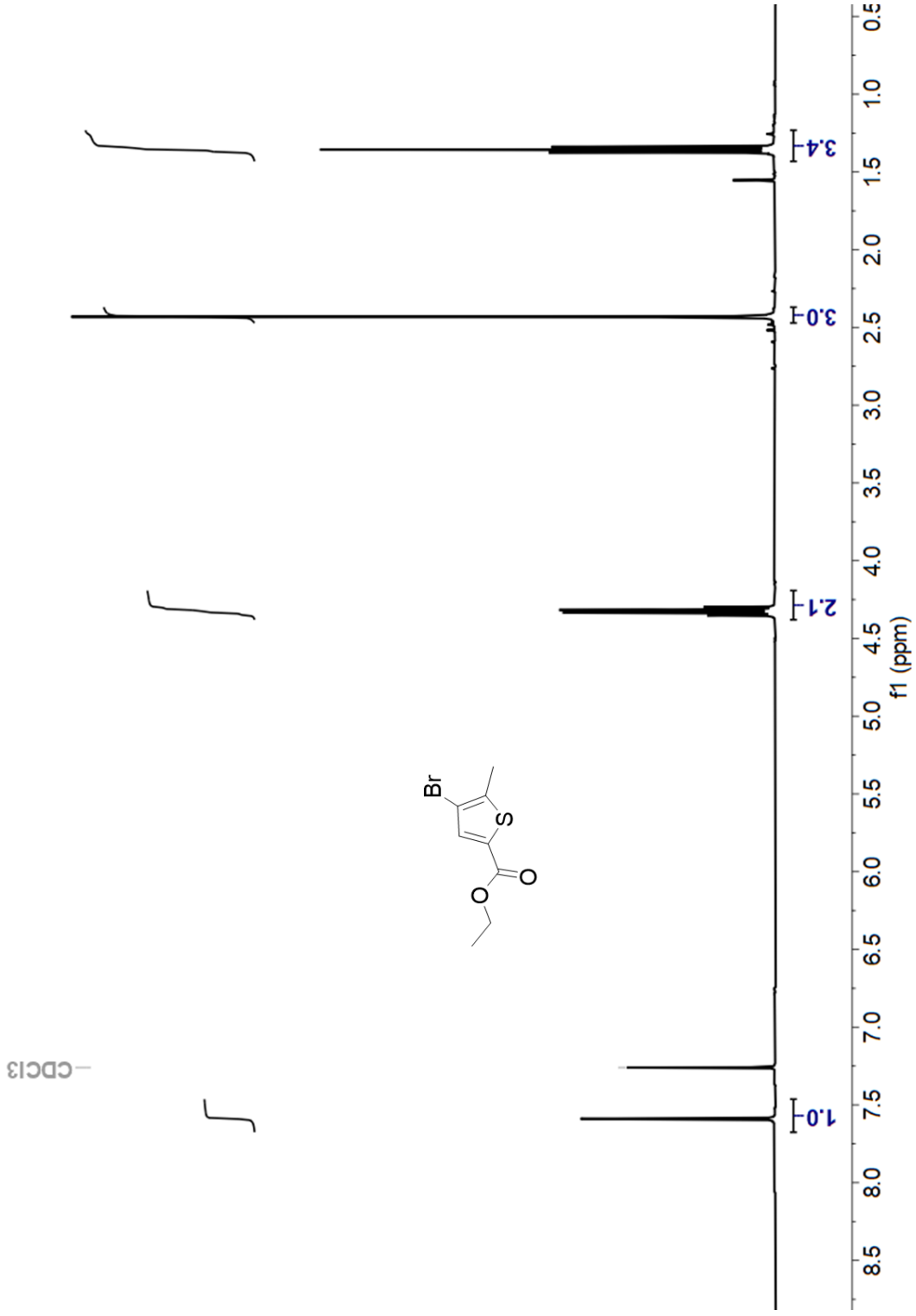
CDCl3
Br
S
O
O
1.0
3.4
3.0
2.1
8.5
8.0
7.5
7.0
6.5
6.0
5.5
5.0
4.5
4.0
3.5
3.0
2.5
2.0
1.5
1.0
0.5
f1 (ppm)

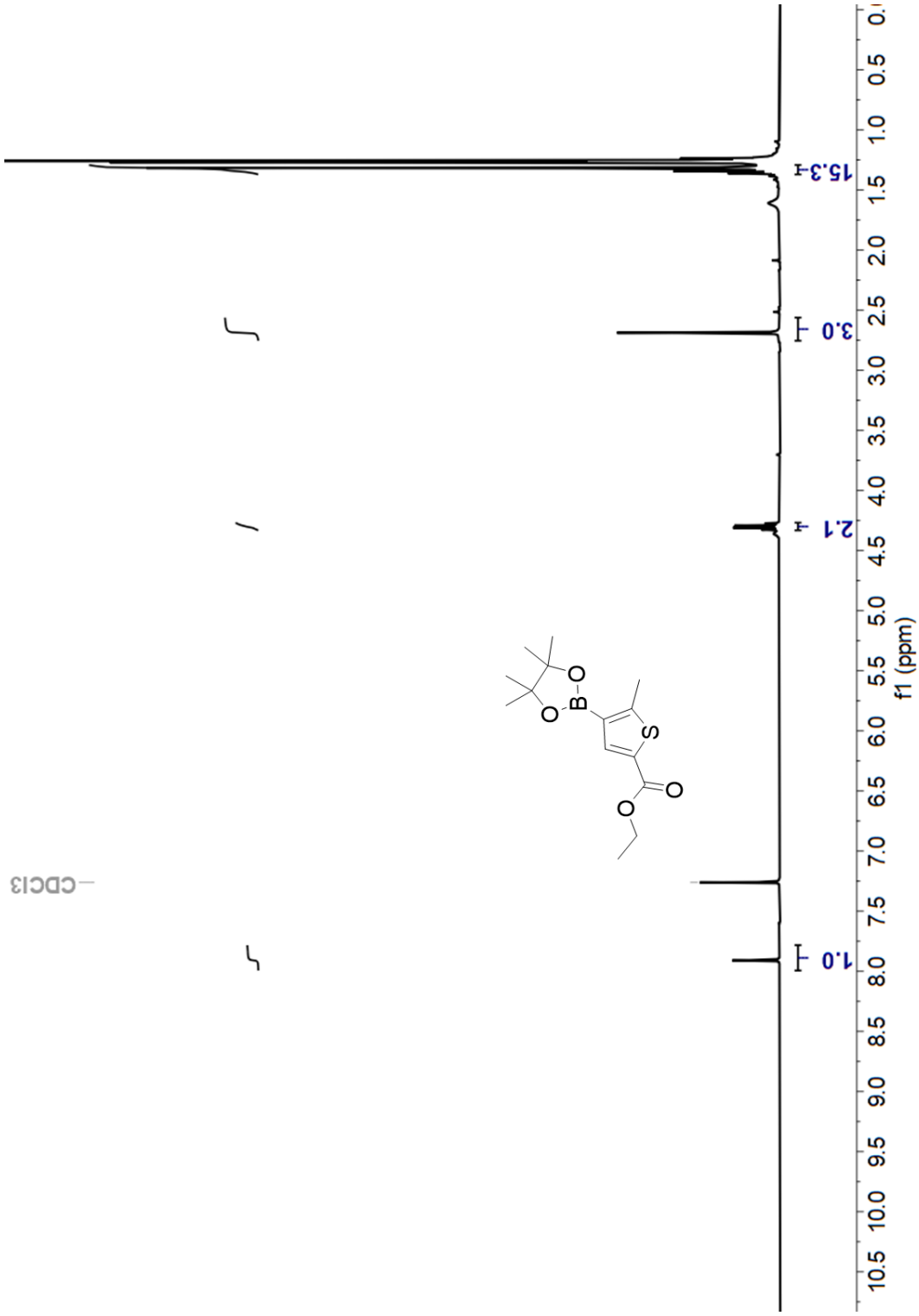
CDCl3
1.0
3.0
2.1
15.3
f1 (ppm)

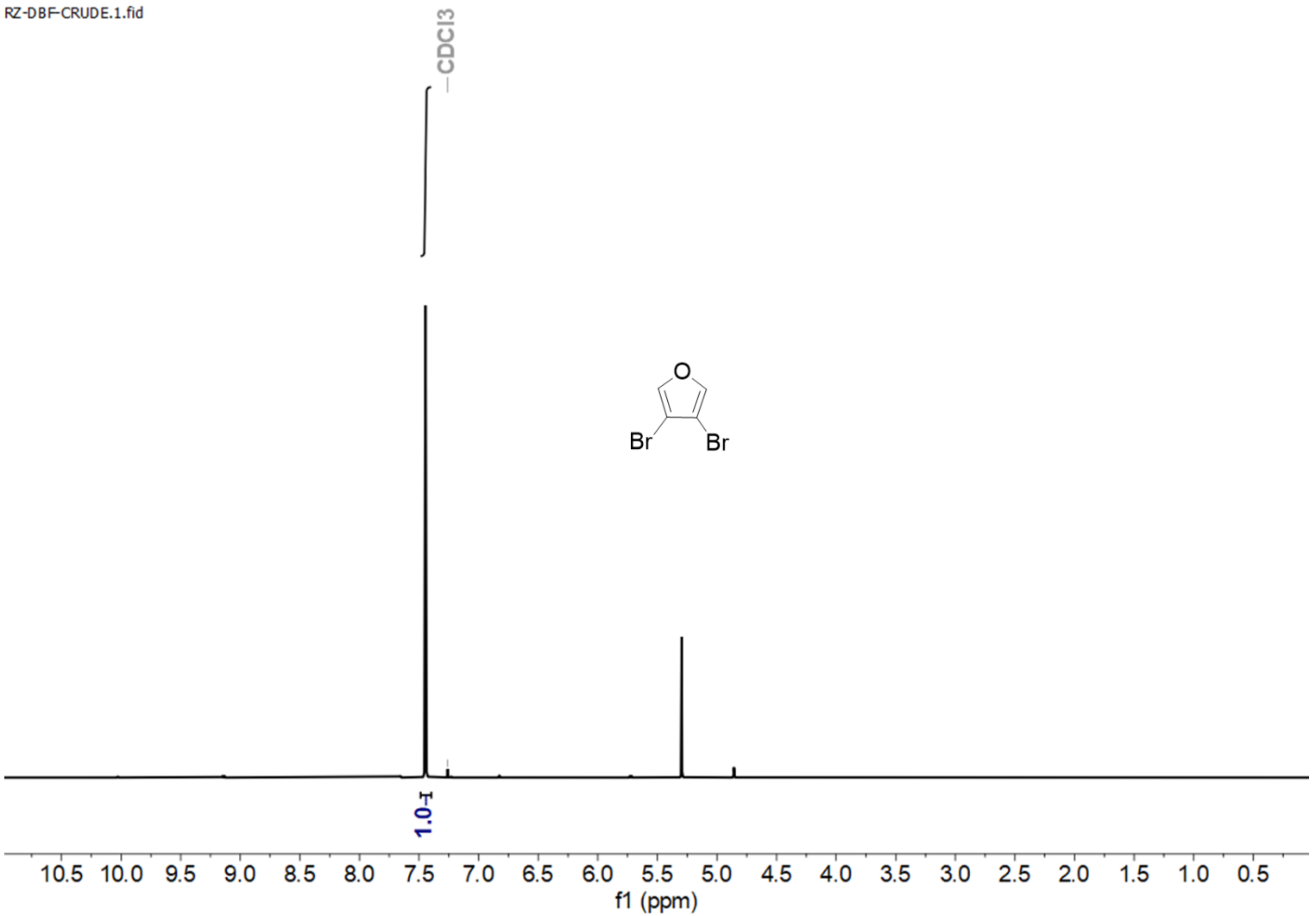
RZ-DBF-CRUDE.1.fid
CDCl3
O
Br
Br
1.0
10.5 10.0 9.5 9.0 8.5 8.0 7.5 7.0 6.5 6.0 5.5 5.0 4.5 4.0 3.5 3.0 2.5 2.0 1.5 1.0 0.5
f1 (ppm)

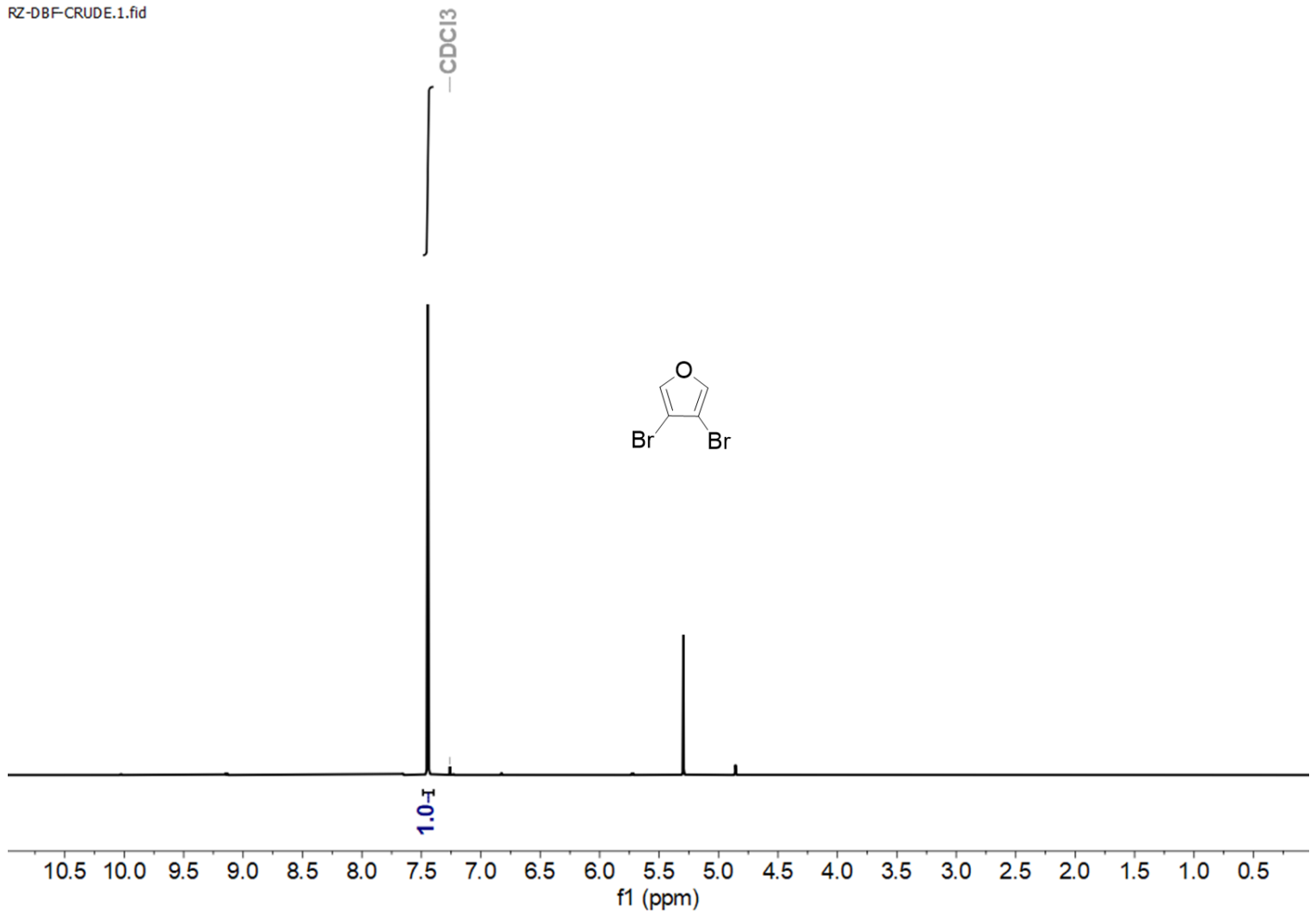
RZ-DBF-CRUDE.1.fid
CDCl3
O
Br
Br
1.0
10.5 10.0 9.5 9.0 8.5 8.0 7.5 7.0 6.5 6.0 5.5 5.0 4.5 4.0 3.5 3.0 2.5 2.0 1.5 1.0 0.5
f1 (ppm)

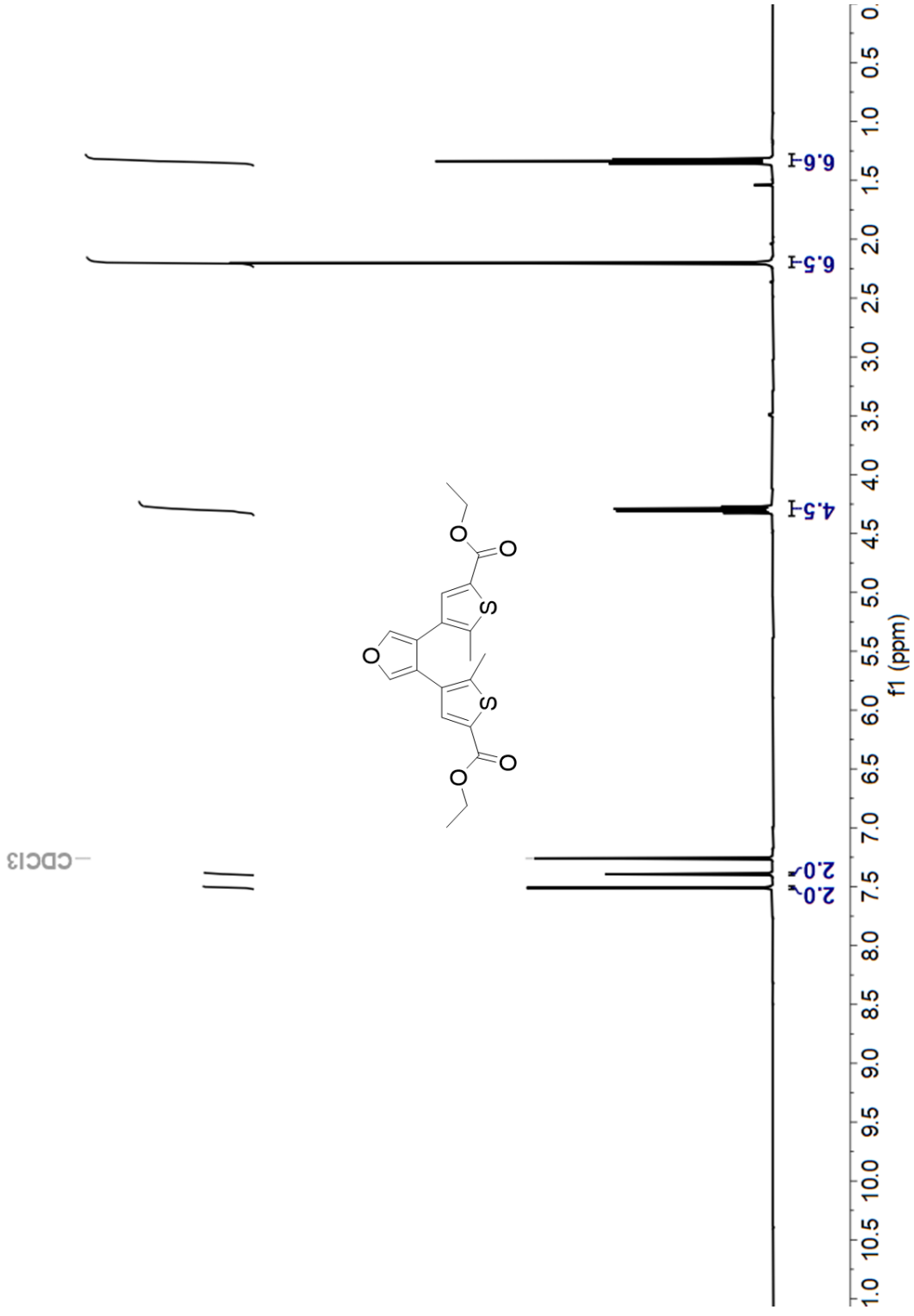
6.6
6.5
4.5
2.0
2.0
CDCl3
f1 (ppm)

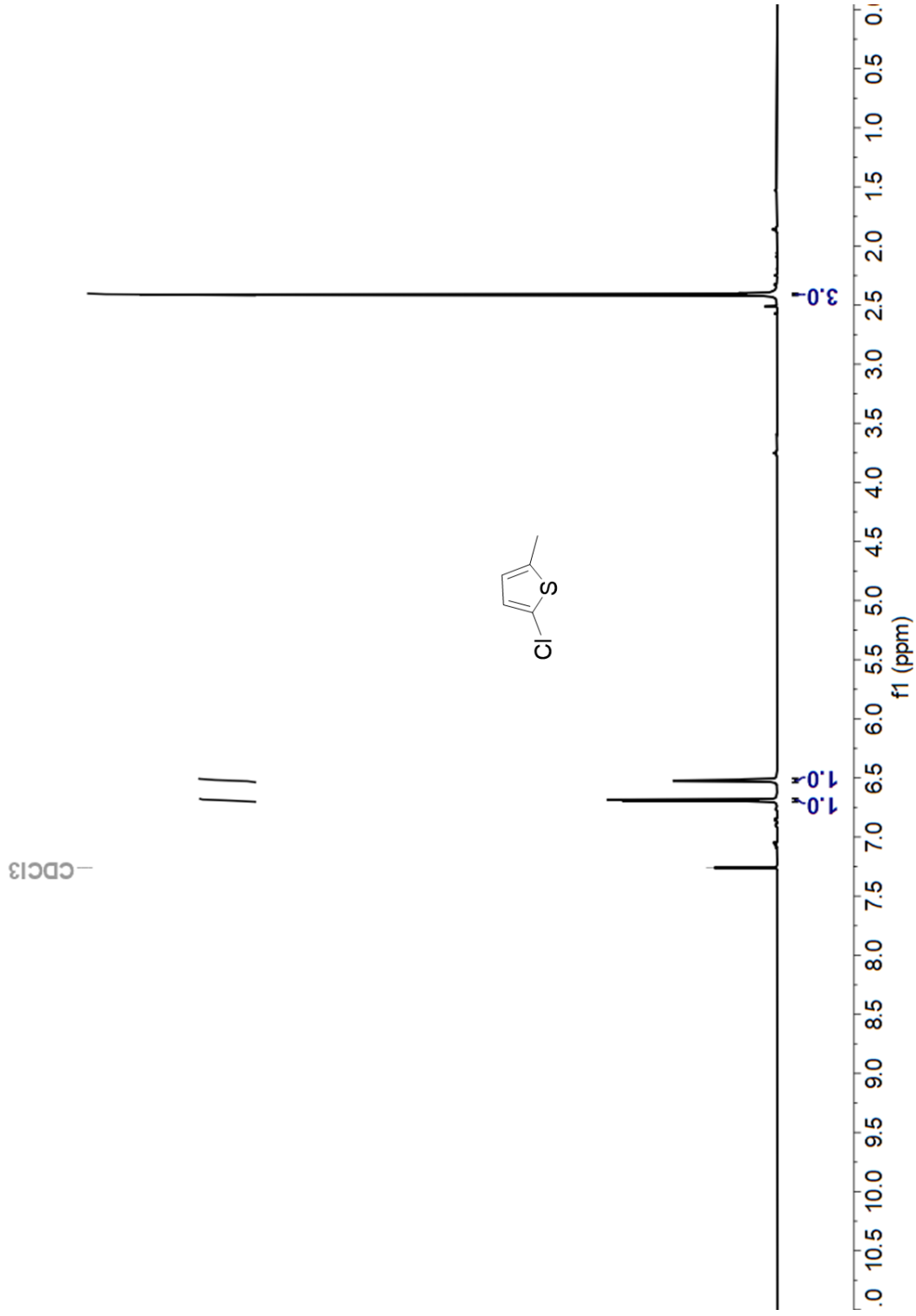
CDCl3
Cl
S
3.0
1.0
1.0
f1 (ppm)

2.0
2.2
3.9
6.5
CDCl3
Cl
S
O
O
S
Cl
10.5 10.0 9.5 9.0 8.5 8.0 7.5 7.0 6.5 6.0 5.5 5.0 4.5 4.0 3.5 3.0 2.5 2.0 1.5 1.0 0.5
f1 (ppm)

CDCl3
2.0
4.2
2.3
6.4
Cl
S
S
Cl
f1 (ppm)

21.4
2.0
4.6
6.2
3.1
f1 (ppm)
Ph
P
Ph
S
S
Ph
P
Ph

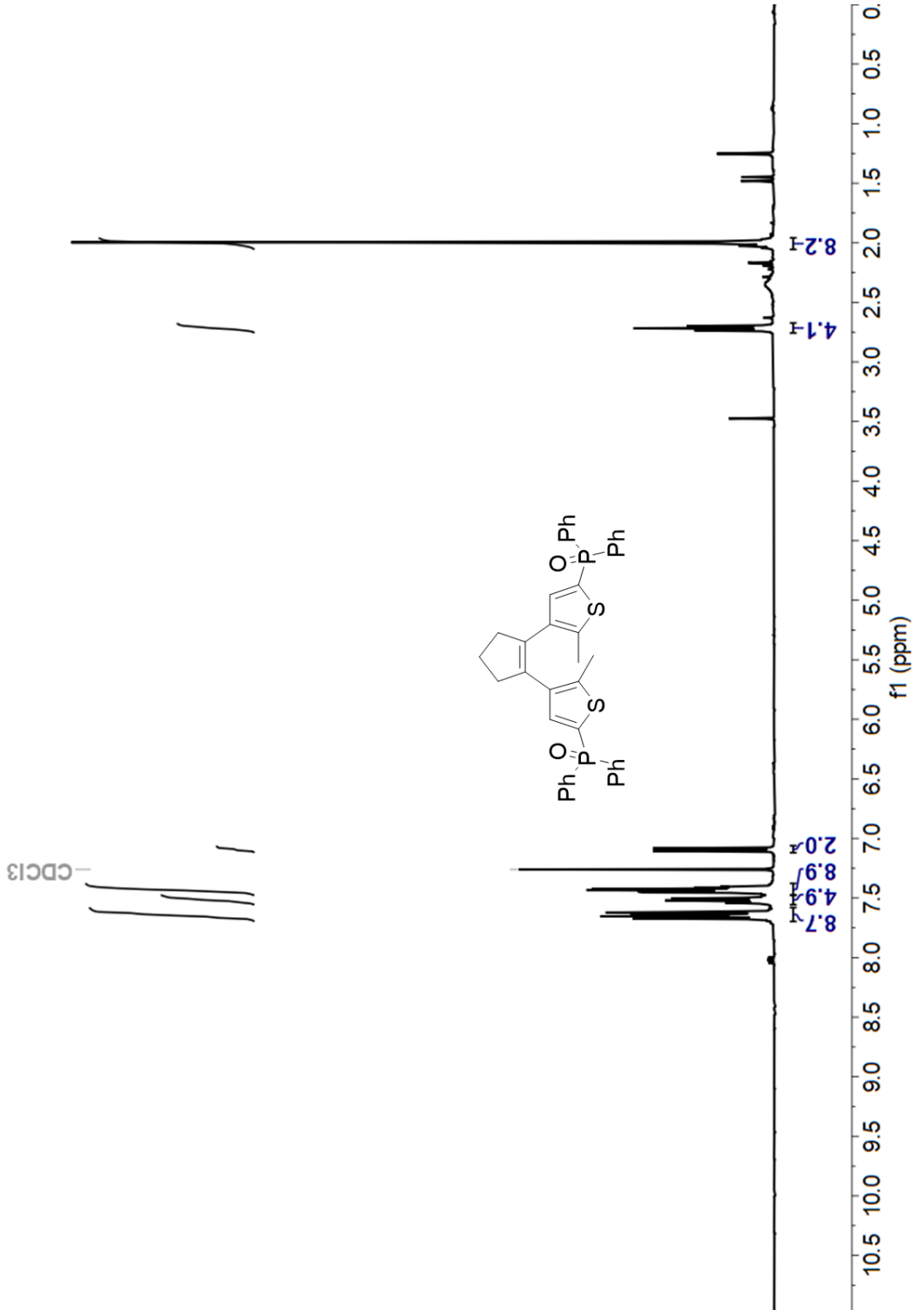
8.2
4.1
2.0
8.9
4.9
8.7
CDCl3
f1 (ppm)

3.0
2.0
3.8
2.0
1.9
CDCl3
O
O
Br
f1 (ppm)

CDCl3
16.7
2.0
4.2
4.5
8.3
6.3
f1 (ppm)

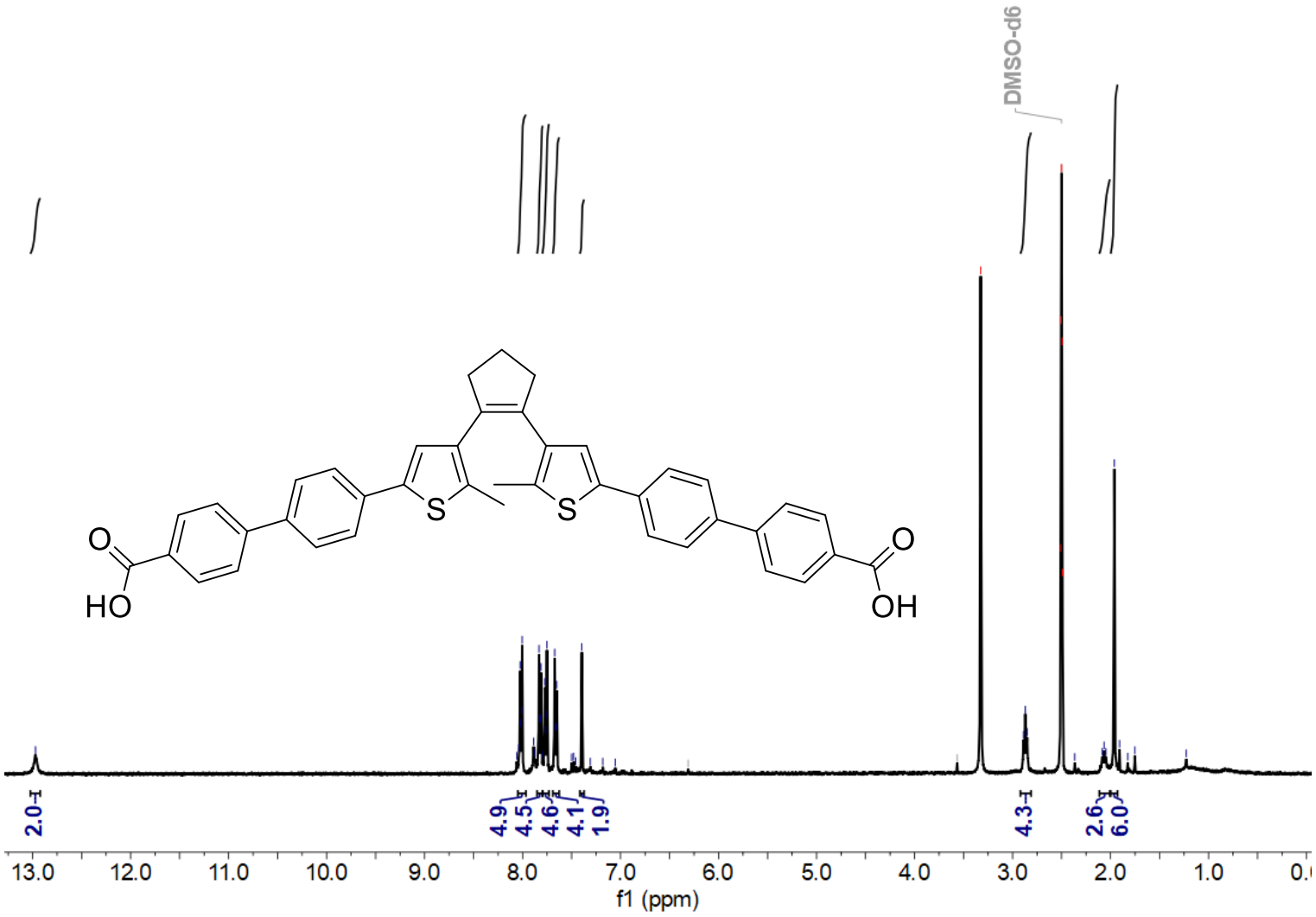
DMSO-d6
O
HO
S
S
O
OH
2.0
4.9
4.5
4.6
4.1
1.9
4.3
2.6
6.0
13.0
12.0
11.0
10.0
9.0
8.0
7.0
6.0
5.0
4.0
3.0
2.0
1.0
f1 (ppm)

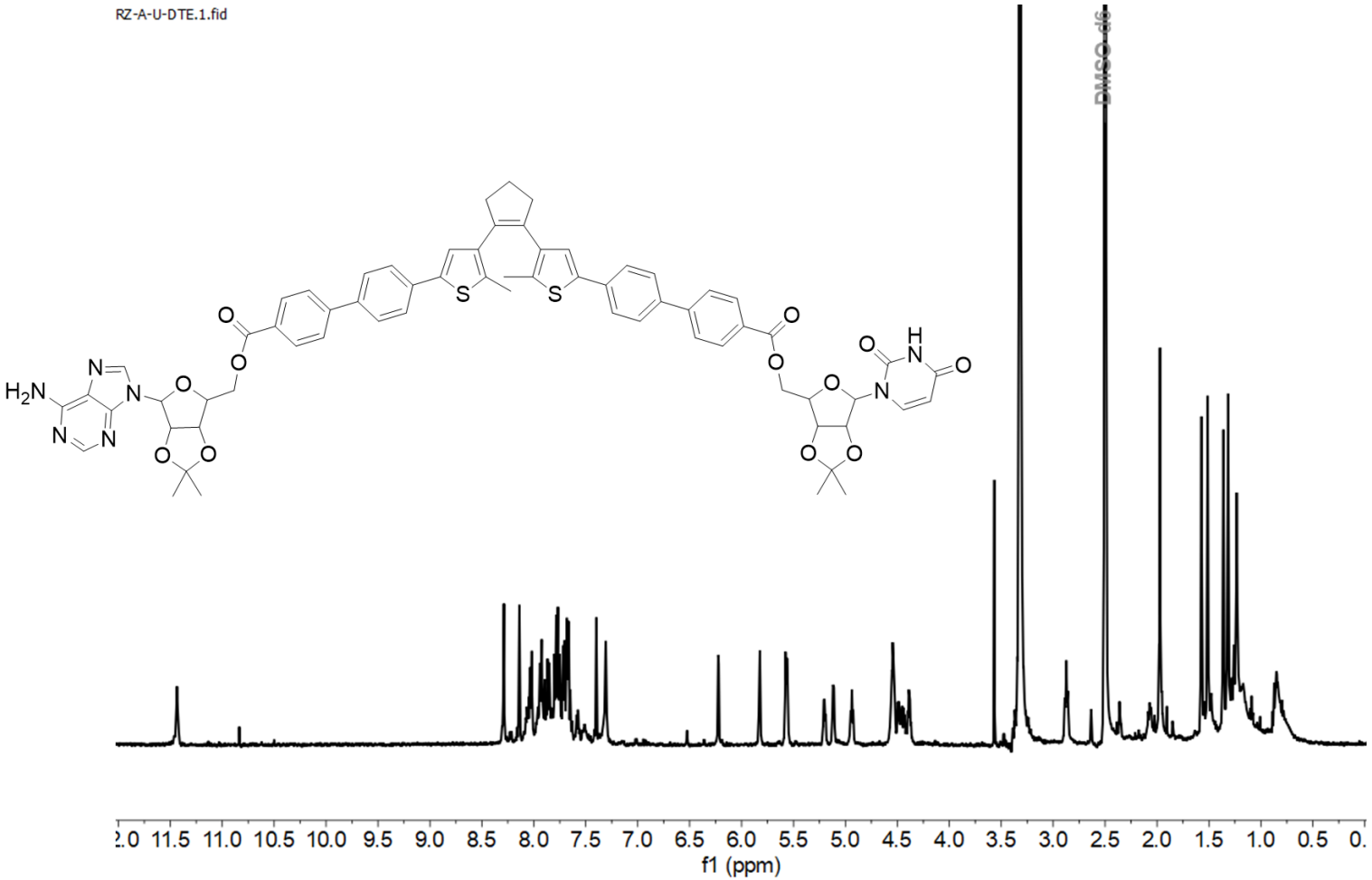
RZ-A-U-DTE.1.fid
DMSO-d6
f1 (ppm)